'Clinical outcomes and mechanisms of mesenteric fibrosis in small bowel neuroendocrine tumours'

by

Dr Faidon-Marios Laskaratos *MBBS MSc MRCP (UK) MRCP (London)*

A thesis submitted to University College London (UCL) in fulfilment of the requirements for the degree of Doctor of Philosophy (PhD)

Centre for Gastroenterology and Institute for Liver and Digestive Health, UCL

Supervisors:

Prof Martyn Caplin & Prof Krista Rombouts

March 2020

Declaration of originality

'I, Faidon-Marios Laskaratos confirm that the work presented in this thesis is my own. Where information has been derived from other sources, I confirm that this has been indicated in the thesis.'

……………………..

Dr F-M. Laskaratos

Acknowledgements

Abstract

Small intestinal neuroendocrine tumours (SI NETs) are relatively rare, indolent tumours arising from the enterochromaffin cells of the small bowel. They can be associated with the development of fibrosis, most commonly in the heart (termed 'carcinoid heart disease') or the mesentery around a metastatic deposit (also known as mesenteric desmoplasia). A concise summary of our current understanding of the pathophysiology of neuroendocrine fibrogenesis is provided in **Chapter 1**. The development of mesenteric fibrosis can be asymptomatic, but in some patients, it can lead to significant complications, such as bowel obstruction or mesenteric ischaemia. However, the epidemiology and pathophysiology of mesenteric fibrosis have not been sufficiently explored. In addition, there is a lack of clinically useful biomarkers for the detection of image-negative mesenteric desmoplasia.

The first aim of our study was to explore different clinical aspects of mesenteric desmoplasia and more specifically the epidemiological characteristics and clinical assessment of mesenteric fibrosis. An additional aim was to delineate further the pathogenesis of this process and evaluate a non-invasive, blood-based biomarker for the early detection of fibrosis.

To investigate the clinical and epidemiological aspects of mesenteric desmoplasia, two large-scale retrospective studies were performed which are described in **Chapter 2**. The first study was a survival analysis of approximately 150 fibrotic SI NETs and the second was a survival analysis of almost 400 metastatic SI NETs investigating the effect of mesenteric fibrosis on prognosis in addition to other epidemiological data. We demonstrated that in a large cohort of almost 400 patients with metastatic small bowel neuroendocrine tumours the prevalence of mesenteric fibrosis was about 35% and that 50% of patients with mesenteric metastases had radiological evidence of desmoplasia. The presence of mesenteric fibrosis was associated with a worse overall survival compared to patients without mesenteric lymphadenopathy by both univariate and multivariate analysis. However, in a retrospective analysis of almost 150 patients with fibrotic small bowel neuroendocrine tumours we did not find a significant difference in overall survival or complications (bowel obstruction, mesenteric ischaemia) among patients with mild, moderate and severe mesenteric desmoplasia

(patients were grouped using a radiological scoring system to grade the severity of desmoplasia). We determined that in midgut neuroendocrine tumours with radiological evidence of mesenteric fibrosis advanced age (>65) and elevated urinary 5-hydroxyindoleacetic acid (a product of serotonin metabolism measured in the urine) were independent predictors of survival.

In addition, to explore the pathophysiology of mesenteric fibrogenesis, we performed a set of co-culture experiments using the small intestinal NET cell lines KRJ-I and P-STS and the stromal cell line HEK293 and these experiments are described in **Chapter 3**. This study evaluated the crosstalk between cancer and stromal cells in terms of effects on cell proliferation, metabolism, gene expression (RT2 PCR Profilers and RNA sequencing) and protein/cytokine secretion. A reduction in cell metabolic activity was observed in both KRJ-I and P-STS cells treated with HEK293 conditioned media, with no significant changes in cell proliferation. Furthermore, no significant changes were observed in HEK293 cell proliferation or metabolic activity upon culturing with conditioned media of cancer cells. The RT2 PCR arrays revealed that several genes with key regulatory functions in cancer biology and fibrogenesis were significantly up- or down-regulated in KRJ-I, P-STS and HEK293 cells (fold-change≥2, p<0.05). In addition, RNA sequencing and Ingenuity Pathway Analysis identified multiple pathways that were significantly activated or inhibited (p<0.05, z score ≥ |2|). These signalling pathways have a wide range of biological functions, such as involvement in protein synthesis (e.g. EIF2 pathway) or regulation of cell metabolism and energy production. Several changes in chemokine and growth factor secretion were also observed.

A specific pathway that was activated in KRJ-I cells as a result of the paracrine effect - the integrin pathway - was further investigated in human tissue using qPCR, immunohistochemistry and Western blotting. This set of experiments is described in **Chapter 4**. A total of 34 patients were recruited into this prospective study and the gene/protein expression was evaluated in patients with graded severity of mesenteric fibrosis. The fibrosis grading was established using a complex and thorough assessment of the mesenteric desmoplasia which included a triangulation of different methodologies incorporating surgical, radiological and histological criteria. Using a variety of techniques, we provided evidence that the integrin pathway is activated in the fibrotic mesenteric mass of SI NETs. The detailed analysis of mesenteric

desmoplasia (incorporating surgical, radiological and histological parameters), that was used to provide the grading of fibrosis severity, also revealed several cases of image-negative mesenteric fibrosis. This is a new concept, as traditionally the diagnosis of mesenteric fibrosis has been based on imaging studies.

Finally, in **Chapter 5**, we evaluated a novel biomarker – the Fibrosome - that included 5 circulating transcripts from the NETest, which collectively exhibited high performance metrics for the detection of mesenteric fibrosis, even in the case of image-negative mesenteric desmoplasia.

In conclusion, this study has provided useful epidemiological data about mesenteric fibrosis and more specifically regarding its prevalence, effect on overall survival and clinical outcomes, and has also provided insight into the assessment of the presence and severity of mesenteric fibrosis, demonstrating for the first time that a radiological evaluation alone is not sufficient. In addition, this is the first study to provide a comprehensive understanding of the bidirectional communication of cancer and stromal cells and we have validated the activation of the integrin pathway in the fibrotic microenvironment of SI NETs (human tissue). Finally, a novel circulating biomarker was developed with promising preliminary results, that warrant further validation in additional independent patient cohorts.

Impact Statement

This study has investigated the poorly understood effects of mesenteric fibrosis on clinical outcomes, as well as the basic pathophysiology involved with the aim of identifying key pathways that may have a translational impact on clinical management. It has also evaluated a novel circulating biomarker for the detection of mesenteric fibrosis, which may have important clinical utility in cases of image-negative desmoplasia. This study was an international collaborative project with the University of Graz in Austria and the Wren Laboratories in the USA, which explored an area of research that is under-investigated despite the substantial morbidity and mortality associated with the development of mesenteric fibrosis. The impact of mesenteric desmoplasia on survival and other clinical outcomes is a topic that has been previously overlooked, partly because this information was not recorded in national and institutional databases that were used in other epidemiological studies. This epidemiological information is likely to be useful for both future researchers and clinicians. Our survival analysis of patients with fibrotic small intestinal NETs has identified specific predictors of poor prognosis which may be helpful to guide clinical management and assist with patient prognostication. Our basic science experiments have also provided further insight into the pathogenesis of mesenteric fibrosis, which has improved our understanding of this process and may lead the way for further studies in this field. In addition, the identification of pathways involved in mesenteric fibrogenesis is a prerequisite for the development of targeted therapies, and these can be tested initially in vitro, followed by in vivo human tissue moving forward to translational medicine. The lack of medical antifibrotic therapies creates a compelling need for such studies, as currently surgical resection is the mainstay for the management of mesenteric fibrosis. Furthermore, our study has revealed for the first time the effect of stroma on cancer progression, and particularly the activation of the integrin pathway in the fibrotic microenvironment of these tumours. This is a novel finding and provides a new direction for future research, as previous studies had mainly focussed on the effect of the cancer cells on the stroma and the stimulation of fibrosis. Finally, the development of a novel biomarker (derived from the NETest) with excellent performance metrics for the detection of mesenteric fibrosis is important given the non-invasive nature of the assessment and the clinical significance

of the early diagnosis of desmoplasia. The methodology used may also be applied in future studies for the evaluation of other circulating profibrotic transcripts (not included in the NETest) and the evaluation of additional, non-invasive biomarkers of fibrosis associated with neuroendocrine neoplasia.

Contents

List of Abbreviations

APLP2:   Amyloid precursor-like protein 2

α-SMA: a-Smooth Muscle Actin

AUC: Area Under the Curve

BNIP3L: BCL2 Interacting Protein 3 Like

BrdU: 5-bromo-2'-deoxyuridine

CCL2:   C-C motif chemokine ligand 2

CgA: Chromogranin A

CHD: Carcinoid Heart Disease

CI: Confidence Interval

CM: Complete Medium

CMF-PBS: Ca^{2+} Mg^{2+} free phosphate buffered saline

COL1A1:   Collagen type I alpha 1 chain

COL3A1:   Collagen type III alpha 1 chain

CondM: Conditioned medium

CPA: Collagen Proportionate Area

CTGF: Connective Tissue Growth Factor

CXCL2:   C-X-C motif ligand 2

CXCL8:   C-X-C motif ligand 8

DAG: Diacylglycerol

DAP12:   DNAX activation protein of 12kDa

DIPNECH: Diffuse idiopathic neuroendocrine cell hyperplasia

DMEM: Dulbecco's Modified Eagle Medium

EBV:	**Epstein-Barr virus**
ECM:	**Extracellular Matrix**
EGFR:	**Epithelial Growth Factor receptor**
ENETS:	**European Neuroendocrine Tumour Society**
ERK:	**Extracellular signal-regulated kinase**
FADD:	**Fas-associated via death domain**
FAPα:	**Fibroblast activation protein α**
FBS:	**Fetal Bovine Serum**
FGF2:	**Fibroblast Growth Factor 2**
FGFR1:	**Fibroblast Growth Factor Receptor 1**
FN1:	**Fibronectin 1**
FZD7:	**Frizzled homolog 7**
GAP:	**GTPase activating protein**
G-CSF:	**Granulocyte colony stimulating factor**
GDF:	**GDI displacement factor**
GDI:	**Guanine nucleoside dissociation inhibitor**
GEF:	**Guanine nucleotide exchange factor**
GEP:	**Gastro-entero-pancreatic**
Grb2:	**Growth factor receptor-bound protein 2**
5-HIAA:	**5-Hydroxy-indole-acetic acid**
HKG:	**Housekeeping gene**
HR:	**Hazard ratio**
HRP:	**Horseradish peroxidase**
5-HT:	**5-hydroxytryptamine**

HTLV1: Human T-cell leukaemia virus 1

IL: Interleukin

IP3: Inositol-1,4,5-triphosphate

IP-10: Interferon gamma-induced protein 10

IPA: Ingenuity Pathway Analysis

ITGAV: Integrin α subunit v

ITGAX: Integrin α subunit x

KSHV: Kaposi sarcoma-associated herpesvirus

LAP: Latency-associated peptide

LTBP: Latent TGF-β Binding Protein

MAPK: Mitogen-activated protein kinases

MAX: Myc-associated protein X

MCP-1: Monocyte chemoattractant protein-1

MEK: Mitogen-activated protein/extracellular signal-regulated kinase

MFI: Median fluorescence intensity

MIP: Macrophage Inflammatory Protein

M-M: Mesenteric mass

MMP: Matrix metalloproteinase

MMT: 3-(4,5-dimethylthiazol-2-yl)-2,5-diphenyltetrazolium bromide

mTOR: Mammalian target of rapamycin

NET: Neuroendocrine Tumour

NFAT: Nuclear factor of activated T-cell

NFκB2: Nuclear Factor Kappa B Subunit 2

N-TIS: Normal tissue (mucosa)

OS: Overall Survival

PBS: Phosphate buffered saline

PDGF: Platelet-derived growth factor

PI3K: Phosphatidylinositol 3-kinase

PIP2: Phosphatidylinositol-4,5-bisphosphonate

pNET: Pancreatic Neuroendocrine Tumour

PLC: Phospholipase C

PKC: Protein kinase C

PRRT: Peptide receptor radionuclide therapy

qRT-PCR: Quantitative reverse transcription-polymerase chain reaction

ROC: Receiver operating characteristic

ROS: Reactive oxygen species

SA-PE: Streptavidin-phycoerythrin

SEER: Surveillance, Epidemiology and End Results

SFM: Serum-Free Medium

SI: Small intestinal

TGF-α: Transforming Growth Factor alpha

TGF-β: Transforming Growth Factor beta

TGFβR1: Transforming Growth Factor beta Receptor 1

TMB: Tetra-methylbenzidine

TNF: Tumour Necrosis Factor

TREM-1: Triggering receptor expressed on myeloid cells-1

T-TIS: (Primary) tumour tissue

VEGF: Vascular Endothelial Growth Factor

Chapter 1

Introduction

1. Introduction

Neuroendocrine tumours (NETs) are relatively rare cancers, but their incidence has increased dramatically over recent decades[1]. They represent a heterogeneous group of neoplasms that arise from cells of the diffuse endocrine system and the most common sites of disease are the gastrointestinal tract followed by the bronchopulmonary tree[1]. NETs are often associated with the development of fibrosis, which may occur at local or distant sites[2].

Carcinoid heart disease (CHD) is a common fibrotic complication of neuroendocrine tumours (typically of small bowel and bronchial origin) that usually manifests with fibrosis of the right-sided heart valves, although in severe cases and usually if a patent foramen ovale is present it may also affect the left-sided chambers[3]. It can rapidly progress to heart failure, if left untreated, and is a well-known poor prognostic factor[4,5]. In addition, mesenteric fibrosis in midgut neuroendocrine tumours is a common finding that has been reported to occur in up to 50% of cases[6,7]. This usually develops around a metastatic mesenteric lymph node and has a typical 'spoke-wheel' appearance on imaging studies, which is considered a pathognomonic sign of small intestinal (SI) NETs[8]. The development of mesenteric desmoplasia is associated with significant morbidity, because it can lead to a variety of local complications, such as bowel obstruction, mesenteric ischaemia and obstructive uropathy[9]. More recently, its effect on overall survival has been evaluated in several studies, which have generally shown an association with poor prognosis[7,10-13]. Although CHD and mesenteric fibrosis are the commonest carcinoid-related fibrotic complications, fibrosis can develop in many other sites, including the retroperitoneum, the pleura and the skin[14-16].

The association of NETs with fibrosis has been known for a long time. However, the pathophysiology of this relationship has not been explored in depth and the underlying mechanisms remain elusive. A small number of review articles have focused on the area of carcinoid-driven fibrogenesis[2,17], including a recent publication in *Cancer* from our research group[9]. In this chapter we will provide a general overview of our existing knowledge of the mechanisms that drive fibrosis development in NETs and the reader is referred to our review article for a more comprehensive analysis of the topic[9]. This chapter will focus on the role of the

tumour microenvironment, and discuss the importance of several factors including serotonin, growth factors, kinins and other peptides that are known to interact with each other (synergistically or antagonistically), thereby contributing to the complex pathogenesis of fibrosis (**Figure 1.1**).
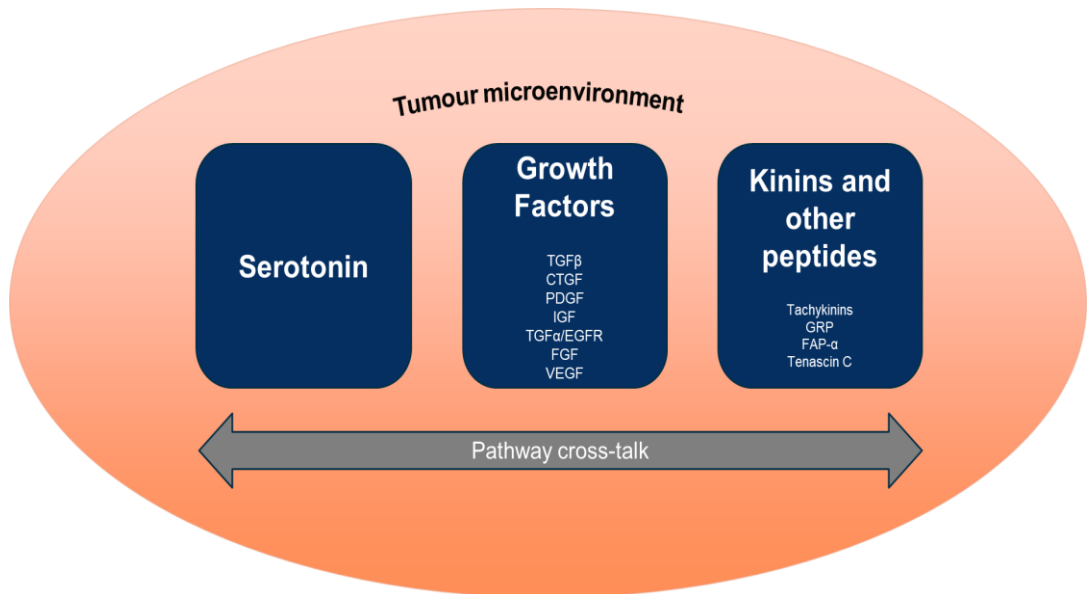
Figure 1.1. Schematic representation of our current understanding of the pathophysiology of fibrosis in NETs. Several factors within the tumour microenvironment play a role in fibrogenesis and are known to interact with each other. The pathway cross-talk largely accounts for the complexity of the process, and the difficulty in establishing effective antifibrotic therapies.

1.1. The role of the tumour microenvironment

The tumour microenvironment consists of neoplastic and non-neoplastic cells (e.g. fibroblasts, epithelial and endothelial cells), as well as a dynamic extracellular matrix (ECM), which contains both structural proteins (such as collagens) and other proteins with a wide range of functional properties (such as growth factors) that can directly interact with the surrounding cells upon their release from the ECM[18]. This complex microenvironment plays a critical role in cancer progression, as well as in fibrogenesis, and the functional interactions between tumour cells and fibroblasts are largely responsible for the development of desmoplasia in many types of cancer[19,20]. There is very limited literature in the

field of NETs evaluating the dynamic interactions of cancer and stromal cells within the tumour microenvironment. Svedja *et al* assessed the cross-talk of the enterochromaffin-derived neuroendocrine cell line KRJ-I with HEK293 cells in a Transwell system (**Figure 1.2**)[21]. This study showed that the addition of a 5-hydroxytryptamine receptor 2B (5-HT$_{2B}$) inhibitor in the tumour compartment led to a significant reduction in cell proliferation and profibrotic gene expression (TGFß1, CTGF, FGF2) not just in the KRJ-I cells but also in the HEK293 cells (that lack 5-HT$_{2B}$ receptors but have 5-HT$_{2A/C}$ receptors). This suggested that the effect of the drug on HEK293 cells was mediated through a reduction in serotonin secretion by the KRJ-I cells, which would normally exert a pro-proliferative and profibrotic effect on HEK293 cells[21].
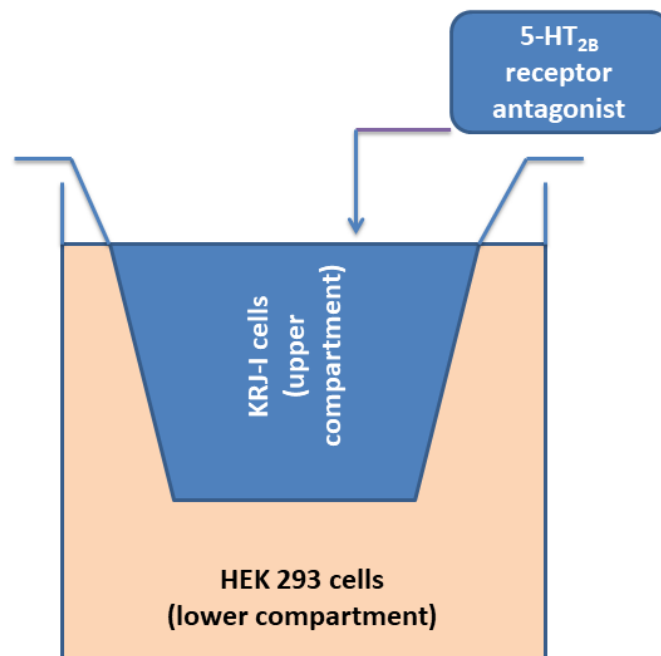
Figure 1.2. Transwell co-culture system of fibroblastic cells (HEK293) and cancer cells (KRJ-I) representing the small intestinal NET microenvironment. The role of serotonin in fibrosis development was investigated with the use of a 5-HT2B receptor antagonist[21].

In another study Kidd *et al* isolated fibroblasts from a patient with a fibrotic midgut NET, which they were able to culture for 5-7 days. Treatment of these fibroblasts with

TGFß1 led to a significantly increased expression of CTGF mRNA in the fibroblasts (relative to untreated fibroblasts) and this suggested a role of the TGFß1-CTGF axis in the development of carcinoid-related fibrosis[22].

1.2. Serotonin

The role of serotonin in the pathogenesis of carcinoid-related fibrosis is unambiguous and strong evidence is available that links serotonin secretion with the development of CHD. Many animal experimental studies[23-32] and numerous prospective[33-40] and retrospective[5,41-44] clinical studies have demonstrated a clear association between serotonin levels (often inferred from levels of its metabolite, 5-hydroxyindoleacetic acid [5-HIAA], in the urine) and the pathogenesis of CHD. The $5-HT_{2B}$ receptor seems to be particularly important for the development of cardiac valvulopathy, and this is also suggested by its involvement in drug-induced valvular heart disease (which has very similar phenotypic features to CHD)[45-59]. Although the exact mechanisms of serotonin-induced fibrogenesis remain elusive, it is known that serotonin has mitogenic properties in a wide range of stromal cells[60-67] and may induce TGFß expression in fibroblasts[68-70].

Serotonin may also be involved in the development of mesenteric fibrosis and this is suggested by the role of serotonin in the cross-talk of KRJ-I and HEK293 cells in a Transwell system, as described earlier[21]. In addition, several retrospective studies have demonstrated an association between urinary 5-HIAA levels and mesenteric fibrosis[11,71], as well as platelet 5-HT with mesenteric mass formation[72]. However, the association of urinary 5-HIAA levels with CHD appears to be stronger compared to that with mesenteric desmoplasia, which implies that other factors (apart from circulating serotonin) are likely to be involved in mesenteric fibrogenesis[11].

Serotonin has also been implicated in the development of fibrosis associated with pancreatic NETs (the so-called 'sclerosing variant'). This is observed on rare occasions (<15% of pancreatic NETs), and these sclerosing tumours have distinct histopathological features and imaging characteristics, and are often associated with adverse clinical outcomes and a more aggressive biological behaviour[73-77].

1.3. Growth factors

Several growth factors have been implicated in the development of carcinoid-related fibrosis. **TGFß** (Transforming Growth Factor ß) seems to play an important role in the cross-talk of cancer and stromal cells due to its known ability to induce collagen synthesis in fibroblasts[78,79] and promote tumour growth in neuroendocrine tumour cells[80,81]. In a previous study of gastroenteropancreatic NETs by Chaudhry *et al*[82], the authors demonstrated expression of all isoforms of TGFß (TGFß1-3) in cancer cells, while stromal cells expressed TGFß2 and latent TGFß binding protein (LTBP). Interestingly, TGFß receptor 2 immunoreactivity was detected mainly in the stromal cells and this suggested that TGFß could be involved in the interaction between cancer cells and fibroblasts to stimulate ECM production[82]. Similarly, another study by Waltenberger *et al* assessed the role of TGFß in the development of CHD[83]. The authors showed that TGFß1 and TGFß3 were immunohistochemically present in fibroblasts of carcinoid fibrotic lesions, while in unaffected heart valves only a limited number of fibroblasts were seen, with weak or no staining for TGFß1, TGFß2 and TGFß3[83]. In addition, in a different study, staining for the latent form of TGFß1 and αSMA (alpha smooth muscle actin - a marker of activated fibroblasts) was higher in fibrotic carcinoid valves compared to healthy valves[70]. Other members of the TGFß family, namely activin A and BMP4 (Bone Morphogenic Protein 4), have also been implicated in the pathogenesis of CHD and mesenteric angiopathy (sclerotic vascular changes) in midgut NETs, respectively[84,85].

In addition, **CTGF/CCN2** (Connective Tissue Growth Factor) is a downstream mediator of TGFß1 that is known to be involved in carcinoid-related fibrogenesis. Kidd *et al* demonstrated that mRNA levels of CTGF and TGFß1 were significantly higher in fibrotic midgut NETs compared to normal mucosa and non-fibrotic (gastric) carcinoids[22]. In addition, these changes were confirmed at protein level by immunohistochemistry. Serum CTGF levels were also higher in patients with fibrotic midgut NETs compared to healthy controls and non-fibrotic (gastric) tumours[22]. In another study of patients with midgut NETs, elevated serum CTGF levels were associated with right heart failure and right-sided valvular regurgitation and a threshold level of ≥77 µg/l was shown to have the best sensitivity and specificity for the prediction of right ventricular dysfunction[86].

Furthermore, **PDGF** (Platelet-derived Growth Factor) is a known fibrotic mediator in scleroderma and other fibrotic disorders[87-89]. Its role in carcinoid-driven fibrosis has been investigated in a small number of studies. Chaudhry *et al* showed that in gastroenteropancreatic NETs PDGF and PDGF α receptors were expressed in both cancer and stromal cells, while PDGF ß receptors were expressed only in the stromal component. This indicated that PDGF could be involved in the stimulation of stromal cells in a paracrine and possibly autocrine manner[82,90]. Another study that included mainly midgut and pancreatic NETs, demonstrated that stromal cells adjacent to cancer cells exhibited a stronger immunohistochemical expression of PDGF ß receptors compared to stromal cells which were distant to the tumour. Therefore, a paracrine effect that could contribute to fibrosis development in the tumour was suggested[91].

The **FGF** (Fibroblast Growth Factor) family includes a large number of growth factors that are known to regulate numerous cellular processes[92] and some of these family members have also been investigated in the context of carcinoid-related fibrosis. As mentioned earlier, FGF2 (also known as basic FGF) is involved in the cross-talk of KRJ-I and HEK293 cells[21], thereby suggesting a possible role in the desmoplastic reaction of midgut NETs, but was also strongly expressed in type 3 gastric NETs associated with diffuse stromal fibrosis[93]. In another study of gastrointestinal NETs, a positive correlation was observed between the amount of fibrous stroma and acidic FGF (αFGF), indicating that αFGF may play a role in fibrogenesis[94]. However, plasma levels of FGF did not appear to be associated with the presence of CHD in midgut NETs[38].

Moreover, **TGFα** (Transforming Growth Factor α) is known to bind to EGFR (Epithelial Growth Factor Receptor) and can thereby mediate several cellular processes, including angiogenesis, tumour cell proliferation and fibrogenesis in NETs[95-97]. In a heterogeneous group of gastroenteropancreatic NETs, TGFα was expressed in most tumours, but EGFR expression was higher in midgut compared to pancreatic NETs. The authors suggested that TGFα produced by the tumour cells might bind to EGFR present in cancer and stromal cells, and this in turn could lead to tumour growth (autocrine mechanism) and also account for the more advanced fibrosis observed in midgut NETs (paracrine effect)[98].

In addition, **IGF** (Insulin Growth Factor) -1 and -2 are known regulators of neuroendocrine tumour growth[99-101]. IGF-1 and IGF-1 receptor expression have been demonstrated in a small series of midgut NETs and stimulation of cultured tumour cells with IGF-1 induced cell proliferation, indicating that this growth factor may lead to tumour growth via an autocrine mechanism[102]. IGF-1 and -2 can also stimulate fibroblast proliferation[103] and therefore may play a role in the fibrogenesis associated with midgut NETs.

Finally, **VEGF** (Vascular Endothelial Growth Factor) is another growth factor that has been implicated in the development of fibrosis in pulmonary NETs. VEGF is a well-known proangiogenic factor and in a small series of patients with pulmonary tumorlets and neuroendocrine cell hyperplasia, tumorlets were seen within hypervascular and fibrotic areas. A higher expression of VEGF and VEGF receptor 2 was noted in endothelial cells and increased expression of VEGF receptor 1 was observed in bronchial epithelial and endothelial cells, compared with healthy lung tissue[104]. A case report of a pulmonary tumorlet associated with fibrosis also demonstrated strong expression of TGFß1 and VEGF in the tumour cells, indicating a role of these growth factors in the development of fibrosis associated with lung carcinoids[105].

1.4. Kinins and other peptides

Kinin peptides (bradykinins and tachykinins) are known to be released in the circulation during episodes of flushing in patients with carcinoid syndrome and have been implicated in the development of fibrosis associated with midgut NETs[106-108]. Tachykinins substance P and neuropeptide K are mitogenic in fibroblasts[109,110] and have been linked to the development of carcinoid heart disease[35]. Neurokinin A has also been associated with fibrotic cardiac involvement[40].

In medullary thyroid cancer (which is derived from calcitonin-secreting cells) a significant association was noted between desmoplasia and expression of tenascin C[111,112] and fibroblast activation protein α (FAPα)[112]. Tenascin C is an extracellular matrix glycoprotein that is upregulated in many malignancies and correlates with increased cancer invasiveness, while FAPα is a serine protease that is involved in ECM remodelling during cancer invasion[112]. Therefore, it was not surprising that desmoplastic tumours exhibited a higher prevalence of lymph node metastases[112].

Gastrin-releasing peptide (GRP) is another peptide that has been implicated in the development of fibrosis in pulmonary NETs. In a case report of a patient with a typical bronchial NET, tumorlets and diffuse idiopathic neuroendocrine cell hyperplasia (DIPNECH) associated with fibrosis, serum GRP levels were elevated pre-operatively and returned to normal after lobectomy, indicating that this peptide was secreted by the tumour cells. Increased immunohistochemical expression of GRP was also noted in the carcinoids and tumorlets, suggesting that this peptide is produced by the cancer cells and may be contributing to the dense fibrosis observed around the tumour cells in a paracrine manner[113].

In addition, neuroendocrine tumour cells secrete numerous other peptides, such as prostaglandins and interleukins, which have not been investigated in carcinoid-related fibrogenesis, but are known mediators of chronic inflammation and may act as profibrotic molecules[114-116].

1.5. Pathway crosstalk

Although several factors and their involvement in fibrosis were described earlier, it would be naïve to assume that these factors act independently via discrete pathways. In contrast, there is significant cross-talk between these fibrotic mediators and their downstream signalling cascades[9]. For example, many growth factors share common downstream molecules and they may act synergistically or antagonistically to each other. Some growth factors may also bind to different receptors[9]. For instance, CTGF which can bind to IGF receptors, that mediate collagen synthesis, as well as EGFR, that activate pathways which induce cell proliferation[97]. This cross-talk adds complexity to the pathophysiology of fibrosis in NETs and makes therapeutic targeting of this pathological process extremely challenging.

In conclusion, NETs are often associated with fibrosis and this development is generally considered an adverse factor linked with worse clinical outcomes and overall survival. The area of mesenteric fibrogenesis remains under-investigated and further research is needed in this field to improve our knowledge of the pathophysiology of this poorly understood condition, given the substantial morbidity and mortality

associated with it. This strategy will allow the development of appropriate targeted therapies. In the following chapters, we will describe our research in this area, which has mainly focused on the *epidemiology and clinical outcomes of mesenteric fibrosis* (**Chapter 2**), the *pathophysiology of the disease using co-culture cell line models* (**Chapter 3**), the *assessment of mesenteric desmoplasia* and *further delineation of the pathophysiology by evaluating alterations in gene/protein expression in human tissue* (**Chapter 4**), and finally, the *development of a circulating biomarker for early detection of fibrosis* (**Chapter 5**).

Chapter 2

Clinical aspects of mesenteric fibrosis in midgut neuroendocrine tumours: Prevalence, clinical outcomes and effect on prognosis

2. Clinical aspects of mesenteric fibrosis in midgut neuroendocrine tumours: Prevalence, clinical outcomes and effect on prognosis

2.1. Introduction

Little is known about the epidemiological features and clinical outcomes associated with mesenteric fibrosis. This is because most epidemiological and prognostic data related to neuroendocrine tumours derive from national registries, such as the Surveillance, Epidemiology and End Results (SEER) database. These analyses are limited by the lack of detailed clinical information in these registries (such as the presence of mesenteric desmoplasia on imaging studies) and the inability to trace individual patient records in order to validate or further explore specific aspects of their disease or management. In addition, due to the rarity of the disease, many institutional studies often analyse heterogeneous patient populations to increase the sample size, which then makes interpretation of the results quite challenging[11]. Therefore, in order to extend our knowledge of the epidemiological and clinical aspects of mesenteric fibrosis, we performed two separate large retrospective studies at the ENETS Centre of Excellence of the Royal Free Hospital.

The *first study* was a survival analysis of 147 patients with SI NETs associated with mesenteric desmoplasia. The focus of this analysis was to identify prognostic factors affecting overall survival in this group of patients, and to assess the effect of the radiological severity of mesenteric fibrosis on clinical outcomes.

The *second study* was a retrospective study of 387 patients with metastatic SI NETs (stage IV), which evaluated the effect of multiple clinical variables on overall survival, although our specific aim was to identify (by multivariate analysis) whether mesenteric fibrosis was a poor prognostic factor for survival in a large group of patients with the same stage of disease (i.e. stage IV). We also assessed the prevalence of mesenteric fibrosis, its association with CHD and urinary 5-HIAA levels. These two studies have now been published as original articles in *Neuroendocrinology*[10,11] and their methodology and results will be presented separately in this chapter, followed by a combined discussion of their main findings in relation to mesenteric fibrosis.

2.2. First retrospective study: Midgut NETs associated with mesenteric fibrosis

2.2.1. Methods

This retrospective study included a total of 147 patients with histopathologically confirmed SI NETs and radiological evidence of mesenteric fibrosis. These patients were treated in our centre during the period 2001-2013. Electronic patient records were reviewed, and detailed information was collected regarding demographic and clinical characteristics, biochemical data and survival status (**Table 2.1**). Data were collected at baseline (diagnosis), although treatments given during the entire follow-up period were also recorded, given their impact on disease status and possible effect on overall survival.

Category of data	Specific information collected
Patient demographics	Age
	Sex
Clinical characteristics	Presenting symptoms
	Performance status
	Smoking history
	Medical comorbidities (including type)
	CHD
	Secondary malignancy
	Medical and surgical treatments relevant to the NET (including type)
	Hospital admissions related to fibrotic complications
	Survival status
Tumour characteristics	Tumour grade
	Extent of liver metastases
	Extra-hepatic metastases (including sites)
	Radiological severity of mesenteric desmoplasia
Biochemical data	Chromogranin A
	Urinary 5-HIAA

Table 2.1. Data collected for the first retrospective study of 147 patients with fibrotic SI NETs.

NETs were classified into histological grades 1-3 based on their mitotic count and proliferation index by performing immunohistochemistry using Ki67 antibody according to the WHO 2010 classification[117].

The extent of liver metastases was classified in 4 categories (absent, occupying <25%, 25-50% or >50% of the liver parenchyma). The assessment was performed by 2 radiologists (Dr Mohammed Khalifa and Dr Henry Walton).

The severity of mesenteric desmoplasia was graded as mild, moderate or severe using a classification system originally proposed by Pantongrag-Brown *et al*, which is based on the number and thickness of radiating fibrotic strands surrounding the mesenteric mass, as shown below:

Mild desmoplasia	<10 thin strands
Moderate desmoplasia	>10 thin strands or <10 thick strands
Severe desmoplasia	>10 thick strands

The assessment was performed by 2 radiologists independently (Dr Mohammed Khalifa and Dr Henry Walton) with a good interobserver variability (90% agreement) and consensus was achieved in cases of discrepancy.

The clinical, pathological, radiological and biochemical data collected were used as variables for the survival analysis. Non-parametric Kaplan-Meier techniques were used to estimate the median overall survival (OS) and associated 95% confidence intervals (CI). Semi-parametric Cox regression models were used to evaluate the association of these variables with OS in both univariate and multivariate analyses. We also assessed the relationship between the number of hospital admissions with fibrotic complications (bowel obstruction and mesenteric ischaemia) during the follow-up period and the severity of desmoplasia at diagnosis. A univariate quasi-poison generalised linear model was used for this statistical analysis. The relationship of desmoplasia severity and urinary 5-HIAA levels was assessed using a Fisher exact test. A p value <0.05 was considered statistically significant. The statistical analysis was performed by statistician Dr Martin Walker (Imperial College London).

2.2.2. Results

The patients' mean age was 60 ± 23 years and there was an equal representation of male and female patients (1:1). The median follow-up period was 82 months (range 2-300). A summary of the patient characteristics is provided in **Table 2.2**.

			N=147	(%)
Age	>65		53	(36)
	≤65		94	(64)
Sex	Male		75	(51)
	Female		72	(49)
Performance status	0-1		139	(95)
	2		8	(5)
Smoking	No		82	(56)
	Yes		35	(44)
Presenting symptom	Carcinoid syndrome	No	81	(55)
		Yes	64	(44)
	Non-specific symptoms	No	55	(37)
		Yes	90	(61)
	Incidental finding	No	129	(88)
		Yes	16	(11)
Tumour grade	1		73	(50)
	2		38	(26)
	3		1	(1)
	N/A		35	(24)
Carcinoid heart disease	No		127	(86)
	Yes		17	(12)
	N/A		3	(2)
Medical comorbidities	0-2		126	(86)
	>2		21	(14)
Secondary malignancy	No		122	(83)
	Yes		19	(13)
	N/A		6	(4)
Desmoplasia	Mild		35	(24)
	Moderate		52	(35)
	Severe		15	(10)
	N/A		45	(31)
Liver tumour burden	None		38	(26)
	<25%		53	(36)
	25-50%		14	(10)
	>50%		22	(15)
	N/A		20	(14)
Bone metastases	No		124	(84)
	Yes		23	(16)
Lung metastases	No		133	(90)
	Yes		12	(8)
	N/A		2	(1)
Other metastases	No		95	(65)
	Yes		51	(35)
	N/A		1	(1)
Chromogranin A	Normal		20	(14)
	<5 x ULN		42	(29)

	5-10 x ULN		27	(18)
	>10 x ULN		39	(27)
	N/A		19	(13)
Urine 5-HIAA	Normal		37	(25)
	<5 x ULN		39	(27)
	5-10 x ULN		25	(17)
	>10 x ULN		22	(15)
	N/A		24	(16)
Primary resection	No		68	(46)
	Yes		79	(54)
Type of surgery	**None**		46	(31)
	Bypass		22	(15)
		Ileo-ileal	13	
		Ileo-colonic	6	
		Gastro-enterostomy	1	
		Defunctioning jejunostomy	1	
		Defunctioning ileostomy	1	
	Resection		79	(54)
		Small bowel resection	38	
		Right hemicolectomy	41	
Somatostatin analogues			136	(93)
Interferon			11	(7)
Targeted radionuclide therapy			53	(36)
	I[131]MIBG		8	
	[90]Yttrium		27	
	[177]Lutetium		11	
	I[131]MIBG and [90]Yttrium		3	
	[90]Yttrium and [177]Lutetium		2	
	I[131]MIBG and [177]Lutetium		2	

Table 2.2. Patient characteristics in a cohort of 147 fibrotic SI NETs. (ULN: Upper limit of normal)

During the follow-up period most patients (77.5%) required at least one admission for management of abdominal complications, while about a third (30.5%) were admitted two or more times. Many of these patients underwent surgical interventions for their SI NETs during follow-up. 54% of cases underwent primary resection, 15% had a surgical bypass operation, while 31% did not require surgery. Of those patients who had primary resection, 72% had elective operations, while 28% needed emergency surgery either for bowel obstruction or mesenteric ischemia.

The median OS for this patient cohort was 8.7 years (95% CI 6.8, 9.9) (**Figure 2.1**)
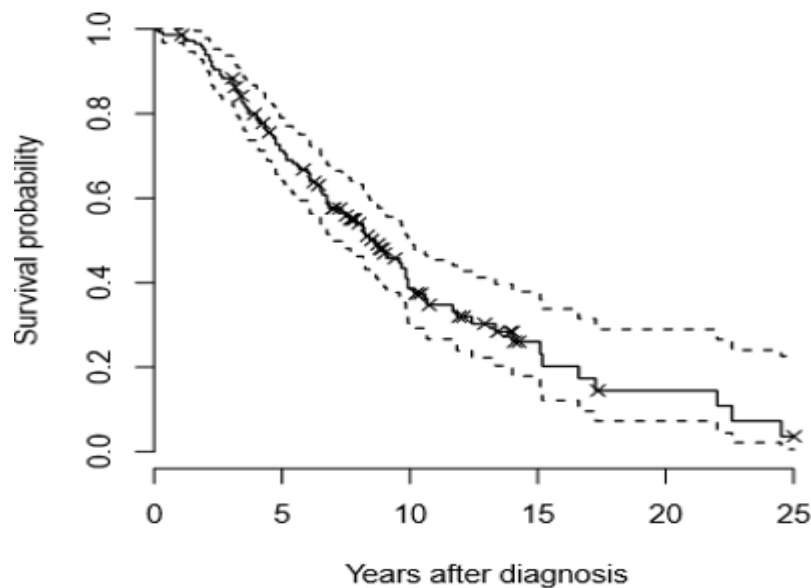
Figure 2.1. Kaplan-Meier curve demonstrating the OS in a cohort of 147 patients with fibrotic SI NETs

The univariate analysis showed that age>65, hepatic tumour burden>50%, CHD, chromogranin A (CgA) levels>10 times the upper limit of normal, and urinary 5-HIAA levels>5 times the upper limit of normal were associated with a significantly shorter OS. On the other hand, primary resection was associated with a significantly longer OS. The other clinical parameters showed no significant association with OS (**Table 2.3**).

Variable	Categories	Records	HR	95% CI	Pr(>|z|)
Age (years)[*]	(0,65]	94			NA
	(65,84]	53	3.03	(1.92, 4.79)	<0.0001
Sex	female	72			NA
	male	75	1.27	(0.84, 1.92)	0.25
Performance status	0	63			NA
	1	76	1.46	(0.93, 2.30)	0.10
	2	8	2.17	(0.95, 4.96)	0.06
Primary Resection[*]	no	68			NA
	yes	79	0.45	(0.29, 0.69)	0.0001
Type of Surgery[*]	none	46			NA
	primary resected	79	0.39	(0.24, 0.63)	<0.001
	bypass	22	0.68	(0.36, 1.28)	0.23
					(Cont'd)

Presenting symptoms (Carcinoid Syndrome)	no	81			NA
	yes	64	0.95	(0.62, 1.44)	0.80
Presenting symptoms at diagnosis (GI symptoms)	no	55			NA
	yes	90	0.96	(0.62, 1.47)	0.86
Presenting symptoms (Incidental diagnosis)	no	129			NA
	yes	16	0.89	(0.45, 1.78)	0.74
Smoking	no	82			NA
	yes	35	1.27	(0.76, 2.11)	0.36
Other Malignancy (secondary)	no	122			NA
	yes	19	1.56	(0.86, 2.83)	0.15
Liver Metastases*	none	38			NA
	<25%	53	1.18	(0.64, 2.19)	0.59
	25%-50%	14	1.62	(0.72, 3.65)	0.24
	>50%	22	3.25	(1.68, 6.30)	<0.001
Bone Metastases	no	124			NA
	yes	23	1.70	(0.99, 2.92)	0.05
Lung Metastases	no	133			NA
	yes	12	1.93	(0.96, 3.88)	0.07
Distant Metastases	no	95			NA
	yes	51	1.00	(0.65, 1.54)	0.99
Carcinoid Heart Disease*	no	127			NA
	yes	17	2.55	(1.44, 4.49)	0.001
Chromogranin A*	normal	20			NA
	<5 upper normal limit	42	1.09	(0.49, 2.44)	0.83
	5-10 upper normal limit	27	1.65	(0.72, 3.78)	0.23
	>10 upper normal limit	39	3.73	(1.75, 7.9)	0.0006
Urine 5-HIAA*	normal	37			NA
	<5 upper normal limit	39	1.73	(0.89, 3.33)	0.10
	5-10 upper normal limit	25	2.31	(1.13, 4.71)	0.02
	>10 upper normal limit	22	5.74	(2.82, 11.68)	<0.0001
Somatostatin analogues	no	11			NA
	yes	136	0.96	(0.42, 2.21)	0.93
Interferon	no	136			NA
	yes	11	1.14	(0.59, 2.20)	0.71
Radionuclide therapy	no	94			NA
	yes	53	0.94	(0.62, 1.44)	0.78
Tumour Grade	1	73			NA
	2	38	1.45	(0.88, 2.40)	0.14
	3	1	NA	NA	NA
Number of Admissions during follow-up	[0,2)	102			NA
	[2,10]	45	1.46	(0.96, 2.23)	0.08
Number of medical comorbidities	[0,2]	126			NA
	(2,5]	21	0.75	(0.39, 1.41)	0.37

Table 2.3. Univariate analysis of predictors of OS in 147 patients with fibrotic SI NETs (*p<0.05)

33

Kaplan-Meier curves showing the survival probability of patients with fibrotic SI NETs stratified by variables identified as significant by univariate analysis are shown in **Figure 2.2**.
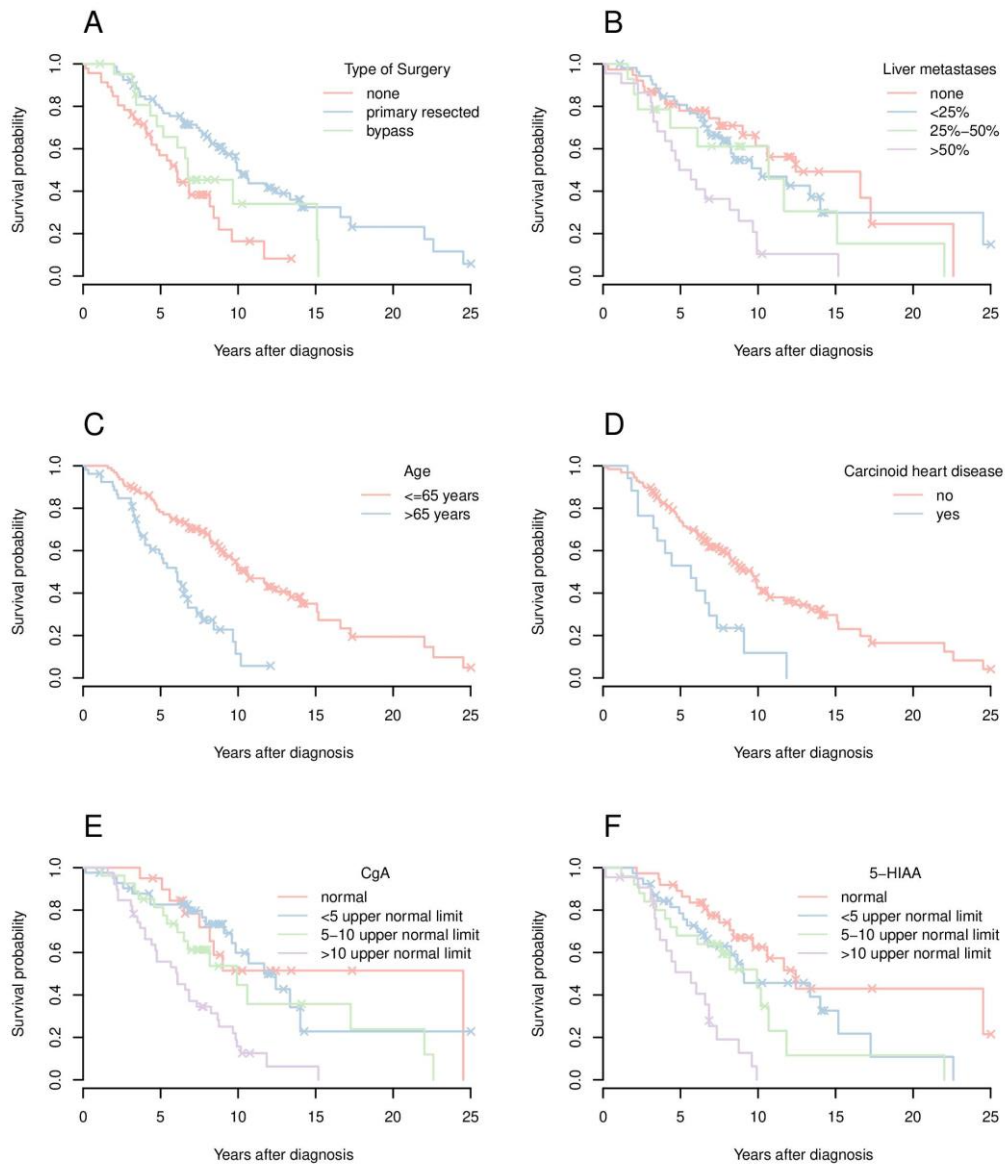
Figure 2.2. Kaplan-Meier curves stratified by clinical and biochemical variables that showed a statistically significant association (p<0.05) with OS (by univariate analysis) in desmoplastic SI NETs.

The multivariate analysis showed that only age>65 and urinary 5-HIAA levels>10 times the upper limit of normal remained statistically significant and predictive of a shorter OS (**Table 2.4**).

Variable	HR	95% CI	*p*
Primary resection	0.54	(0.26, 1.11)	0.09
Bypass surgery	0.86	(0.32, 2.30)	0.77
Carcinoid heart disease	0.93	(0.35, 2.46)	0.88
CgA <5 times ULN	1.02	(0.34, 3.02)	0.98
CgA 5-10 times ULN	1.05	(0.30, 3.64)	0.94
CgA >10 times ULN	1.36	(0.39, 4.76)	0.63
Urine 5-HIAA <5 times ULN	1.47	(0.57, 3.77)	0.42
Urine 5-HIAA 5-10 times ULN	1.95	(0.66, 5.82)	0.23
Urine 5-HIAA >10 times ULN[*]	5.82	(1.74, 19.42)	0.004
Volume of liver metastases <50%	1.10	(0.51, 2.41)	0.80
Volume of liver metastases >50%	1.31	(0.46, 3.75)	0.61
Age >65[*]	4.89	(2.53, 9.45)	<0.0001

Table 2.4. Multivariate analysis of factors associated with OS in 147 fibrotic SI NETs (*p<0.05).

The severity of desmoplasia did not affect OS at a statistically significant level (**Figure 2.3a**) and did not correlate with the number or annual frequency of hospital admissions during the follow-up period (**Figures 2.3b and 2.3c**).
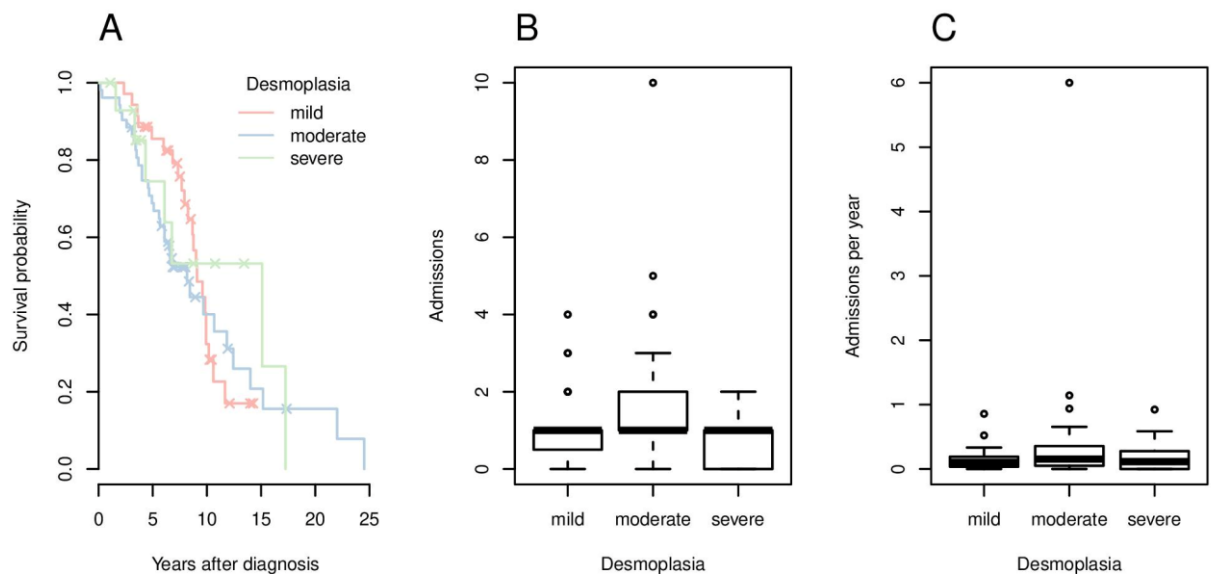
Figure 2.3. Kaplan-Meier curves demonstrating the OS of patients with fibrotic SI NETs stratified according to the severity of desmoplasia (A). Number (B) and annual frequency (C) of hospital admissions with abdominal complications during follow-up in patients with mild, moderate and severe desmoplasia.

There was no significant association between the desmoplasia severity and urinary 5-HIAA levels (p=0.64), but there was a positive association between the severity of fibrosis and hepatic tumour burden (p=0.017), suggesting that patients with extensive desmoplasia had more advanced metastatic disease in the liver.

2.3. Second retrospective study: Metastatic midgut NETs

Although the *severity* of mesenteric desmoplasia did not seem to significantly affect OS or other clinical outcomes in patients with fibrotic SI NETs, we were interested to assess whether the *presence* of mesenteric fibrosis was associated with a shorter OS. We therefore evaluated a large cohort of 387 patients with SI NETs with and without mesenteric fibrosis. In order to limit patient heterogeneity (which was shown to be a significant limitation in previous studies involving SI NETs), we selected patients with the same stage of disease (stage IV).

2.3.1. Methods

This retrospective study included 387 patients with metastatic (stage IV) SI NETs treated in our centre from 2000-2014. Demographic, clinical and biochemical data were collected using electronic patient records and the specific information for each data category is provided in **Table 2.5**.

Category of data	Specific information collected
Patient demographics	Age
	Sex
Clinical data	Presenting symptoms
	Symptom duration before diagnosis
	Medical comorbidities
	Secondary malignancy
	CHD
	Medical and surgical therapies relevant to NET
	Survival status
Tumour characteristics	Grade
	Extent of liver disease
	Extrahepatic metastases (including site)
	Locoregional lymph node metastases
	Desmoplasia
Biochemical data	CgA
	Urinary 5-HIAA

Table 2.5. Data collected for a cohort of 387 patients with metastatic SI NETs

SI NETs were histologically graded (grade 1-3) using the WHO 2010 classification[117]. The extent of the liver disease was evaluated by 3 radiologists (Dr Lee Grant, Dr Anthie Papadopoulou and Dr Lorna Woodbridge) based on the volume of liver parenchyma replaced by tumour (no liver disease, <25%, 25-50% or >50%). Interobserver variability was not assessed in this study, and the extent of liver disease volume reported by each specialist radiologist was used for the analysis. The presence of mesenteric desmoplasia was also assessed radiologically. The presence of a mesenteric mass with surrounding fibrotic strands and a typical 'spoke-wheel' appearance was considered pathognomonic.

These clinical, radiological and biochemical parameters were used as variables for the survival analysis of this large patient cohort of 387 metastatic SI NETs. Non-parametric Kaplan-Meier techniques were used to estimate the median OS and 95% CI both overall and *in strata* defined by the exploratory variables described earlier. A semi-parametric Cox regression model was used to identify (in a univariate fashion) statistically significant predictors of survival (using a Bonferroni correction for multiple testing). A multivariate Cox regression model was fitted to a subset of subjects with complete data for variables identified as statistically significant at univariate analysis. In addition, we evaluated the association of mesenteric fibrosis with CHD. The association of urinary 5-HIAA levels with both CHD and mesenteric fibrosis was also assessed. A Fisher's exact test was used to evaluate these associations. A p value<0.05 was considered statistically significant. The statistical analysis was performed by statistician Dr Martin Walker (Imperial College London).

2.3.1. Results

Patients in this cohort had a mean age (±SD) of 60 (±12) years and there was a balanced representation of male and female sex (1.2:1). The median follow-up period was 62.9 months (range 2.4-348). The majority (94.5%) of patients had liver metastases. Mesenteric lymphadenopathy was present in 64.6% of cases, and approximately half of those patients (54%) had mesenteric desmoplasia.

A summary of patient baseline characteristics is provided in **Table 2.6**.

Characteristic	Category	N	%
Age	<65	228	59
	≥65	159	41
Sex	Female	179	46
	Male	208	54
Onset of symptoms prior to diagnosis	No symptoms	38	10
	<12 months	116	30
	12-36 months	56	14
	>36 months	103	27
	N/A	74	19
Presenting symptoms	Incidental diagnosis	38	10
	Abdominal symptoms	140	36
	Carcinoid syndrome	63	16
	Carcinoid syndrome and abdominal symptoms	94	24
	N/A	52	13
Tumour grade	1	201	52
	2	127	33
	3	6	2
	N/A	53	14
Liver tumour burden	None	21	5
	<25%	96	25
	25-50%	26	7
	>50%	45	12
	N/A	199	51
Carcinoid heart disease	No	326	84
	Yes	61	16
Mesenteric lymphadenopathy	No	137	35
	Present without desmoplasia	114	29
	Present with desmoplasia	136	35
Bone metastases	No	335	87
	Yes	52	13
Lung metastases	No	365	94
	Yes	22	6
Other distant metastases	No	373	96
	Yes	14	4
Medical co-morbidities	Diabetes mellitus	33	9
	Hypertension	114	29
	Ischaemic heart disease	22	6
	Chronic renal failure	9	2
	Congestive cardiac failure	8	2
Secondary malignancy	Gastrointestinal	6	2
	Breast	13	3
	Prostate	9	2
	Gynaecological	5	1
	Other	5	1
Chromogranin A	Normal	52	13
	<5 x ULN	83	21
	5-10 x ULN	63	16
	>10 x ULN	105	27
	N/A	84	22
Urinary 5-HIAA levels	Normal	58	15
	<5 x ULN	90	23
	5-10 x ULN	38	10
	>10 x ULN	64	17
	N/A	137	35

Table 2.6. Patient baseline characteristics in a cohort of 387 metastatic midgut NETs. (ULN:

Upper limit of normal)

Patients in this cohort of advanced SI NETs received a wide range of medical and surgical treatments, which are summarised in **Table 2.7**. All patients were commenced on somatostatin analogues at baseline and upon progression, treatment escalation to peptide receptor radionuclide therapy (PRRT) was the usual choice (40%). Surgical resection of the primary tumour (and mesenteric mass, if present) was performed within 6 months of diagnosis in 45% of cases (of which, 58% elective, 26% emergency, 16% unknown), while 5% had a surgical bypass and the remaining 50% did not have any surgical intervention at baseline (i.e. within 6 months of diagnosis). A small proportion of patients had surgery during the follow-up period (>6 months after diagnosis).

Treatment		N	%
Systemic therapies	Somatostatin analogues	387	100
	Interferon	26	7
	PRRT	153	40
	^{131}I-MIBG	37	10
	Chemotherapy	39	10
Surgical intervention	Primary resection within 6 months of diagnosis	173	45
	➢ Elective	100	26
	o Curative intent	48	12
	o Palliative (symptomatic)	31	8
	o Palliative (prophylactic)	13	3
	o Incidental finding	2	1
	o N/A	6	2
	➢ Emergency	45	12
	o Bowel obstruction	30	8
	o Perforation	7	2
	o Mesenteric ischaemia	8	2
	➢ N/A	28	7
	❖ Small bowel resection	79	20
	❖ Right hemicolectomy	77	20
	❖ N/A	17	4
	Surgical bypass within 6 months of diagnosis	18	5
	Primary resection at follow-up (>6 months after diagnosis)	23	6
	Surgical bypass at follow-up	4	1
	Liver resection at follow-up	13	3
Transarterial embolization		41	11

Table 2.7. Treatments during the follow-up of 387 patients with metastatic SI NETs.

The median OS in this patient cohort was 101 months (95% CI 84, 118) (**Figure 2.4**).
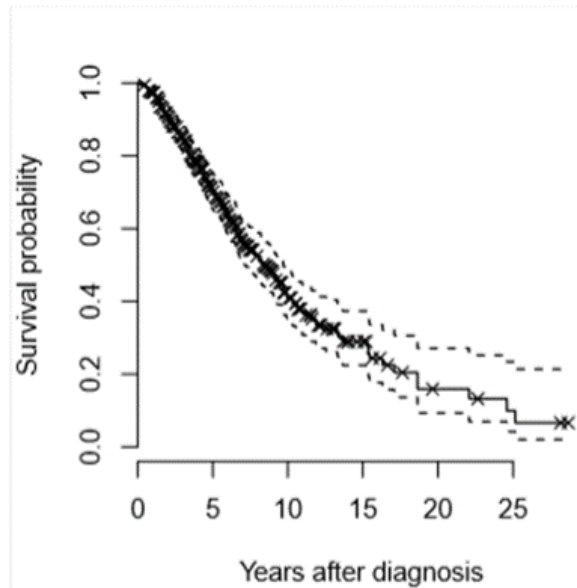
Figure 2.4. Kaplan-Meier curve demonstrating the overall survival in a cohort of 387 patients with metastatic SI NETs.

The univariate analysis (after application of the Bonferroni correction for multiple testing) showed that the following parameters were associated with shorter OS at a statistically significant level: age>65, hepatic tumour burden>50%, mesenteric lymphadenopathy with and without associated desmoplasia, bone metastases, CHD, CgA levels>5 times the upper limit of normal, urinary 5-HIAA levels>5 times the upper limit of normal and grade 2 and 3 tumours. On the other hand, primary resection at baseline was predictive of a longer OS. Other clinical variables were not associated with OS ($p \geq 0.05$). The results of the univariate analysis are shown in **Table 2.8**.

Variable	Category	Records	HR	95% CI	P value	P adj[*]
Age	<65	228				
	≥65	159	2.23	1.93, 2.53	<0.001	<0.001[+]
Sex	Female	179				
	Male	208	1.01	0.72, 1.30	0.96	1
Onset of symptoms prior to diagnosis	No symptoms	38				
	<12 months	116	1.89	1.29, 2.51	0.04	1
	12-36 months	56	2.08	1.42, 2.75	0.03	1
	>36 months	103	1.71	1.09, 2.33	0.09	1
Presenting symptoms	Incidental diagnosis	38				
	Abdominal symptoms	140	1.66	1.06, 2.26	0.09	1
	Carcinoid syndrome	63	1.74	1.09, 2.39	0.09	1
	Carcinoid syndrome and abdominal symptoms	94	1.89	1.27, 2.50	0.04	1
Tumour grade	1	201				
	2	127	2.55	2.22, 2.88	<0.001	<0.001[+]
	3	6	11.43	10.49, 12.37	<0.001	<0.001[+]
Liver tumour burden	None	21				
	<25%	96	1.99	1.05, 2.93	0.15	
	25-50%	26	1.54	0.41, 2.66	0.45	
	>50%	45	5.03	4.07, 5.99	<0.001	0.001[+]
Carcinoid heart disease	No	326				
	Yes	61	1.85	1.49, 2.21	0.001	0.03[+]
Mesenteric lymphadenopathy	No	137				
	Present without desmoplasia	114	1.84	1.43, 2.24	0.003	0.04[+]
	Present with desmoplasia	136	1.75	1.42, 2.09	0.001	0.04[+]
Bone metastases	No	335				
	Yes	52	1.97	1.56, 2.37	0.001	0.03[+]
Lung metastases	No	365				
	Yes	22	1.28	0.63, 1.92	0.45	1
Other distant metastases	No	373				
	Yes	14	1.63	1.02, 2.39	0.12	1
Diabetes mellitus	No	353				
	Yes	33	0.69	0.05, 1.33	0.25	1
Hypertension	No	272				
	Yes	114	0.88	0.56, 1.21	0.45	1
Ischaemic heart disease	No	364				

	Yes	22	1.51	0.91, 2.11	0.18	1
Chronic renal failure	No	377				
	Yes	9	0.57	-0.57, 1.71	0.34	1
Congestive cardiac failure	No	378				
	Yes	8	1.26	0.44, 2.07	0.58	1
Secondary malignancy						
➤ **Gastrointestinal**	No	381				
	Yes	6	1.13	-0.01, 2.28	0.83	1
➤ **Breast**	No	374				
	Yes	13	1.21	0.45, 1.96	0.63	1
➤ **Prostate**	No	378				
	Yes	9	0.54	-0.61, 1.68	0.28	1
➤ **Gynaecological**	No	382				
	Yes	5	1.05	-0.34, 2.45	0.94	1
➤ **Other**	No	382				
	Yes	5	1.05	-0.34, 2.45	0.94	1
Chromogranin A	Normal	52				
	<5 x ULN	83	1.19	0.60, 1.77	0.57	
	5-10 x ULN	63	1.93	1.34, 2.52	0.03	
	>10 x ULN	105	3.61	3.09, 4.12	<0.001	<0.001[+]
Urinary 5-HIAA levels	Normal	58				
	<5 x ULN	90	0.89	0.37, 1.41	0.67	
	5-10 x ULN	38	1.84	1.26, 2.42	0.04	
	>10 x ULN	64	2.41	1.92, 2.89	<0.001	<0.001[+]
Surgical intervention at baseline (within 6 months of diagnosis)	None	196				
	Primary resection	173	0.44	0.13, 0.76	<0.001	<0.001[+]
	Surgical bypass	18	0.87	0.25, 1.49	0.67	

Table 2.8. Univariate analysis of predictors of overall survival in 387 patients with metastatic SI NETs. Adjusted p-values (Bonferroni correction for multiple testing) are indicated in the relevant column.

Kaplan-Meier curves of the OS of patients with metastatic SI NETs stratified by variables identified as statistically significant by univariate analysis are shown in **Figure 2.5**.
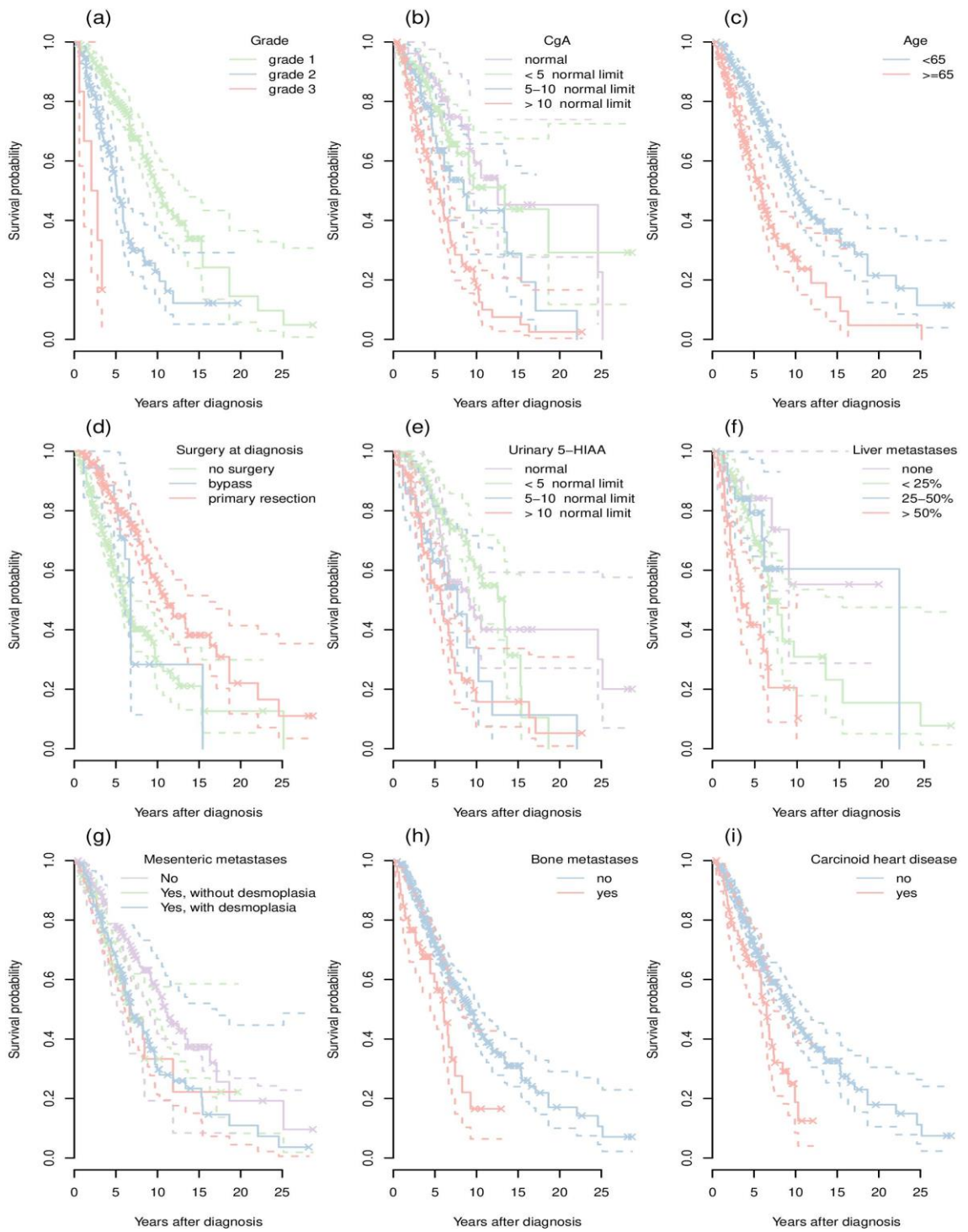
Figure 2.5. Kaplan-Meier curves of OS in 387 patients with metastatic SI NETs stratified by factors identified as statistically significant by univariate analysis (having applied a Bonferroni correction for multiple testing).

The multivariate analysis showed that the following variables were associated with a statistically significantly shorter OS: age>65, mesenteric metastases with and without desmoplasia, presence of liver metastases and bone metastases, while CHD showed a trend towards significance. Primary resection was associated with a longer OS (**Table 2.9**). Further analysis of this result based on patient symptomatology showed that the benefit of surgical resection was limited to symptomatic patients, while those who were diagnosed incidentally did not demonstrate a significant survival benefit with surgery compared to conservative management (median OS [95% CI] 12.1 years [9.34, 14.9] versus 9.67 years [2.3, 17.0], log-rank test, p=0.25).

Variable	Category	HR	95% CI	p-value
Age	≥65	1.98	1.46, 2.68	<0.001
Surgery	Primary resection	0.51	0.37, 0.70	<0.001
	Surgical bypass	0.79	0.41, 1.53	0.487
Presence of liver metastases		2.49	1.01, 6.15	0.048
Mesenteric lymphadenopathy	With desmoplasia	1.83	1.29, 2.60	0.001
	Without desmoplasia	1.84	1.21, 2.79	0.004
Bone metastases		1.54	1.01, 2.34	0.045
CHD		1.46	0.99, 2.13	0.052

Table 2.9. Multivariate analysis of predictors of OS in 387 patients with metastatic SI NETs. The presence of mesenteric lymphadenopathy with a desmoplastic reaction was an adverse factor associated with a hazard ratio (HR) of 1.83 which was highly significant (p=0.001).

Next, we assessed the relationship of 5-HIAA with fibrotic complications of neuroendocrine neoplasia (CHD and mesenteric fibrosis). As expected, there was a strong relationship with CHD (p<0.001) (**Table 2.10a**). In addition, there was a positive (but less potent) association with mesenteric fibrosis (p=0.02) (**Table 2.10b**). However, there was no significant correlation between CHD and mesenteric fibrosis (p=0.72) (**Table 2.10c**).

a. Association of CHD with urinary 5-HIAA levels (Fisher's exact test, $p<0.001$)

Urinary 5-HIAA levels	No CHD	CHD	N
Normal	57	1	58
<5 ULN	84	6	90
5-10 ULN	31	7	38
>10 ULN	41	23	64
TOTAL	213	37	250

b. Association of mesenteric fibrosis with urinary 5-HIAA levels (Fisher's exact test, $p=0.02$)

Urinary 5-HIAA levels	No mesenteric lymphadenopathy	Mesenteric lymphadenopathy without desmoplasia	Mesenteric lymphadenopathy with desmoplasia	N
Normal	20	18	20	90
<5 ULN	30	18	42	64
5-10 ULN	4	13	21	38
>10 ULN	22	23	19	58
TOTAL	76	72	102	250

c. Association of CHD with mesenteric fibrosis (Fisher's exact test, $p=0.72$)

Mesenteric lymphadenopathy	No CHD	CHD	N
None	113	24	137
Present without desmoplasia	96	18	114
Present with desmoplasia	117	19	136
TOTAL	326	61	387

Table 2.10. Association of CHD (a) and mesenteric fibrosis (b) with urinary 5-HIAA levels in a large institutional series of metastatic SI NETs. The correlation of mesenteric desmoplasia with the presence of CHD is also shown (c). (ULN: Upper limit of normal, CHD: Carcinoid heart disease)

2.4. Discussion

There is limited literature regarding the epidemiology and clinical outcomes associated with mesenteric fibrosis in midgut neuroendocrine tumours. As mentioned earlier, this is due to the lack of information about the radiological presence of fibrosis in cancer registries, and the fact that most previous retrospective studies of SI NETs do not make a distinction between fibrotic and non-fibrotic patients. Our data and those of others[7,118] suggest that the presence of mesenteric fibrosis is associated with worse clinical outcomes, and in our metastatic SI NET cohort a shorter OS. However, the severity of mesenteric fibrosis (graded radiologically) did not appear to affect OS or the likelihood of abdominal complications in fibrotic SI NETs. This may be because the amount of fibrosis *per se* is not a crucial factor, and perhaps the location of the mesenteric mass (in relation to other vital structures, such as small bowel loops and mesenteric vessels) is more important for the development of complications and the effect on survival. The impact of mesenteric fibrosis on overall survival mainly reflected disease-specific survival, since the cause of death was related to the tumour in at least 70% of cases (predominantly related to disease progression and severe CHD). This is in keeping with the literature which suggests that the principal cause of death in patients with advanced SI NETs is disease-related, usually due to CHD or cachexia due to disease progression or mesenteric-intestinal involvement[4]. Therefore, although a minority of patients will die of local complications (e.g. bowel obstruction or perforation), mesenteric fibrosis may also be a (previously unrecognised) risk factor for disease progression, which was the cause of death in most of our patients with advanced SI NETs. The mechanisms through which mesenteric fibrosis could contribute to cancer progression are currently unclear, but we believe that the liaison of cancer cells with fibroblasts within the fibrotic microenvironment may promote cancer cell invasion, migration and metastasis. This phenomenon is known to exist in other cancer types[19] and is supported by our experimental work (**Chapter 4**). Interestingly, another study from Germany also showed that desmoplastic SI NETs were a more aggressive patient cohort (compared to non-fibrotic tumours) with a higher prevalence of distant metastases and a significantly shorter progression-free survival[118]. This is perhaps not surprising, since the presence of desmoplasia is a known risk factor for cancer progression in many cancers[18], and not simply an association with cancer, because this is supported by functional studies of tumour-

stromal interactions[19]. Certainly, a better understanding of this phenomenon is needed in neuroendocrine neoplasia. Several studies have assessed the effect of mesenteric lymphadenopathy on OS, without specifically evaluating the presence of desmoplasia. Hellman *et al* showed that the presence of pathological lymph nodes in the mesentery was linked to shorter OS and this effect was independent of the presence of liver disease[13]. Similarly, Landry *et al* demonstrated that more aggressive lymphadenectomy was associated with better OS in midgut NETs[119].

Primary tumour resection (with en block resection of the mesenteric mass, if present) was associated with a significantly longer OS in our metastatic SI NET cohort, but the benefit of resection was limited to symptomatic patients. Although there is certainly a potential surgical bias in retrospective analyses, a relatively recent systematic review of studies assessing the effect of primary resection in midgut NETs with unresectable liver metastases concluded that there was a trend towards better OS in the surgical group. Similar to our data, another study from Uppsala showed that prophylactic primary resection in stage IV SI NETs conferred no survival benefit in asymptomatic patients[120]. The ENETS guidelines also suggest that primary resection in the setting of metastatic disease should be reserved for symptomatic patients, while in asymptomatic cases an individualised multidisciplinary approach is essential[121].

Another interesting finding was that the prevalence of desmoplasia (by radiological detection) in our metastatic SI NET cohort was 35%. This is in keeping with other studies[6,12], although the evaluation of mesenteric fibrosis by standard cross-sectional imaging is problematic and does not always correlate with the histological assessment of fibrosis[8]. Our observations from the multidimensional assessment of mesenteric desmoplasia that we performed prospectively in 34 surgically-resected SI NETs (**Chapter 4**) revealed several discrepancies between the radiological detection of mesenteric fibrosis and the surgical and histopathological findings, indicating that radiology often underestimates the true prevalence of fibrosis.

The role of circulating serotonin in the development of mesenteric fibrosis is also an area of controversy. In our metastatic SI NET cohort there was a positive association between urinary 5-HIAA levels and mesenteric fibrosis, although this was less potent than the (known) association of urinary 5-HIAA and CHD. This suggests that other factors apart from serotonin are likely to be involved in the pathogenesis of mesenteric

desmoplasia and clearly several other factors are known to be implicated in this process (such as TGFß and CTGF)[9]. In our cohort of fibrotic SI NETs we did not find a significant association between the severity of desmoplasia and urinary 5-HIAA levels, which again suggests that other molecules are responsible for the progression of fibrosis. Clearly, a better understanding of the pathways leading to fibrosis is needed, including the role of possible changes in serotonin metabolism at a local level in the mesentery. Other studies have also evaluated the association of urinary 5-HIAA levels and a significant link has been shown in some[12,71], but not all[6] the studies. In addition, the presence of significantly elevated urinary 5-HIAA levels appeared to be associated with a significantly shorter OS in our cohort of fibrotic SI NETs and this was independent of other factors (such as CHD). The mechanisms through which elevated serotonin can affect OS remain elusive, but perhaps it is a risk factor for disease progression given the known mitogenic properties of serotonin on neuroendocrine tumour cells[64,122]. Interestingly, another study of SI NETs also demonstrated that elevated urinary 5-HIAA levels were associated with poor prognosis by multivariate analysis[123].

Finally, the association of mesenteric fibrosis with other carcinoid-related fibrotic complications, and particularly CHD, has not been evaluated in other studies. Our data showed that these two fibrotic complications of SI NETs do not usually co-exist, which suggests that the pathophysiology of these fibrotic conditions is substantially different. This is perhaps not surprising because the microenvironment of the mesentery and the heart valves is completely different and certainly the most significant distinction between the two conditions is the presence of cancer cells in the mesenteric microenvironment which can directly interact with other stromal cells that are in close proximity. In contrast, the fibrosis in the heart valves is driven mainly by fibroblasts stimulated by tumour-derived circulating factors, of which serotonin seems to be the most important, since it can stimulate cell proliferation and collagen synthesis in fibroblasts, although other factors such as TGFβ are also known to play a role[124]. Unfortunately, the pathophysiology of CHD remains largely unknown and further research would be needed to understand the differences in the underlying mechanisms between mesenteric and cardiac fibrogenesis, which would account for our observation that these conditions do not usually co-exist.

In conclusion, these retrospective studies from our centre have provided useful epidemiological information about mesenteric fibrosis in midgut NETs both in terms of its prevalence, and its effect on OS and other clinical outcomes. However, we clearly need to gain a better understanding of the pathophysiology of mesenteric desmoplasia, and in particular the pathways of disease development, as well as the role of local serotonin in this process. The pathogenesis of CHD appears to be different and probably less complex, but requires also investigation in separate, appropriately designed studies. In the following two chapters we will focus on the pathophysiology of mesenteric fibrosis by evaluating the functional interaction of neuroendocrine tumour cell lines with stromal cells (**Chapter 3**), as well as changes in gene and protein expression in fibrotic and non-fibrotic midgut NETs (**Chapter 4**).

Chapter 3

Investigation of the pathophysiology of mesenteric fibrosis in midgut neuroendocrine tumours using an *in vitro* model of the fibrotic mesenteric microenvironment

3. Investigation of the pathophysiology of mesenteric fibrosis in midgut neuroendocrine tumours using an *in vitro* model of the fibrotic mesenteric microenvironment

3.1. Introduction

As described in Chapter 1, only a small number of studies have included functional assessments of the mesenteric fibrotic microenvironment and as a result the complex, dynamic processes that underlie the pathophysiology of fibrosis in SI NETs remain elusive. The lack of progress in elucidating the mechanisms of mesenteric fibrogenesis is also due to significant limitations of previous studies. These include, for example, the use of models that are not representative of the mesenteric microenvironment, such as the use of the BON-1 cell line (which is of pancreatic origin and therefore not representative of an enterochromaffin cell line[125]) or AKR-2B (mouse) fibroblasts (not of human origin) to investigate the paracrine effect in the work of Beauchamp and colleagues[126]. Other studies have used appropriate models of the mesenteric microenvironment, but are limited by the investigation of only a small number of factors (such as CTGF), rather than assessing entire pathways of disease[21,22], which would have contributed to a better understanding of the underlying pathophysiology. The investigation of pathways of disease is of paramount importance in a complicated process, such as fibrosis, where multiple factors are involved, often with significant cross-talk between different pathways[9]. Therefore, the development of antifibrotic therapies would require a deep understanding of these complex interactions, as targeting a single factor (such as CTGF) is unlikely to be effective.

In our *in vitro* study of the mesenteric tumour microenvironment we aimed to investigate the crosstalk of human SI NET cell lines (KRJ-I and P-STS) with a human stromal cell line (HEK293). This required a collaboration with the University of Graz, Austria (Prof Roswitha Pfragner), as the KRJ-I and P-STS cell lines were not widely available and could be used only in the institution in which they were developed. A Mutual Transfer Agreement was signed in December 2017, in order to allow us access to P-STS/KRJ-I cell derivatives (RNA/cell culture supernatants) and their analysis was performed in our laboratory (Institute for Liver and Digestive Health, UCL). These cancer cell lines were established from small bowel carcinoids and are a suitable

enterochromaffin model[127,128]. The HEK293 cell line is a stromal cell line of human origin. Despite being one of the most commonly used cell lines in cell biology studies, its precise origin is still debated, but they have been used as a fibroblast model in several studies[129], including a recent study by Svedja and colleagues, that investigated the cross-talk of HEK293 with KRJ-I cells in a Transwell system[21].

Before embarking on this study, we performed a preliminary set of experiments in our laboratory using BON-1 cells (as a NET cell line) and assessed their crosstalk with HEK293 cells. Although this model was not representative of the SI NET microenvironment (since BON-1 is a pancreatic neuroendocrine tumour cell line), these experiments were important to optimise several aspects of the co-culture system prior to our collaboration with the University of Graz and to demonstrate the feasibility of this study. These experiments will also be described in this section, although they served mainly as a pilot study prior to using a more appropriate *in vitro* model of the mesenteric microenvironment.

3.2. Materials and methods

3.2.1. Investigation of the crosstalk between BON-1 and HEK293 cells

Preliminary co-culture experiments were performed using the pancreatic neuroendocrine tumour cell line BON-1 and the fibroblastic cell line HEK293 and changes in gene expression (single gene expression), cell proliferation and metabolism were assessed.

The BON-1 cell line was a kind gift from Prof Tim Meyer, UCL Cancer Institute and the HEK293 cell line was a kind gift from Dr Alan Holmes, Division of Medicine, UCL.

Conditioned media of both cell types (BON-1 and HEK293) were initially collected. Briefly, cells were plated in Petridishes (10cm) at a cell density of 2 million cells per dish using 8 ml of complete medium (Dulbecco's Modified Eagle Medium [DMEM] supplemented with 10% of Fetal Bovine Serum [FBS] and 1% pen-strep) (day 1). After 24h cells were washed twice with 8ml of HBSS (without Ca/Mg) and serum starved with 8ml of serum free medium (DMEM supplemented with 0.5% FBS and 1% pen-strep) (day 2). 48 h later the conditioned media of both cell types were

collected in 15ml falcon tubes and centrifuged at 1500rpm for 8 minutes. Supernatants were then transferred into new 15 ml falcon tubes and stored at -20ºC (day 4).

To assess **changes in gene expression**, cells were plated in 6-well plates at a cell density of 500,000 cells/well using 2ml of complete medium per well (day 1). After 24h (day 2), cells in rows 2 & 3 (see **Figure 3.1**) were washed twice with HBSS and serum starved (using 2 ml of serum free medium per well). 24h later (day 3) the culture media from the third row of cells were removed and 2 mls of conditioned media of the other cell type were added (e.g. HEK293 conditioned media were added on BON-1 cells and vice versa). 48h later (day 5), RNA was extracted from the cells using the RNAeasy Mini Kit (Qiagen®) and changes in gene expression were assessed.

ROW 1	BON-1 (CM)	BON-1 (CM)	BON-1 (CM)
ROW 2	BON-1 (SFM)	BON-1 (SFM)	BON-1 (SFM)
ROW 3	BON-1 (CondM)	BON-1 (CondM)	BON-1 (CondM)

ROW 1	HEK293 (CM)	HEK293 (CM)	HEK293 (CM)
ROW 2	HEK293 (SFM)	HEK293 (SFM)	HEK293 (SFM)
ROW 3	HEK293 (CondM)	HEK293 (CondM)	HEK293 (CondM)

Figure 3.1: Experimental design to investigate changes in gene expression occurring due to the crosstalk between neuroendocrine tumour cells (BON-1) and stromal cells (HEK293). Each row of cells has 3 biological repeats representing the same experimental condition. CM: Complete medium, SFM: Serum Free Medium, CondM: Conditioned medium of the other cell line (e.g. Conditioned medium of stromal cells added to cancer cells)

Changes in cell proliferation were assessed using the BrdU ELISA assay. This assay detects 5-bromo-2'-deoxyuridine (BrdU) incorporated into cellular DNA during cell proliferation using an anti-BrdU antibody. When cells are cultured with labelling medium that contains BrdU, this pyrimidine analog is incorporated in place of thymidine into the newly synthesized DNA of proliferating cells. After removing labelling medium, cells are fixed and the DNA is denatured with a fixing/denaturing solution. Then a BrdU mouse monoclonal antibody (detection antibody) is added to

detect incorporated BrdU. An anti-mouse IgG, HRP (Horseradish peroxidase)-linked antibody is then used to recognise the bound detection antibody. HRP substrate TMB (tetra-methylbenzidine) is added to develop colour. The magnitude of the absorbance for the developed colour is proportional to the quantity of BrdU incorporated into cells, which is a direct indication of cell proliferation.

To measure changes in cell proliferation, BON-1 and HEK293 cells were plated in 96-well plates at a density of 20,000 cells/well using 200 µl of complete medium per well (day 1). After 24h, cells in columns 2 and 3 (see **Figure 3.2**) were washed once with 200 µl of HBSS and then 200 µl of serum free medium was added in each well (day 2). After a further 24h, all media were removed, cells were washed once with HBSS and media changed (200 µl of complete medium/well were added in column 1, 200 µl of serum free medium/well in column 2, and 200 µl of conditioned medium of the other cell line were added in column 3 (e.g. HEK 293 conditioned media were added to BON-1 cells). In addition, 20 µl of BrdU were added in each well. After 24h, changes in cell proliferation were measured using the cell proliferation ELISA assay, BrdU (colorimetric assay) and changes in absorbance were read at 370nm (day 4).

COLUMN 1	COLUMN 2	COLUMN 3	COLUMN 1	COLUMN 2	COLUMN 3	
BON-1 (CM)	BON-1 (SFM)	BON-1 (CondM)	HEK (CM)	HEK (SFM)	HEK (CondM)	BLANK
BON-1 (CM)	BON-1 (SFM)	BON-1 (CondM)	HEK (CM)	HEK (SFM)	HEK (CondM)	BLANK
BON-1 (CM)	BON-1 (SFM)	BON-1 (CondM)	HEK (CM)	HEK (SFM)	HEK (CondM)	BLANK
BON-1 (CM)	BON-1 (SFM)	BON-1 (CondM)	HEK (CM)	HEK (SFM)	HEK (CondM)	BLANK

Figure 3.2: Experimental design to investigate changes in cell proliferation occurring due to the crosstalk between neuroendocrine tumour cells (BON-1) and stromal cells (HEK293). Columns 1-3 represent different experimental conditions with 4 biological repeats for each condition. CM: Complete Medium, SFM: Serum-Free Medium, CondM: Conditioned medium of the other cell line (e.g. HEK 293 conditioned media added on BON-1 cells).

Changes in cell metabolism were measured using the MTT assay. This assay is based on the conversion of water soluble MTT (3-(4,5-dimethylthiazol-2-yl)-2,5-diphenyltetrazolium bromide) compound to an insoluble formazan product. Viable

cells with active metabolism convert MTT into formazan (mitochondrial dehydrogenases of viable cells cleave the tetrazolium ring, which results in reduction of MTT to insoluble formazan crystals). Dead cells, on the other hand, lose this ability and therefore show no signal. Thus, colour formation serves as a useful marker of only the viable cells. The measured absorbance at 590nm is therefore proportional to the number of viable cells.

To measure changes in cell metabolic activity, BON-1 and HEK293 cells were plated in 96-well plates at a density of 20,000 cells/well using 200 µl of complete medium per well (day 1) using an experimental design similar to that shown in Figure 3.2. After 24h, cells in columns 2 and 3 (see **Figure 3.2**) were washed once with 200 µl of HBSS and then 200 µl of serum free medium was added (day 2). After a further 24h, all media were removed, cells were washed once with HBSS and media were changed. 200 µl of complete medium/well were added in column 1, 200 µl of serum free medium/well in column 2 and 200 µl of conditioned medium of the other cell line/well were added in column 3 (e.g. HEK 293 conditioned media were added on BON-1 cells) (day 3). After 24h, 40 µl of MTT (Sigma; St Louis, MO, USA) was added in each well. After a 2h incubation for HEK293 cells and a 1h incubation for BON-1 cells (as cancer cells are more metabolically active than stromal cells) the optical density was read at 590 nm using a microplate reader (day 4).

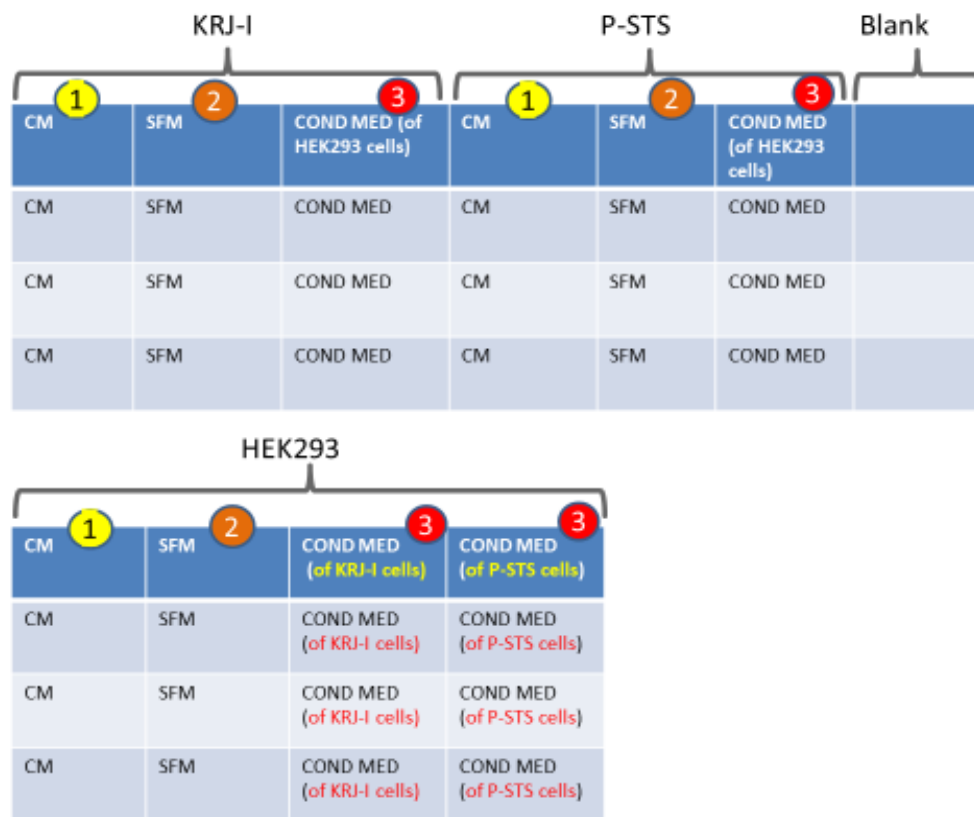### 3.2.2. Investigation of the crosstalk between KRJ-I/P-STS cells and HEK293 cells

For this set of experiments, we collaborated with the University of Graz, Austria (Prof Roswitha Pfragner) and were able to have access to P-STS/KRJ-I cell derivatives (RNA/cell culture supernatants). Due to the nature of the Mutual Transfer Agreement between UCL and the University of Graz, we could not have access to the actual cancer cell lines, but only their derivatives. Thus, the experiments involving culturing of cells, cell proliferation and cell metabolism studies were performed at the University of Graz, and the experiments involving the analysis of RNA and cell culture supernatants were performed in our laboratory (Institute for Liver and Digestive Health, UCL) after shipment of the cell derivatives. The analyses of all the results were also performed by our team at UCL.

The cancer cell lines KRJ-I and P-STS have been isolated from SI-NET primary tumours and are not widely available[127,128]. Thus, in a first set of experiments designed to explore new genes important in tumour-stromal interactions in SI-NETs, a screening platform was optimised, which consisted of fibroblast cells (HEK293) and SI-NET cell lines (P-STS and KRJ-I) to screen for paracrine effects. Initially, both cell lines were cultured in the same medium (1:1 dilution of Ham's F12 and DMEM [4.5 g/l glucose] supplemented with 10% FBS and 1% pen strep) at a cell density of 2 million cells in 8ml of media, followed by 48h of serum starvation to obtain conditioned media. These were centrifuged at 1500 rpm for 8 minutes and stored at - 80° C.

Changes in cell proliferation and **cell metabolic activity** of cancer cells (P-STS/KRJ-I) after treatment with conditioned media of fibroblasts were assessed by means of the BrdU ELISA (CellTiter 96 Aqueous, Promega) and WST-1 assay (Cell proliferation reagent WST-1, Roche), respectively. The water-soluble tetrazolium (WST) assay is equivalent to the MTT assay, and detects the metabolic activity of the respiratory chain of cultured cells. The assay is based on changes in the light absorbance resulting from the metabolism of WST-1 into formazane by mitochondrial succinate reductase. Similarly, changes in cell proliferation and metabolism were investigated in fibroblastic cells (HEK293) treated with conditioned media of SI-NET cells (KRJ-I/P-STS). These *in vitro* culture experiments were performed at the University of Graz, Austria, where the SI NET cell lines (KRJ-I/P-STS) were initially developed[127,128] and were based upon our previous *in vitro* experiments with the BON-1 cells (described earlier). In brief, to assess changes in cell proliferation, KRJ-I, P-STS and HEK293 cells were plated in 96 well plates at a density of 25,000 cells per well using 100 µl of complete medium (1:1 dilution of Ham's F12 nutrient mixture and DMEM supplemented with 10% FBS and 1% pen-strep) per well. After 24h, cells in conditions 2 and 3 (see **Figure 3.3**) were washed once with 100 µl of Ca^{2+} Mg^{2+} free phosphate buffered saline (CMF-PBS) pH=7.4 and then 100 µl of serum free medium (1:1 dilution of Ham's F12 nutrient mixture and DMEM supplemented with 0.5% FBS and 1% pen-strep) was added in each well. Spinning steps were required at each washing step or change in media for KRJ-I cells, since these are floating (suspension) cells. After a further 24h, all media were removed, cells washed once with washing buffer and media were changed (100 µl of complete medium/well were

added in condition 1, 100 µl of serum free medium/well in condition 2. In condition 3, for KRJ-I and P-STS cells, 100 µl of conditioned medium of the HEK293 cell line/well were added, while for HEK293 cells, 100 µl of conditioned medium of the KRJ-I and P-STS cells were added. In addition, 10 µl of BrdU was added in each well. After 24h, changes in cell proliferation were measured using the cell proliferation BrdU ELISA assay (Cat No 11 647 229 001), as previously described.

Figure 3.3. Experimental design to investigate changes in cell proliferation due to the crosstalk between neuroendocrine tumour cells (KRJ-I/P-STS) and stromal cells (HEK293). Columns 1-3 represent different experimental conditions with 4 biological repeats for each condition. CM: Complete Medium, SFM: Serum-Free Medium, CondM: Conditioned medium of the other cell line (e.g. HEK 293 conditioned media added on KRJ-I and P-STS cells)

To assess changes in cell metabolic activity, KRJ-I, P-STS and HEK293 cells were plated in 96 well plates at a density of 25,000 cells per well using 100 µl of complete medium (1:1 dilution of Ham's F12 nutrient mixture and DMEM supplemented with 10% FBS and 1% pen-strep) per well. After 24h, cells in conditions 2 and 3 (see Figure 3.3, as the plate design used was similar to the one used for the BrdU assay) were washed once with 100 µl of CMF-PBS (Ca Mg free phosphate buffered saline) pH=7.4 and then 100 µl of serum free medium (1:1 dilution of Ham's F12 nutrient mixture and DMEM supplemented with 0.5% FBS and 1% pen-strep) were added in each well. After a further 24h, all media were removed, cells were washed once with washing buffer and media were changed (100 µl of complete medium/well were added in condition 1 and 100 µl of serum free medium/well in condition 2. In condition 3, for KRJ-I and P-STS cells, 100 µl of conditioned medium of the HEK293 cell line/well were added, while in HEK293 cells, 100 µl of conditioned medium of the KRJ-I and P-STS cells were added). After 24h, 10 µl of WST-1 reagent was added in each well and changes in cell metabolic activity were measured (WST-1 assay, Roche, Cat. No. 11 644 807 001).

To assess **changes in gene expression**, cells (KRJ-I, P-STS and HEK293) were plated in 6-well plates at a cell density of 500,000 cells/well using 2ml of complete medium (1:1 dilution of Ham's F12 and DMEM [4.5 g/l glucose] supplemented with 10% FBS and 1% pen strep) per well (day 1). After 24h (day 2), KRJ-I and P-STS cells in rows 2 & 3 and HEK293 cells in rows 2-4 (see **Figure 3.4**) were washed twice with CMF-PBS and serum starved (using 2 ml of serum free medium per well). 24h later (day 3) culture media were changed in all the wells. In row 1, the old media were removed, cells were washed twice with CMF-PBS and 2ml of complete media were added in each well. In row 2, the old media were removed, washed twice with CMF-PBS and 2ml of serum free media were added in each well. For KRJ-I and P-STS cells, the old media were removed from row 3, cells were washed twice with CMF-PBS and 2ml of HEK293 conditioned media were added. For HEK293 cells, the old media were removed from rows 3&4, cells were washed twice with CMF-PBS and 2 ml of conditioned media of the cancer cells, KRJ-I and P-STS, were added in each well of rows 3&4, respectively. 48h later (day 5), cell culture supernatants were collected. RNA was extracted from cells, using the RNeasy mini kit (Qiagen®) and stored at -

80ºC. The cell culture supernatants and extracted RNA were then sent to our laboratory (Institute for Liver and Digestive Health, UCL).

ROW 1	KRJ-I (CM)	KRJ-I (CM)	KRJ-I (CM)
ROW 2	KRJ-I (SFM)	KRJ-I (SFM)	KRJ-I (SFM)
ROW 3	KRJ-I (CondM)	KRJ-I (CondM)	KRJ-I (CondM)

ROW 1	P-STS (CM)	P-STS (CM)	P-STS (CM)
ROW 2	P-STS (SFM)	P-STS (SFM)	P-STS (SFM)
ROW 3	P-STS (CondM)	P-STS (CondM)	P-STS (CondM)

ROW 1	HEK (CM)	HEK (CM)	HEK (CM)
ROW 2	HEK (SFM)	HEK (SFM)	HEK (SFM)
ROW 3	HEK (CondM KRJ-I)	HEK (CondM KRJ-I)	HEK (CondM KRJ-I)
ROW 4	HEK (CondM P-STS)	HEK (CondM P-STS)	HEK (CondM P-STS)

Figure 3.4: Experimental design to investigate changes in gene expression due to the crosstalk between neuroendocrine tumour cells (KRJ-I/P-STS) and stromal cells (HEK293). Each row of cells has 3 biological repeats representing the same experimental condition. CM: Complete medium, SFM: Serum Free Medium, CondM: Conditioned medium of the other cell line (e.g. Conditioned medium of stromal cells added to cancer cells. Note that HEK293 cells were treated with conditioned media of both KRJ-I and P-STS cells).

Next, changes in gene expression profile in HEK293 fibroblasts were assessed using the **"Human Fibrosis" RT²Profiler PCR Array (Qiagen®)** which contains 84 genes encoding ECM remodelling enzymes, TGFß signaling molecules and inflammatory cytokines, as well as additional genes important for fibrosis development. Moreover, the **Bio-rad® RT²Profiler PCR Array "Human Molecular Mechanisms Of Cancer"** was employed for the P-STS/KRJ-I cancer cells. This panel includes 92 target genes linked to important cancer-related pathways, and its results can suggest pathways that are potentially activated or inhibited in tumour cells.

Briefly, in order to perform the RT2 PCR Profiler arrays, cells were washed twice with cold PBS before being lysed directly in the well with β-mercaptoethanol containing lysis buffer provided in the RNeasy Mini kit (QIAGEN, Denmark), followed by the use of QIA shredder spin columns (QIAGEN). Subsequent RNA preparation was done

according to the protocol for the RNeasy Mini kit. RNA concentration was determined using a NanoDrop Spectrophotometer.

RT2 PCR Profiler Human Fibrosis (Qiagen®)

The Human Fibrosis RT PCR Profiler (Qiagen®) was used to investigate changes in gene expression in the HEK293 cells (stromal cells in our *in vitro* model). Samples were prepared from pooled RNA extracted from HEK293 cells using the RNeasy Mini Kit (Qiagen®). More specifically, 3 RNA samples from the same experimental condition (0.33 µg per sample) were pooled together. cDNA synthesis based on 0.33 µg total RNA of each pooled sample was performed using the RT2First Strand Kit (Qiagen®). Real-time PCR was performed in triplicate for each pooled sample using the RT2 qPCR SYBR green mastermix and Human Fibrosis RT2 Profiler PCR 96-well Array (Catalogue number PAHS-120Z, Qiagen®) and the following PCR cycling program (holding stage: 10 min 95°C (1 cycle), cycling stage: 15 s 95°C plus 60 s 60°C (40 cycles), melt curve stage: 15 s 95°C, 1 min 60°C, 30 s 95°C, 15 s 65°C).

The PCR array data passed the Qiagen online quality control. Data analysis of relative gene expression was performed using the ΔΔCt method. Array analysis of the results was performed using the software provided by the Qiagen web portal (http://www.qiagen.com/geneglobe) and normalization was done on automatic HKG (housekeeping gene) panel.

RT2 PCR Profiler Molecular Mechanisms of Cancer (Bio-rad®)

The Molecular Mechanisms of Cancer RT2 PCR Profiler was used to investigate changes in gene expression in the KRJ-I and P-STS cells (tumour cells in our *in vitro* model). Samples were prepared from pooled RNA extracted from HEK293 cells using the RNeasy Mini Kit (Qiagen®). More specifically, 3 RNA samples from the same cell type and experimental condition (0.33 µg per sample) were pooled together. cDNA synthesis based on 0.33 µg total RNA of each pooled sample was performed using the iScript gDNA Clear cDNA synthesis kit (Bio-rad®). Real-time PCR was performed in triplicate for each pooled sample using the RT2 qPCR SYBR green mastermix and Molecular Mechanisms of Cancer RT2 Profiler PCR 96-well Array (Bio-rad®) and the following PCR cycling program (holding stage: 10 min 95°C (1

cycle), cycling stage: 15 s 95°C plus 60 s 60°C (40 cycles), melt curve stage: 15 s 95°C, 1 min 60°C, 30 s 95°C, 15 s 65°C).

The PCR array data passed the Bio-rad online quality control. Data analysis of relative gene expression was performed using the ΔΔCt method. Array analysis of the results was performed using the Bio-rad PrimePCR Analysis software (http://www.biorad.com) and normalization was done on automatic HKG (housekeeping gene) panel.

Changes in gene expression in both cell types (cancer and stromal cells) were further investigated with **RNA sequencing (UCL Genomics)**, using the following methodology:

Library preparation

100ng total RNA were processed using the NEBNext RNA Ultra II kit with Poly A+ selection (p/n E7760 & E7490) according to manufacturer's instructions.

Briefly, mRNA was isolated from total RNA using paramagnetic Oligo dT beads to pull down poly-adenylated transcripts. The purified mRNA was fragmented using chemical hydrolysis (heat and divalent metal cation) and primed with random hexamers. Strand-specific first strand cDNA was generated using Reverse Transcriptase in the presence of Actinomycin D. This allowed for RNA dependent synthesis while preventing spurious DNA-dependent synthesis. The second cDNA strand was synthesised using dUTP in place of dTTP, to mark the second strand.

The resultant cDNA was then "A-tailed" at the 3' end to prevent self-ligation and adapter dimerisation.

Full length xGen adaptors (IDT), containing two unique 8bp sample specific indexes, a unique molecular identifier (N8) and a T overhang were ligated to the A-Tailed cDNA. Successfully ligated cDNA molecules were then enriched with limited cycle PCR (14 cycles – the actual number was dependent on the amount of input RNA). The high-fidelity polymerase employed in the PCR was unable to extend through uracil. This meant only the first strand cDNA was amplified for sequencing, making the library strand specific (first-strand).

Sequencing

Libraries to be multiplexed in the same run were pooled in equimolar quantities, calculated from Qubit and Bioanalyser fragment analysis.

Samples were sequenced on the NextSeq 500 instrument (Illumina, San Diego, US) using a 75bp single read run with a corresponding 8bp unique molecular identifier (UMI) read.

Data Analysis

Run data were demultiplexed and converted to fastq files using Illumina's bcl2fastq Conversion Software v2.19. Fastq files were then aligned to the human genome UCSC hg38 using RNA-STAR 2.5.2b then UMI deduplicated using Je-suite (1.2.1). Reads per transcript were counted using FeatureCounts and differential expression was estimated using the BioConductor package SARTools, a DESeq2 wrapper.

All annotation and sequences were obtained from Illumina iGenomes (http://emea.support.illumina.com/sequencing/sequencing_software/igenome.html)

RNA sequencing data were further analysed by **Ingenuity Pathway Analysis (IPA)** in collaboration with Dr Dong Xia (Royal Veterinary College, London). Both generic and tissue-specific (using the following selections: small intestine, lymph node, fibroblast [both primary tissue and cell line] and immune cells) IPA analyses were performed. However, to avoid an unnecessarily complicated presentation of our results, we have included here only the generic IPA analyses, which are probably more useful, as the Qiagen IPA software does not include a specific option for 'neuroendocrine tumour'-related pathways. The tissue-specific analysis was also useful in some selected cases, where the generic analysis was inadequate, and this will be discussed later.

Furthermore, it is known that cytokine and pro-inflammatory factor production and release are important in tumour development. To further dissect the stromal-tumour interaction on **cytokine and inflammatory protein secretion profile**, the conditioned media of cancer cells and fibroblasts were collected and a **Bio-Plex Pro™ Human Cytokine 27-plex Assay (BioRad - Luminex)** was performed. The Bio-Plex Pro™ assays are essentially immunoassays using magnetic fluorescently dyed microspheres (also known as beads), each with a distinct spectral address to allow detection of

individual analytes within a multiplex suspension. The assay principle is similar to that of a sandwich ELISA, as shown in **Figure 3.5**. *Capture antibodies* directed against the desired biomarker (analyte) are covalently coupled to the beads. Coupled beads react with the sample containing the biomarker. After a series of washes to remove unbound protein, a *biotinylated detection antibody* is added to create a sandwich complex. The final detection complex is formed with the addition of streptavidin-phycoerythrin conjugate. Phycoerythrin serves as a fluorescent indicator (or reporter). When a multiplex assay suspension is placed into the Luminex-based reader, a red (635nm) laser illuminates the fluorescent dyes within each bead to provide bead classification. At the same time, a green (532nm) laser excites phycoerythrin to generate a reporter signal. A high-speed digital processor manages data output, and the Bio-Plex Manager ™ software presents data as median fluorescence intensity (MFI). The concentration (pg/ml) of analytes bound to each bead is proportional to the MFI of the reporter signal and is also provided by the software.
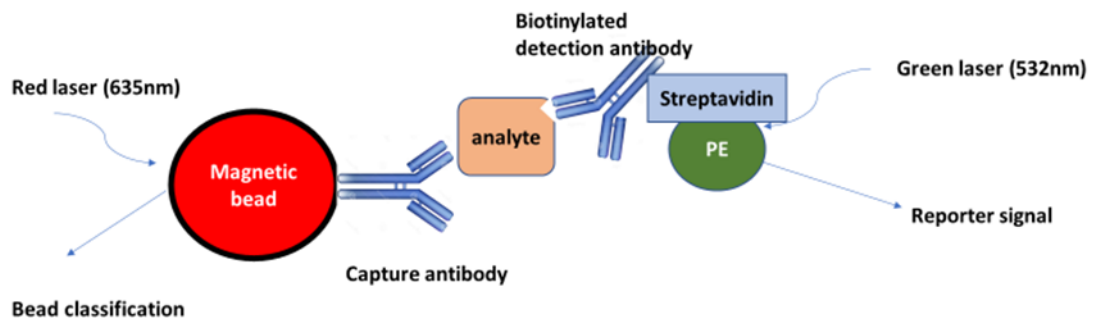
Figure 3.5. Schematic representation of bead-based multiplex assay using Luminex technology.
PE: Phycoerythrin fluorescent reporter

The cell culture supernatants were analysed using the Bio-Plex Pro™ Human Cytokine 27-plex Assay (BioRad - Luminex). In brief, as the levels of each analyte in the cell culture supernatants were unknown, we used undiluted samples, as well as 1:2

and 1:4 dilutions of each sample (using serum free medium as the diluent). Standards (1-8) were also prepared using serum free medium as diluent and following a serial dilution technique as per manual protocol. The blank solution consisted of serum free medium. Next, **coupled beads** were diluted from a 10x stock concentration (575 µl) to a final 1x concentration (5,750 µl) using assay buffer (5,175 µl) as a diluent. Diluted (1x) coupled beads were vortexed for 30 seconds at medium speed and 50 µl was transferred to each well of a 96-well plate. The plate was placed on a magnet and each well washed twice with 100µl of Bio-Plex wash buffer. The plate was then taken off the magnet and 50 µl of each **sample** (undiluted, 1:2, 1:4), **standard** (1-8) and the **blank** were added in each well of the 96-well plate. The plate was covered with sealing tape and incubated on a shaker at 850 rpm for 30 minutes at room temperature. The plate was then placed on a magnet and each well washed three times with 100 µl wash buffer. Next, the plate was taken off the magnet and the 1x **detection antibody solution** (3,000 µl) was prepared (by diluting 300 µl of 10x stock detection antibodies with 2,700 µl of detection antibody diluent). 25 µl of 1x detection antibody solution was added in each well. The plate was covered with a sealing tape and incubated on a shaker at 850 rpm for 30 minutes at room temperature. The plate was then placed on a magnet and each well washed three times with 100 µl wash buffer. Next, the 1x **streptavidin-phycoerythrin (SA-PE) solution** (6,000 µl) was prepared by diluting the stock 100x SA-PE solution (60 µl) with 5,940 µl assay buffer. 50 µl of 1x SA-PE solution was added in each well. The plate was covered with sealing tape and incubated on a shaker at 850 rpm for 10 minutes at room temperature. The plate was then placed again on the magnet and each well washed three times of 100 µl of wash buffer. The plate was subsequently taken off the magnet and the beads were re-suspended in 125 µl of assay buffer per well. The plate was covered and shaken at 850 rpm for 30 seconds at room temperature before placing the plate on the reader.

3.3. Results

### 3.3.1. Investigation of the crosstalk between BON-1 and HEK293 cells: Single gene expression

A set of preliminary co-culture experiments was performed using the pancreatic neuroendocrine tumour cell line BON-1 and fibroblastic cell line HEK293. Changes

in single gene expression were assessed in a set of pro-fibrotic genes (IL-8, TGFβ1, TGFβR1, TNF, NFκB2, CCL2, CXCL2) known to be expressed by the BON-1 and/or HEK293 cells[21,130-134]. A brief description of the role of these genes is given in **Table 3.1**.

Gene	Function
IL8	Proinflammatory chemokine involved in neutrophil chemotaxis
TGFβ1	Growth factor involved in fibrosis
TGFβR1	TGFβ receptor
TNF	Growth factor involved in inflammation (acute phase response), apoptosis and fibrosis
NFKB2	Transcription factor induced by TNF and other signalling pathways. Involved in inflammation and cell proliferation
CCL2	Cytokine involved in inflammation (monocyte, memory T cell and dendritic cell chemotaxis)
CXCL2	Chemokine involved in immunoregulatory and inflammatory processes

Table 3.1. Brief description of the function of a set of profibrotic genes expressed by BON-1 and/or HEK293 cells. Changes in gene expression were measured in BON-1 and/or HEK293 cells after exposure to the conditioned media of the other cell type (e.g. HEK293 conditioned media on BON-1 cells), in order to investigate their potential involvement in the crosstalk between cancer and stromal cells.

CCL2 expression was significantly upregulated in HEK293 cells treated with BON-1 conditioned media relative to control. NFKB2 expression was significantly upregulated in BON-1 cells treated with the conditioned media of HEK293 cells relative to control, while IL-8 expression was significantly downregulated in BON-1 cells treated with conditioned media of HEK293 cells relative to control (**Figure 3.6**). No other significant changes were noted in the evaluated genes.
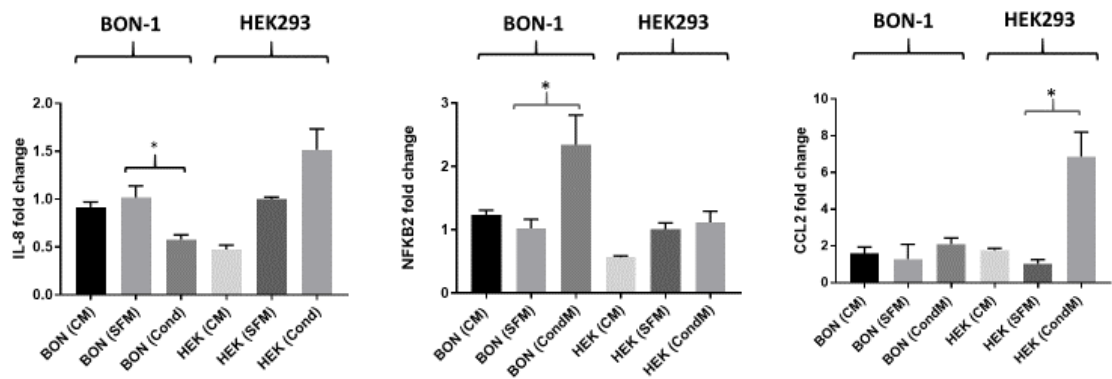
Figure 3.6. Changes in pro-fibrotic gene expression observed in BON-1 and HEK293 cells following exposure to the conditioned medium of the other cell line (presented as fold change to control [serum free medium]). CM: Complete medium, SFM: Serum free medium, CondM: Conditioned medium of the other cell line (e.g. HEK293 conditioned medium on BON-1 cells). In BON-1 cells there was a significant downregulation of IL-8 (*$p < 0.05$) and a significant upregulation of NFκB2 (*$p < 0.05$) in response to exposure to HEK293 conditioned media. In HEK293 cells there was a significant upregulation of CCL2 in response to BON-1 conditioned media (*$p < 0.05$). Results are from one experiment with 3 samples per condition (n=3).

No significant changes were noted in cell proliferation (BrdU assay) or cell metabolism (MTT assay) in either the BON-1 or HEK293 cells after treatment with the conditioned media of the other cell line (compared to control) (**Figure 3.7**).
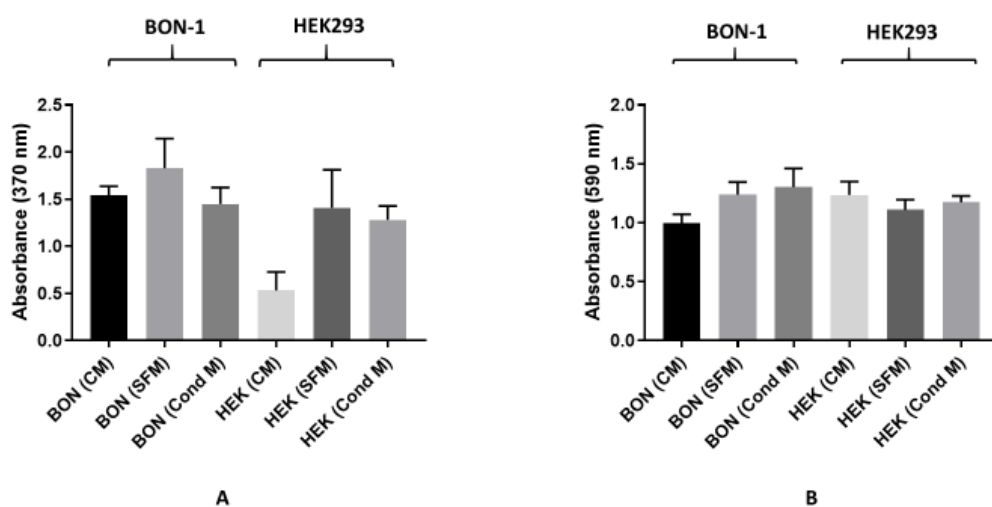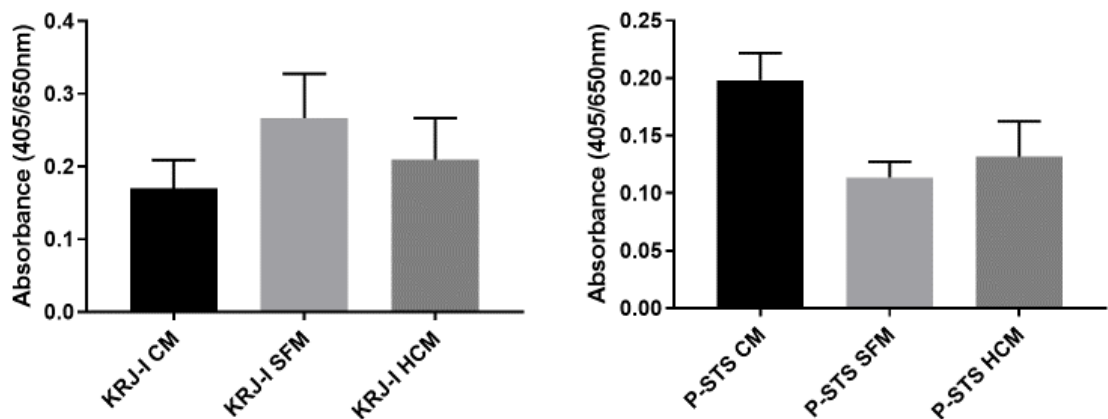
Figure 3.7. (A) Changes in cell proliferation in BON-1 and HEK293 cells measured using a BrdU assay. No significant changes were noted in BON-1 cells cultured with HEK293 conditioned media compared to control. Similarly, no significant changes were seen in HEK293 cells cultured with BON-1 conditioned media compared to control. **(B) Changes in cell metabolic activity of BON-1 and HEK293 cells measured using an MTT assay.** No significant changes were noted in BON-1 cells cultured with HEK293 conditioned media compared to control. Similarly, no significant changes were seen in HEK293 cells cultured with BON-1 conditioned media compared to control. CM: complete media, SFM: serum free media, Cond M: conditioned media.

3.3.2. Investigation of the crosstalk between KRJ-I/P-STS and HEK293 cells

A reduction in **cell metabolic activity** was observed in both KRJ-I and P-STS cells treated with HEK293 conditioned media (**Figure 3.8**), with no significant changes in **cell proliferation (Figure 3.9)**.
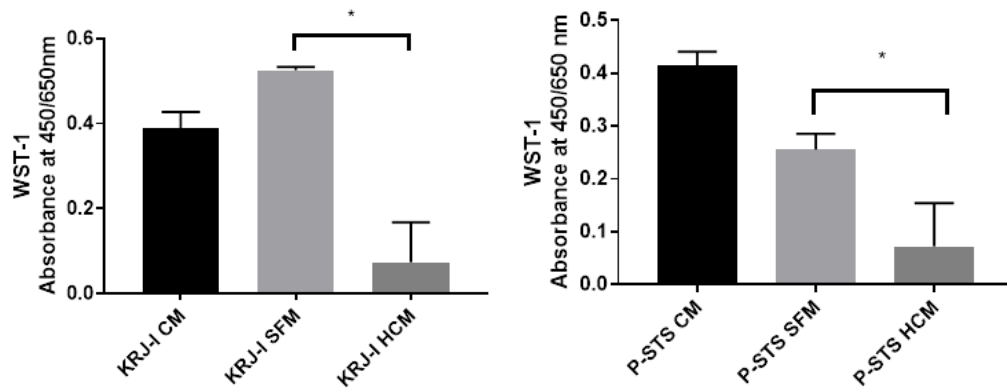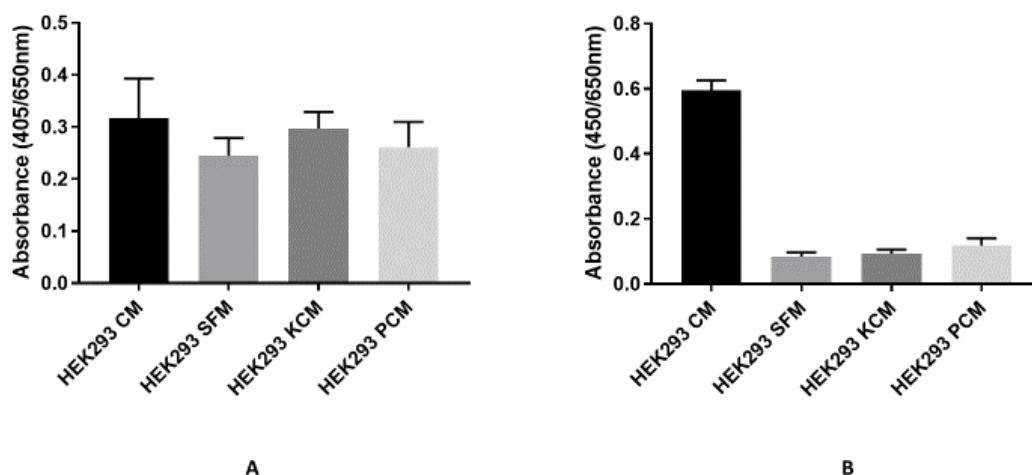
Figure 3.8. Changes in cell metabolic activity observed in the SI NET cell lines KRJ-I and P-STS in different experimental conditions. Changes in absorbance were assessed using the WST-1 assay. Absorbances were read at 450/650nm and measured 2 hours after adding the WST-1 reagent. A statistically significant reduction in cell metabolic activity was seen in KRJ-I and P-STS cells treated with HEK293 conditioned media compared to control (serum free media) (*p=0.0002). Results are from 2 independent experiments (n= 8 samples per condition). CM: complete media, SFM: serum free media, HCM: HEK293 conditioned media.

Figure 3.9. Changes in cell proliferation observed in KRJ-I and P-STS cells in different experimental conditions. Changes in absorbance were assessed using the BrdU assay. Absorbances were read at 405/650nm. No statistically significant changes were noted in cell proliferation of KRJ-I and P-STS cells exposed to HEK293 conditioned media compared to control. Results are from one experiment with 3 samples (n=3) per condition. CM: complete media, SFM: serum free media, HCM: HEK293 conditioned media.

Furthermore, no significant changes were observed in HEK293 cell proliferation or metabolic activity upon culturing with conditioned media of cancer cells (**Figure 3.10**).


Figure 3.10. (A) Changes in cell proliferation in HEK293 in different experimental conditions. Changes in absorbance were assessed using the BrdU assay. Absorbances were read at 405/650nm. No statistically significant changes were noted in cell proliferation of HEK293 cells exposed to KRJ-I and P-STS conditioned media compared to control. Results are from one experiment with 3 samples (n=3) per condition. **(B) Changes in cell metabolic activity of HEK293 cells in different experimental conditions.** Changes in absorbance were assessed using the WST-1 assay. Absorbances were read at 450/650nm and measured 2 hours after adding the WST-1 reagent. No statistically significant changes in cell metabolic activity were seen in HEK293 cells treated with KRJ-I and P-STS conditioned media compared to control (serum free media). Results are from 2 independent experiments (n= 8 samples per condition). CM: complete media, SFM: serum free media, HCM: HEK293 conditioned media.

The **RT PCR Profiler** "Molecular Mechanisms of Cancer" revealed that several genes with important roles in cancer biology were significantly (fold-change≥2, $p<0.05$) up- or down-regulated in cancer cells treated with HEK293 conditioned media. More specifically, KRJ-I cells exhibited a significant upregulation of the following genes: PIK3R1, NFKB2, ITGAV, MAPK1, MAX and MAP2K1 (**Figure 3.11**), while P-STS

cells responded with a significant downregulation in the following genes: Grb2 and FADD (**Figure 3.12**). These changes are summarised in **Table 3.2**.

KRJ-I		P-STS	
	⬆		⬇
PIK3R1	2.61-fold	Grb2	-4.48-fold
NFκB2	2.25-fold	FADD	-3.95-fold
ITGAV	2.91-fold		
MAPK1	2.27-fold		
MAX	2.19-fold		
MAP2K1	11.93-fold		

Table 3.2. Summary of significant changes (≥2-fold, p<0.05) in gene expression in cancer cells KRJ-I and P-STS treated with HEK293 conditioned media compared to control. Fold changes are shown for each gene. Red up arrow indicates upregulation and green down arrow indicates down-regulation.
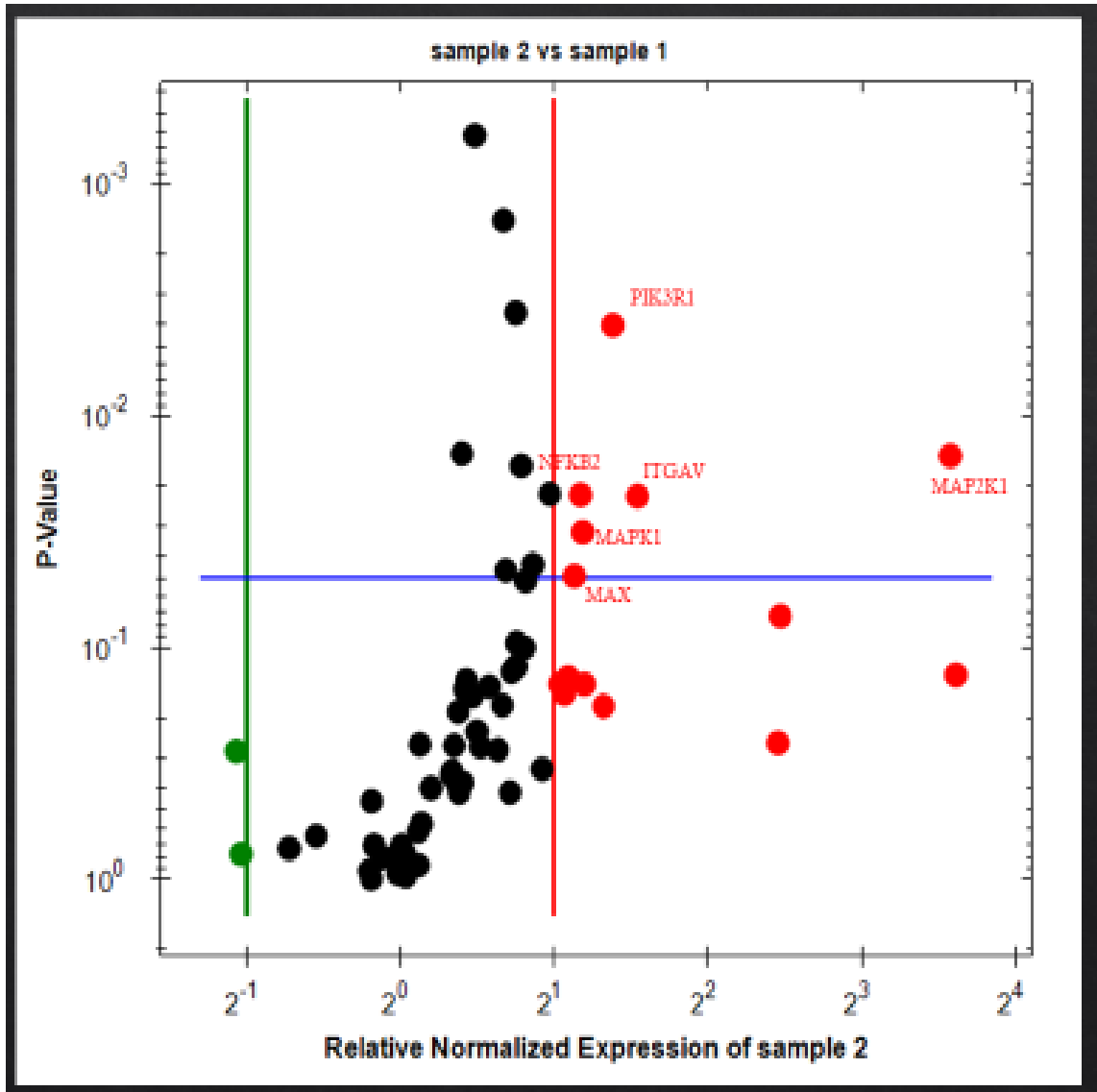
Figure 3.11. Volcano plot representing changes in gene expression in KRJ-I cells treated with HEK293 conditioned media. Each dot in this graph represents a gene included in the RT Profiler "Molecular Mechanisms of Cancer". The y-axis represents the p-value and genes with statistically significant changes ($p<0.05$) are represented above the blue horizontal line of the graph. The x axis indicates the fold change (compared to control) and genes located to the right of the red vertical line have a fold up-regulation of ≥ 2, while genes located to the left of the vertical green line have a fold down-regulation of ≥ 2. Thus, the genes in the right upper corner of this Volcano plot (PIK3R1, NFKB2, ITGAV, MAPK1, MAX and MAP2K1) have a fold up-regulation of ≥ 2, which is statistically significant ($p<0.05$). Results are from 1 experiment with 3 samples (n=3) per condition. In the graph, sample 2 indicates KRJ-I cells treated with HEK293 conditioned media; Sample 1 refers to KRJ-I cells in serum free media.
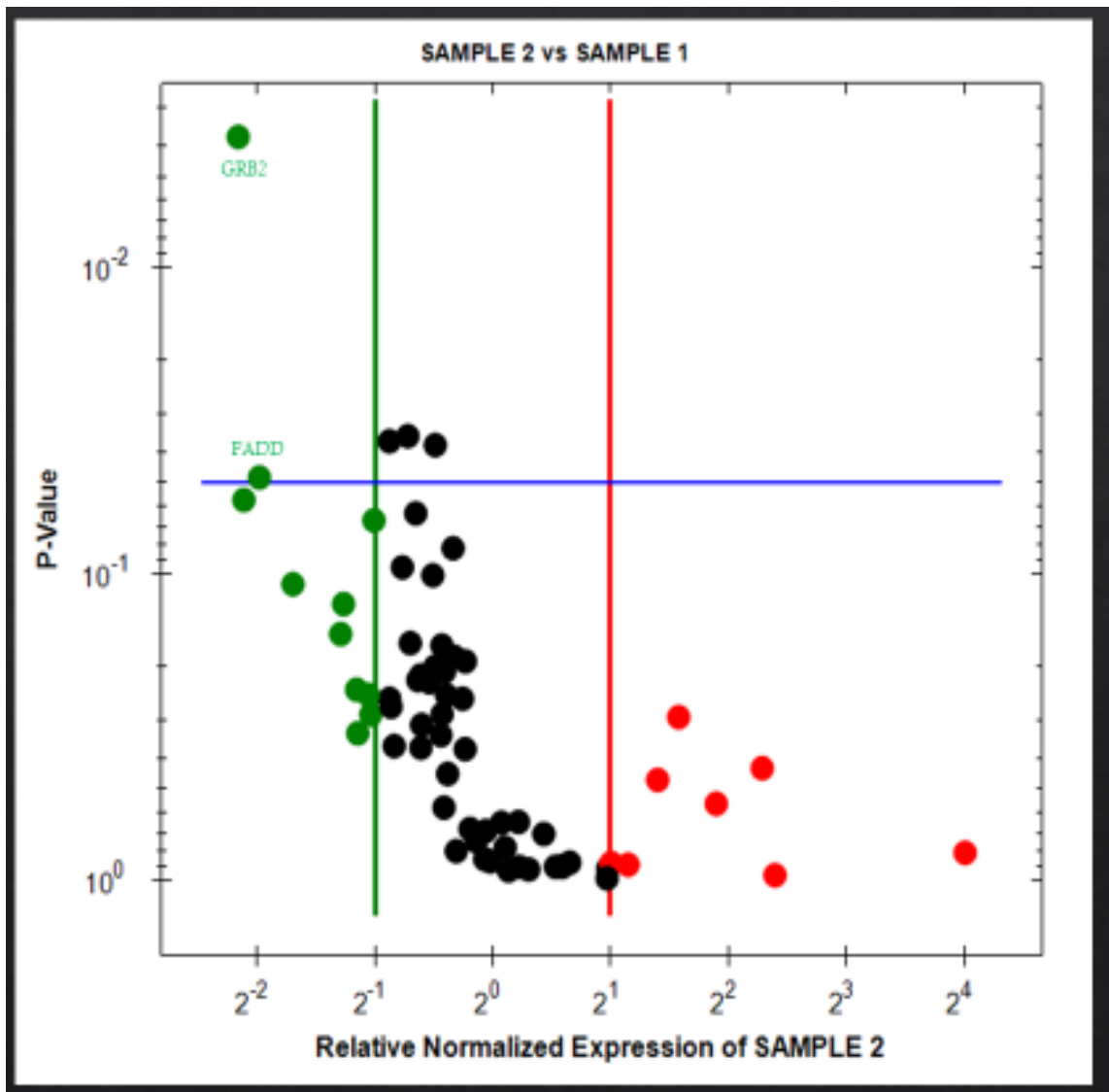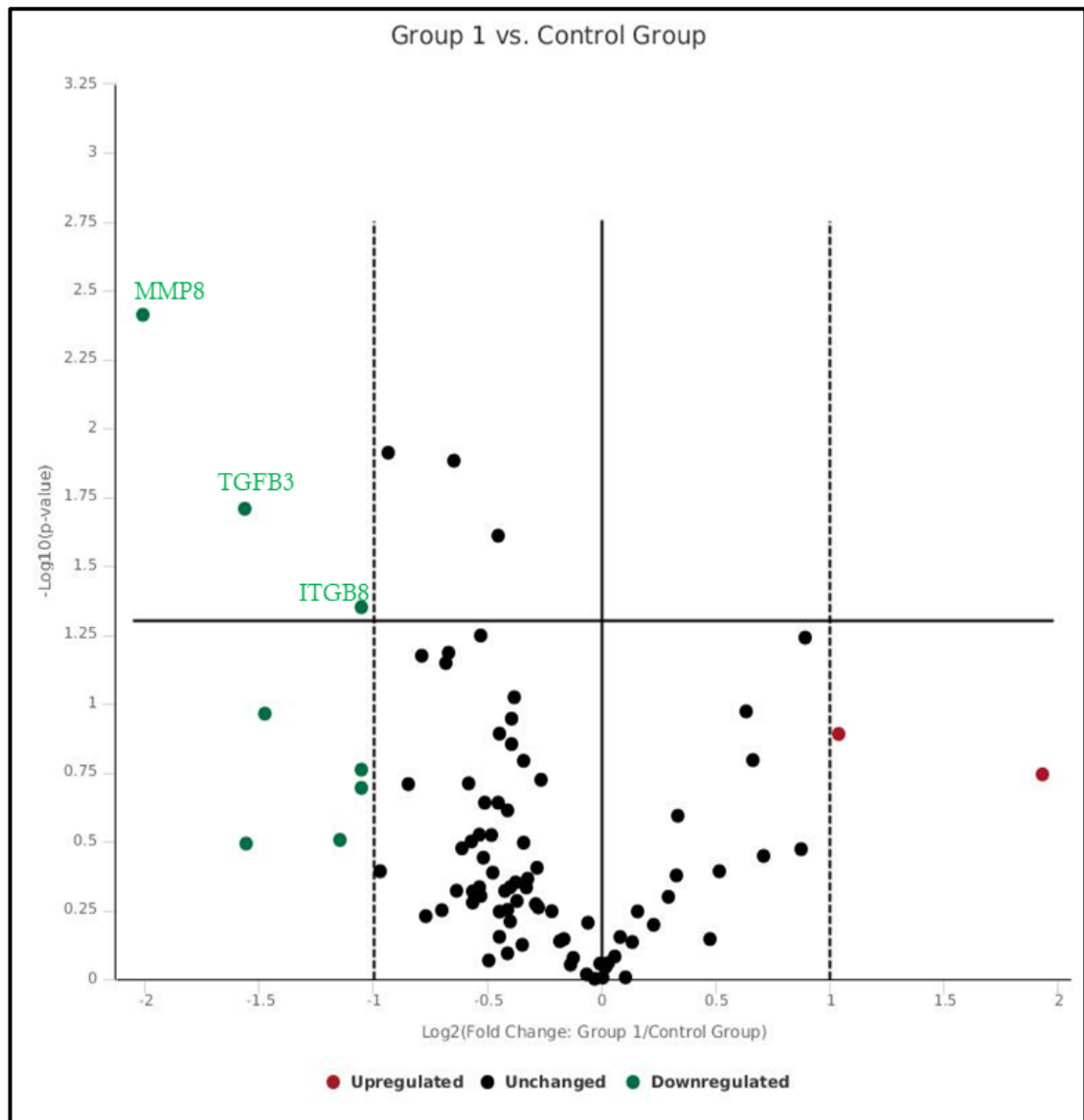
Figure 3.12. Volcano plot representing changes in gene expression in P-STS cells treated with HEK293 conditioned media. Each dot in this graph represents a gene included in the RT Profiler "Molecular Mechanisms of Cancer". The y-axis represents the p-value and genes with statistically significant changes ($p<0.05$) are represented above the blue horizontal line of the graph. The x axis indicates the fold change (compared to control) and genes located to the right of the red vertical line have a fold up-regulation of ≥2, while genes located to the left of the vertical green line have a fold down-regulation of ≥2. Thus, the genes in the left upper corner of this Volcano plot (Grb2 and FADD) have a fold down-regulation of ≥2, which is statistically significant ($p<0.05$). Results are from 1 experiment with 3 samples per condition. In the graph, sample 2 indicates P-STS cells treated with HEK293 conditioned media; sample 1 refers to P-STS in serum free media.
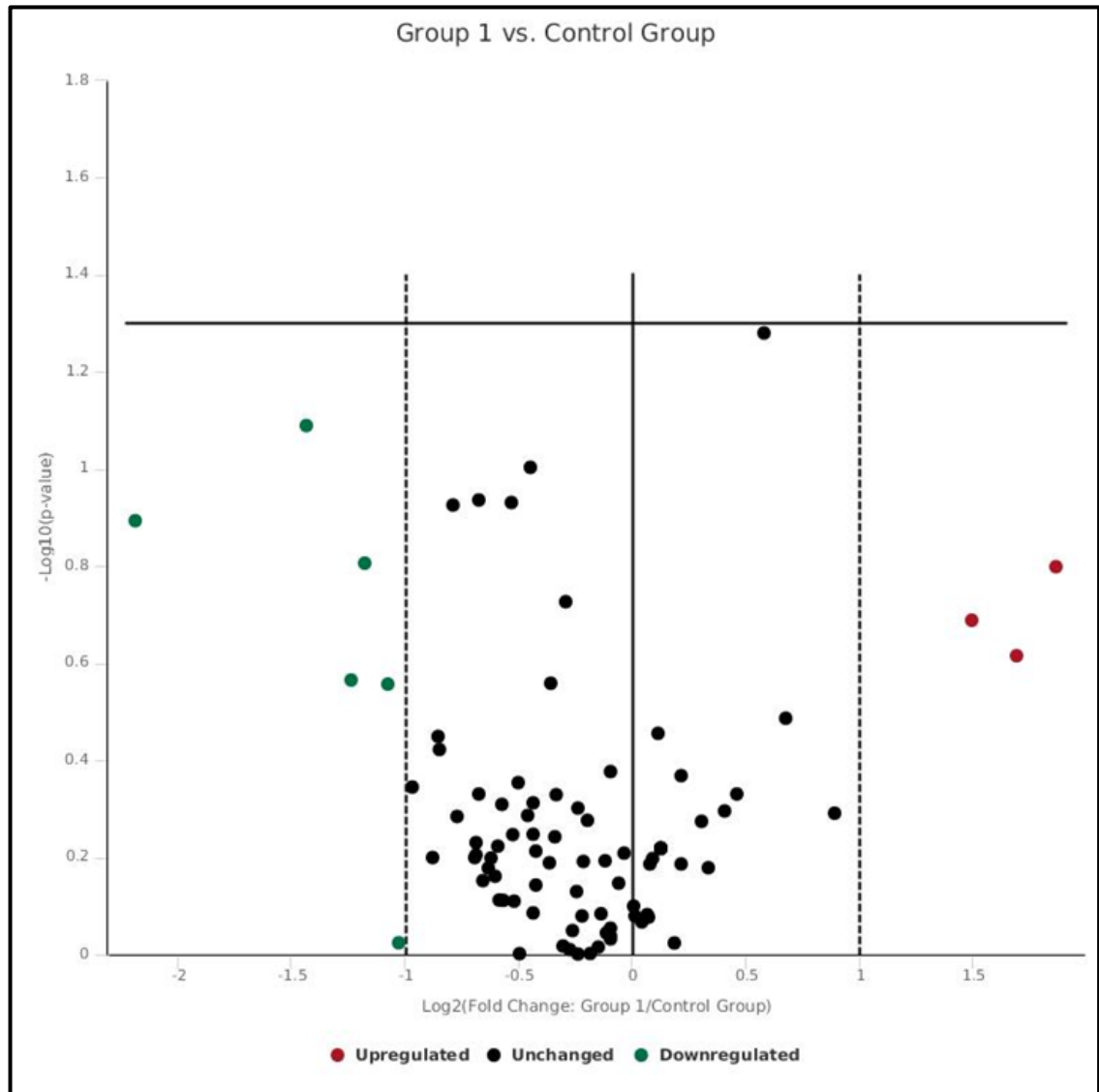
To assess changes in gene expression of HEK293 cells, the "Human Fibrosis" RT PCR Profiler was used. HEK293 cells treated with KRJ-I conditioned media exhibited a significant downregulation of the following genes: MMP8, TGFβ3 and ITGB8

(**Figure 3.13**), while no significant changes were noted in gene expression of HEK293 cells treated with P-STS conditioned media (**Figure 3.14**).

Figure 3.13. Volcano plot representing changes in gene expression in HEK293 cells treated with KRJ-I conditioned media. Each dot in this graph represents a gene included in the Human Fibrosis RT Profiler. The y-axis represents the p-value and genes with statistically significant changes ($p<0.05$) are represented above the black horizontal line of the graph. The x axis indicates the fold change (compared to control) and genes located to the right of the second vertical dotted line (shown as red dots) have a fold up-regulation of ≥ 2, while genes located to the left of the first vertical dotted line (shown as green dots) have a fold down-regulation of ≥ 2. Thus, the genes in the left upper corner of this Volcano plot (MMP8, TGFβ3 and ITGB8) have a fold down-regulation of ≥ 2, which is statistically significant ($p<0.05$). Results are from 1 experiment with 3 samples per condition. In the graph, group

1 refers to HEK293 cells treated with KRJ-I conditioned media, while the control group is HEK293 cells in serum free media.

Figure 3.14. Volcano plot representing changes in gene expression in HEK293 cells treated with P-STS conditioned media. Each dot in this graph represents a gene included in the Human Fibrosis RT Profiler. The y-axis represents the p-value and genes with statistically significant changes (p<0.05) are represented above the black horizontal line of the graph. The x axis indicates the fold change (compared to control) and genes located to the right of the second vertical dotted line (shown as red dots) have a fold up-regulation of ≥2, while genes located to the left of the first vertical dotted line (shown as green dots) have a fold down-regulation of ≥2. In this Volcano plot no genes exhibited a fold-change of ≥2 that is statistically significant. Results are from 1 experiment with 3 samples per condition. In the graph, group 1 refers to HEK293 cells treated with P-STS conditioned media, while the control group is HEK293 cells in serum free media.

Changes in gene expression in KRJ-I, P-STS and HEK293 cells were further assessed with **RNA sequencing (UCL Genomics)** (using 3 samples per condition from one experiment) **and Ingenuity Pathway Analysis (IPA)** (Qiagen Bioinformatics) was performed to identify transcriptional pathways that are significantly activated or inhibited ($p < 0.05$, z score $\geq |2|$) as a result of the cross-talk between cancer and stromal cells.

In KRJ-I cells the following pathways were activated: NF-KB activation by viruses, Tec kinase signalling, dendritic cell maturation, TREM1 signalling, role of NFAT in regulation of the immune response, cdc42 signalling, PI3K signalling in B lymphocytes, TNFR1 signalling, integrin signalling, neuroinflammation signalling pathway, IL-8 signalling, cardiac hypertrophy signalling and phospholipase signalling, while the RhoGDI signalling pathway was inhibited (**Figure 3.15**).
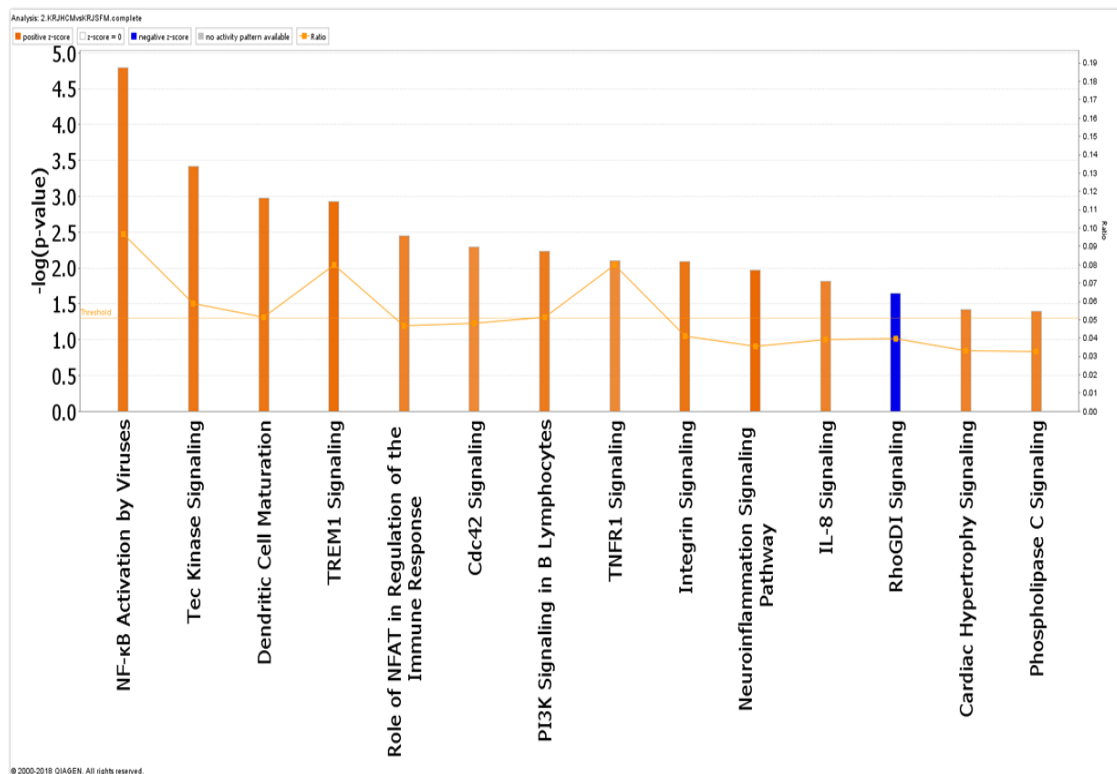
Figure 3.15. IPA analysis showing transcriptional pathways that are significantly altered in KRJ-I cells treated with HEK293 conditioned media. The x-axis represents the pathways identified. Orange bars represent pathways whose transcription is activated, while blue bars represent pathways whose transcription is inhibited. The y-axis (left) shows the -log of the p-value calculated based on the Fisher's exact test. The horizontal orange line represents the threshold of statistical significance ($p < 0.05$). The ratio (y-axis, right [represented by the orange points]) is calculated as follows: number
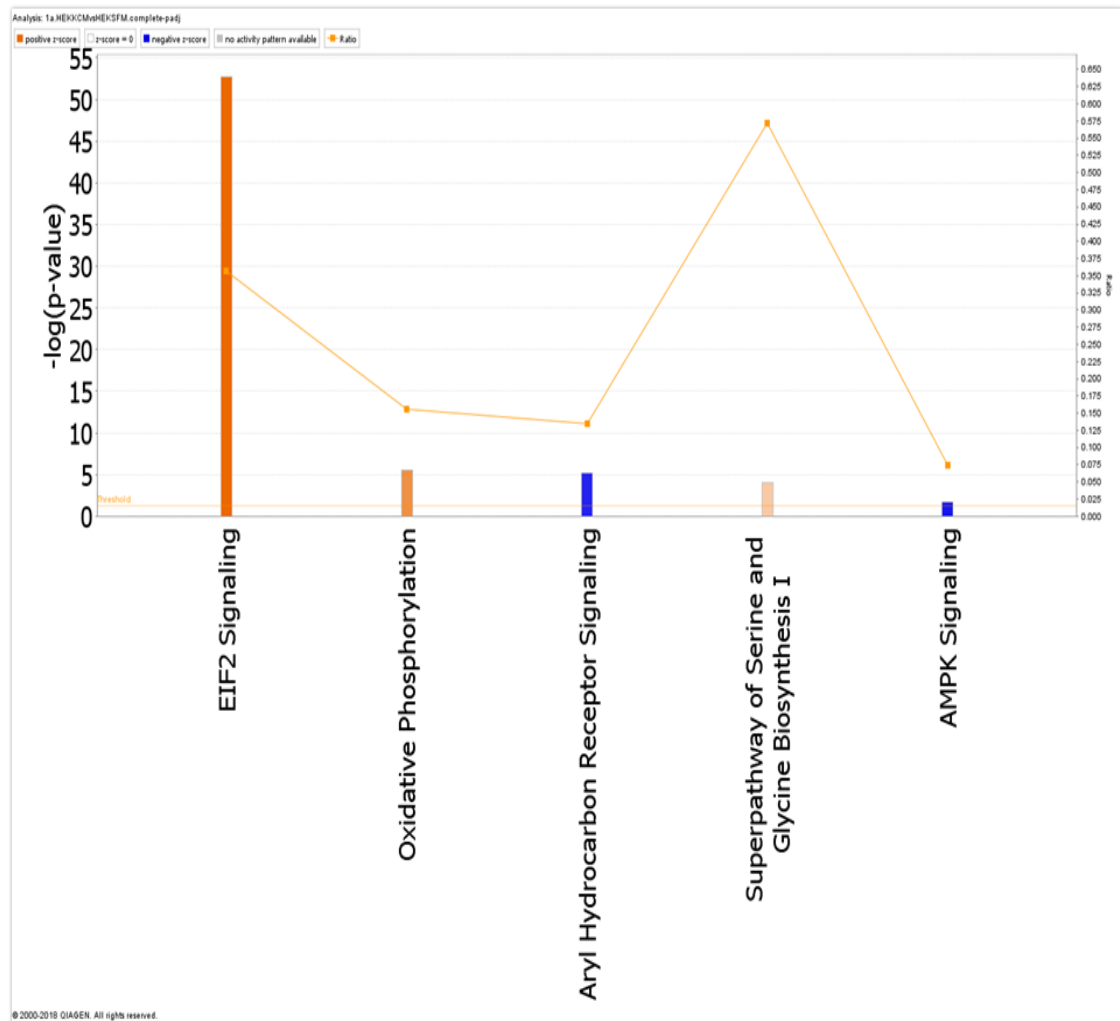
of genes in a given pathway that meet cut-off criteria, divided by the total number of genes that make up that pathway.

In P-STS cells treated with HEK293 conditioned media the following pathways were significantly activated: EIF2 signalling, oxidative phosphorylation and Gas signaling, while the superpathway of cholesterol biosynthesis was inhibited (**Figure 3.16**).
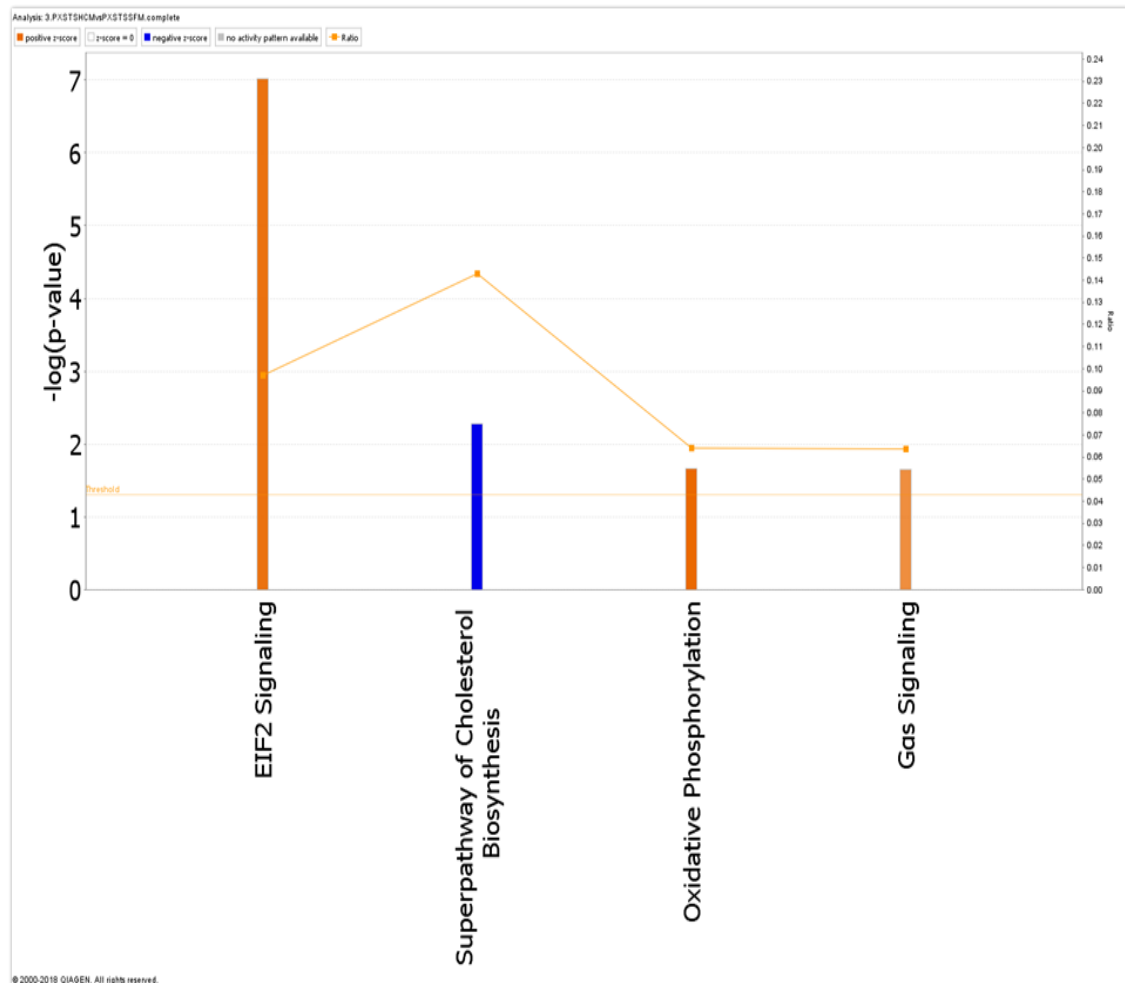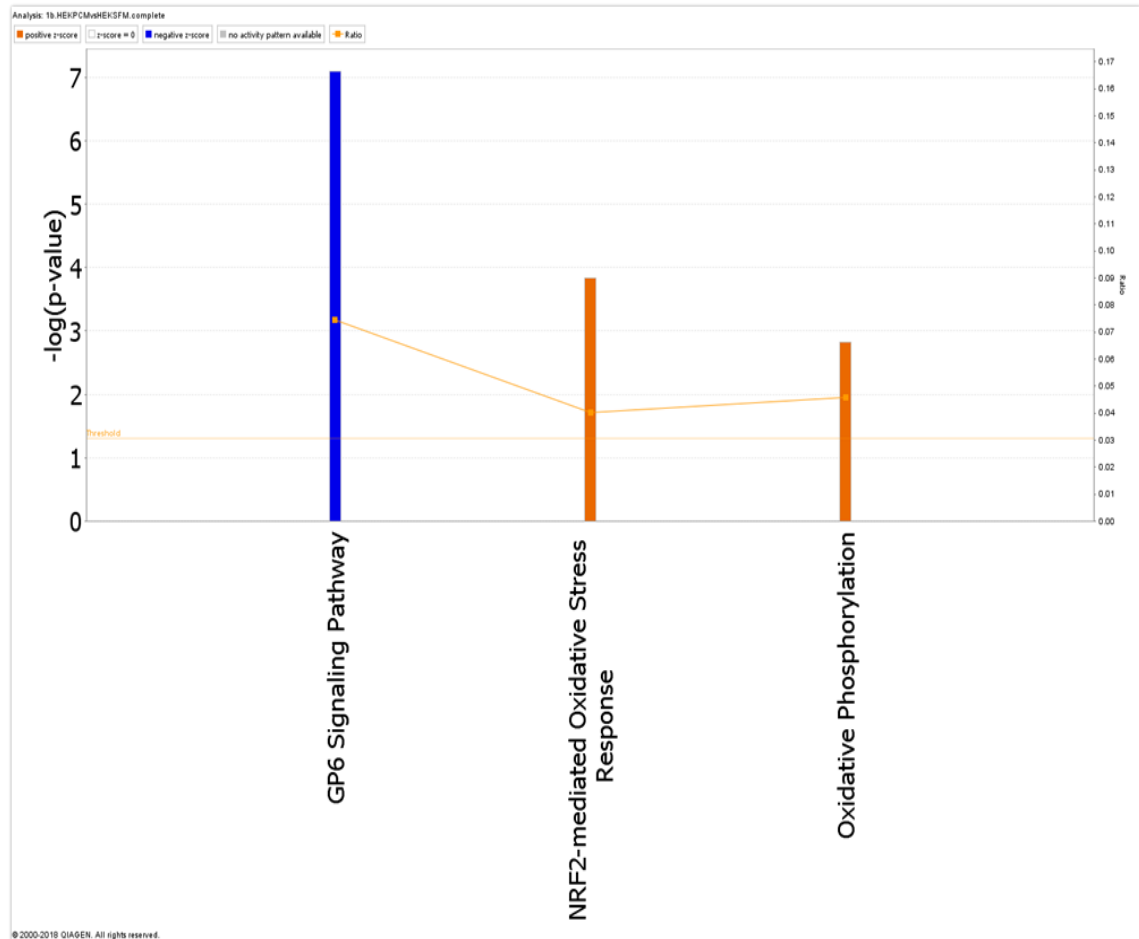

Figure 3.16. IPA analysis showing transcriptional pathways that are significantly altered in P-STS cells treated with HEK293 conditioned media. The x-axis represents the pathways identified. Orange bars represent pathways whose transcription is activated, while blue bars represent pathways whose transcription is inhibited. The y-axis (left) shows the -log of the p-value calculated based on the Fisher's exact test. The horizontal orange line represents the threshold of statistical significance ($p<0.05$). The ratio (y-axis, right [represented by the orange points]) is calculated as follows: number of genes in a given pathway that meet cut-off criteria, divided by the total number of genes that make up that pathway.

In HEK293 cells treated with KRJ-I conditioned media, the following pathways were significantly activated: EIF2 signaling, oxidative phosphorylation, superpathway of serine and glycine biosynthesis, while the aryl hydrocarbon receptor and AMPK pathways were inhibited (**Figure 3.17**).

Figure 3.17. IPA analysis showing transcriptional pathways that are significantly altered in HEK293 cells treated with KRJ-I conditioned media. The x-axis represents the pathways identified. Orange bars represent pathways whose transcription is activated, while blue bars represent pathways whose transcription is inhibited. The y-axis (left) shows the -log of the p-value calculated based on the Fisher's exact test. The horizontal orange line represents the threshold of statistical significance ($p < 0.05$). The ratio (y-axis, right [represented by the orange points]) is calculated as follows: number of genes in a given pathway that meet cut-off criteria, divided by the total number of genes that make up that pathway.

In HEK293 cells treated with P-STS conditioned media, the following pathways were significantly activated: NRF2-mediated oxidative stress response and oxidative phosphorylation, while the GP6 signalling pathway was inhibited (**Figure 3.18**).

Figure 3.18. IPA analysis showing transcriptional pathways that are significantly altered in HEK293 cells treated with P-STS conditioned media. The x-axis represents the pathways identified. Orange bars represent pathways whose transcription is activated, while blue bars represent pathways whose transcription is inhibited. The y-axis (left) shows the -log of the p-value calculated based on the Fisher's exact test. The horizontal orange line represents the threshold of statistical significance (p<0.05). The ratio (y-axis, right [represented by the orange points]) is calculated as follows: number of genes in a given pathway that meet cut-off criteria, divided by the total number of genes that make up that pathway.

Intriguingly, a significantly different pattern of pathway activation or inhibition was noted in HEK293 cells in response to KRJ-I and P-STS conditioned media, despite the fact that these two cancer cell lines (KRJ-I and P-STS) were both established from a primary SI NET (**Figures 3.19 and 3.20**).
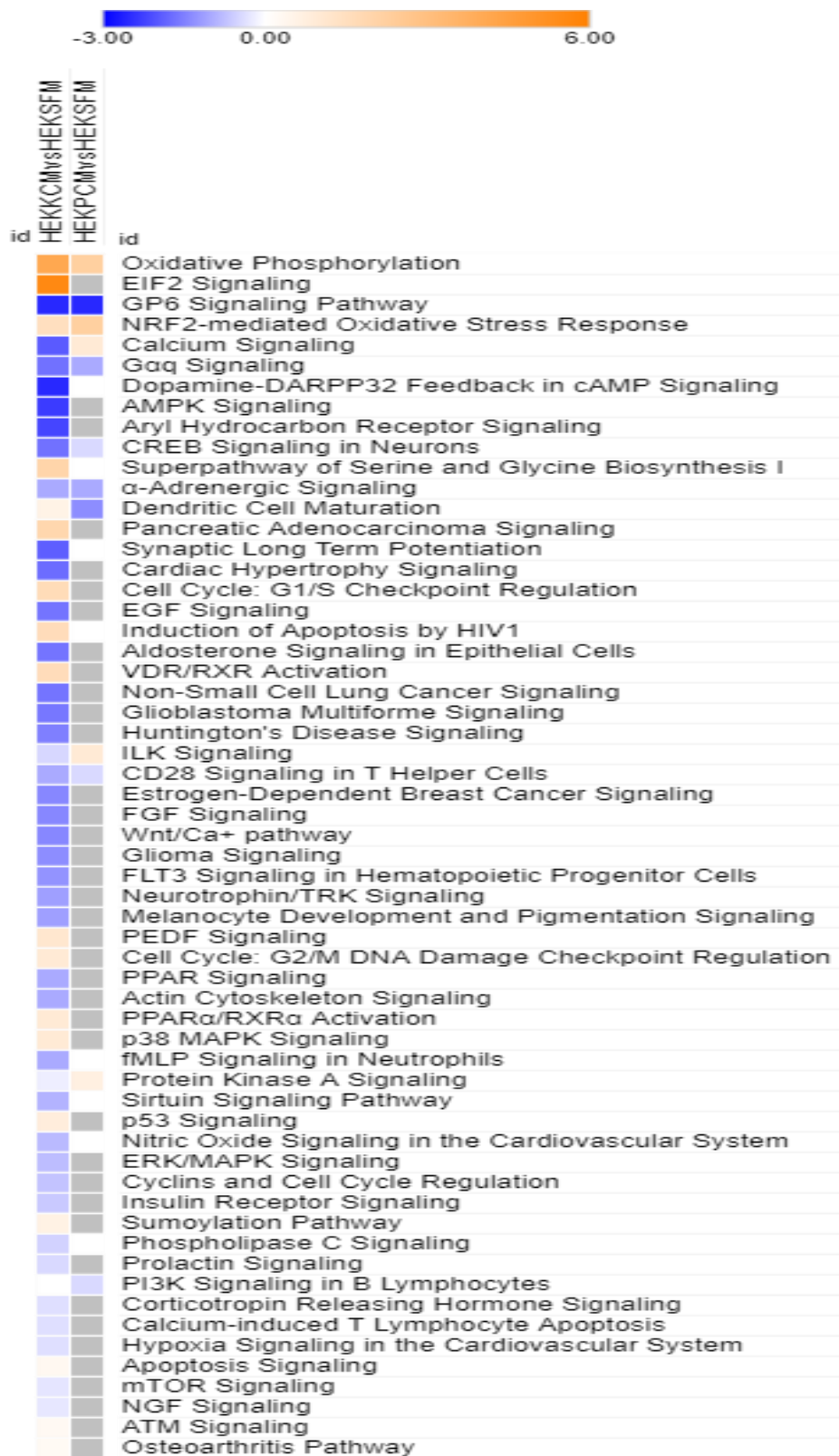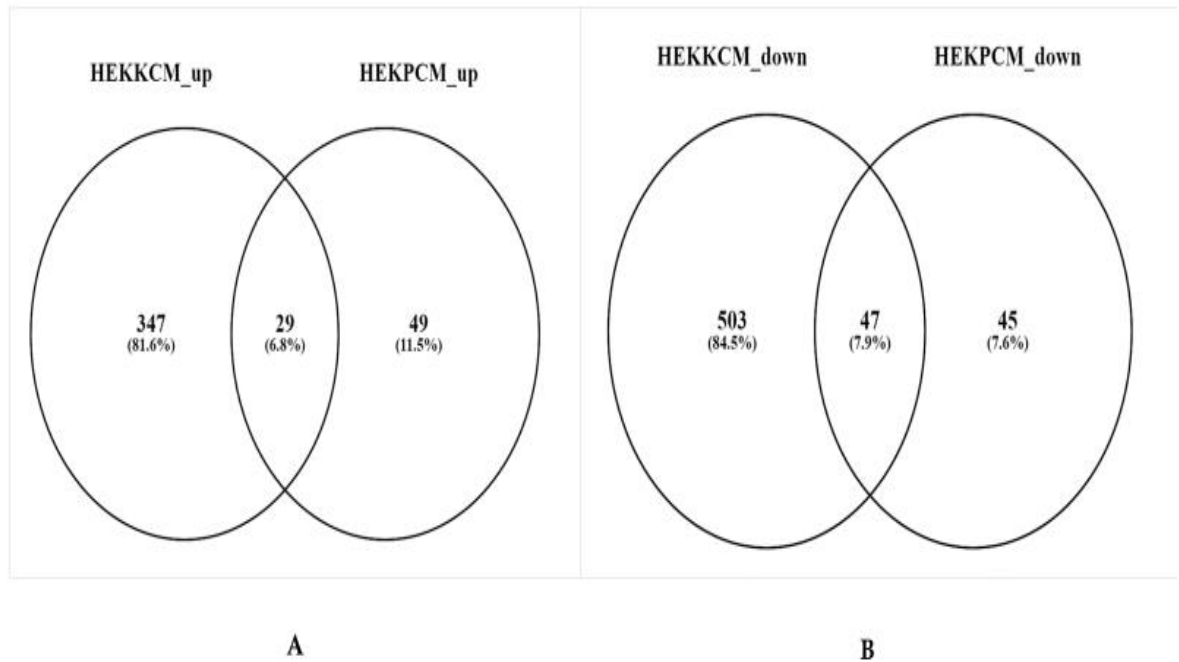
Figure 3.19. Heat map comparison of pathway scores for HEK293 cells treated with KRJ-I (left column) and P-STS (right column) conditioned media. The score magnitudes are shown as a gradient

colour from light to dark orange for induced pathway activity, and from light to dark blue for suppressed pathway activity.

Figure 3.20. A. Venn diagram demonstrating the differential expression in <u>upregulated</u> genes between HEK293 cells treated with conditioned media of KRJ-I (left circle) and P-STS cells (right circle). There was a small overlap (6.8%) in gene expression, but the majority of upregulated genes were differentially expressed. **B. Venn diagram demonstrating the differential expression in <u>downregulated</u> genes between HEK293 cells treated with conditioned media of KRJ-I (left circle) and P-STS cells (right circle).** There was a small overlap (7.9%) in gene expression, but the majority of downregulated genes were differentially expressed.

In addition, we evaluated **changes in cytokine/chemokine and growth factor secretion** by performing a 27-plex Luminex assay using cell culture supernatants of KRJ-I, P-STS and HEK293 cells. As mentioned earlier, this assay allows the simultaneous measurement of a panel of cytokines/chemokines and growth factors in culture media. We compared the concentration of these proteins in cell culture supernatants of cancer cells treated with HEK293 conditioned media *versus* control (cancer cells in serum free media). We also assessed the concentration of these proteins in cell culture supernatants of HEK293 cells treated with cancer cell conditioned media *versus* control (HEK293 cells in serum free media). It should be noted that these proteins were also present in the conditioned media that were used to treat the cells and this was taken into account during data interpretation. Changes in

gene expression for these specific cytokines/chemokines and growth factors were assessed using our RNA sequencing data and this data provided some further information for the interpretation of the results. A ≥2-fold up- or down-regulation was considered as a threshold to determine a significant change in gene expression. We observed three different main patterns of response, which are outlined below along with some examples which are provided for clarity:

1. *A discordance between gene expression and protein secretion (i.e. no significant change at RNA level with a significant increase or decrease in the levels of secreted proteins)*

In this pattern of response, there was no significant change in gene expression, but there was a significantly higher or lower protein concentration in the cell culture media of cells exposed to conditioned media of the other cell line relative to control (cells in serum free media). Our interpretation of this pattern of response is that the significant increase or decrease in protein concentration is mainly due to the concentrating or diluting effect of the conditioned media that were added to the treated cells.

An example is given in **Figure 3.21** which illustrates changes in FGF2 levels measured in cell culture supernatants of HEK293 cells. FGF2 protein levels were significantly higher in the culture media of HEK293 cells treated with KRJ-I conditioned media, compared to HEK293 cells in serum free media. There was a 0.91-fold change (p=0.11) in FGF2 gene expression in HEK293 cells treated with KRJ-I conditioned media (relative to control). Of note, the concentration of FGF2 protein in KRJ-I conditioned media was significantly higher (as shown in the graph) and it is likely that the increase observed in FGF2 protein levels reflects the relatively high FGF2 concentration in the KRJ-I conditioned media that were added to treat HEK293 cells.

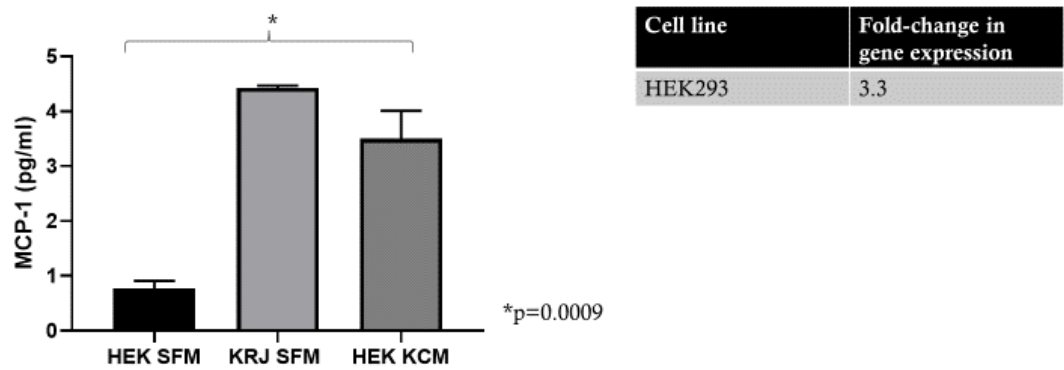| Cell line	Fold-change in gene expression
HEK293	0.91

*p<0.0001
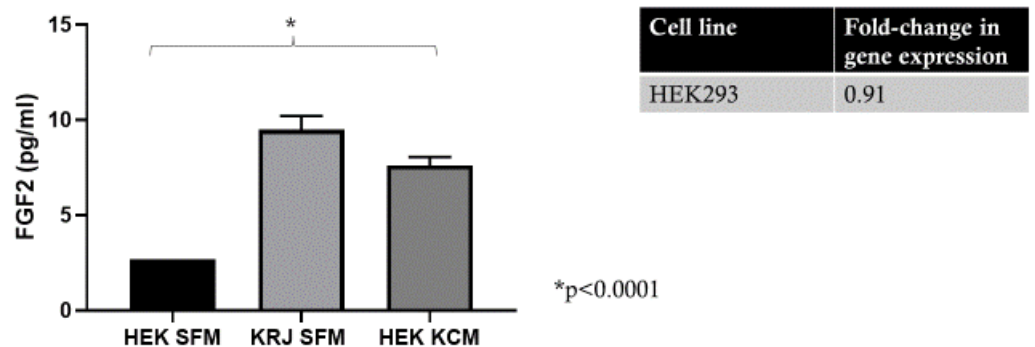
Figure 3.21. FGF2 concentration (pg/ml) in cell culture supernatants of HEK293 cells as measured with a 27-plex Luminex assay. FGF2 protein levels were significantly higher in culture media of HEK293 cells treated with KRJ-I conditioned media relative to control. In the absence of significant changes in FGF2 gene expression, this is likely to mainly reflect the significantly higher FGF2 concentration in the conditioned media that were added to the treated cells, as shown in the graph. An unpaired t-test was used for statistical comparison. Results are from 1 experiment with 3 samples per condition. HEK SFM indicates HEK conditioned media, KRJ-I SFM refers to KRJ-I conditioned media, and HEK KCM indicates culture media of HEK cells treated with KRJ-I conditioned media.

2. *A concordance between gene expression and protein secretion*

In this pattern of response, there was a significant change ($\geq$2-fold) in gene expression with a significant change in protein secretion in the same direction. For example, as shown in **Figure 3.22**, MCP-1 levels were significantly higher in cell culture media of HEK293 cells treated with KRJ-I conditioned media compared to control (HEK293 cells in serum free media). This change was accompanied by a significant upregulation (3.3-fold) in MCP-1 gene expression, which is likely to have contributed to the higher protein levels measured in cell culture supernatants. However, MCP-1 was also present in conditioned media of KRJ-I cells (as shown in the graph), that were added to treat HEK293 cells. Therefore, some of the measured MCP-1 in treated HEK293 cell culture supernatants may have conceivably been produced by KRJ-I cells. It is

difficult to be absolutely certain about the source of the MCP-1, as the *in vitro* half-lives of most cytokines in different experimental conditions are not known and also depend on handling and storage conditions[135].

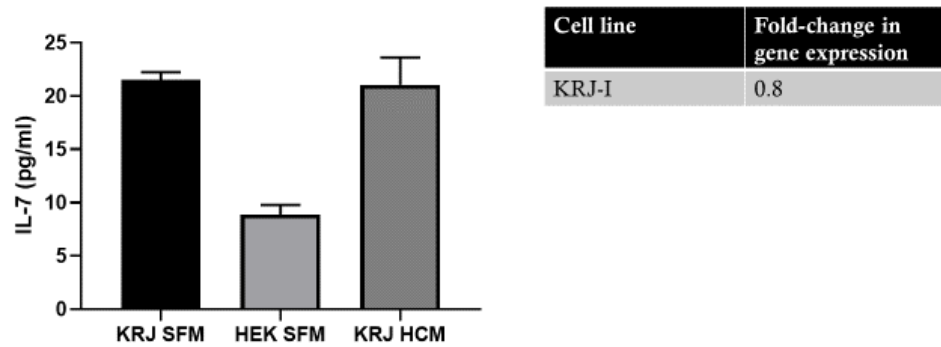| Cell line	Fold-change in gene expression
HEK293	3.3

*p=0.0009

Figure 3.22. MCP-1 concentration (pg/ml) in cell culture supernatants of HEK293 cells as measured with a 27-plex Luminex assay. MCP-1 levels were significantly higher in cell culture supernatants of HEK293 cells treated with KRJ-I conditioned media (relative to control) and a 3.3-fold upregulation was also noted in MCP-1 gene expression. Therefore, an increase in MCP-1 transcription appears to be accompanied by higher secretion of MCP-1 in cell culture supernatants, but the possibility that some of the measured MCP-1 protein derived from the KRJ-I conditioned media (that were added on treated HEK293 cells) cannot be excluded. An unpaired t-test was used for statistical comparison. Results are from 1 experiment with 3 samples per condition. HEK SFM indicates HEK conditioned media, KRJ-I SFM refers to KRJ-I conditioned media, and HEK KCM indicates culture media of HEK cells treated with KRJ-I conditioned media.

3. No significant changes in protein secretion

In this pattern of response, there was no significant change in protein secretion between treated cells and controls. This suggests that the crosstalk of cancer and stromal cells did not affect secretion of these cytokines/chemokines or growth factors. An example is shown in **Figure 3.23**. Here, there was no significant change in IL-7 secretion between KRJ-I cells treated with HEK293 conditioned media relative to control (KRJ-I cells in serum free media) ($p=0.7844$). Similarly, there was no

significant change in gene expression of IL-7 in treated KRJ-I cells relative to control (0.8-fold change, $p=0.15$).

Figure 3.23. IL-7 concentration (pg/ml) in cell culture supernatants of KRJ-I cells as measured with a 27-plex Luminex assay. No significant changes were observed at gene expression or protein secretion level in KRJ-I cells treated with HEK293 conditioned media compared to control (KRJ-I cells in serum free media). An unpaired t-test was used for statistical comparison. Results are from 1 experiment with 3 samples per condition. KRJ SFM indicates KRJ-I conditioned media, HEK SFM refers to HEK conditioned media and KRJ HCM indicates culture media of KRJ-I cells treated with HEK conditioned media.

Table 3.3 summarises the results of the 27-plex Luminex for measured cytokines/chemokines and growth factors in cell culture supernatants of KRJ-I, P-STS and HEK293 cells, which are grouped appropriately based on their pattern of response.

Pattern	KRJ-I (HCM vs SFM)	P-STS (HCM vs SFM)	HEK293 (KCM vs SFM)	HEK293 (PCM vs SFM)
1	IL-1β, IL-1ra, IL-6, IL-8, IL-9, IL-10, IL-13, IL-17A, Eotaxin, FGF2, G-CSF, IP-10, MCP-1, MIP-1, MIP-1B	IL-8	IL-6, IL-7, IL-8, IL-9, IL-10, IL-12, IL-13, IL-17A, Eotaxin, FGF2, PDGF-BB, MIP-1B, TNF	MCP-1
2		IP-10	IP-10, MCP-1	
3	IL-7, IL-12, PDGF-BB, TNF	IL-1β, IL-6, IL-7, IL-9, IL-10, MIP-1B, IL-17A, Eotaxin, FGF2, MCP-1, PDGF-BB, TNF	G-CSF	IL-1β, IL-6, IL-7, IL-8, IL-9, IL-10, IL-17A, Eotaxin, IP-10, PDGF-BB, MIP-1B, TNF

Table 3.3. Patterns of response in cytokine/chemokine and growth factor secretion in KRJ-I, P-STS and HEK293 cells. As described in the text, three main patterns of response were observed, when the RNA sequencing and 27-plex Luminex data were reviewed jointly for these cytokines/chemokines and growth factors. SFM: Serum Free Medium, HCM: HEK293 conditioned media, KCM: KRJ-I conditioned media, PCM: P-STS conditioned media.

3.4. Discussion

In our preliminary experiments, the crosstalk of neuroendocrine tumour and stromal cells was initially investigated using a co-culture model of BON-1 and HEK293 cells. As mentioned earlier, this model has the significant limitation that the BON-1 cell line is a pancreatic neuroendocrine tumour cell line and therefore it is not ideal for studying the mesenteric tumour microenvironment. A comparison of BON-1 with the small intestinal KRJ-I cells revealed significant differences in gene expression and receptor profile expression, wide variability in neuroendocrine marker transcript levels and substantially different responses in proliferative and secretory studies, suggesting that the BON-1 cell line is not an appropriate enterochromaffin cell neuroendocrine tumour model[125]. However, a recent study from Sweden questioned the authenticity of the KRJ-I cell line due to its lymphoblastoid phenotype, while the P-STS cell line was considered to represent a genuine small intestinal neuroendocrine tumour cell line[136]. Unfortunately, it is generally accepted that NET cell lines as a model for human cancer

have significant limitations, are often not widely available or well characterised and this poses significant challenges in basic science experiments aiming to delineate cancer biology[137]. However, our preliminary experiments with the BON-1 and HEK293 cells were important to demonstrate the feasibility of this study and optimise several aspects of the co-culture system prior to the collaboration with the University of Graz, which gave the unique opportunity to study the crosstalk of KRJ-I and P-STS cells with the fibroblastic HEK293 cells. These experiments have delineated further the complex interactions within the tumour microenvironment, and these dynamic processes seem to involve multiple signalling pathways and factors, sometimes with significant crosstalk involved in the regulation of downstream mediators. Certainly, these *in vitro* data would need to be validated in human tissue. However, our functional studies using appropriate cell line models of the mesenteric microenvironment provide the first in-depth analysis of the tumour-stromal interactions in this context and are a platform that can be utilised to investigate **pathways of disease**, instead of assessing single factors (such as CTGF or VAP-1) as in previous studies. This structured approach is more likely to advance our knowledge and improve our understanding of mesenteric fibrogenesis in SI NETs.

In our preliminary experiments we did not find a significant crosstalk between BON-1 and HEK293 cells. We did not identify any significant changes in cell proliferation or metabolic activity and there were only a few changes in gene expression in response to conditioned media of the other cell line. This is perhaps not surprising, considering the relative lack of stromal fibrosis in pancreatic NETs (pNETs). Although a so-called 'sclerosing variant' of pNETs has been described, it is rare and accounts for less than 15% of cases. This variant has distinct pathologic features and biomarker expression profiles, and a significantly higher percentage of these tumours are serotonin-secreting neoplasms compared with non-fibrotic pNETs[9]. In our experiments, we found that CCL2 expression was significantly upregulated in HEK293 cells after exposure to BON-1 conditioned media. CCL2 (also known as monocyte chemoattractant protein-1 [MCP-1]) is a potent monocyte-attracting chemokine, which plays an important role in tumour-stromal interactions and is known to promote tumour progression[138]. MCP-1 has several key roles in tumorigenesis, due to its ability to directly stimulate proliferation, cell migration and angiogenesis[138]. In BON-1 cells NFKB2 expression was significantly upregulated, while IL-8 expression was downregulated in response

to HEK293 conditioned media. NFKB2 is a transcription factor that regulates inflammation, survival, proliferation and other biological processes. It has been previously shown (in a mouse model) that increased NFKB2 activity can lead to fatal lung inflammation, characterised by diffuse alveolar damage, marked peribronchial fibrosis and a significant accumulation of myofibroblasts in the lungs[139,140]. Cytokines (such as IL-8, IL-6 and other molecules) are secreted in the tumour microenvironment by both cancer and stromal cells and are also known to play an important role in inflammation and tumour progression[141]. We observed a downregulation of IL-8 in BON-1 cells (in response to HEK293 conditioned media) and no other changes in gene expression were detected as a result of the BON-1/HEK293 crosstalk. These findings are in keeping with the rare development of fibrosis in pancreatic neuroendocrine tumours[9].

There are only a few studies in the literature that have investigated the crosstalk of neuroendocrine tumour and stromal cells. As mentioned earlier, Svejda *et al* used a Transwell co-culture system to investigate the cross-talk of small intestinal KRJ-I cells and HEK293 stromal cells[21]. The authors demonstrated that targeting the 5-HT2B receptor of KRJ-I cells with an antagonist (PRX-08066) led to inhibition of proliferation and serotonin secretion, as well as reduced synthesis of profibrotic growth factors (TGFβ1, CTGF, FGF2). In addition, this led to inhibition of proliferation and reduced synthesis of profibrotic growth factors (TGFβ1, CTGF, FGF2) in HEK293 cells despite the absence of a 5-HT2B receptor in these cells, suggesting that there is a cross-talk between cancer and stromal cells which contributes to the development of fibrosis[21]. An older study by Beauchamp et al investigated the effect of BON-1 conditioned media on AKR-2B (mouse) fibroblasts[126]. The authors showed that BON-1 conditioned media stimulated DNA synthesis, soft agar growth and TGFβ1 and fibronectin gene expression in AKR-2B fibroblasts. They also demonstrated the presence of several different molecules in the BON-1 conditioned media, including TGFβ1, TGFβ2, TGFβ3, TGFα, PDGF-β chain and basic FGF (also known as FGF2). The authors suggested that this model provided evidence that multiple growth factors are involved in the desmoplastic reaction accompanying carcinoid tumours. Of course, there are several significant limitations to this study, which do not make it representative of the mesenteric tumour microenvironment of

midgut NETs, such as the use of a pancreatic neuroendocrine tumour cell line (not of small intestinal origin) and mouse fibroblasts (not of human origin).

In view of the limited literature in this research area, in collaboration with the University of Graz, we performed a detailed assessment of the crosstalk of SI NET cell lines KRJ-I and P-STS with the stromal cell line HEK293. We observed a significant reduction in cell metabolic activity of KRJ-I and P-STS cells in response to HEK293 conditioned media, but the physiological significance of this finding is unclear, particularly as there was no change in cell proliferation. On the other hand, HEK293 cell proliferation and metabolic activity did not change significantly upon exposure to KRJ-I and P-STS conditioned media.

The RT PCR Profiler arrays revealed that several changes in gene expression occurred as a result of the paracrine effect. **KRJ-I cells exposed to HEK293 conditioned media demonstrated a significant upregulation of the following genes: PIK3R1, MAPK1, MAP2K1, NF-κB2, ITGAV and MAX.** The first 3 of these genes encode proteins that are components of the MAPK (mitogen-activated protein kinases) and mTOR (mammalian target of rapamycin) pathways (**Figures 3.24 and 3.25**), suggesting that these pathways are activated in KRJ-I cells during tumour-stromal interactions. Both these pathways have a central role in the pathophysiology of carcinogenesis, as they regulate critical biological functions, such as cell survival, proliferation, angiogenesis and 'death-related' pathways (apoptosis and autophagy)[97,142,143]. There is also significant cross-talk between these pathways via feedback loops[142,144]. The **PIK3R1** gene encodes the regulatory unit of PI3K (Phosphatidylinositol 3-kinase), known as p85α. PI3K also has a catalytic unit (PIK3CA or p110α). PI3K is considered a key upstream component of the mTOR pathway (**Figure 3.24**), which is known to be activated in both SI NET cell lines (KRJ-I, P-STS, L-STS and H-STS)[144] and neuroendocrine tumours[145]. The mTOR inhibitor everolimus has also been shown to be effective in the clinical management of non-functioning small bowel NETs[146,147], although it is not known to affect the desmoplastic reaction in the mesentery. The **MAPK1** (mitogen-activated protein kinase 1) gene encodes the ERK2 (extracellular signal-regulated kinase 2) protein, which is a downstream mediator of the MAPK pathway[143,148], and **MAP2K1** encodes the MEK1 (mitogen-activated protein/extracellular signal-regulated kinase 1) protein, which together with MEK2, are the exclusively specific activators of ERK1/2[143]

(**Figure 3.25**). The MAPK pathway is known to play a critical role in neuroendocrine neoplasia[97,144], as well as in other cancers[143], due to its known ability to regulate multiple physiological processes, such as cell proliferation, differentiation, invasion and metastasis[97,143].
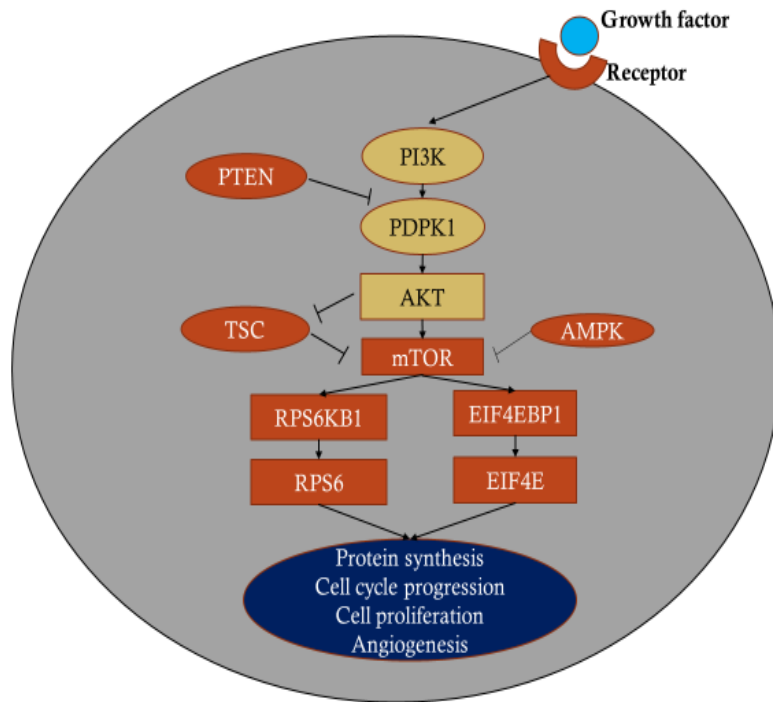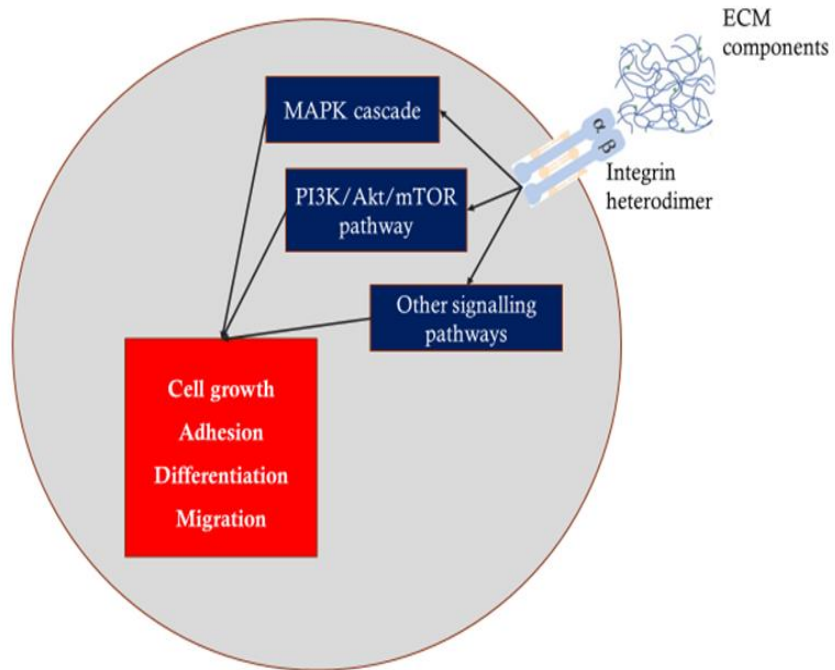

Figure 3.24. Simplified schematic overview of the mTOR pathway. Extracellular stimuli (such as growth factors) regulate the mTOR pathway. Activation of this pathway may alter several cellular processes, such as cell proliferation and protein synthesis. AMPK: 5'-adenosine monophosphate-activated protein kinase, PI3K: Phosphatidylinositol 3-kinase, PDPK1: 3-phosphoinositide dependent protein kinase 1, mTOR: mammalian target of rapamycin, TSC: Tuberosis sclerosis complex, EIF4EBP1: eukaryotic translation initiation factor 4E-binding protein, RPS6KB1: ribosomal protein S6 kinase, RPS6: ribosomal protein S6.
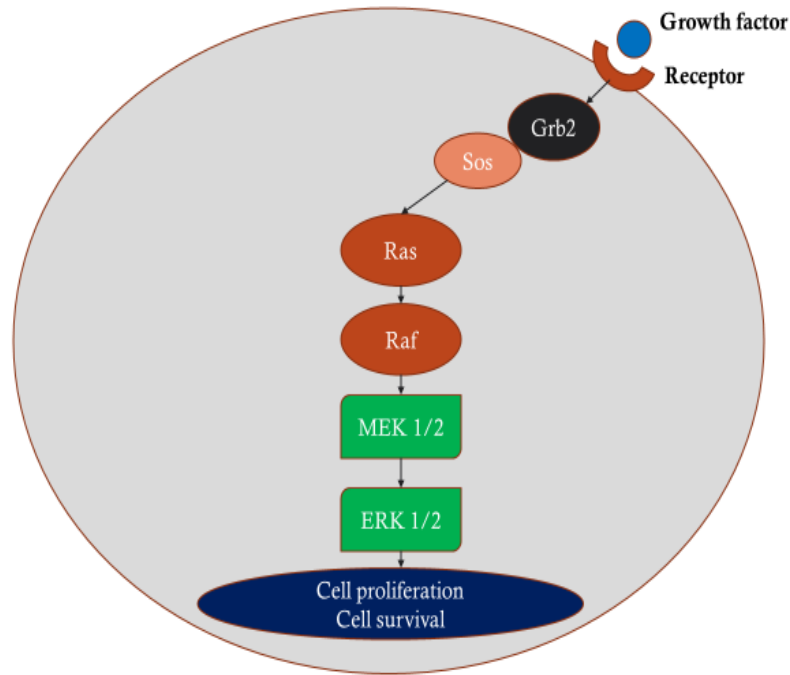
Figure 3.25. Simplified schematic overview of the Raf/MEK/ERK pathway. Extracellular stimuli (such as growth factors) regulate the Raf/MEK/ERK pathway typically via the adapter protein Grb2 (Growth factor receptor-bound protein 2), the guanine nucleotide exchange factor Sos (Son of sevenless) and the small GTPase, Ras. Activation of this pathway results in increased cell proliferation and cell survival. MEK: mitogen-activated protein/extracellular signal-regulated kinase, ERK: extracellular signal-regulated kinase.

The **ITGAV** (integrin subunit alpha v) gene encodes integrin αv. Integrins are a family of transmembrane receptors composed of two subunits, α and β[149]. These receptors allow the interaction of cells with the extracellular matrix and play important roles in cell signalling[149]. Several signalling pathways (including MAPK and mTOR) are activated by integrin αv, which may regulate a wide range of cellular processes in cancer biology, including proliferation, chemotaxis, epithelial-to-mesenchymal transition, invasion and metastasis[149-151] (**Figure 3.26**). The integrin pathway was also shown in the IPA analysis to be significantly activated in KRJ-I cells treated with HEK293 conditioned media (**Figure 3.15**) and will be discussed in more detail later.

Figure 3.26. Simplified schematic overview of the integrin pathway. The ECM contains matrix (e.g. collagens, fibronectin) and non-matrix proteins (e.g. growth factors such as TGFβ). These can interact with the integrin receptors, which can transmit 'outside-in' signals via multiple downstream pathways, including the MAPK and mTOR pathways. These pathways affect multiple cellular processes ultimately leading to cancer progression. Integrins are also involved in a complex cross-talk with TGFβ, as well as in 'inside-out' signalling, whereby receptor activation can alter integrin-binding capacity[152,153].

The **NF-κB2** gene encodes NF-κB2/p52, which is generated from a large precursor protein known as p100 via the non-canonical NF-κB pathway[154]. NF-κB2/p52 is a transcription factor which does not act as a single protein, but instead forms NF-κB dimers with other NF-κB proteins. Upon activation of the NF-κB pathway by specific stimuli these dimers are able to translocate to the nucleus and activate the transcription of target genes, which are involved in immunity, inflammation and cell survival[154]. Therefore, sustained activation of the NF-κB pathway is implicated in the development of autoimmune diseases and cancer, particularly haematological malignancies[154]. The pathway 'NF-κB activation by viruses' was activated in KRJ-I cells treated with HEK293 conditioned media, as shown in the IPA analysis (**Figure 3.15**), suggesting that the activation of this pathway may be important in the cross-talk of SI NET and stromal cells. In addition, it is interesting that in our preliminary

experiments this gene was also found to be upregulated in BON-1 cells treated with HEK293 conditioned media.

The **MAX** (Myc-associated protein X) gene encodes Max, which acts as a partner for Myc and together these proteins form a dimeric transcription factor, that regulates the expression of multiple genes. The Myc/Max complex targets genes that are involved in a wide range of biological processes, including ribosome biogenesis, protein translation, cell-cycle progression and metabolism, and therefore regulate multiple functions, such as cell proliferation, survival and differentiation (**Figure 3.27**)[155]. It is also interesting that Myc protein translation is activated by mTORC1 (mTOR complex 1)[155], a downstream mediator of the mTOR pathway, which is activated in KRJ-I cells (as described earlier).
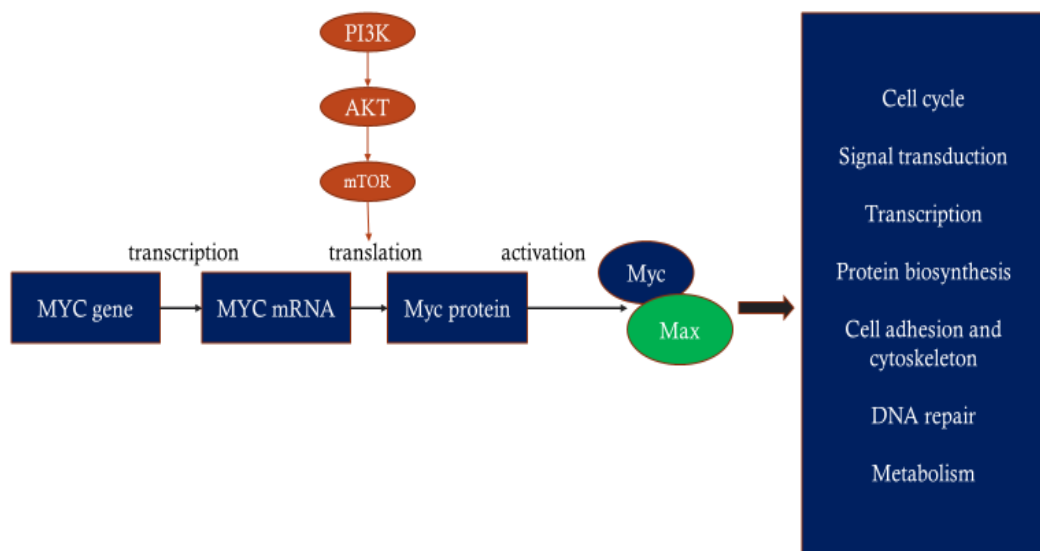
Figure 3.27. The Myc oncoprotein can regulate a wide range of cellular biological processes by altering the transcription of multiple genes (thus called a 'super-transcription factor'). This requires an activated mTOR pathway and dimerization with its partner, **Max**, with which it forms a heterodimeric transcription factor, known as the Myc-Max complex.

The RT Profiler 'Molecular Mechanisms of Cancer' revealed that in P-STS cells treated with HEK293 conditioned media, the following genes were significantly down-regulated: Grb2 and FADD. The **Grb2** gene encodes the Grb2 (Growth factor receptor-bound protein 2), which was briefly mentioned in **Figure 3.25**. This is a key

adaptor protein involved in intracellular signal transduction, linking cell surface receptors to downstream signalling pathways, such as the MAPK cascade. It is known to play a critical role in oncogenesis, due to its ability to affect many cellular processes involved in the multi-step cascade of cancer metastasis, such as cell adhesion, extracellular matrix remodelling, cell motility, tumour angiogenesis and tumour cell dissemination[156]. Thus, the downregulation of Grb2 seems paradoxical, as it would have a protective effect against tumour growth. On the other hand, **FADD** (Fas-associated via death domain) is another cytosolic adaptor protein, which is recruited to ligated death receptors, such as Fas (**Figure 3.28**). It is involved in apoptosis signalling due to its ability to interact with pro-caspase 8, which is then activated to caspase 8. This in turn can activate downstream executioner caspases 3 and 7, which can lead to apostosis[157,158]. Therefore, the downregulation of FADD would usually promote tumour growth through inhibition of apoptosis. Although FADD is a critical mediator of cell death pathways, it may in some cases promote cell growth through activation of NF-κB signalling pathways, but this is less common[157,158].
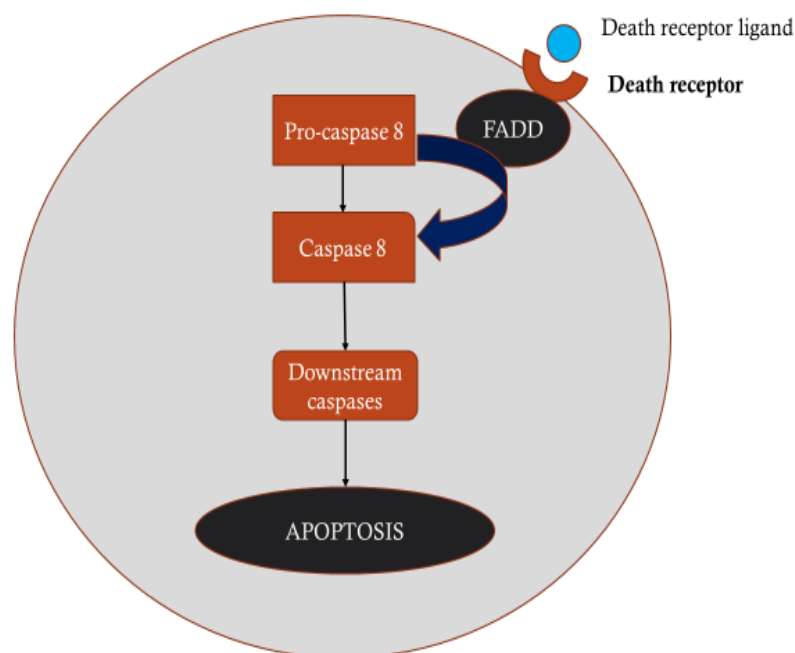
Figure 3.28. Simplified schematic overview of the extrinsic pathway of apoptosis mediated by FADD. Upon ligand binding on a death receptor (such as Fas receptor by its ligand FasL) FADD is recruited to the cell surface and activates caspase 8. Caspase 8 catalyses the activation of downstream caspases that induce apoptotic cell death.

The Human Fibrosis RT PCR Profiler was applied to HEK293 cells. **HEK293 cells exposed to KRJ-I conditioned media exhibited a significant downregulation of MMP8, TGFβ3 and ITGB8**. **MMP8** (metalloproteinase 8), also known as collagenase-2, is a metalloproteinase that has the ability to degrade fibrillar collagens, as well as other substrates, such as other extracellular matrix proteins, proteases, growth factors and chemokines[159]. It is involved in a wide range of inflammatory disorders, in which it is usually associated with progression of inflammation, while in cancer a dual role of MMP8 (tumorigenic and tumour suppressive) has been reported[160]. Although the precise role of MMP8 in cancer progression seems to depend on the type and stage of the tumour, in most cases wild-type MMP8 exhibits a tumour suppressive activity by inhibiting cell migration, invasion and metastasis. However, mutant MMP8 enhances tumorigenic phenotypes[160]. Therefore, the downregulation of MMP8 in HEK293 cells suggests that these cells could exert a pro-proliferative effect on cancer cells (in a paracrine manner). In addition, **TGFβ3** was downregulated in treated HEK293 cells and this reflects a profibrotic response, as TGFβ3 is known to have antifibrotic effects in several conditions, such as wound healing and systemic sclerosis[161,162]. Furthermore, **ITGB8**, which was downregulated in HEK293 cells treated with KRJ-I conditioned media, is involved in the synthesis of integrin αvβ8. This integrin acts as a cell surface receptor for the latency-associated peptide (LAP) of TGFβ. Binding of latent (inactive) TGFβ to αvβ8 leads to recruitment of the metalloproteinase 14 (MMP14), which cleaves the LAP peptide and therefore activates TGFβ with induction of fibrosis[163]. Therefore, reduction of ITGB8 expression in HEK293 cells suggests an antifibrotic effect.

In this in vitro model no changes were seen in gene expression in HEK293 cells exposed to P-STS conditioned media using the Human Fibrosis RT Profiler. This suggests a weak paracrine effect in this direction.

In addition, the IPA analysis provided information about specific signalling pathways that are activated or inhibited in these cell lines as a result of the paracrine effect. In **KRJ-I cells treated with HEK293 conditioned media**, the following pathways were activated: NF-κB activation by viruses, Tec kinase signalling, dendritic cell maturation, TREM1 signalling, role of NFAT in regulation of the immune response, cdc42 signalling, PI3K signalling in B lymphocytes, TNFR1 signalling, integrin signalling, neuroinflammation signalling pathway, IL-8 signalling, cardiac

hypertrophy signalling and phospholipase signalling, while the RhoGDI signalling pathway was inhibited (see **Figure 3.15**).

The **integrin signalling pathway** is of particular interest, as several components of this pathway were also shown to be upregulated at gene expression level in KRJ-I cells in the Molecular Mechanisms of Cancer RT Profiler (**Figure 3.11**). This pathway was shown to be significantly activated in our RNA sequencing and IPA analysis data (**Figure 3.29**).
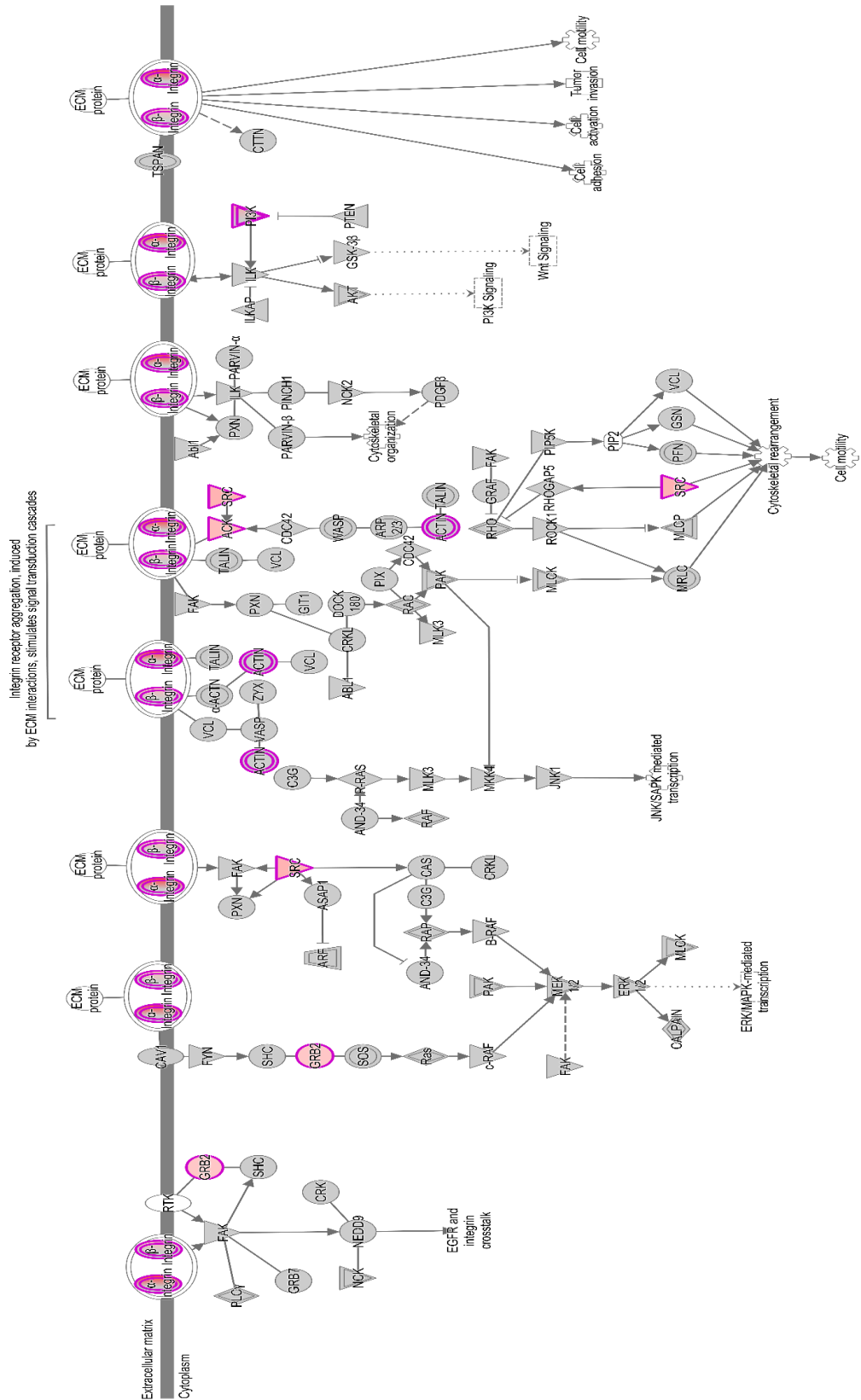
Figure 3.29. Activation of the integrin pathway in KRJ-I cells treated with HEK293 conditioned media. As shown in the figure, this pathway involves downstream activation of the MAPK, mTOR and

97

other signalling cascades that ultimately affect multiple cellular processes, such as tumour invasion, cell motility and adhesion.

The integrin pathway is a complex pathway, and a more simplified representation is provided in **Figure 3.26**. As previously mentioned, integrins consist of an α and β-subunit and form transmembrane proteins, which bind extracellularly to ECM components, such as fibronectin and several members of the laminin and collagen families[164]. They transduce signals into the cell ('outside-in' signalling) via multiple signalling pathways, including the Ras/Raf/MEK/ERK and mTOR pathways, which were also shown to be transcriptionally active in treated KRJ-I cells. These pathways regulate a wide range of cellular processes, including cell adhesion, proliferation, survival and migration, which contribute to cancer progression[165,166]. In addition, there is extensive crosstalk between integrins and TGFβ signalling, which is important in both cancer progression and fibrosis development[164]. Integrins also participate in 'inside-out' signalling, whereby receptor activation can regulate integrin-binding activity[152,153]. The integrin pathway is investigated *in vivo* in **Chapter 4**. Although this pathway is known to contribute to cancer progression in other cancers[164,166], its role in the mesenteric microenvironment of carcinoid tumours has not been previously explored. It is interesting however that a recent study by Bosch and colleagues demonstrated that patients with small bowel NETs associated with a desmoplastic reaction are a more aggressive cohort with a significantly shorter progression-free survival, and a higher prevalence of distant metastases, lymphatic vessel and perineural invasion compared to patients with non-fibrotic tumours[118]. We have also shown recently that mesenteric fibrosis is associated with a significantly shorter overall survival in patients with advanced midgut NETs[11] (see **Chapter 2**), and it is possible that the fibrotic microenvironment may mediate tumour progression by this and other pathways in these tumours.

NF-κB activation by viruses is another pathway that was activated in KRJ-I cells treated with HEK293 conditioned media (**Figure 3.30**). This pathway is known to be activated by oncogenic viruses and particularly human T-cell leukaemia virus 1 (HTLV1), Kaposi sarcoma-associated herpesvirus (KSHV), and Epstein-Barr virus (EBV). These viruses encode specific oncogenic proteins that are able to activate the NF-κB pathway via the canonical and non-canonical route[167]. Deregulation of the NF-κB pathway is known to lead to abnormal transcription of multiple target genes,

involved in inflammatory and immune responses, as well as in cell survival and proliferation. As a result, activation of this pathway by oncogenic viruses is associated with the development of wide range of malignancies, such as adult-T cell leukaemia (HTLV-1), Kaposi sarcoma (KSHV) and Burkitt's lymphoma (EBV)[167]. Therefore, this pathway may also play a role in the survival and growth of cancer cells within the fibrotic microenvironment of midgut NETs.
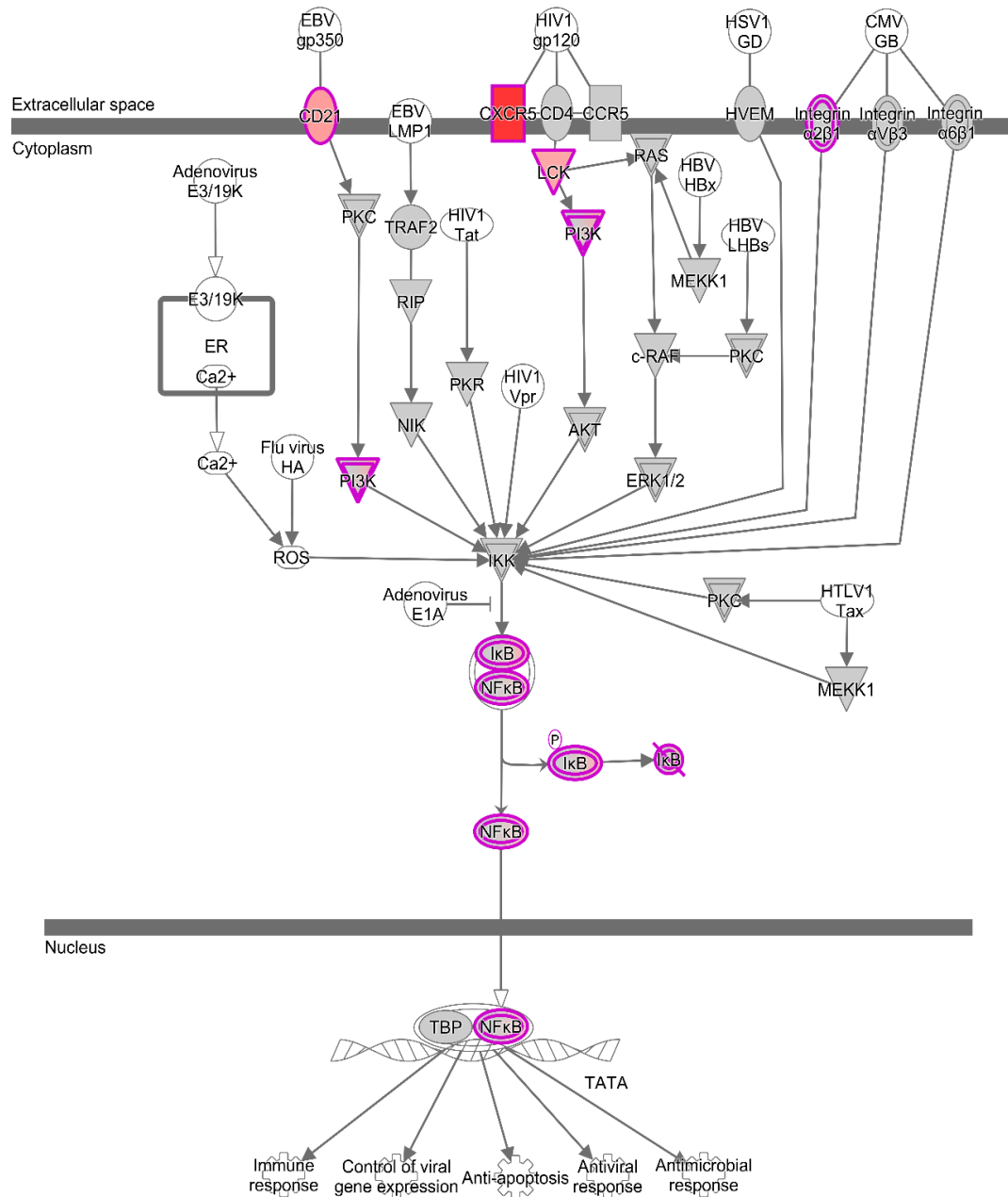
Figure 3.30. Schematic representation of the NF-κB activation by viruses pathway, that was found to be activated in KRJ-I cells treated with HEK293 cells. As shown in the figure, this pathway can

be activated by a variety of oncogenic viruses (such as EBV, HSV, CMV and HIV), which through various signalling cascades can promote nuclear translocation of NFκB. This in turn leads to transcription of multiple genes that control many cellular processes, such as anti-apoptosis and the immune response.

In addition, the **Tec kinase signalling pathway** was found to be activated in treated KRJ-I cells. Tec kinases are a family of non-receptor tyrosine kinases, which are known to play a role in lymphocyte development and transformation[168]. They can be activated by binding of various antigens on antigen receptors of B- and T-lymphocytes, as well as by other types of receptors, such as integrins and receptor tyrosine kinases. Tec kinases can lead to activation of multiple downstream mediators (such as NF-κB and PLCγ [phosphoinositide phospholipase C]), which can control a wide range of cellular processes, including cell survival and proliferation, and constitutive activation of this pathway is associated with lymphoproliferative disorders[168]. Here, it is interesting to mention the recent paper by Hofving *et al* which reviewed the phenotype of gastroenteropancreatic (GEP) NET cell lines and concluded that KRJ-I cells are of lymphoblastoid origin[136]. This will be discussed later in some more detail.

The **dendritic cell maturation** was another pathway, which was activated in treated KRJ-I cells. This is a complex pathway (**Figure 3.31**), which is critical for dendritic cell maturation. Dendritic cells are characterised as the 'gatekeepers of the immune system', but this ability depends on a cellular differentiation program, called 'maturation', which allows them to activate antigen-specific naïve T-cells[169-171]. Dendritic cells play an important and complicated role in cancer. They normally have the ability to induce anti-tumour immunity and control tumour growth, but often the tumour microenvironment can reduce their survival and functionality, or may alter their activity towards an immunosuppressive and tolerogenic phenotype that may support tumour progression[169]. Although at first sight it seems strange that the dendritic cell maturation pathway is activated in cancer cells (which do not undergo this cellular process), this pathway exerts many of its effects by downstream activation of the canonical and non-canonical NFκB pathways. As shown in **Figure 3.31**, we believe that the main reason why this pathway is 'activated' in the IPA analysis is the fact that many components of the canonical and non-canonical NF-κB pathways are activated in KRJ-I cells. The IPA analysis was performed using a 'generic' approach,

but when a more 'tissue-specific' approach was used, the NF-κB activation by viruses pathway remained significantly activated in KRJ-I cells, while the dendritic cell maturation pathway was no longer significantly activated (**Figure 3.32**).

Figure 3.31. Overview of the dendritic cell maturation pathway, that was activated in treated KRJ-I cells.
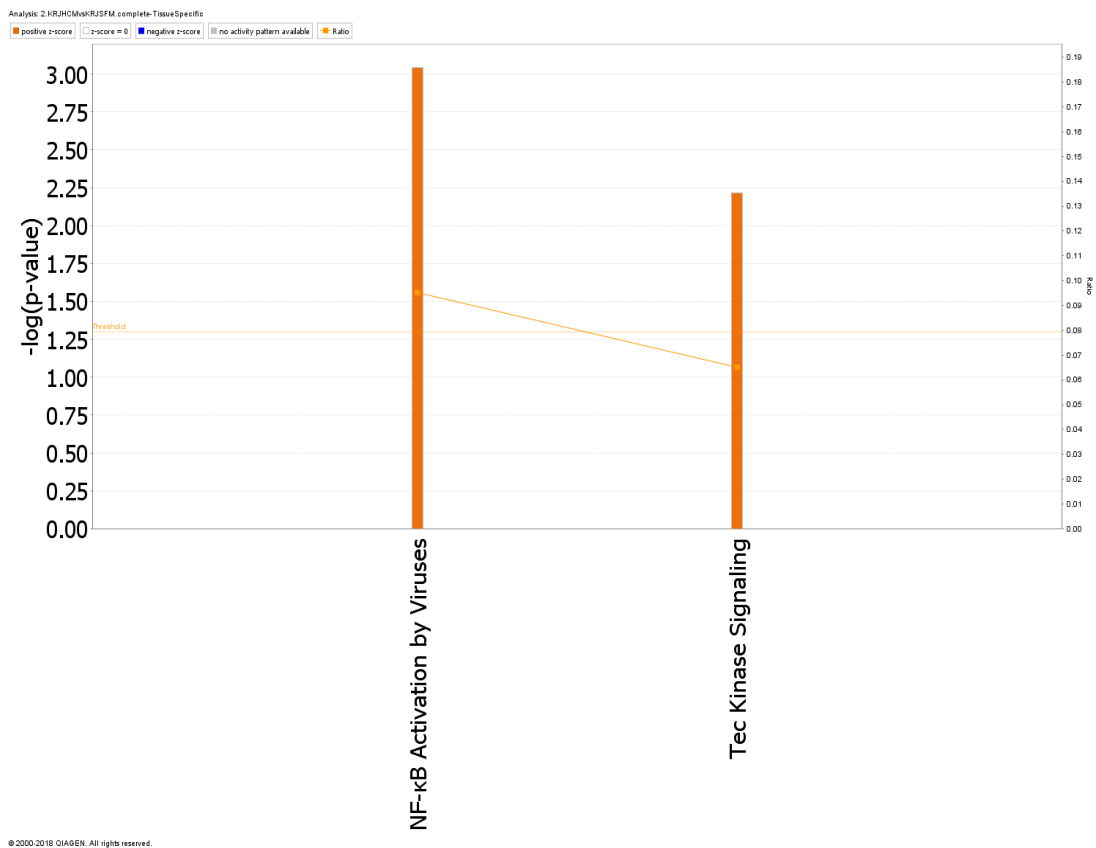
Figure 3.32. 'Tissue-specific' IPA analysis of pathways activated in KRJ-I cells treated with HEK293 conditioned media. This was based on a specific selection of options (see methodology section) and showed that the dendritic maturation pathway was no longer significantly activated based on a more stringent search, as this is not a cancer-specific pathway.

Furthermore, the **TREM-1 signaling pathway** was found to be activated in KRJ-I cells in response to HEK293 conditioned media. This pathway is known to play a role in the inflammatory response of myeloid cells[172]. The TREM-1 receptor (triggering receptor expressed on myeloid cells-1) is able to phosphorylate (upon its activation) multiple proteins, including the adaptor protein DAP12 (DNAX activation protein of 12kDa), phospholipase Cγ, ERK1/2 and NF-κB (via the canonical pathway), which ultimately lead to the transcription of genes involved in inflammation, such as cytokines and chemokines[172]. In addition, the TREM-1 pathway is able to induce reactive oxygen species (ROS) production, which can lead to apoptosis in neutrophils[172]. Therefore, this pathway may have a role in cancer development by maintaining an inflammatory response within the tumour microenviroment, which is important for cancer progression.

The **role of NFAT in regulation of the immune response** and **phospholipase signalling** are closely linked pathways that were found to be activated in KRJ-I cells as a result of the paracrine effect. NFAT (nuclear factor of activated T-cell) is a transcription factor that is regulated by the phosphatase calcineurin, which controls its transport from the cytoplasm to the nucleus by dephosphorylation (**Figure 3.33**). NFAT proteins are able to alter target gene expression, which is important in many physiological and pathological biological processes, including regulation of the immune system, inflammation, angiogenesis and development and metastasis of cancer[173]. As shown in **Figure 3.33**, activation of the NFAT pathway starts with receptor activation (e.g. Toll-like receptors, G-coupled receptors etc.) which leads to phospholipase C activation. This process catalyses the hydrolysis of PIP2 (phosphatidylinositol-4,5-bisphosphonate) to DAG (diacylglycerol) and IP3 (inositol-1,4,5-triphosphate). DAG activates PKC (protein kinase C), which in turn can activate a number of signalling pathways (e.g. Ras/Raf/ERK, NF-κB, Akt), that play important roles in carcinogenesis and metastasis[174]. On the other hand, IP3 binds to its receptor (IP3R) on the endoplasmic reticulum (ER), resulting in calcium efflux from the ER to the cytoplasm. This activates the calcium sensor STIM, which binds and activates a channel (Orai1) in the plasma membrane, that allows influx of calcium and formation of the calcium/calmodulin/calcineurin complex. This complex dephosphorylates NFAT, which can translocate to the nucleus and lead to target gene transcription. These genes play important roles in inflammatory disorders, and in cancer development, cell proliferation, angiogenesis, metastasis and drug resistance[173,175]. The NFAT pathway is also known to interact with other major oncogenic pathways[173]. Therefore, this pathway may play a role in the growth of neuroendocrine tumours within the fibrotic microenvironment.
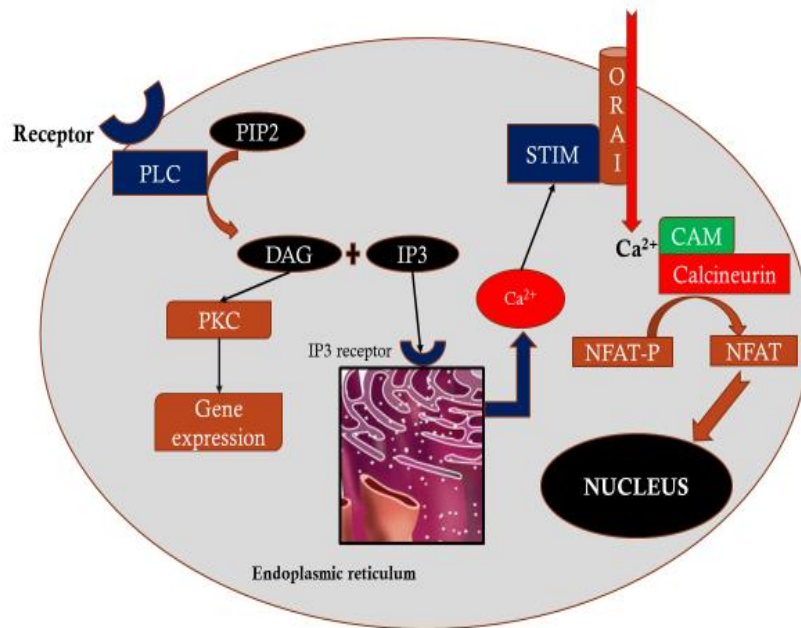
Figure 3.33. Simplified schematic overview of the NFAT and phospholipase pathways, which are activated in KRJ-I cells in response to HEK293 conditioned media. DAG: diacylglycerol; IP3: inositol-1,4,5-triphosphate; NFAT: nuclear factor of activated T-cell; PIP2: phosphatidylinositol-4,5-bisphosphonate.

In addition, the **cdc42 signalling** pathway was activated, while the **RhoGDI signalling** pathway was inhibited in KRJ-I cells exposed to HEK293 conditioned media. These two pathways are very closely linked and will be discussed together. The Rho GTPases, such as Cdc42 and RhoA, are Ras-related small GTP-binding proteins that perform several important cellular functions, such as regulation of cell morphology and motility, transcriptional regulation and ROS production[176]. Their activation is controlled by a number of regulatory factors, as shown in **Figure 3.34**. Inactive cdc42-GDP binds to GDI (guanine nucleoside dissociation inhibitor). The dissociation from GDI is accomplished by GDF (GDI displacement factor), which in turn allows GEF (guanine nucleotide exchange factor) to incorporate GTP to cdc42. Active cdc42 is then able to bind to effector proteins and initiate various signalling pathways, which regulate multiple cellular functions. GAP (GTPase activating protein) acts as a negative regulator of cdc42 signalling[177]. Deregulation of the cdc42 signalling pathway can lead to several pathogenic processes related to cancer, such as cellular transformation, changes in cell metabolism, formation of invadopodia and filopodia, invasion and cell migration[177].
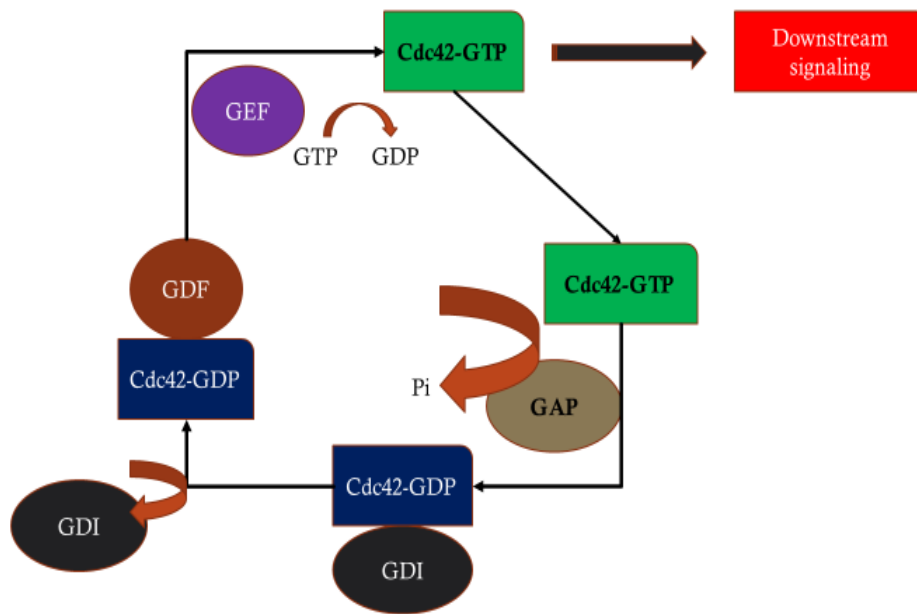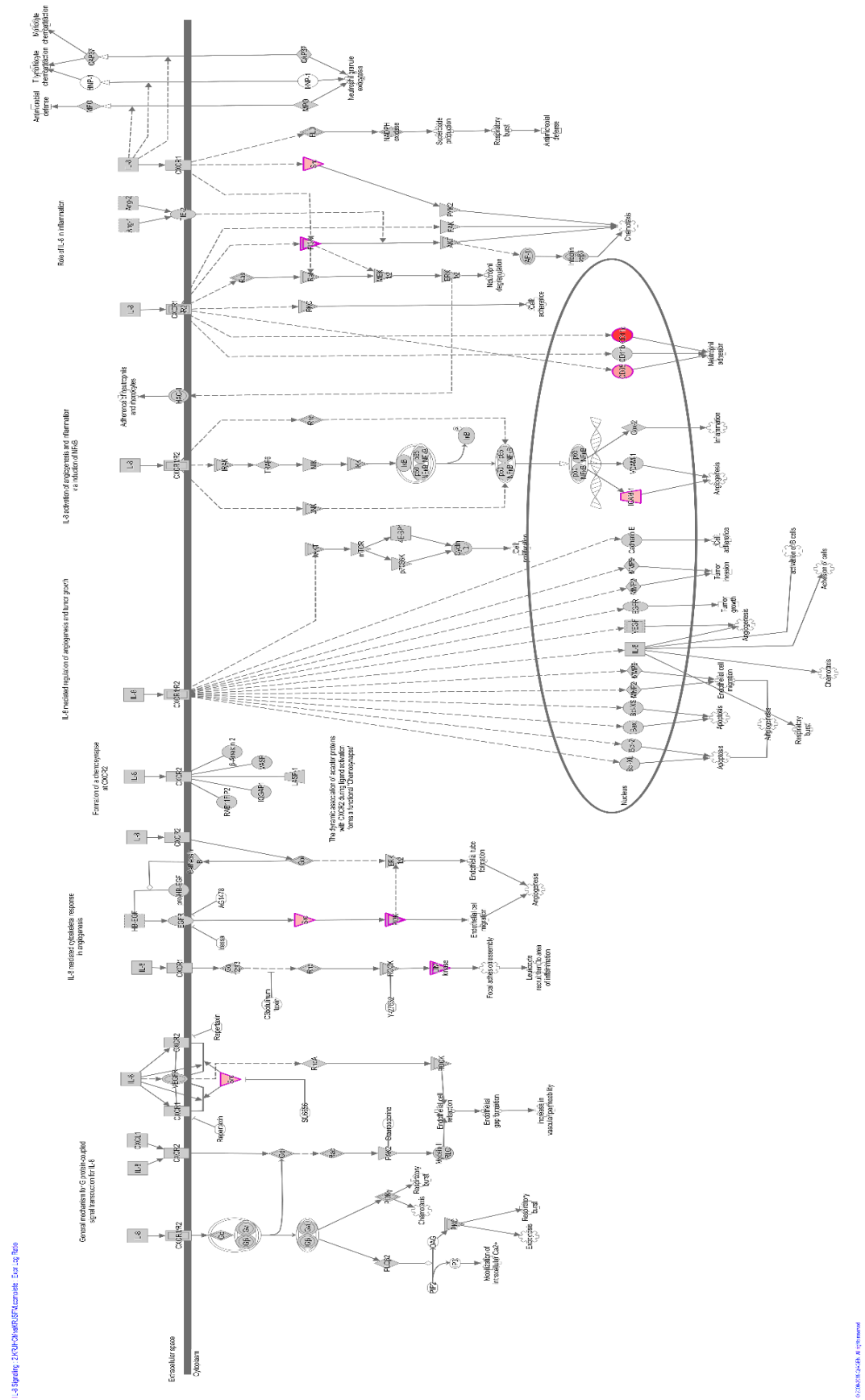
Figure 3.34. Simplified schematic overview of the regulation of Rho GTPases. Activation of the Cdc42 pathway can initiate multiple downstream pathways that affect a wide range of cellular functions, such as cell division, enzyme activity and cell adhesion[177]. GDI: guanine nucleoside dissociation inhibitor; GDF: GDI displacement factor; GEF: guanine nucleotide exchange factor; GAP: GTPase activating protein.

In addition, the **PI3K signalling in B lymphocytes** was activated in KRJ-I cells treated with HEK293 conditioned media. This pathway has been presented previously (see **Figure 3.24**). In B lymphocytes PI3K signalling is initiated downstream of the B-cell receptor and it plays an important role in B cell growth and proliferation[178]. It is known to regulate B cell development and differentiation, cell metabolism and mitochondrial function. Pathological activation of this pathway is associated with the development of B cell-derived malignancies, such as diffuse large B cell lymphomas[178]. As mentioned earlier, the PI3K-Akt-mTOR pathway is also involved in other cancers, including neuroendocrine neoplasms, and its activation within the fibrotic microenvironment of midgut NETs needs to be validated *in vivo*.

TNFR1 signalling pathway is another pathway that was found to be activated in KRJ-I cells in response to the paracrine effect. TNF is a growth factor involved in the pathogenesis of many inflammatory disorders, including inflammatory bowel disease

and rheumatoid arthritis. By binding to its receptor TNFR1, it can activate the canonical NF-κB pathway and lead to the transcriptional upregulation of many proinflammatory genes[179]. This pathway has two sequential "cell death checkpoints", and if these are disrupted (under pathological conditions), this pathway can induce apoptosis and necroptosis[179]. Therefore, the usual role of this pathway is the development of an inflammatory response and the transduction of survival signals, which are clearly important for cancer progression.

The **IL-8 signalling pathway** was also significantly activated in KRJ-I cells treated with HEK293 conditioned media. This is a complicated pathway and is shown in **Figure 3.35**. IL-8, also known as CXCL8 (C-X-C motif ligand 8), is a chemokine that is produced by many cell types and can bind to two receptors, CXCR1 (IL-8RA) and CXCR2 (IL-8RB). These receptors are then able to initiate a number of signalling cascades, the most important of which are the PI3K/Akt, phospholipase C/protein kinase C (PLC/PKC) and Ras/Raf/ERK pathways[180]. These pathways regulate critical cellular functions and ultimately lead to cell proliferation, invasion, angiogenesis and metastasis[180]. IL-8 is upregulated in a wide range of malignancies, including breast, prostate, lung and ovarian cancer, due to its ability to contribute to multiple hallmarks of cancer[180], but its role in neuroendocrine neoplasia within the fibrotic microenvironment has not been previously explored.

Figure 3.35. Schematic overview of the IL-8 signalling pathway, which was activated in KRJ-I cells in response to HEK293 conditioned media. As shown in the figure, IL-8 binds to its receptors

(CXCR1 and CXCR2) and can thereby initiate several signalling cascades, the most important of which are the PI3K/Akt, phospholipase C/protein kinase C (PLC/PKC) and Ras/Raf/ERK pathways. These pathways regulate critical cellular functions and ultimately lead to cell proliferation, invasion, angiogenesis and metastasis.

The **neuroinflammation signalling pathway** was also activated in treated KRJ-I cells. This is also another complicated pathway (**Figure 3.36**) which is involved in immune and inflammatory responses in the central nervous system and the pathophysiology of neurodegenerative diseases[181]. This pathway is activated in macrophages in the central nervous system (called microglia) in response to pathogens, infection or injury, and leads to the production of inflammatory mediators and chemokines (such as IL-1β and TNFα), which cause neuronal dysfunction, damage and cell death[181]. Multiple signalling cascades are activated downstream of cell surface receptors, including the PI3K/Akt, MAPK and NF-κB pathways, which lead to transcription of proinflammatory genes. In addition, the neuroinflammation pathway leads to the production of ROS and gaseous signalling molecules (nitric oxide), which also contribute to cell death and inflammation[181]. Whether these pathways contribute to inflammation within the cancer microenvironment of midgut neuroendocrine tumours and therefore promote tumour growth needs to be investigated *in vivo*.
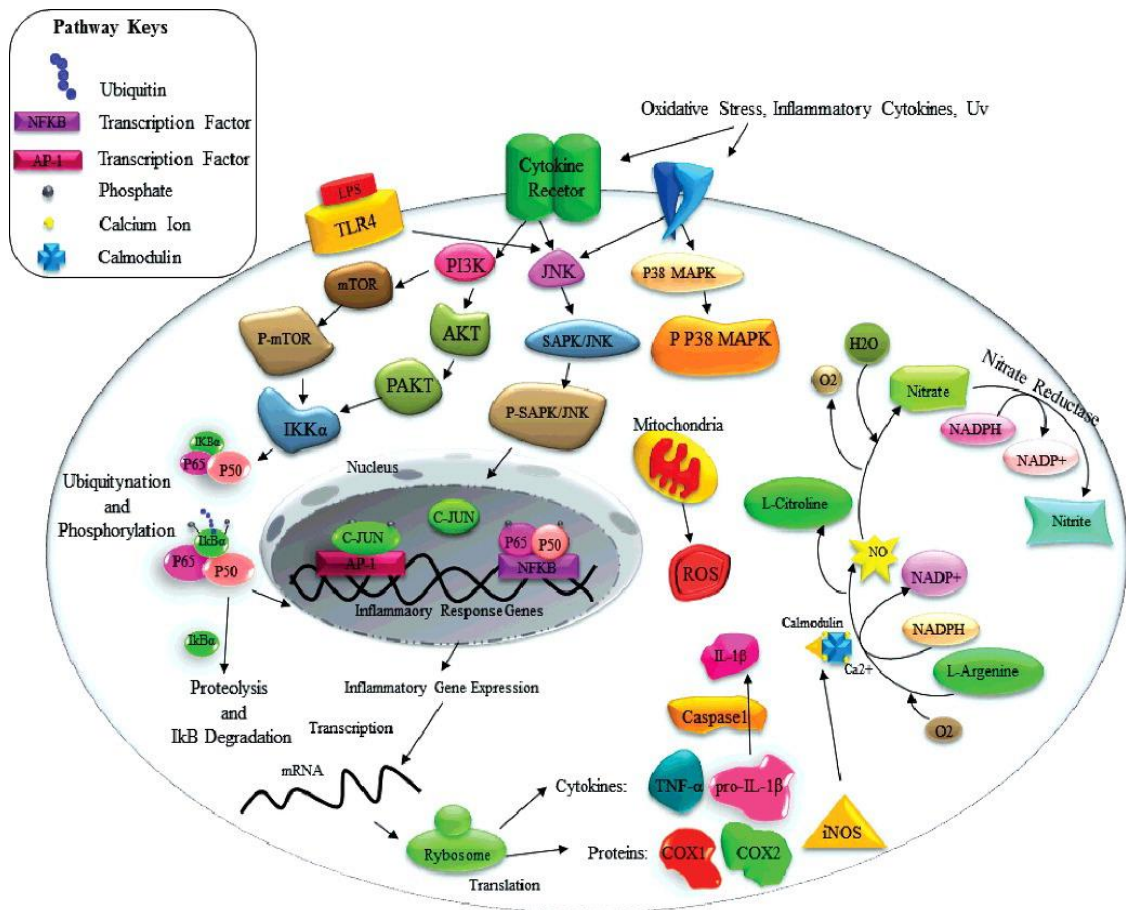
Figure 3.36. Neuroinflammation pathways. (From Shabab et al. International Journal of Neuroscience. 2017. Reprinted with permission)

The **cardiac hypertrophy signalling** pathway was also activated in KRJ-I cells exposed to HEK293 conditioned media. This complicated pathway (see **Figure 3.37**) is involved in cardiac remodelling and incorporates a wide range of biological processes, including gene transcription, protein synthesis, changes in cell metabolism, inflammatory responses and cell death[182]. These processes are driven by a number of signalling cascades, the most important of which are the IGF1-PI3K-Akt pathway, MAPK signalling, the phospholipase C pathway and calcium-dependent pathways[182]. Although 'cardiac hypertrophy' *per se* is not a cancer-related process, many of the pathways illustrated in the pathway figure are known to play critical roles in oncogenesis and most of them have been presented earlier. This shows clearly the complex pathway crosstalk that may be involved in the pathophysiology of mesenteric fibrosis, which most probably involves complicated pathway networks, rather than simply single factors that have been the focus of most previous studies of mesenteric fibrosis in neuroendocrine tumours.
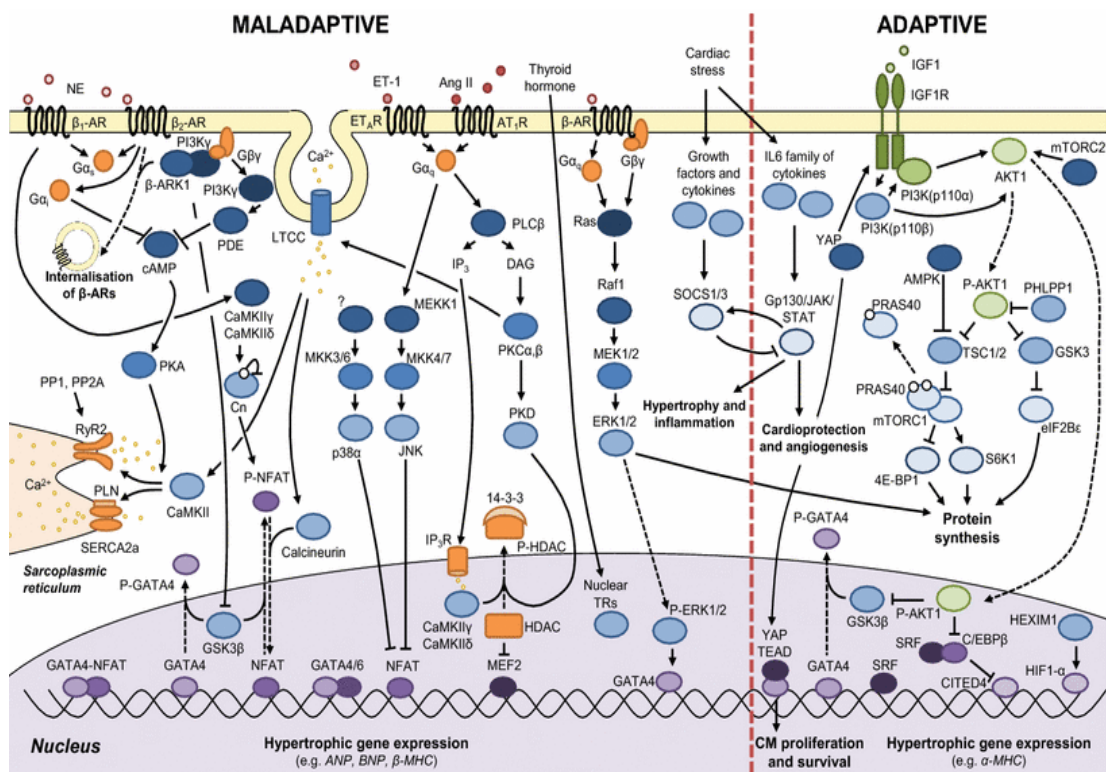
Figure 3.37. Schematic overview of the cardiac hypertrophy signalling. (From Tham et al. Arch Toxicol 2015 89:1401-1438. Reprinted with permission).

In **P-STS cells treated with HEK293 conditioned media** the following pathways were significantly activated: EIF2 signalling, oxidative phosphorylation and Gas signaling, while the superpathway of cholesterol biosynthesis was inhibited. **EIF2 (eukaryotic initiation factor 2) signalling** is a pathway that is involved in protein synthesis. It is of critical importance for cell survival and plays a major role in the integrated stress response[183]. It will be described in more detail later. **Gas signalling** is another pathway that involves gaseous signalling molecules, such as carbon monoxide (CO), nitric oxide (NO) and hydrogen sulphide (H_2S). These gasotransmitters play important roles in several cellular processes, including proliferation, cytoprotection and apoptosis. They exert many of their effects on cell function through their ability to regulate potassium channel activity in mitochondria[184]. In addition, the **oxidative phosphorylation** pathway (**Figure 3.38**) was activated in P-STS cells treated with HEK293 conditioned media. The mitochondrial oxidative phosphorylation system is an important functional unit

comprising of the electron transport chain (complexes I-IV) and the ATP synthase (complex V), which are involved in energy production[185]. The oxidative phosphorylation machinery is also involved in ROS production and apoptosis[185]. The activation of this pathway in neuroendocrine tumour cells is interesting, because most cancers do not rely on respiration to meet their energy demands, but instead they depend on glycolysis. This switch from aerobic to glycolytic energy production (known as the Warburg effect) is a typical metabolic change in de-differentiated cancers. However, the majority of midgut neuroendocrine tumours are well-differentiated with a low proliferation index (Ki67) and do not exhibit increased glucose metabolism, as also evidenced by the generally low tracer uptake of these tumours on ^{18}F-FDG PET imaging studies [186]. On the other hand, the **superpathway of cholesterol biosynthesis** was inhibited in P-STS cells exposed to HEK293 conditioned media. Lipid biogenesis is thought to play an important role in cancer growth and signalling[187], but to the best of our knowledge changes in lipid metabolism and their effect on disease progression have not been investigated in small bowel neuroendocrine tumours. Sterol composition of cell membranes is known to affect many membrane-based properties, such as receptor signalling and vesicular trafficking, and thus cholesterol homeostasis plays a critical role in cell growth[187].
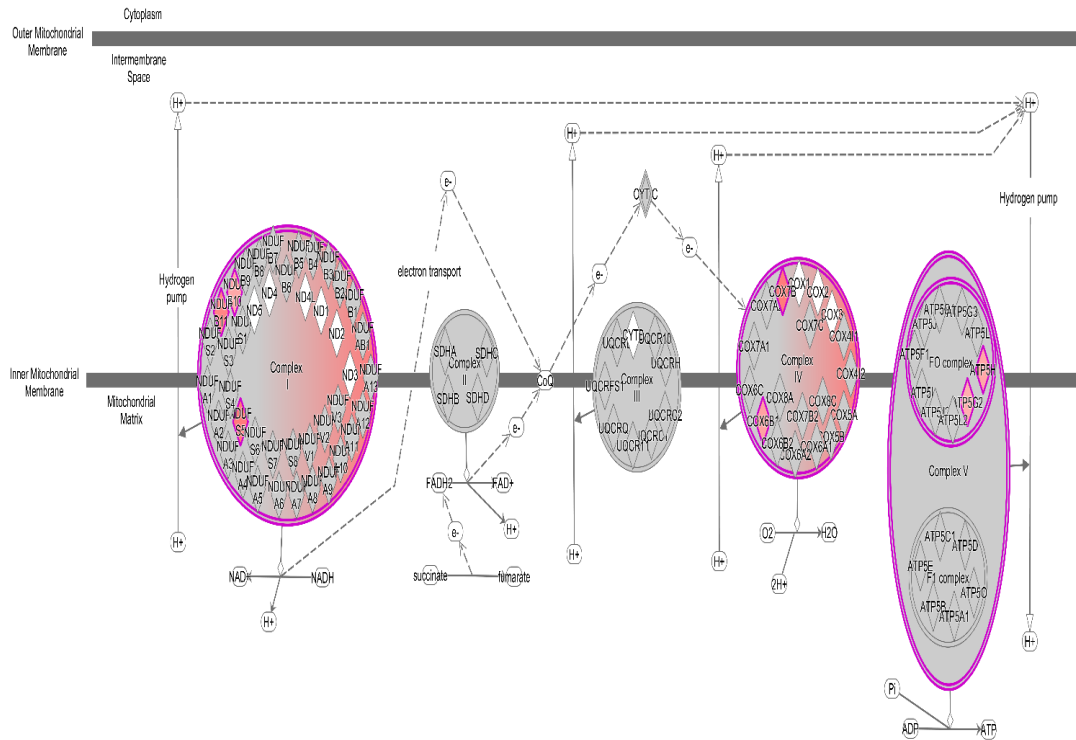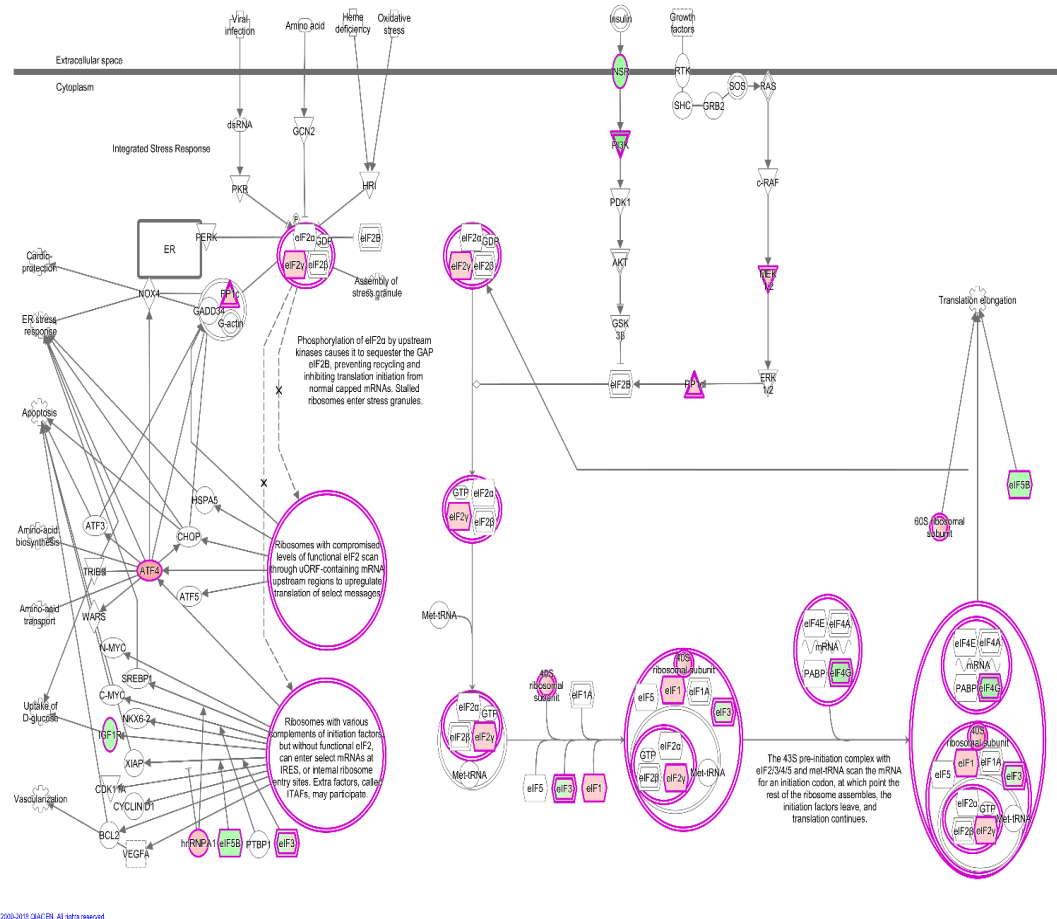
Figure 3.38. Schematic representation of the oxidative phosphorylation pathway, which was activated in P-STS cells treated with HEK293 conditioned media.

In **HEK293 cells treated with KRJ-I conditioned media**, the following pathways were significantly activated: EIF2 signaling, oxidative phosphorylation, superpathway of serine and glycine biosynthesis, while the aryl hydrocarbon receptor and AMPK pathways were inhibited. The **EIF2 pathway** plays a key role in the regulation of protein synthesis and is shown in **Figure 3.39**. The eIF2 (eukaryotic initiation factor 2) is a protein that mediates the binding of the initiator methionyl-tRNA to the ribosome for initiation of translation of all cytoplasmic mRNAs. Therefore, this pathway is important for overall protein synthesis in eukaryotic cells[183]. As shown in the figure, this pathway is also regulated by other signalling pathways, which are normally activated by insulin and growth factors, and are mediated downstream by PI3K-Akt and MAPK signalling cascades, respectively. This adds some complexity to this pathway and illustrates the effect of hormones and growth factors on cell metabolism. In addition, the eIF2 pathway is known to play a role in the integrated stress response. As shown in figure 3.36 (left section), the cell responds to stress

113

signals by activating several eIF2 kinases, which phosphorylate the eIF2 subunit α and inhibit global protein synthesis. At the same time, under stress conditions the translation of a few specific mRNAs is paradoxically upregulated (e.g. ATF4). These are involved in the synthesis of specific proteins that regulate the stress response and the induction of apoptotic pathways[183].

Figure 3.39. Schematic representation of the EIF2 signalling pathway, which was activated in HEK293 cells treated with KRJ-I conditioned media. As shown in the figure, this pathway controls global protein synthesis and its activation can be influenced by several external factors, such as hormones (insulin), growth factors and oxidative stress.

The **oxidative phosphorylation** pathway was also activated in HEK293 cells treated with KRJ-I conditioned media, suggesting an increase in cell energy production as a result of the paracrine effect, as described earlier. In addition, the **superpathway of serine and glycine biosynthesis** was activated in HEK293 cells exposed to KRJ-I conditioned media. This is a pathway that provides precursor molecules for protein synthesis, nucleic acid production and lipogenesis[188]. It is also involved in cell

antioxidant capacity and therefore is considered important for cell survival and proliferation[188]. On the other hand, the **aryl hydrocarbon receptor (Ahr) pathway** was inhibited in HEK293 cells treated with KRJ-I conditioned media. This pathway regulates the expression of genes that are involved in a wide range of cellular processes, including cell growth, cell-cell adhesion and matrix remodelling[189]. The Ahr signalling pathway can alter ECM composition by regulating the expression of ECM proteins (e.g. collagen I and IV), but also the expression and activity of proteolytic enzymes, such as metalloproteinases[189]. In addition, it plays an important role in cell-matrix interactions by regulating the expression of important membrane-associated proteins, such as integrins[189]. It is also known to contribute to matrix remodelling by interacting with a number of other signalling pathways, such as the TGFβ and oestrogen receptor pathways[189]. This is interesting, because a recent publication from Rotterdam suggested that young female patients (≤52 years) with midgut neuroendocrine tumours were less likely to have a desmoplastic mesenteric mass and suggested a possible role of sex hormones in the pathogenesis of mesenteric fibrosis[12]. The crosstalk between the Ahr and oestrogen receptor pathway in the process of matrix remodelling may provide a pathophysiological basis for this interesting observation (which the authors could not explain in their paper). The **AMPK pathway** was also inhibited in HEK293 cells in response to KRJ-I conditioned media (**Figure 3.40**). AMPK (adenosine monophosphate -activated protein kinase) is an enzymatic complex which regulates cell metabolism. It is activated in low-energy conditions (low ATP/high AMP) and generally switches off ATP-consuming pathways (such as fatty acid and cholesterol synthesis), while it activates ATP-generating pathways (such as glycolysis and fatty acid oxidation)[190]. As mentioned earlier, it also inhibits mTOR complex 1 and therefore also has an antiproliferative role, which is enhanced further by its ability to act on the cell metabolic status[190]. Therefore, the effect of cancer cells on the cell metabolic activity and proliferation of stromal cells needs to be further explored in fibrotic midgut neuroendocrine tumours.
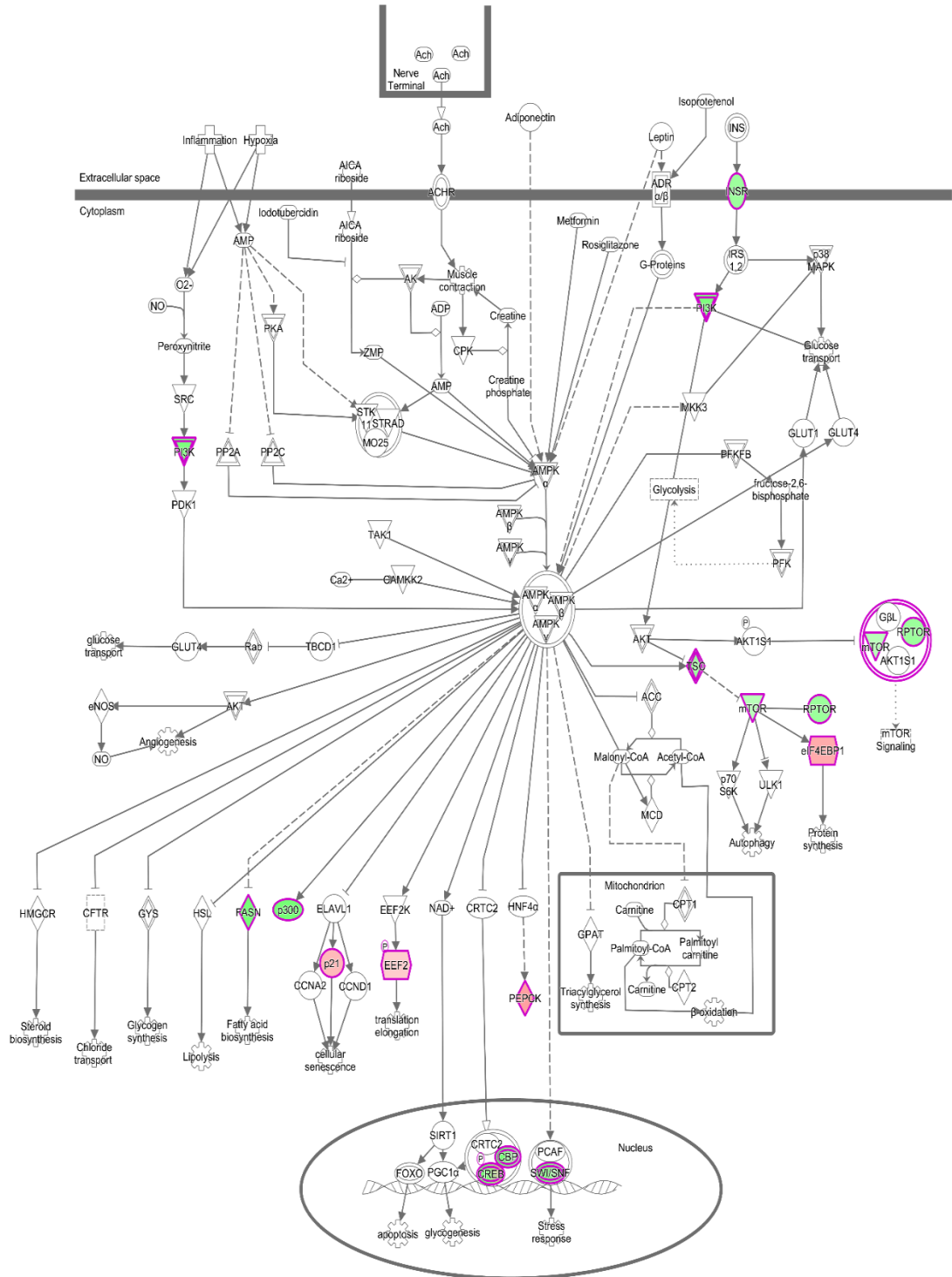
Figure 3.40. Schematic representation of the AMPK pathway, which was inhibited in HEK293 cells treated with KRJ-I conditioned media. As shown in the figure, AMPK is an enzyme that has a central role in cellular metabolism due to its ability to activate ATP-generating pathways, such as fatty acid oxidation, while it inhibits energy consuming pathways, such as fatty acid biosynthesis.

116

In **HEK 293 cells treated with P-STS conditioned media** the following pathways were significantly activated: NRF2-mediated oxidative stress response and oxidative phosphorylation, while the GP6 signalling pathway was inhibited. **NRF2 signalling in oxidative stress** is an important pathway that plays a major role in cell survival in the context of oxidative stress (**Figure 3.41**). Under these conditions a number of downstream mediators (e.g. MAPK cascade, PI3K/Akt and protein kinase C) are activated and ultimately lead to the nuclear translocation of NRF2. In the nucleus NRF2 binds with other proteins (such as Jun) and forms heterodimeric transcription factors which control the expression of a wide range of genes encoding detoxifying enzymes and antioxidant proteins[191]. These mechanisms are important for cell protection against oxidative stress, prevention of apoptosis and survival[191]. The role of oxidative stress in carcinoid-related fibrogenesis has not been sufficiently explored, except in one study which investigated the role of oxidative stress in the development of cardiac fibrosis[192]. Therefore, the involvement of this pathway in mesenteric fibrosis of midgut carcinoids requires further evaluation. In addition, the activation of **oxidative phosphorylation** in HEK293 cells treated with P-STS conditioned media suggests a paracrine effect on mitochondrial metabolism of stromal cells.
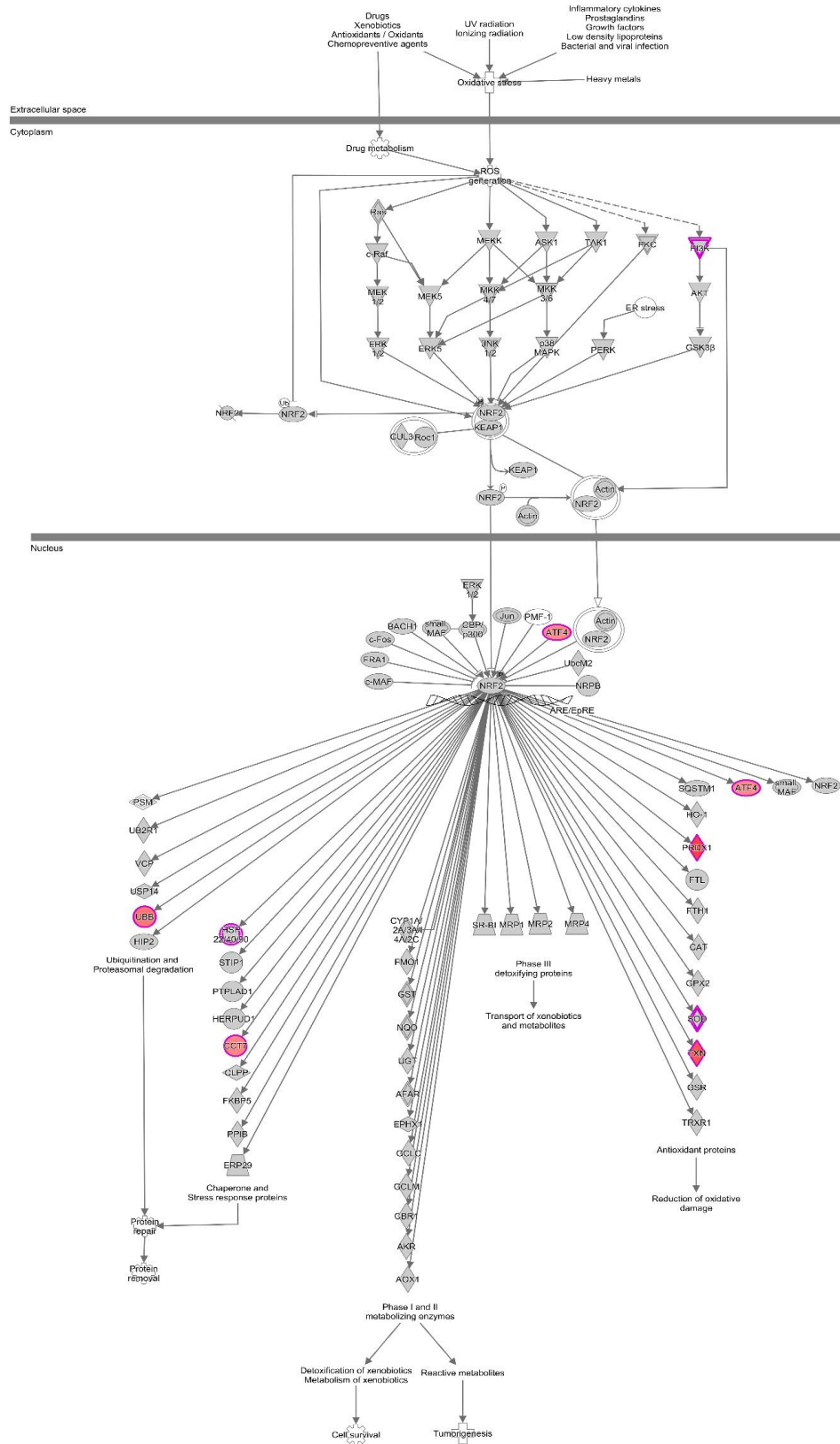
Figure 3.41. Schematic overview of the pathway NRF2 signalling in oxidative stress, which was activated in HEK293 cells treated with P-STS conditioned media. Oxidative stress and ROS generation promote NRF2 nuclear translocation. NRF2 is a trancription factor that controls multiple

genes involved in the oxidative stress response, such as antioxidant proteins and detoxifying enzymes. This pathways is important for cell survival in oxidative stress conditions.

In addition, the **GP6 signalling** pathway was inhibited in HEK293 cells treated with P-STS conditioned media, as shown in **figure 3.42**. This pathway is involved in platelet activation and thrombosis. GP6 is found in platelets and megakaryocytes and is a platelet receptor, which interacts with ECM proteins, such as collagen and laminin[193]. This interaction leads to the activation of a downstream pathway, sequentially involving PI3K, phospholipase C (PLC) and protein kinase C (PKC) and calcium mobilisation into the cytosol, which results in integrin αIIbβ3 activation. This integrin is important for platelet adhesion and aggregation in disrupted blood vessels and this process leads to thrombosis formation[193]. It seems a bit strange that this pathway is inhibited in HEK293 cells (in both the generic and tissue-specific IPA analyses), as it is a platelet-specific pathway and its physiological significance in this context remains unclear.

Figure 3.42. Schematic overview of the GP6 signalling pathway, which was found to be inhibited in HEK293 cells treated with P-STS conditioned media.

Apart from changes in gene expression, we investigated **changes in cytokine/chemokine and growth factor secretion** by performing a 27-plex Luminex on cell culture supernatants of KRJ-I, P-STS and HEK293 cells. These results were then reviewed alongside the RNA sequencing data to identify consistent alterations at both mRNA and protein level as a result of the paracrine effect. Using this approach, 3 distinct patterns of response were identified. Cytokines/chemokines and growth factors that were included in the second pattern of response (i.e. significant upregulation at both mRNA and protein level after exposure to conditioned media of the other cell line) are likely to represent proteins, whose expression is altered as a result of the paracrine effect. On the other hand, in cases where there was inconsistency between mRNA and protein expression, the changes at protein level in the culture media of treated cells (with conditioned media of the other cell line may be explained by the presence of these proteins in the conditioned media that were used for the cell treatments. Alternatively, the discordance between RNA and protein expression data may be due to post-transcriptional and/or post-translational modifications[194-197]. A wide range of post-translational modifications exists and some of these may affect protein levels after biosynthesis. For example, ubiquitination is an evolutionary conserved process with a cardinal role in proteostasis, whereby ubiquitin or ubiquitin-like proteins are added to target proteins, and this event may direct proteins for proteasome degradation[196,197]. In addition, miRNAs are small, non-coding RNA molecules that have been investigated in neuroendocrine neoplasia[195], and are known to regulate not only transcriptional but also post-transcriptional gene expression through a variety of different mechanisms[194]. Finally, discrepancies between RNA and protein measurements in the cell culture supernatants, may relate to the fact that the protein is not secreted after its biosynthesis in the cell. This issue could be further explored by simultaneous measurements of protein levels in cell lysates and cell culture supernatants, which were not performed in our experiments, as the focus was on the secretome of the cells, which is important in cell-to-cell interactions.

In HEK293 cells treated with KRJ-I conditioned media there was a significant upregulation of MCP-1 at both gene expression and protein level in the culture supernatants of these cells. **MCP-1 (monocyte chemoattractant protein 1)**, also known as CCL2 (CC chemokine ligand 2), is an important cytokine which is not only

involved in inflammatory responses, but is also known to be secreted in the tumour microenvironment by both cancer and stromal cells, depending on the tumour type[198]. MCP-1 plays an important role in cancer development and progression[198]. Therefore, in our *in vitro* model we believe that the conditioned media of KRJ-I cells contain certain factors that stimulate the secretion of MCP-1 by HEK293 cells and this response may in turn allow the survival and metastatic spread of the cancer cells in midgut neuroendocrine tumours. It is interesting to note that MCP-1/CCL2 was also upregulated at mRNA level in HEK293 cells treated with BON-1 conditioned media in our preliminary experiments, although we did not assess protein secretion in this model. In addition, **IP-10 (interferon γ-inducible protein 10**, also known as CXCL10) was significantly upregulated at both mRNA and protein secretion level in P-STS cells treated with HEK293 conditioned media, as well as in HEK293 cells treated with KRJ-I conditioned media. CXCL10 is an angiostatic factor that is secreted by both tumour and stromal cells in the tumour microenvironment[199]. It plays an important role in anti-tumour immunity by regulating the function of CD4+ T helper cells and effector CD8+ cells, but also may have a direct suppressive effect on cancer cells[199]. It can also reduce tumour growth by inhibiting angiogenesis[199]. The role of CXCL10 in fibrogenesis is more complex and seems to depend on the model studied[200,201]. For example, in the heart CXCL10 seems to play an antifibrotic role following ischaemic cardiac injury[200], while in the liver it induces chronic inflammation, which eventually leads to liver fibrosis in chronic hepatitis C infection[201]. Therefore, the role of this cytokine in the development of fibrosis in midgut neuroendocrine tumours would need to be investigated further.

In conclusion, this study has provided a comprehensive analysis of the crosstalk of two enterochromaffin-derived neuroendocrine tumour cell lines, KRJ-I and P-STS, with a stromal cell line, HEK293. Unlike previous studies that have focussed on single profibrotic factors, such as TGFβ1 and CTGF, this analysis of an *in vitro* model of the mesenteric tumour microenvironment has revealed **pathways of disease** that provide further insight into the mechanisms of fibrogenesis in midgut neuroendocrine tumours. As described earlier, multiple pathways appear to be involved in these complex interactions, and many of those signalling cascades play important roles in both carcinogenesis and fibrosis. There is also significant crosstalk between these pathways, which further complicates the underlying processes. An intriguing result,

however, was the fact that different pathways were activated or inhibited in KRJ-I and P-STS cells, even though these cell lines are both derived from primary midgut neuroendocrine tumours. Similarly, different pathways were activated or inhibited in HEK293 cells treated with KRJ-I and P-STS conditioned media, suggesting that there are differences in the secretome of these cancer cells. Although a recent paper challenged the neuroendocrine origin of the KRJ-I cell line[136], this cell line has been well-characterised in previous studies that have demonstrated its enterochromaffin origin[125,202]. Therefore, it is quite difficult to explain the different results observed in the IPA analysis between these two cell lines. One possible explanation (other than the potential different origin of these cell lines) is that this discrepancy is due to heterogeneity of cancer cells within the primary tumour. It may be that the KRJ-I cell line represents a pro-metastatic cell and it may have its known 'lymphoblastoid' phenotype as part of an escape mechanism which facilitates invasion and metastasis, while the P-STS cell line may be more typical of cells in the primary tumour without metastatic potential. This unpublished hypothesis was suggested by Dr Mark Kidd, who was involved in the characterisation of the KRJ-I cell line[125], but of course this remains to be proven. If this assumption were true, it would also explain the more significant cross-talk that we observed between KRJ-I and HEK293 cells, compared with the relatively weak interaction between P-STS and HEK293 cells, because it is known that fibrosis tends to develop around the mesenteric mass and not the primary tumour. However, at present this is an unclear area which requires further clarification and research. Of course, our results would need to be further validated *in vivo* and could lead to the development of previously unrecognised druggable targets for mesenteric fibrosis.

Chapter 4

Assessment of mesenteric desmoplasia in midgut neuroendocrine tumours and further delineation of the pathophysiology of mesenteric fibrosis using human tissue

4. **Assessment of mesenteric desmoplasia in midgut neuroendocrine tumours and further delineation of the pathophysiology of mesenteric fibrosis using human tissue**

4.1. Introduction

The assessment of mesenteric fibrosis is a problematic area, because there is very limited literature on the multidimensional evaluation of fibrosis using a triangulation of different methodologies. In clinical practice and in most studies the presence of mesenteric desmoplasia is determined radiologically and is defined as a mesenteric mass (a pathological lymph node measuring ≥ 10mm) with radiating soft tissue strands in a typical 'spoke-wheel' pattern[71]. However, often there are atypical appearances, such as subtle spiculation around the mesenteric lymph node or a 'misty' mesentery, but a histopathological correlation with these unusual radiological patterns is lacking[10]. In addition, often there may be a solitary mesenteric mass without evident mesenteric desmoplasia on radiology, but it is unclear whether this radiological appearance rules out the presence of minimal desmoplasia around the lymph node. The accurate evaluation of mesenteric desmoplasia using a multidimensional approach is therefore essential for research studies investigating the pathophysiology of mesenteric fibrosis, in order to accurately classify patients as 'fibrotic' or 'non-fibrotic'. This approach may also allow the development of different categories of severity for mesenteric fibrosis. This is of critical importance for the evaluation of changes in gene and protein expression in different groups of patients, which may provide further insight into the mechanisms of mesenteric fibrogenesis, as we will discuss later in this chapter.

Chapter 4 includes two parts, which are closely linked:

The **first part** focuses on the multidimensional assessment of mesenteric fibrosis in 34 patients with midgut neuroendocrine tumours enrolled in our study. This includes a triangulation of cross-sectional imaging, intra-operative (surgical) evaluation and histological measurements (**Figure 4.1**). Using this approach, we were able to group patients in different categories of mesenteric fibrosis severity.
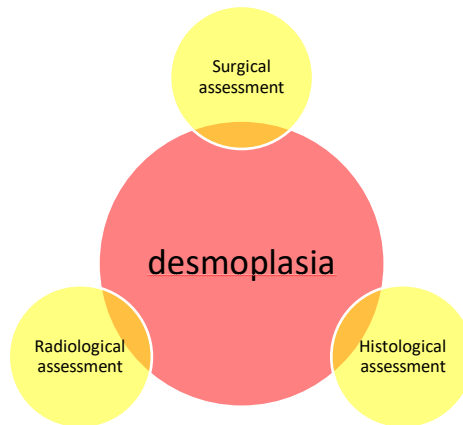
Figure 4.1. A multidimensional assessment of mesenteric desmoplasia incorporating radiological, surgical and histological criteria was performed to accurately evaluate the severity of fibrosis and categorise patients in different groups.

The **second part** of this chapter focuses on changes in gene and protein expression in these different patient groups. A preliminary study was initially performed to assess changes in gene expression in the first 26 patients recruited in the study, using a set of genes that have been previously implicated in the development of mesenteric fibrosis in midgut neuroendocrine tumours[9]. As we will discuss later, this was performed to assess the robustness of our methodological approach and evaluate if differences in gene expression are seen among different (fibrotic and non-fibrotic) patient groups. We then investigated the integrin pathway in our entire cohort of 34 patients. This pathway was shown to be activated in cancer cells (KRJ-I) exposed to HEK293 conditioned media, as demonstrated in our *in vitro* functional studies (**Chapter 3**).

These two parts will be presented separately, followed by a combined discussion of the main findings.

4.2. Multidimensional assessment of mesenteric desmoplasia in midgut neuroendocrine tumours

4.2.1. Methods

A total of 34 patients with midgut neuroendocrine tumours were prospectively recruited into this study. A summary of their clinical characteristics is provided in **Table 4.1**.

	Patients with midgut NETs who underwent surgery (n=34) n (%)
Age (mean±SD)	61±13
Sex	
Male	23 (68%)
Female	11 (32%)
Grade	
1	21 (62%)
2	13 (38%)
Extent of disease	
Localised	3 (9%)
Locoregional	9 (26%)
Metastatic	22 (65%)
Mesenteric mass	31 (91%)
Liver metastases	17 (50%)
Distant extrahepatic metastases	10 (29%)
Macroscopic mesenteric fibrosis	25 (74%)
Medical therapy	
Octreotide LAR	10 (29%)
Lanreotide Autogel	8 (24%)
Surgical therapy	
Small bowel resection	1 (3%)
Right hemicolectomy (R0)	24 (71%)
Right hemicolectomy (R1)	9 (26%)

Table 4.1. Demographic and clinical characteristics of patients with midgut NETs enrolled in the study.

A multidimensional assessment of mesenteric fibrosis was used to evaluate the accuracy of standard cross-sectional imaging for the detection of fibrosis and categorise patients in different fibrosis severity groups. The components of this assessment are described below:

A. The <u>radiological</u> severity of mesenteric desmoplasia was based on the scoring system originally proposed by Pantongrag-Brown et al[8] using the following categories:

Category	Criteria
No radiological evidence of mesenteric desmoplasia	Absence of radiating strands
Mild desmoplasia	<10 thin radiating strands
Moderate desmoplasia	>10 thin strands or <10 thick strands
Severe desmoplasia	>10 thick strands

B. The <u>histological</u> assessment of mesenteric fibrosis was based on the histological slide with the maximum amount of fibrous tissue. The histological slide was stained with a collagen stain (Sirius Red) and two parameters were measured:

1. The width of the thickest fibrous band surrounding the mesenteric mass. This technique was used previously by Pantongrag-Brown et al and showed a correlation with the radiological assessment of mesenteric fibrosis[8]. In their publication, Pantongrag-Brown et al introduced a new histological parameter, the so-called *'fibrosis grade'*, which is based on the maximum width (*grade 1*: width<1mm, *grade 2*:1-2mm, *grade 3*:>2mm)[8].

2. The Collagen Proportionate Area (CPA), which represents the percentage of collagen in the stroma surrounding the mesenteric metastatic tumour. This is a quantitative method of measuring fibrous tissue using digital image analysis and has been validated in liver cirrhosis by the Royal Free department of cellular pathology[203,204].

A simplified schematic representation of these histological measurements is provided in **Figure 4.2.**
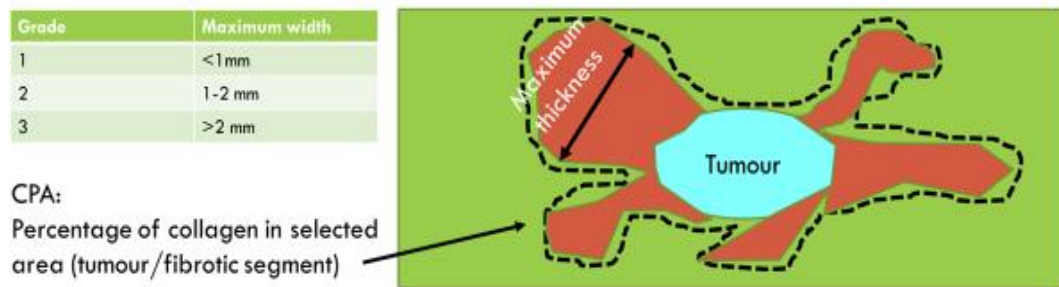
Figure 4.2. Schematic representation of histological slide containing mesenteric tumour tissue (light blue) surrounded by fibrosis (orange). The width of the thickest fibrotic band can be measured (maximum width). The histological grade is calculated based on the maximum width. The Collagen Proportionate Area (CPA) can also be measured in a selected area containing the mesenteric tumour and surrounding fibrotic component, as shown (dotted line).

Optimisation/characterisation of the inter-observer variability

The cross-sectional imaging (CT/MRI scan) and histology (mesenteric mass with surrounding fibrosis) were assessed independently by 2 assessors with good inter-observer variability. There was a 91% agreement in the radiological assessment of mesenteric desmoplasia between the two assessors. In a small number of cases (n=3) a minor discrepancy was observed between the two assessments and consensus was reached between the assessors to determine the radiological severity of the mesenteric desmoplasia after a final review of the imaging studies. The inter-observer variability in the histological measurements is shown in **Figure 4.3**. There was a very good correlation for both CPA (Spearman's correlation r=0.86998, $p<0.0001$) and width of fibrous band measurements (Spearman's correlation r=0.9174, $p<0.0001$) between the two assessors. In the case of minor discrepancies (<20% difference between the two assessments) the mean value of the two assessments was calculated and used for our analysis. In the small number of cases with more significant discrepancies (>20% difference between the two assessments), consensus was reached between the two assessors regarding the CPA and width of fibrous band measurements after a final review of the histology slides.

A   B
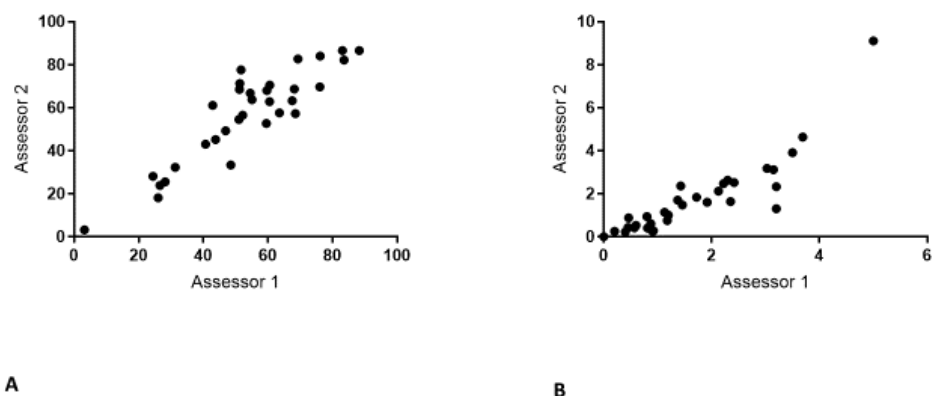
Figure 4.3. A. Interobserver correlation of CPA measurements between assessors 1 and 2 (r=0.86998 [95% CI 0.7487, 0.9347], *p*<0.0001). B. Inter-observer correlation of fibrous band maximum width between assessors 1 and 2 (r=0.9174 [95% CI 0.8366, 0.9591], *p*<0.0001).

C. An <u>intra-operative</u> assessment of the extent of mesenteric fibrosis in relation to the entire small bowel mesentery was also provided using the following categories:

Category	Criteria
No desmoplasia	No mesenteric fibrosis
Mild desmoplasia	Mesenteric fibrosis involving <25% of the small bowel mesentery
Moderate desmoplasia	Mesenteric fibrosis involving 25-50% of the small bowel mesentery
Severe desmoplasia	Mesenteric fibrosis involving >50% of the small bowel mesentery

This assessment was provided by the same operating surgeon (Mr Olagunju Ogunbiyi, Department of Colorectal Surgery, Royal Free Hospital performed the macroscopic assessment of mesenteric desmoplasia in all the cases). Two examples of this assessment are illustrated in **Figure 4.4**.
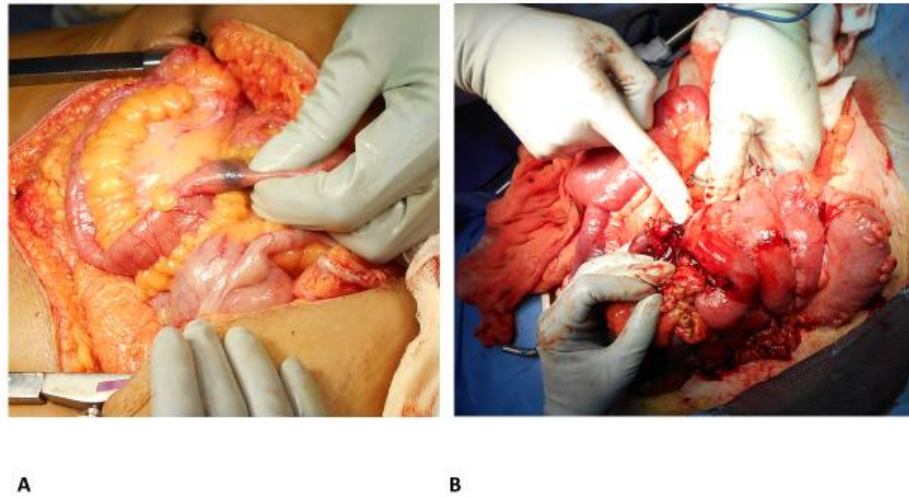
Figure 4.4. Surgical assessments of mesenteric fibrosis in midgut neuroendocrine tumours. (A) Non-fibrotic midgut neuroendocrine tumour diagnosed at double-balloon enteroscopy performed to investigate overt, obscure gastrointestinal bleeding. A tattoo mark is seen indicating the site of the primary tumour. (B) Moderately fibrotic mesenteric mass involving several loops of small bowel.

4.2.2. Results

4.2.2.1. Correlation of surgical and radiological assessments of mesenteric fibrosis

There was a statistically significant correlation between the clinical (surgical and radiological) methods of assessment of mesenteric fibrosis (Fisher's exact test, p=0.014), as shown in **Table 4.2**.

		Surgical				Total
		None	Mild	Moderate	Severe	
Radiological	None	9	5	1	0	15
	Mild	3	2	1	0	6
	Moderate	0	7	1	1	9
	Severe	0	4	0	0	4
Total		12	18	3	1	34

Table 4.2. Correlation of surgical and radiological assessment of mesenteric desmoplasia. Overall, a statistically significant correlation (Fisher's exact test, p=0.014) was observed.

4.2.2.2. Correlation of radiological and histological assessments of mesenteric fibrosis

Correlations were assessed using the fibrosis grade, maximum width and CPA. There was no statistical correlation between the **fibrosis grade** and the radiological assessment of fibrosis (Fisher's exact test, p=0.129) (**Table 4.3**).

		Fibrosis Grade				
		0	1	2	3	Total
Radiological	None	3	6	3	3	15
	Mild	0	0	1	5	6
	Moderate	0	4	2	3	9
	Severe	0	2	2	0	4
Total		3	12	8	11	34

Table 4.3. Correlation of fibrosis grade and the radiological assessment of mesenteric fibrosis. There was no statistical correlation between these methods of assessment.

Similarly, the **maximum width** of fibrous bands did not correlate with the radiological assessment of mesenteric fibrosis at a statistically significant level (Kruskal-Wallis test, p=0.08) (**Figure 4.5**).
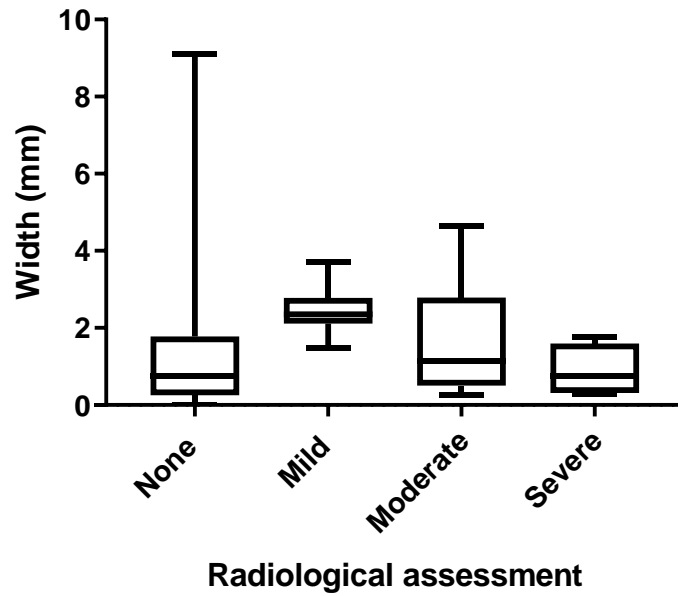
Figure 4.5. Correlation of the radiological assessment of mesenteric fibrosis with the maximum width of fibrous bands. There was no statistical correlation between these methods of assessment.

On the other hand, the correlation of CPA with the radiological assessment of mesenteric fibrosis was statistically significant (One-way ANOVA test, p=0.02) (**Figure 4.6**).
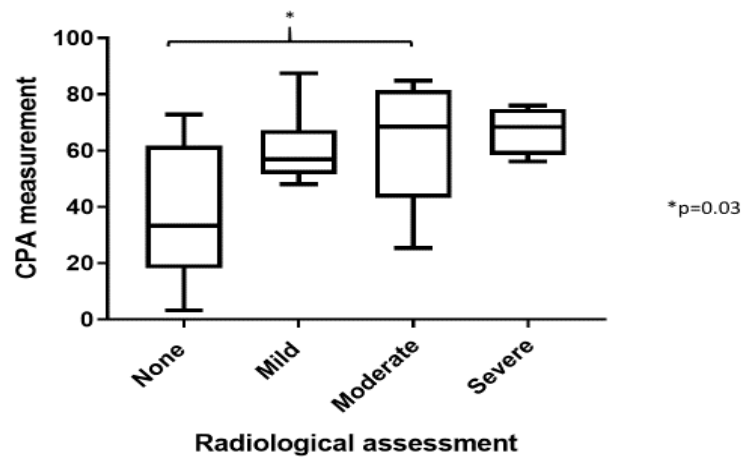
Figure 4.6. Correlation of CPA measurements with the radiological assessment of mesenteric fibrosis. This correlation was statistically significant (One-way ANOVA, p=0.02) and after adjusting for multiple comparisons a significantly higher CPA was noted in the moderately fibrotic radiological group vs. non-fibrotic radiological group (p=0.03) and a trend towards significance was seen in the

CPA difference in the severely fibrotic radiological group vs. the non-fibrotic radiological group (p=0.07).

Interestingly, in several cases there was histological evidence of fibrosis around the mesenteric mass which was not seen radiologically, as shown in **Figures 4.7 and 4.8**.
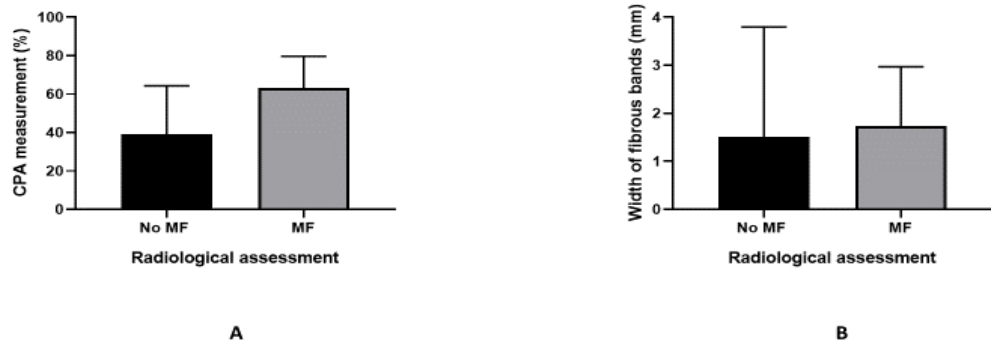
Figure 4.7. Correlation of the radiological presence of mesenteric fibrosis with histological measurements of fibrosis. In several cases, there was histological evidence of fibrosis which was not seen at imaging studies. MF: Mesenteric fibrosis.
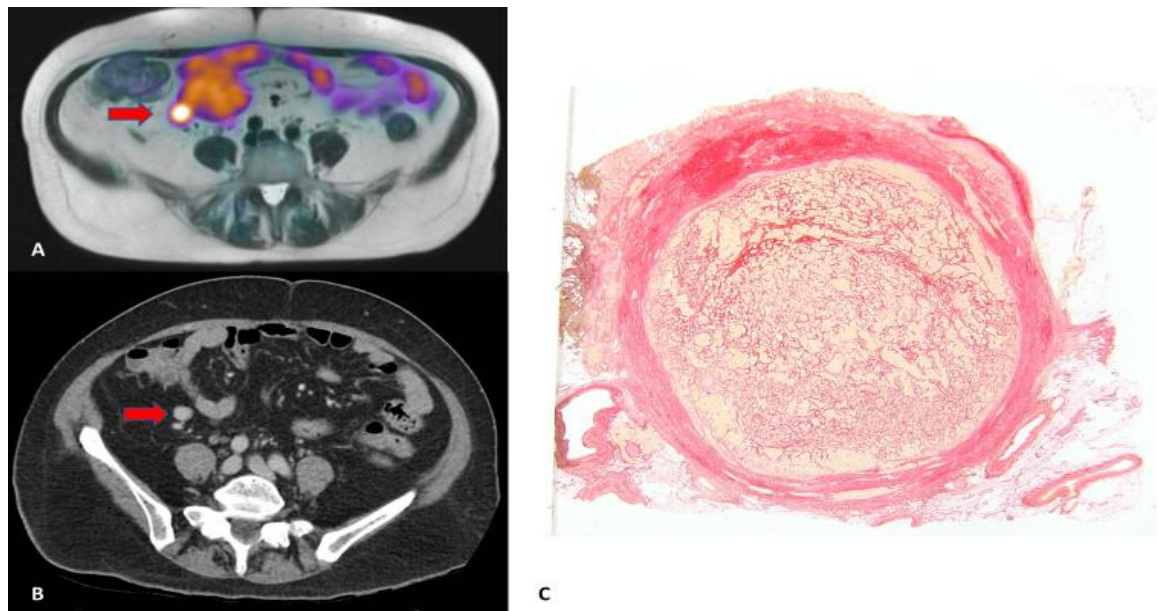
Figure 4.8. Correlation of ^{68}Ga PET/MRI (A), CT abdomen (B) and histology (C) in a patient with a midgut neuroendocrine tumour. (A+B) A gallium-avid mesenteric mass is seen without surrounding desmoplasia on imaging. (C) However, on histology a thin fibrotic capsule is seen surrounding the mesenteric lymph node (lymph node diameter ~14mm), indicating the presence of image-negative mesenteric desmoplasia.

4.2.2.3. Correlation of surgical and histological assessments of mesenteric fibrosis

The surgical evaluation of mesenteric desmoplasia was correlated with the histological fibrotic grade, the width of fibrous bands and the CPA. There was no statistically significant correlation between the fibrotic grade and the surgical assessment (Fisher's exact test, *p*=0.264), as shown in **Table 4.4**.

| | | Fibrosis Grade | | | | |
		0	1	2	3	Total
Surgical	None	3	3	3	3	12
	Mild	0	8	4	6	18
	Moderate	0	0	1	2	3
	Severe	0	1	0	0	1
Total		3	12	8	11	34

Table 4.4. Correlation between the surgical assessment of mesenteric fibrosis and the fibrosis grade. There was no statistically significant association between these assessments (Fisher's exact test, p=0.264).

However, a statistically significant correlation was noted between the surgical assessment of desmoplasia and width of fibrous bands on histology (One-way ANOVA test, p=0.04) (**Figure 4.9**).
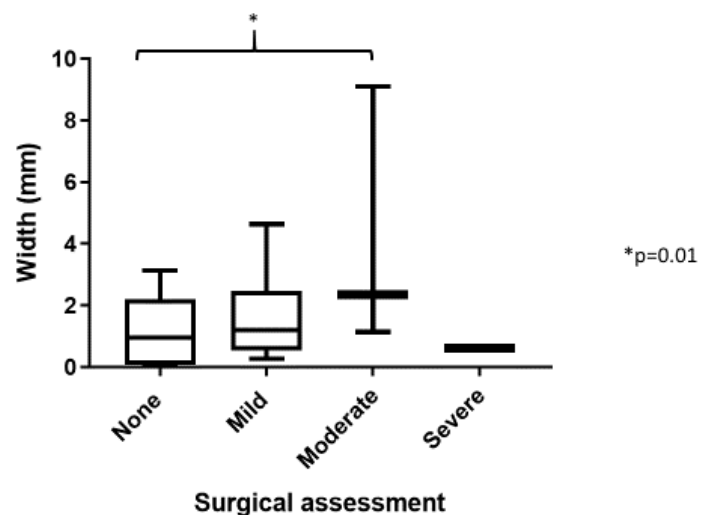
Figure 4.9. Correlation of surgical assessment of mesenteric desmoplasia with width of fibrous bands. There was a statistically significant relationship between these assessments (One-way ANOVA

test, p=0.04) and after adjusting for multiple comparisons a significant difference was noted in the moderately fibrotic surgical group vs. the non-fibrotic group (p=0.01).

In addition, there was a statistically significant association between CPA and the surgical assessment of fibrosis (One-way ANOVA test, p=0.02) (**Figure 4.10**).
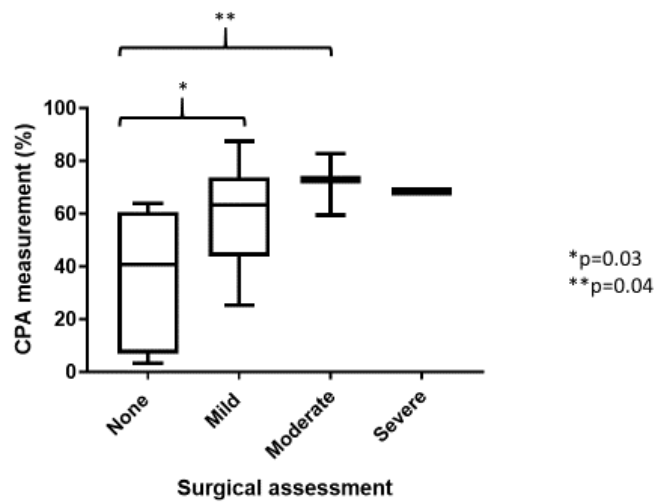
Figure 4.10. Correlation of surgical assessment of mesenteric desmoplasia with CPA. There was a statistically significant relationship between these assessments (One-way ANOVA, p=0.02) and after adjusting for multiple comparisons a significant difference was noted in the mildly fibrotic vs. the non-fibrotic surgical group (p=0.03) as well as the moderately fibrotic vs. non-fibrotic surgical group (p=0.04).

4.2.2.4. Optimal cut-off points of histological parameters (maximum width and CPA) for the prediction of clinical fibrosis

A receiver operating characteristic (ROC) curve was used to establish the optimal cut-off points of CPA and maximum width of fibrous bands that predicted with the best sensitivity and specificity the presence of clinical (radiological and/or surgical) fibrosis.

A width of fibrous band > 0.505mm and a CPA >37.6% were identified as the optimal cut-off points (Width of fibrous bands: AUC 0.751 [95% CI 0.535, 0.967], $p=0.027$ and CPA (AUC 0.804 [95% CI 0.634, 0.975], $p=0.007$) (**Figure 4.11**).
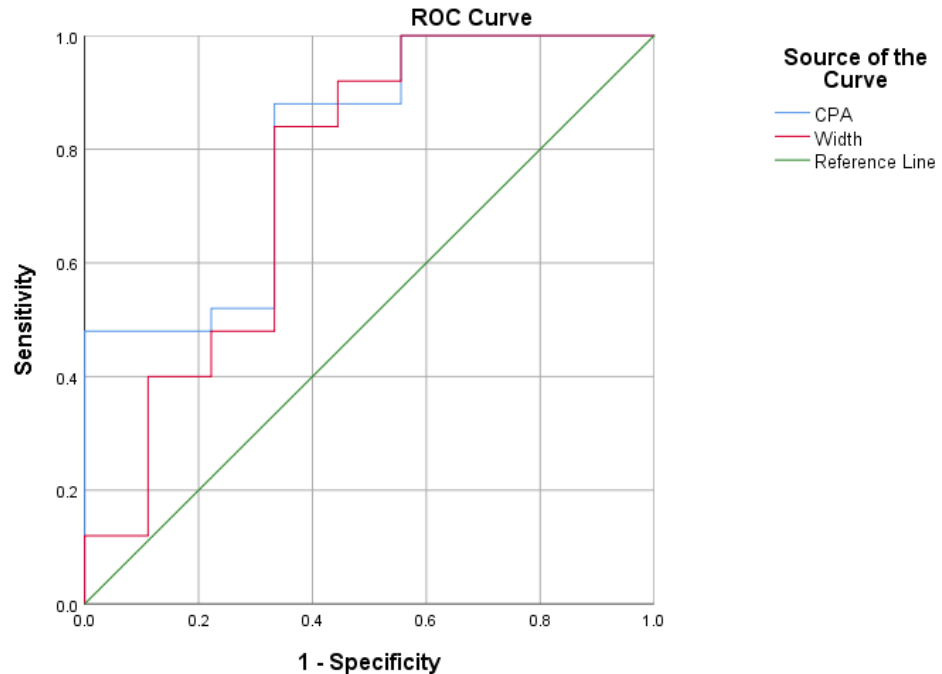
Figure 4.11. Receiver operating characteristic (ROC) curve used for the evaluation of the optimal cut-off points of histological parameters (CPA, width of fibrous band) for the prediction of clinical (radiological and/or intra-operative) fibrosis. A width of fibrous band > 0.505 mm and a CPA > 37.6% were identified as the cut-off points with best sensitivity and specificity.

4.2.2.5. Development of different patient groups of mesenteric fibrosis severity

A total of 34 patients were grouped in different categories of mesenteric fibrosis severity:

1. *Non-fibrotic group*: No evidence of mesenteric fibrosis (n=3)

2. *Minimally fibrotic group*: Only histological (but no clinical evidence of) fibrosis (n=6). In this group of patients, a mesenteric metastasis was present and surrounded by a small amount of fibrosis detected only histologically.

3. *Mildly and severely fibrotic groups*: These patients had evidence of clinical fibrosis (n=25). The group of patients with clinical fibrosis was further sub-divided into 2 smaller subgroups: A group of patients with mild fibrosis (n=14) and another group

with advanced fibrosis (n=11). A scoring system was developed to group patients in different categories of clinical fibrosis severity. This scoring system incorporated surgical (macroscopic), radiological and histological parameters, which have been described previously (**Table 4.5**).

A total score of 6 was arbitrarily chosen as a cut-off point to allow a fairly equal distribution of patients in the two subgroups of clinical fibrosis (mild <6, advanced ≥6).

Interestingly, the non-fibrotic group was characterised by the absence of a mesenteric mass, while all patients with a mesenteric metastasis had evidence of fibrosis development, and the extent of the desmoplastic reaction varied significantly, from minimal (detected only histologically) to more advanced.

Surgical evidence of fibrosis	Radiological evidence of fibrosis	Histological evidence of fibrosis
0: None	0: None	0: None
1: <25% of small bowel mesentery	1: ≤10 thin strands	1: Yes, but CPA<37.6% AND width of fibrous band <0.505 mm
2: 25-50% of small bowel mesentery	2: >10 thin and <10 thick strands	2: Yes, CPA>37.6% OR width of fibrous band >0.505 mm
3: >50% of small bowel mesentery	3: ≥10 thick strands	3: Yes, CPA>37.6% AND max width >0.505mm

Table 4.5. Scoring system used to assess the severity of mesenteric fibrosis. This system is not validated, but incorporates surgical, radiological and histological measurements, therefore allowing for a more objective, multidimensional assessment of the severity of mesenteric fibrosis. CPA: Collagen Proportionate Area**.**

4.3. Investigation of the pathophysiology of mesenteric fibrosis using human tissue

4.3.1. Evaluation of genes that have been previously implicated in mesenteric fibrogenesis associated with midgut neuroendocrine tumours

4.3.1.1. Methods

A preliminary evaluation of changes in profibrotic gene expression was initially performed in the first 26 patients enrolled into the study. Fresh frozen tissue of normal small bowel mucosa, primary tumour and mesenteric mass of recruited patients was prospectively collected and stored in the RFH-UCL Biobank. The study protocol for the tissue analyses was approved by the RFH-UCL Biobank Ethics Committee (reference ID NC2017.003, IRAS ID 208955).

Several profibrotic genes (CTGF, TGFβ1, TGFβ3, FGFR1, PDGF β receptor, TNF, COL1A1, COL3A1, EGFR, FGF2) were assessed and their expression was evaluated by qPCR in the normal mucosa, primary tumour and mesenteric metastasis of patients with different degrees of mesenteric fibrosis severity (ranging from *none* to *advanced* using the classification system described earlier). More specifically, fresh frozen tissue samples of normal mucosa, primary tumour and mesenteric mass were homogenised using a TissueLyser II (Qiagen) and RNA was extracted using the RNeasy Mini Kit (Qiagen). RNA concentration and purity were determined using a NanoDrop 2000 spectrophotometer and an aliquot was analysed on a denaturing gel using electrophoresis to check the quality of isolated RNA. 400 ng of total RNA were used for reverse transcription using the High Capacity cDNA Reverse Transcription Kit (Thermo Fisher Scientific). The following Assays-on-Demand primers were used: CTGF (Hs00170014), TGFβ1 (Hs00998133), TGFβ3 (Hs01086000), FGFR1 (Hs00241111), PDGF β receptor (Hs01019589), TNF (Hs00174128), COL1A1 (Hs00164004), COL3A1 (Hs00943809), EGFR (Hs01076090) and GAPDH (Hs02786624). RT-qPCR was performed on an ABI 7500 Fast Sequence Detection System using the Taqman Universal Mastermix (Thermo Fisher) and the following PCR conditions: 50º for 2 mins, then 95º for 10 mins, followed by 40 cycles at 95ºC/15 s and 60ºC/1 min. Gene expression was normalised to normal SI mucosa (control) using GAPDH as a housekeeping gene.

Many of the selected genes have been previously investigated in smaller studies of NET-related fibrogenesis. One of these genes is known to be expressed only by tumour cells (TGFβ3), some only by stromal cells (FGFR1, PDGF β receptor), while the remaining genes are expressed by both the tumour and stromal components (TGFβ1, CTGF, FGF2, EGFR)[9]. We also investigated a few additional genes which have not been previously assessed in NET-related fibrosis studies, but are either known stromal markers (COL1A1, COL3A1) or are involved in fibrosis development in other conditions (TNF).

The research questions for this analysis were the following:

1. In **fibrotic** midgut neuroendocrine tumours:
(a) Are there differences in profibrotic gene expression between normal and tumour tissue (primary & metastatic)?
(b) Are these differences evident in each of the fibrosis severity groups (minimally fibrotic, mildly fibrotic and severely fibrotic)?
2. In **non-fibrotic** midgut neuroendocrine tumours:
   (a) Are there differences in profibrotic gene expression between normal and tumour tissue?
   (b) How does this compare with fibrotic NETs (with paired normal and primary tumour tissue)?
3. In midgut neuroendocrine tumours are there differences in profibrotic gene expression between different types of tumour tissue (primary and metastatic) **among different fibrosis groups** (unpaired samples)?

4.3.1.2. Results

4.3.1.2.1 Fibrotic SI NETs

In fibrotic SI NETs, as expected, there was a significant upregulation in gene expression of most of the selected genes (CTGF, TGFβ1, TGFβ3, COL1A1, COL3A1, PDGF β receptor, FGFR1) in the desmoplastic mesenteric mass compared to control (normal SI mucosa). Significant upregulation in gene expression was also noted in some genes (TGFβ1, COL1A1, COL3A1, PDGF β receptor, FGFR1) in the primary tumour compared to control (normal SI mucosa). In addition, a significantly higher expression was seen in several genes (TGFβ1, CTGF, COL1A1, TGFβ3, PDGF β receptor, FGFR1) in the desmoplastic mass compared to the primary tumour. Finally,

no significant differences in gene expression were seen between the desmoplastic mass and the normal mucosa for a small number of selected genes (TNF, FGF2, EGFR), suggesting that these are unlikely to play a major role in carcinoid-related mesenteric fibrogenesis. The qPCR results for each of the selected genes are illustrated in **Figures 4.12-4.21**. Data in each of these figures are shown for the entire group of fibrotic SI NETs (A), as well as for each fibrotic subgroup separately, i.e. minimally fibrotic (B), mildly fibrotic (C) and severely fibrotic (D).
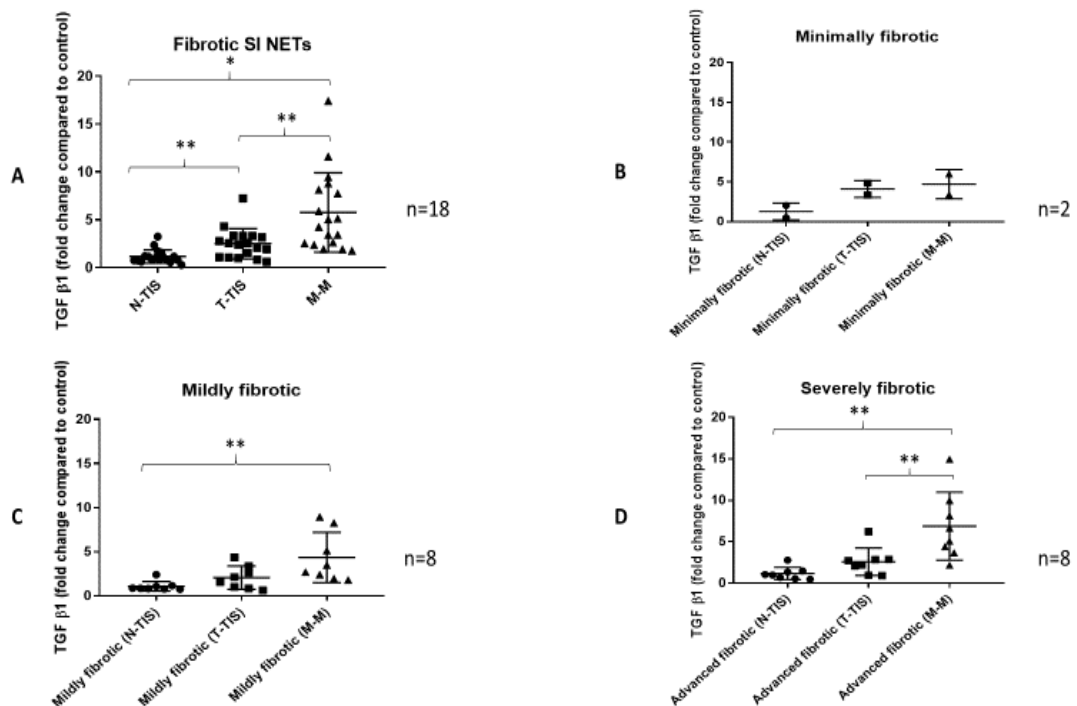
Figure 4.12. TGFβ1 expression in the normal mucosa, primary tumour and mesenteric mass of fibrotic SI NETs. (A) In the entire group of fibrotic SI NETs, a significantly higher expression of TGFβ1 was seen in the mesenteric mass compared to normal mucosa and primary tumour tissue. In addition, TGFβ1 expression was significantly higher in the primary tumour compared to normal mucosa. Data are also shown for each fibrotic subgroup separately, i.e. minimally fibrotic (B), mildly fibrotic (C) and severely fibrotic groups (D). Statistical analysis was performed using a Wilcoxon test. Levels of statistical significance are indicated by asterisks: *p<0.001, **p<0.01, ***p<0.05. N-TIS: normal mucosa, T-TIS: primary tumour tissue, M-M: mesenteric mass.
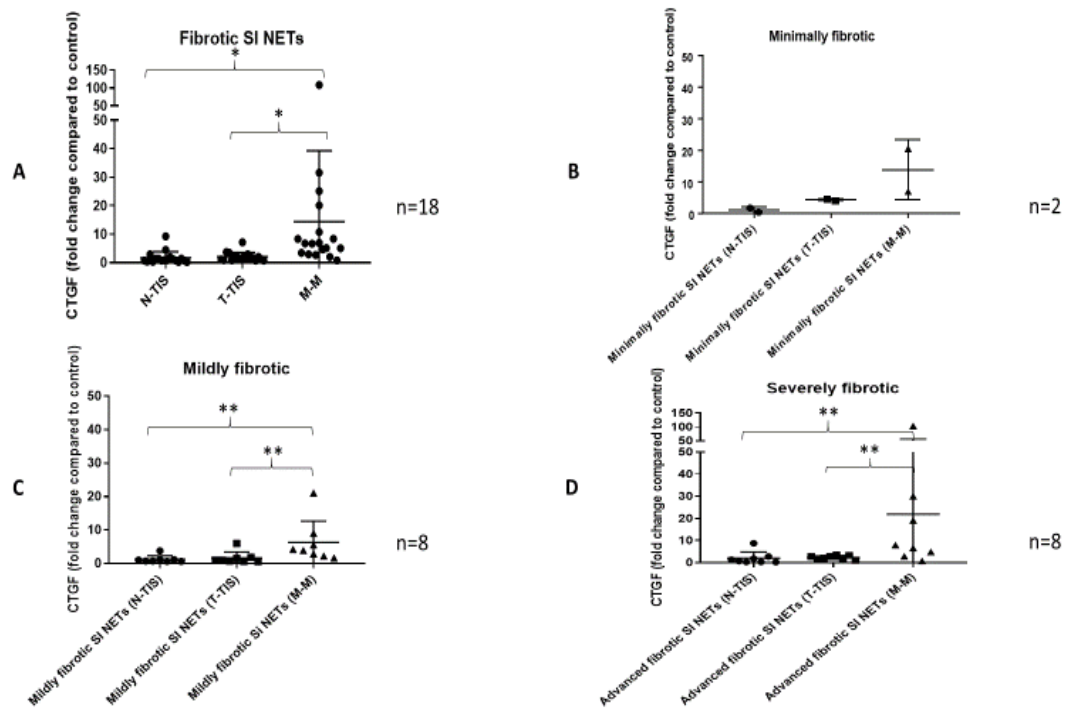
Figure 4.13. CTGF expression in the normal mucosa, primary tumour and mesenteric mass of fibrotic SI NETs. (A) In the entire group of fibrotic SI NETs, a significantly higher expression of CTGF was seen in the mesenteric mass compared to normal mucosa and primary tumour tissue. Data are also shown for each fibrotic subgroup separately, i.e. minimally fibrotic (B), mildly fibrotic (C) and severely fibrotic groups (D). Statistical analysis was performed using a Wilcoxon test. Levels of statistical significance are indicated by asterisks: *$p < 0.001$, **$p < 0.01$, ***$p < 0.05$. N-TIS: normal mucosa, T-TIS: primary tumour tissue, M-M: mesenteric mass.
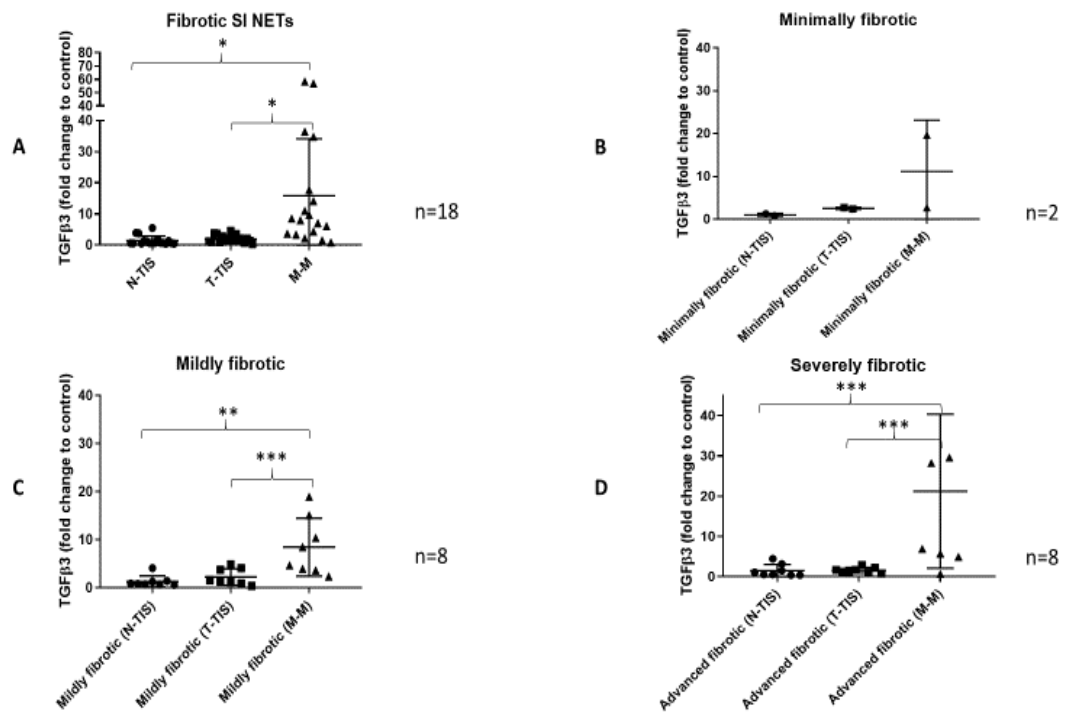
Figure 4.14. TGFβ3 expression in the normal mucosa, primary tumour and mesenteric mass of fibrotic SI NETs. (A) In the entire group of fibrotic SI NETs, a significantly higher expression of TGFβ3 was seen in the mesenteric mass compared to normal mucosa and primary tumour tissue. Data are also shown for each fibrotic subgroup separately, i.e. minimally fibrotic (B), mildly fibrotic (C) and severely fibrotic groups (D). Statistical analysis was performed using a Wilcoxon test. Levels of statistical significance are indicated by asterisks: *p<0.001, **p<0.01, ***p<0.05. N-TIS: normal mucosa, T-TIS: primary tumour tissue, M-M: mesenteric mass.
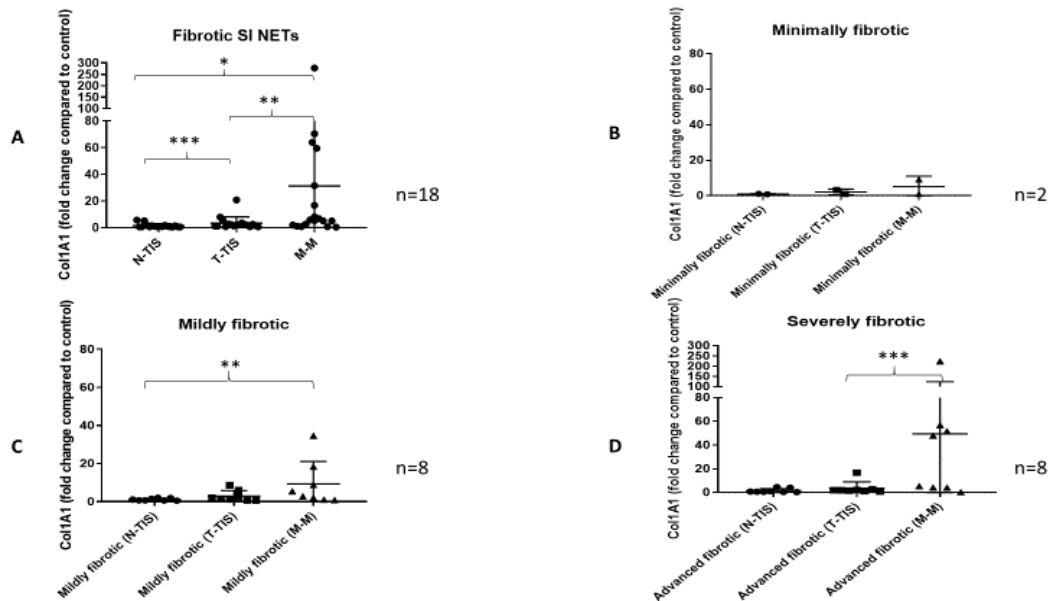
Figure 4.15. COL1A1 expression in the normal mucosa, primary tumour and mesenteric mass of fibrotic SI NETs. (A) In the entire group of fibrotic SI NETs, a significantly higher expression of COL1A1 was seen in the mesenteric mass compared to normal mucosa and primary tumour tissue. In addition, COL1A1 gene expression was significantly higher in the primary tumour compared to normal mucosa. Data are also shown for each fibrotic subgroup separately, i.e. minimally fibrotic (B), mildly fibrotic (C) and severely fibrotic groups (D). Statistical analysis was performed using a Wilcoxon test. Levels of statistical significance are indicated by asterisks: *p<0.001, **p<0.01, ***p<0.05. N-TIS: normal mucosa, T-TIS: primary tumour tissue, M-M: mesenteric mass.
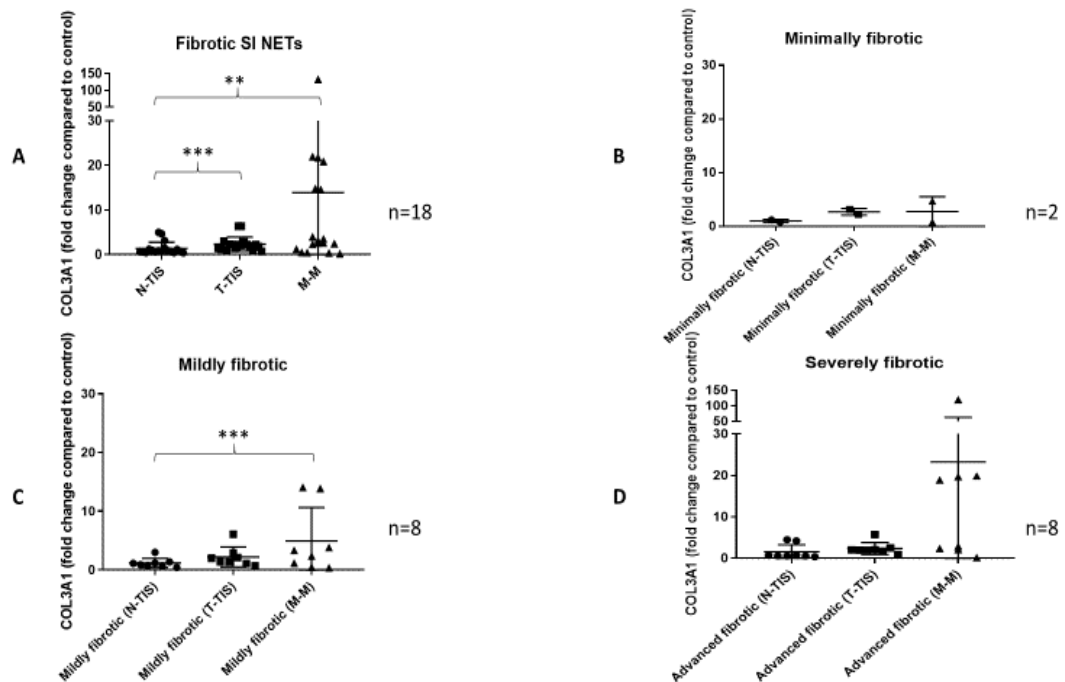

Figure 4.16. COL3A1 expression in the normal mucosa, primary tumour and mesenteric mass of fibrotic SI NETs. (A) In the entire group of fibrotic SI NETs, a significantly higher expression of

143

COL3A1 was seen in the mesenteric mass compared to normal mucosa. In addition, COL3A1 gene expression was significantly higher in the primary tumour compared to normal mucosa. Data are also shown for each fibrotic subgroup separately, i.e. minimally fibrotic (B), mildly fibrotic (C) and severely fibrotic groups (D). Statistical analysis was performed using a Wilcoxon test. Levels of statistical significance are indicated by asterisks: *p<0.001, **p<0.01, ***p<0.05. N-TIS: normal mucosa, T-TIS: primary tumour tissue, M-M: mesenteric mass.

Figure 4.17. PDGF receptor β expression in the normal mucosa, primary tumour and mesenteric mass of fibrotic SI NETs. (A) In the entire group of fibrotic SI NETs, a significantly higher expression of PDGF receptor β was seen in the mesenteric mass compared to normal mucosa and primary tumour tissue. In addition, PDGF receptor β gene expression was significantly higher in the primary tumour compared to normal mucosa. Data are also shown for each fibrotic subgroup separately, i.e. minimally fibrotic (B), mildly fibrotic (C) and severely fibrotic groups (D). Statistical analysis was performed using a Wilcoxon test. Levels of statistical significance are indicated by asterisks: *p<0.001, **p<0.01, ***p<0.05. N-TIS: normal mucosa, T-TIS: primary tumour tissue, M-M: mesenteric mass.
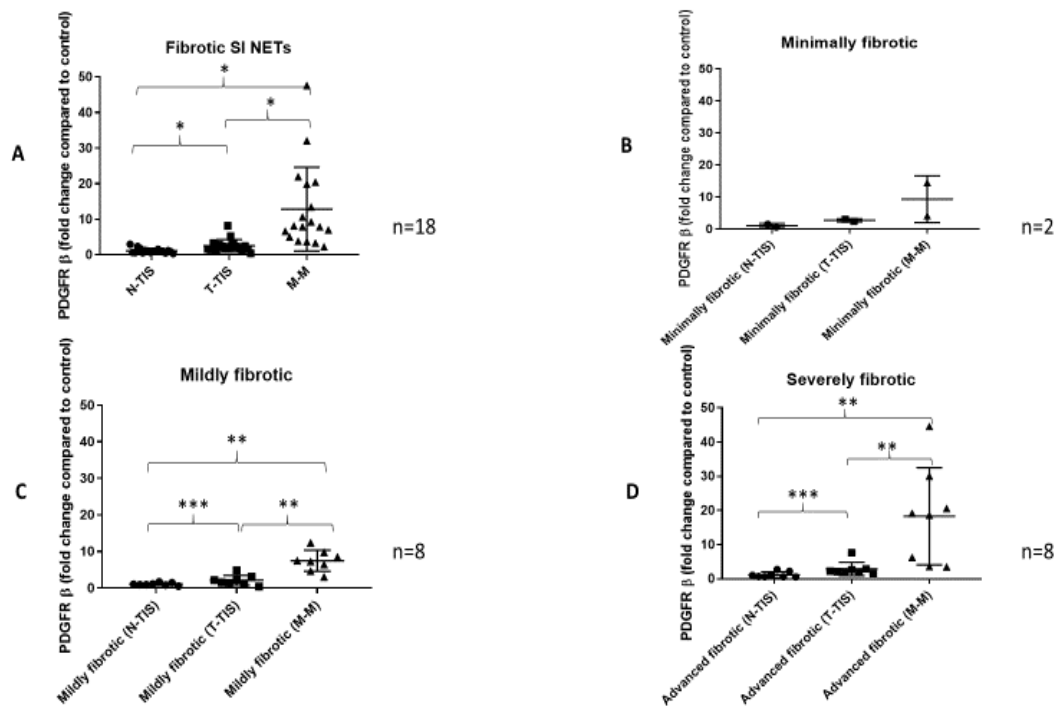
144

Figure 4.18. FGFR1 expression in the normal mucosa, primary tumour and mesenteric mass of fibrotic SI NETs. (A) In the entire group of fibrotic SI NETs, a significantly higher expression of FGFR1 was seen in the mesenteric mass compared to normal mucosa and primary tumour tissue. In addition, FGFR1 gene expression was significantly higher in the primary tumour compared to normal mucosa. Data are also shown for each fibrotic subgroup separately, i.e. minimally fibrotic (B), mildly fibrotic (C) and severely fibrotic groups (D). Statistical analysis was performed using a Wilcoxon test. Levels of statistical significance are indicated by asterisks: *$p < 0.001$, **$p < 0.01$, ***$p < 0.05$. N-TIS: normal mucosa, T-TIS: primary tumour tissue, M-M: mesenteric mass.
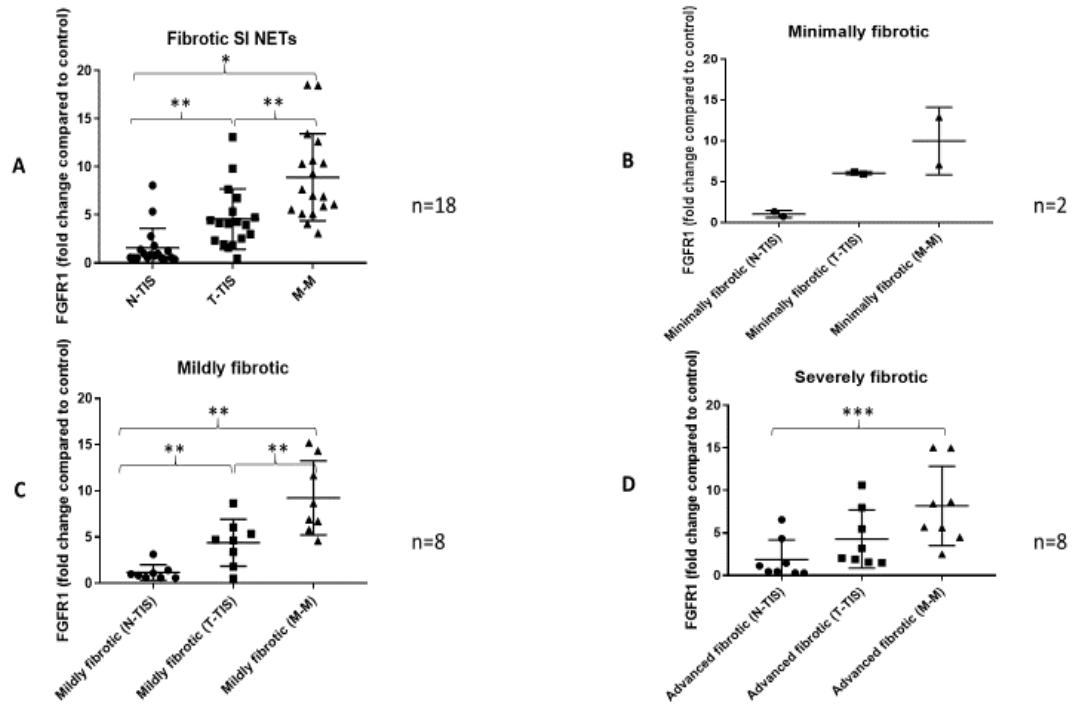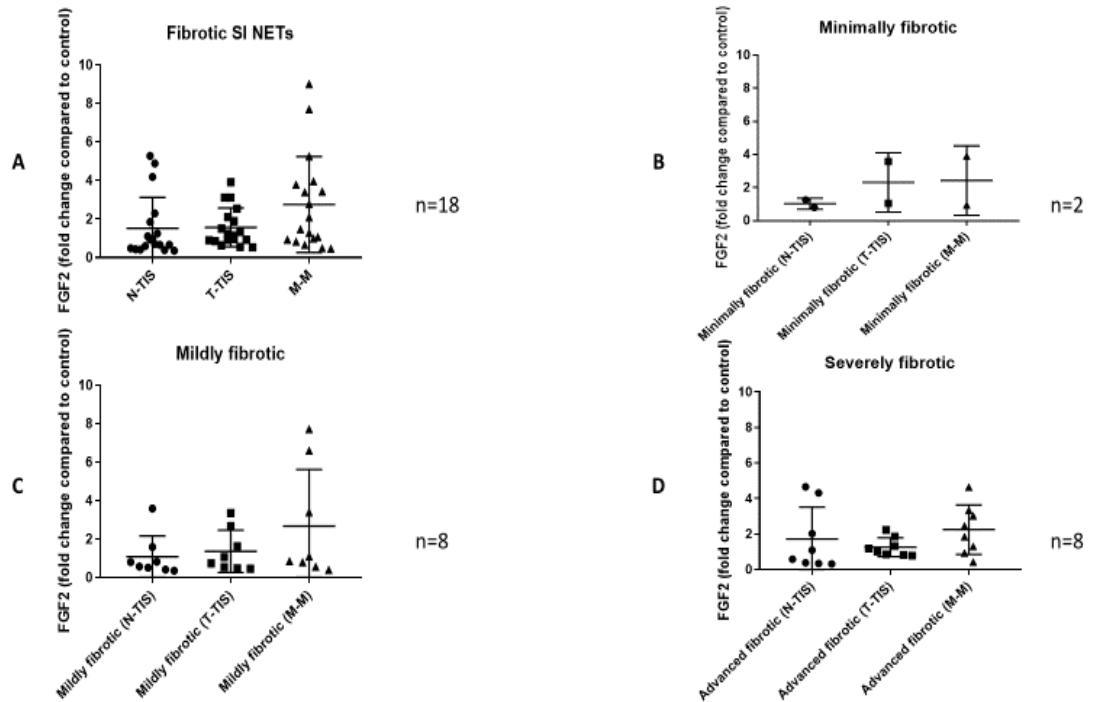
Figure 4.19. FGF2 expression in the normal mucosa, primary tumour and mesenteric mass of fibrotic SI NETs. No significant differences were seen in the mesenteric mass compared to control (normal mucosa) in the whole group of fibrotic SI NETs (A) and the various subgroups (B-D). Statistical analysis was performed using a Wilcoxon test. N-TIS: normal mucosa, T-TIS: primary tumour tissue, M-M: mesenteric mass.
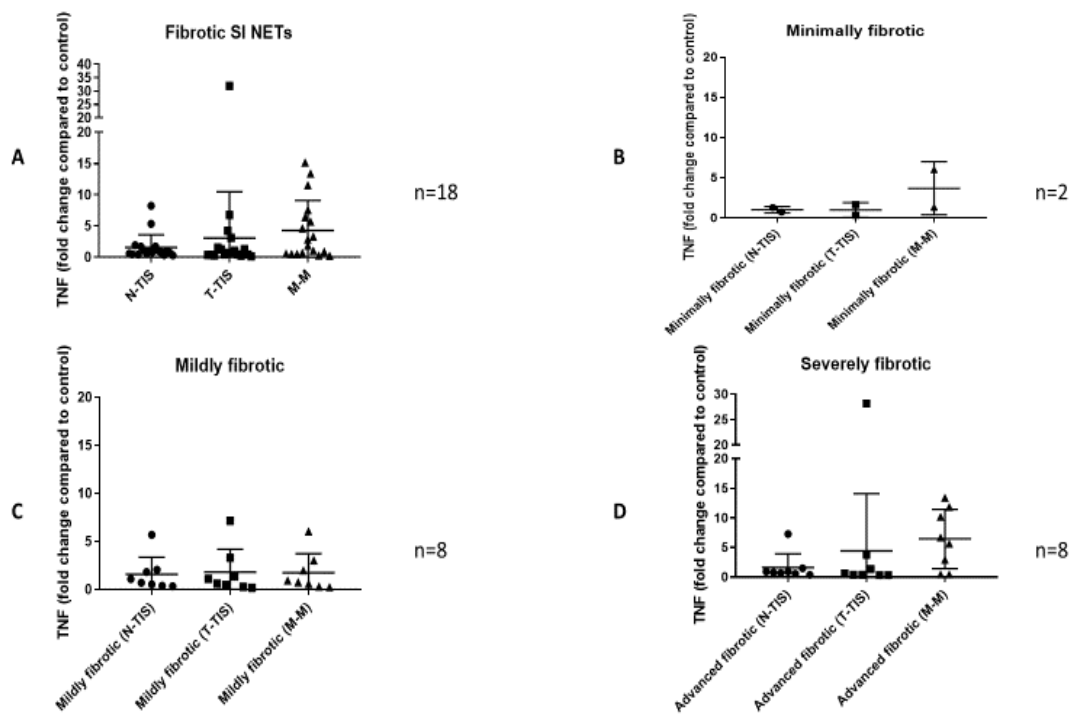
Figure 4.20. TNF expression in the normal mucosa, primary tumour and mesenteric mass of fibrotic SI NETs. No significant differences were seen in the mesenteric mass compared to control

146

(normal mucosa) in the whole group of fibrotic SI NETs (A) and the various subgroups (B-D). Statistical analysis was performed using a Wilcoxon test. N-TIS: normal mucosa, T-TIS: primary tumour tissue, M-M: mesenteric mass.
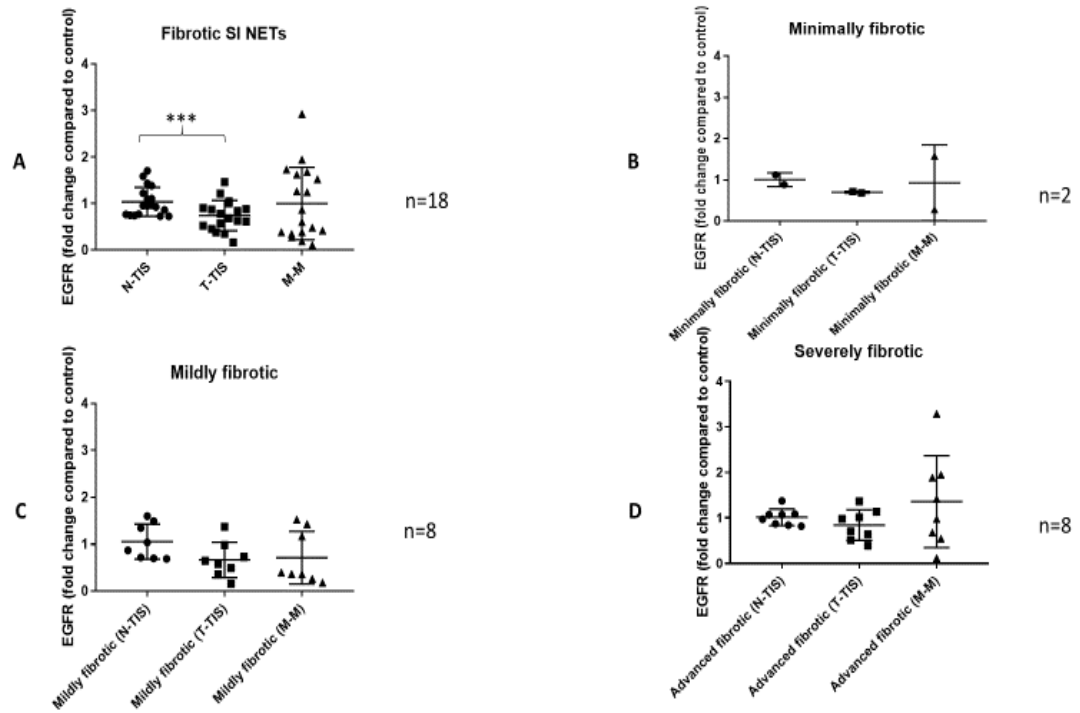
Figure 4.21. EGFR expression in the normal mucosa, primary tumour and mesenteric mass of fibrotic SI NETs. No significant differences were seen in the mesenteric mass compared to control (normal mucosa) in the whole group of fibrotic SI NETs (A) and the various subgroups (B-D). Statistical analysis was performed using a Wilcoxon test. Levels of statistical significance are indicated by asterisks: *p<0.001, **p<0.01, ***p<0.05. N-TIS: normal mucosa, T-TIS: primary tumour tissue, M-M: mesenteric mass.

4.3.1.2.2. Non-fibrotic SI NETs

In non-fibrotic SI NETs, there was no mesenteric mass present and changes in gene expression were assessed in the primary tumour compared to normal SI mucosa. No significant changes were noted in profibrotic gene expression in the primary tumour compared to control (n=3 patients), as shown in **Figure 4.22**.
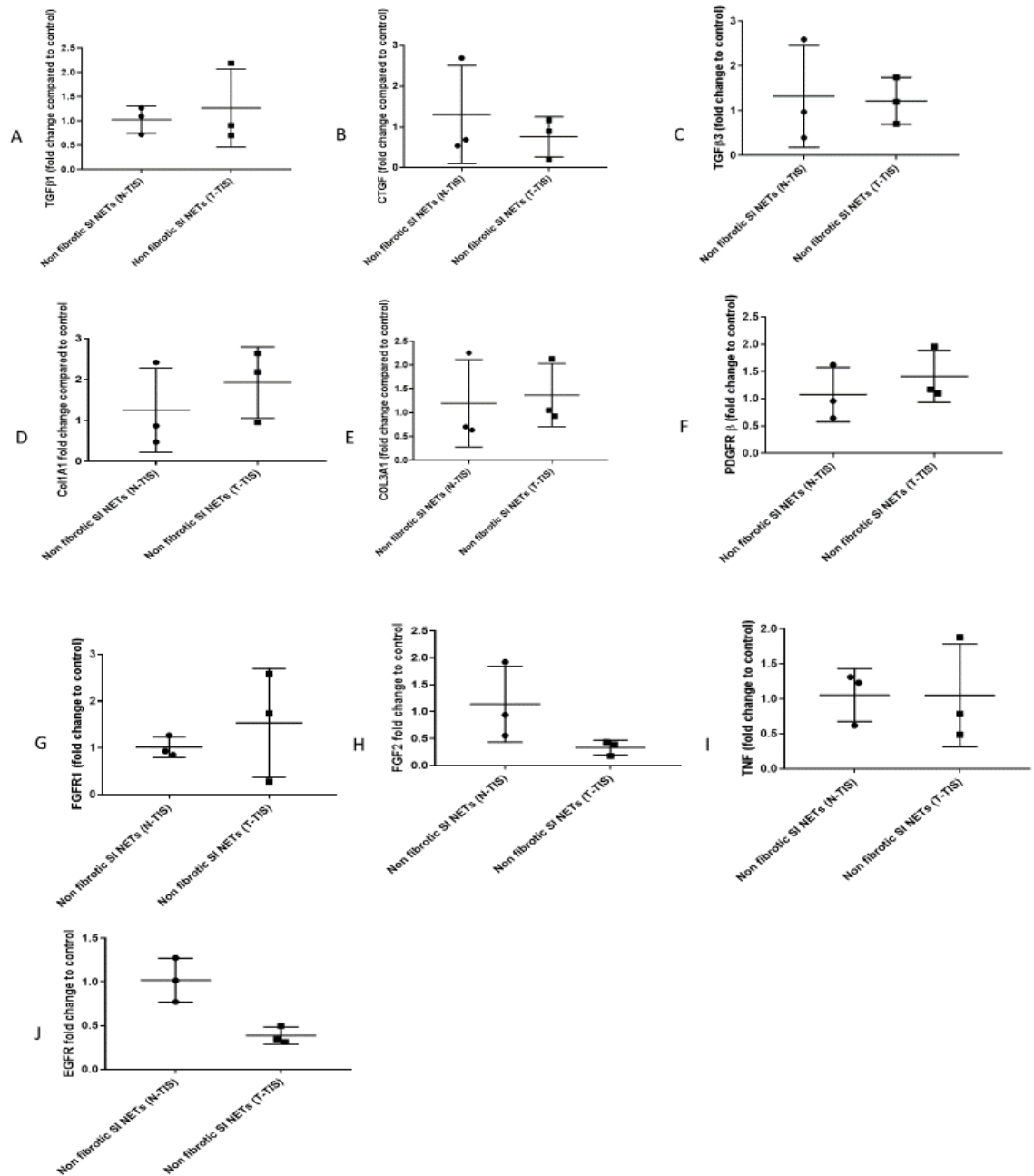
Figure 4.22. Gene expression in the normal mucosa and primary tumour of non-fibrotic SI NETs.
No significant changes were noted in the expression of selected profibrotic genes (A-J). Statistical analysis was performed using a Wilcoxon test. N-TIS: normal mucosa, T-TIS: primary tumour tissue, M-M: mesenteric mass.

4.3.1.2.3. Differences in profibrotic gene expression between different types of tumour tissue among different fibrosis groups

In this analysis, normalised gene expression between primary tumour and mesenteric mass was compared among different fibrosis subgroups using unpaired samples. A Kruskal-Wallis test was performed, and group differences were assessed using a Dunn's correction for multiple comparisons. The results of this analysis for each of the selected genes are shown in **Figures 4.23-4.32**. Generally, as demonstrated in these graphs, a significant upregulation in profibrotic gene expression was noted in the mesenteric mass of patients with established clinical fibrosis (mildly and severely fibrotic groups). This indicates that the mesenteric metastasis of fibrotic SI NETs exhibits a unique pattern of profibrotic gene expression, which is not present in other tissue types, where a desmoplastic reaction is not seen (such as the primary tumour of fibrotic and non-fibrotic SI NETs).
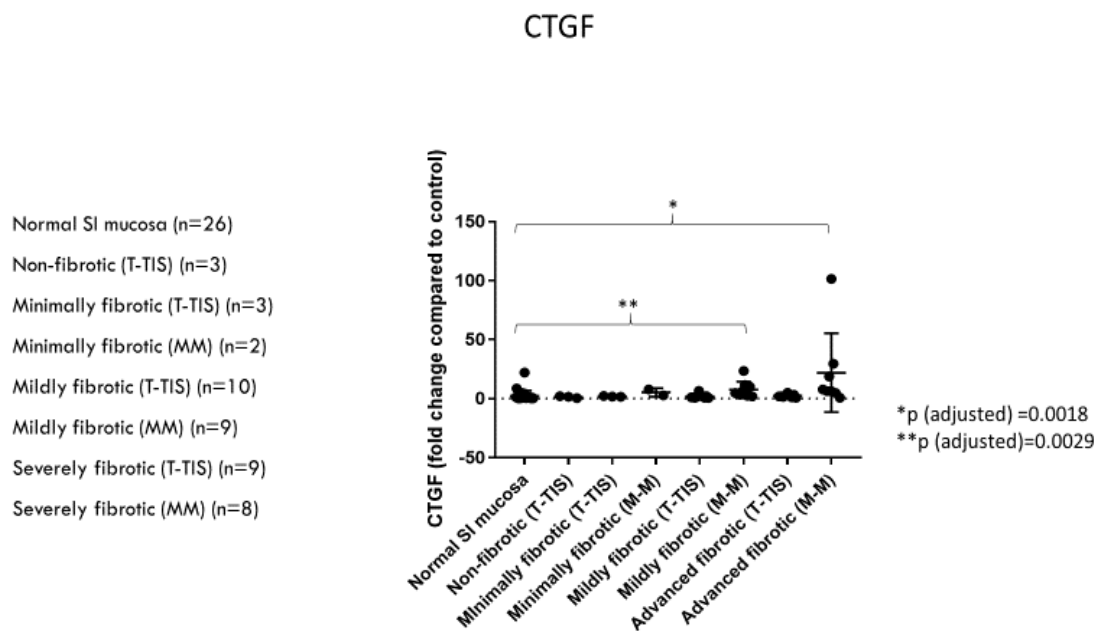
Figure 4.23. CTGF gene expression in different tissue types categorised by mesenteric fibrosis severity. CTGF expression was significantly higher in the mesenteric mass of mildly fibrotic and severely fibrotic patients compared to normal mucosa. (T-TIS: primary tumour, M-M: mesenteric mass)
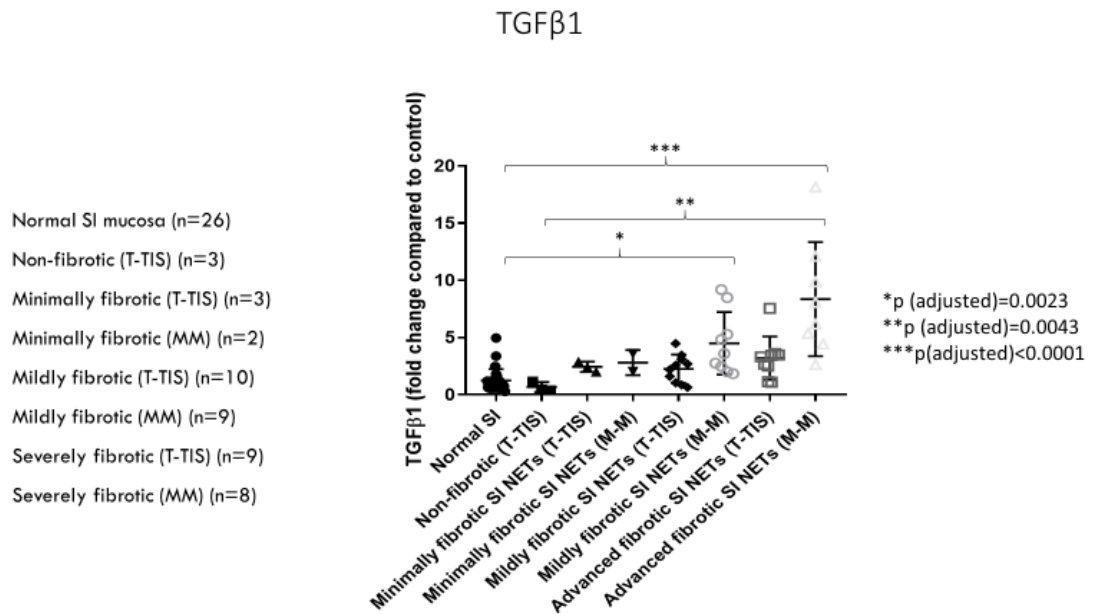
Figure 4.24. TGFβ1 gene expression in different tissue types categorised by mesenteric fibrosis severity. TGFβ1 expression was significantly higher in the mesenteric mass of mildly fibrotic and severely fibrotic patients compared to normal mucosa. In addition, TGFβ1 expression was substantially higher in the mesenteric mass of severely fibrotic tumours compared to the primary tumour of non-fibrotic tumours. (T-TIS: primary tumour, M-M: mesenteric mass)
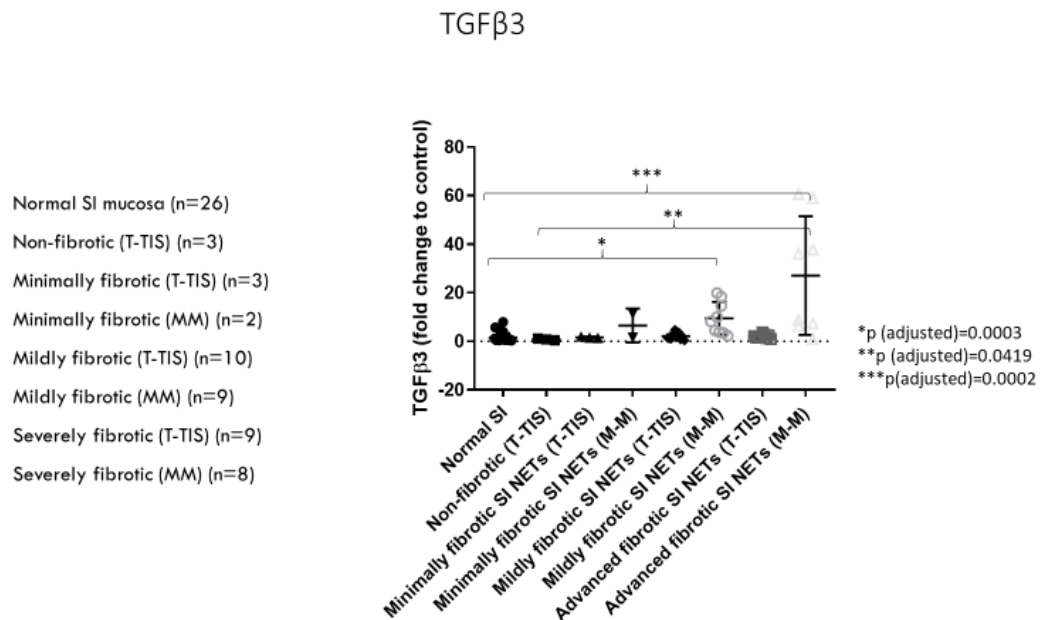
Figure 4.25. TGFβ3 gene expression in different tissue types categorised by mesenteric fibrosis severity. TGFβ3 expression was significantly higher in the mesenteric mass of mildly fibrotic and severely fibrotic patients compared to normal mucosa. In addition, TGFβ3 expression was substantially higher in the mesenteric mass of severely fibrotic tumours compared to the primary tumour of non-fibrotic tumours. (T-TIS: primary tumour, M-M: mesenteric mass)

Col1A1

Normal SI mucosa (n=26)
Non-fibrotic (T-TIS) (n=3)
Minimally fibrotic (T-TIS) (n=3)
Minimally fibrotic (MM) (n=2)
Mildly fibrotic (T-TIS) (n=10)
Mildly fibrotic (MM) (n=9)
Severely fibrotic (T-TIS) (n=9)
Severely fibrotic (MM) (n=8)

*p (adjusted)=0.0210
**p (adjusted)=0.0020

Figure 4.26. COL1A1 gene expression in different tissue types categorised by mesenteric fibrosis severity. COL1A1 expression was significantly higher in the mesenteric mass of mildly fibrotic and severely fibrotic patients compared to normal mucosa. (T-TIS: primary tumour, M-M: mesenteric mass)

Col3A1

Normal SI mucosa (n=26)
Non-fibrotic (T-TIS) (n=3)
Minimally fibrotic (T-TIS) (n=3)
Minimally fibrotic (MM) (n=2)
Mildly fibrotic (T-TIS) (n=10)
Mildly fibrotic (MM) (n=9)
Severely fibrotic (T-TIS) (n=9)
Severely fibrotic (MM) (n=8)

*p (adjusted)=0.0183

Figure 4.27. COL3A1 gene expression in different tissue types categorised by mesenteric fibrosis severity. COL3A1 expression was significantly higher in the mesenteric mass of severely fibrotic patients compared to normal mucosa. (T-TIS: primary tumour, M-M: mesenteric mass)

PDGF Receptor β

Normal SI mucosa (n=26)
Non-fibrotic (T-TIS) (n=3)
Minimally fibrotic (T-TIS) (n=3)
Minimally fibrotic (MM) (n=2)
Mildly fibrotic (T-TIS) (n=10)
Mildly fibrotic (MM) (n=9)
Severely fibrotic (T-TIS) (n=9)
Severely fibrotic (MM) (n=8)

*p (adjusted) <0.0001
**p (adjusted)=0.0091
***p (adjusted)=0.0053

Figure 4.28. PDGF receptor β gene expression in different tissue types categorised by mesenteric fibrosis severity. PDGF receptor β expression was significantly higher in the mesenteric mass of mildly and severely fibrotic patients compared to normal mucosa. In addition, PDGF receptor β expression was substantially higher in the mesenteric mass of mildly and severely fibrotic patients compared to the primary tumour of non-fibrotic patients. (T-TIS: primary tumour, M-M: mesenteric mass)

FGFR1

Normal SI mucosa (n=26)
Non-fibrotic (T-TIS) (n=3)
Minimally fibrotic (T-TIS) (n=3)
Minimally fibrotic (MM) (n=2)
Mildly fibrotic (T-TIS) (n=10)
Mildly fibrotic (MM) (n=9)
Severely fibrotic (T-TIS) (n=9)
Severely fibrotic (MM) (n=8)

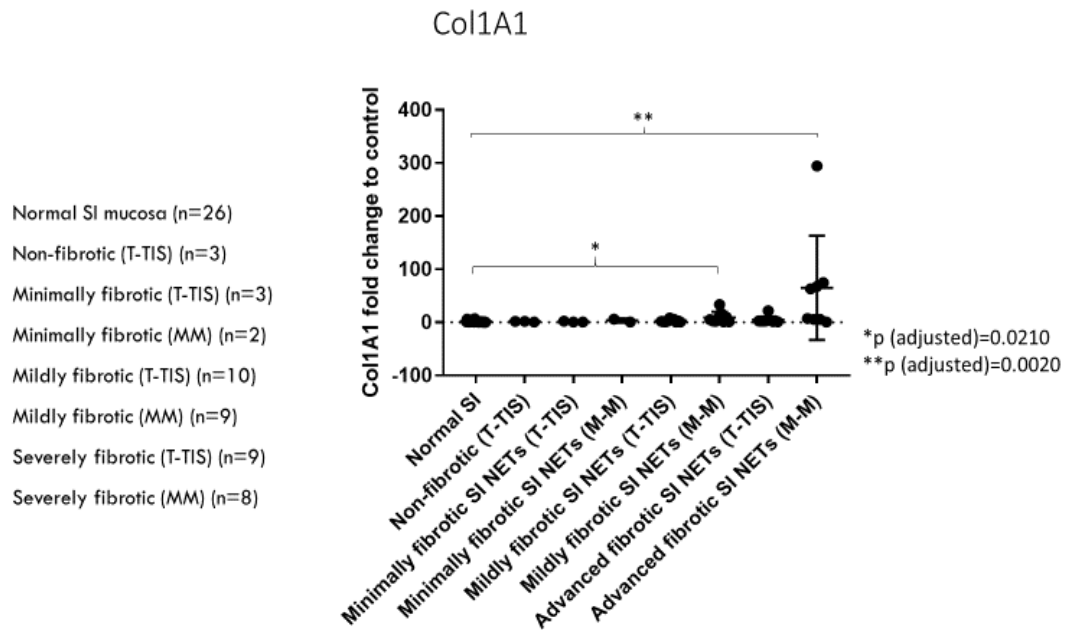*p (adjusted)=0.0003
**p (adjusted)=0.0002

Figure 4.29. FGFR1 gene expression in different tissue types categorised by mesenteric fibrosis severity. FGFR1 expression was significantly higher in the mesenteric mass of mildly fibrotic and severely fibrotic patients compared to normal mucosa. (T-TIS: primary tumour, M-M: mesenteric mass)
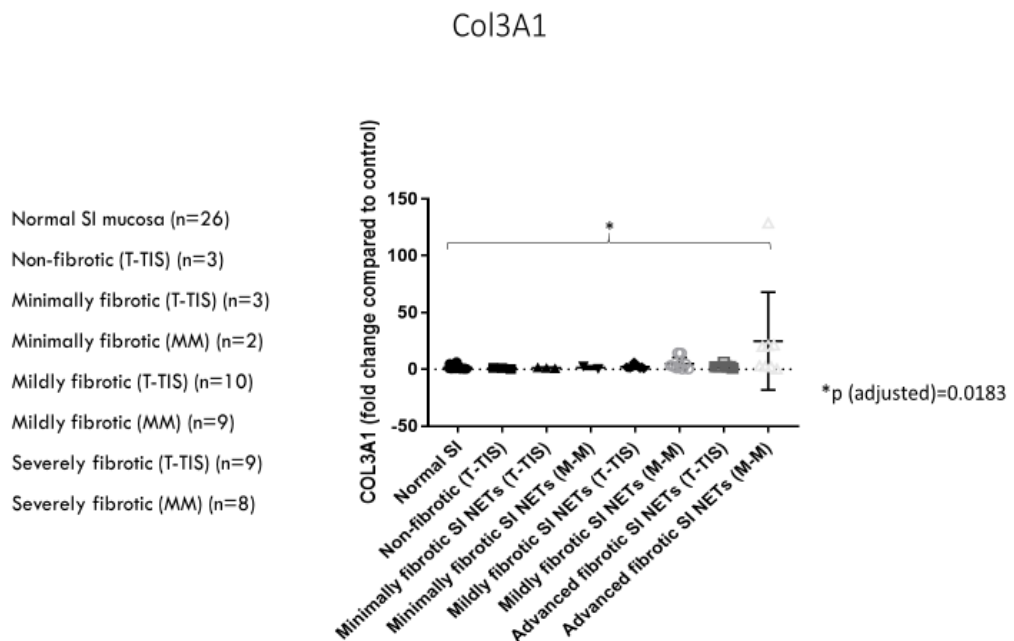
FGF2

Normal SI mucosa (n=26)

Non-fibrotic (T-TIS) (n=3)

Minimally fibrotic (T-TIS) (n=3)

Minimally fibrotic (MM) (n=2)

Mildly fibrotic (T-TIS) (n=10)

Mildly fibrotic (MM) (n=9)

Severely fibrotic (T-TIS) (n=9)

Severely fibrotic (MM) (n=8)
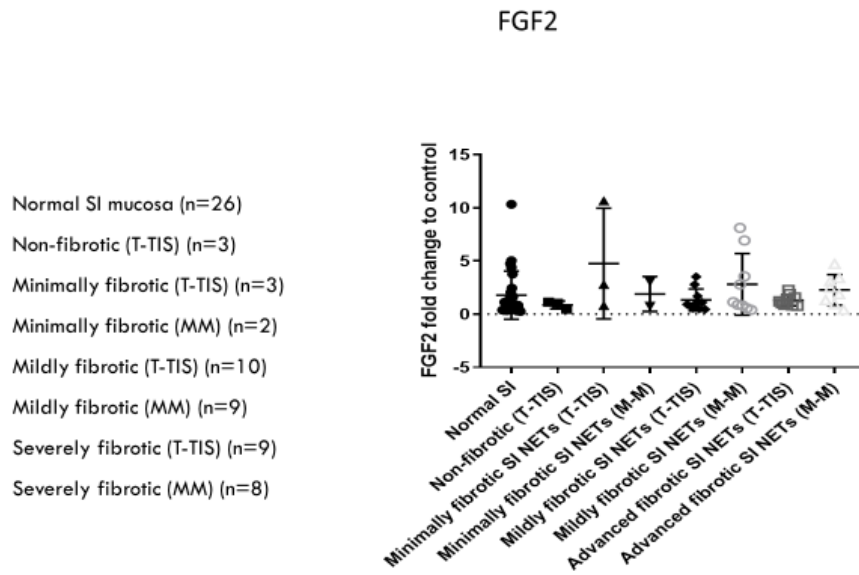
Figure 4.30. FGF2 gene expression in different tissue types categorised by mesenteric fibrosis severity. No significant differences were noted. (T-TIS: primary tumour, M-M: mesenteric mass)

TNF

Normal SI mucosa (n=26)

Non-fibrotic (T-TIS) (n=3)

Minimally fibrotic (T-TIS) (n=3)

Minimally fibrotic (MM) (n=2)

Mildly fibrotic (T-TIS) (n=10)

Mildly fibrotic (MM) (n=9)

Severely fibrotic (T-TIS) (n=9)

Severely fibrotic (MM) (n=8)
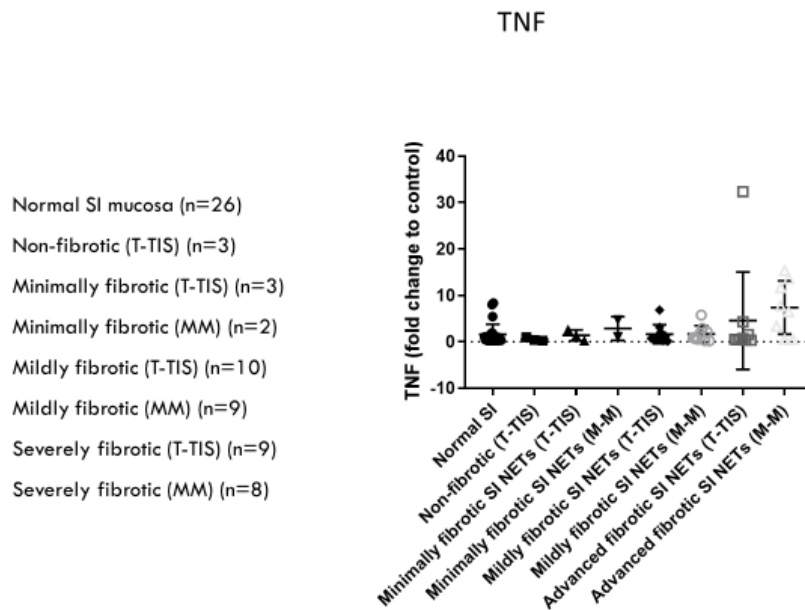
Figure 4.31. TNF gene expression in different tissue types categorised by mesenteric fibrosis severity. No significant differences were noted. (T-TIS: primary tumour, M-M: mesenteric mass)

EGFR

Normal SI mucosa (n=26)
Non-fibrotic (T-TIS) (n=3)
Minimally fibrotic (T-TIS) (n=3)
Minimally fibrotic (MM) (n=2)
Mildly fibrotic (T-TIS) (n=10)
Mildly fibrotic (MM) (n=9)
Severely fibrotic (T-TIS) (n=9)
Severely fibrotic (MM) (n=8)
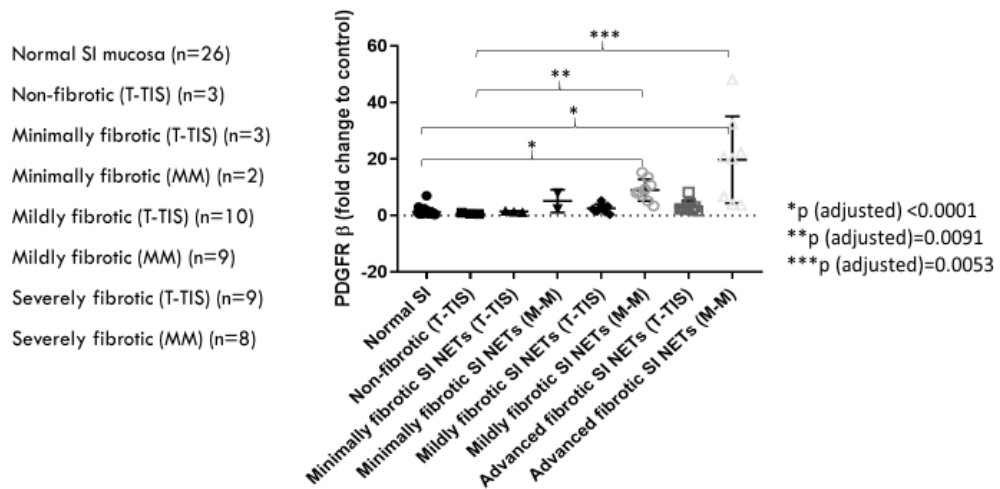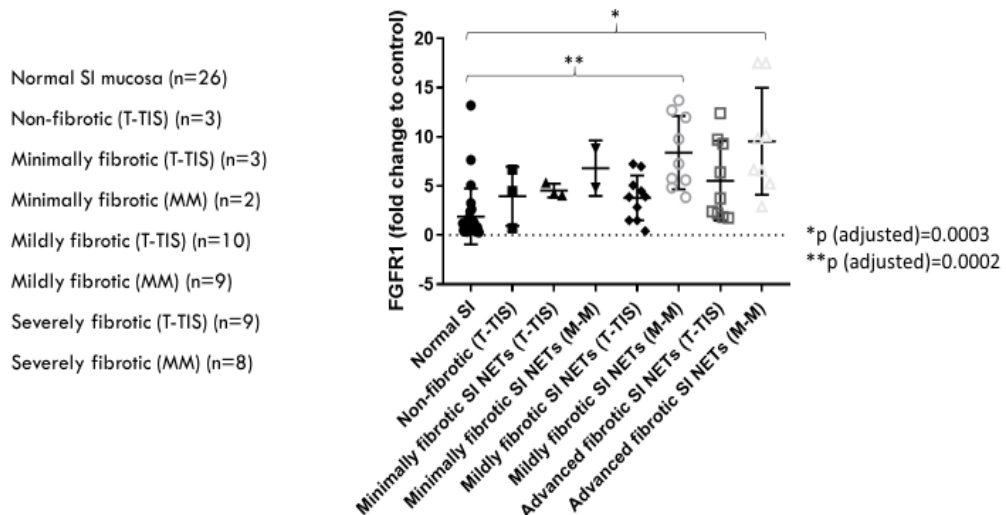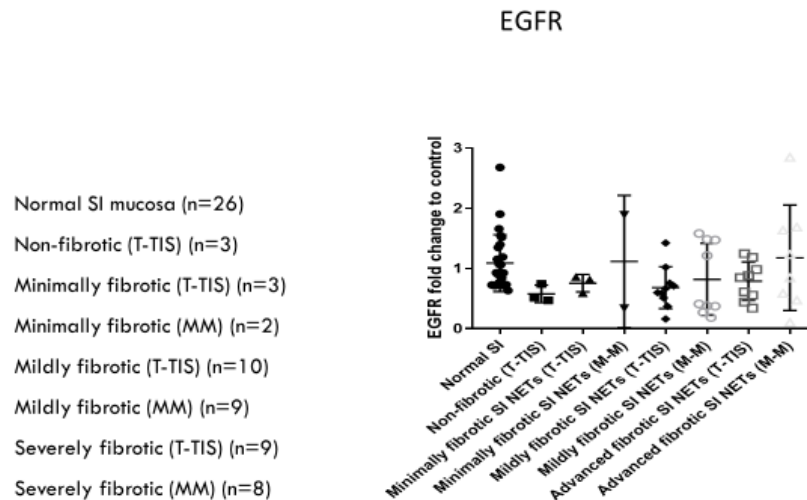
Figure 4.32. EGFR gene expression in different tissue types categorised by mesenteric fibrosis severity. No significant differences were noted. (T-TIS: primary tumour, M-M: mesenteric mass)

4.3.2. Evaluation of the integrin pathway

As described in **Chapter 3**, our *in vitro* functional experiments suggested that the integrin signalling pathway is significantly activated in KRJ-I cells exposed to HEK293 conditioned media. Both our RNA sequencing and Ingenuity Pathway Analysis (IPA), as well as the RT PCR Profiler data indicated that the *integrin pathway* (shown in **Figures 3.23** and **3.26**) is important for tumour-stromal interactions in the indirect co-culture model utilising KRJ-I and HEK293 cells. Therefore, we decided to evaluate this pathway in human tissue collected prospectively from fibrotic and non-fibrotic patients with midgut NETs. The integrin signalling pathway is known to play a critical role in both cancer-related fibrogenesis and tumour progression[164]. As mentioned earlier, integrins can interact with the TGFβ pathway and other components of the ECM, such as fibronectin, and can induce multiple transduction pathways intracellularly[164,166]. These actions can collectively promote cell growth, epithelial-mesenchymal transition and metastasis[150,164]. The role of the integrin pathway has not been previously explored in midgut NETs in relation to fibrogenesis.

4.3.2.1. Methods

A total of 34 patients enrolled into this study, and were grouped into non-fibrotic, minimally fibrotic, mildly and severely fibrotic groups, as described earlier. Fresh frozen tissue of normal small bowel mucosa, primary tumour and mesenteric mass of recruited patients was prospectively collected and stored in the RFH-UCL Biobank.

Components of the **integrin pathway** were assessed by a variety of different methods:

i. **qPCR (gene expression)**. qPCR was performed as previously described (see section 4.3.1.1) The following genes were assessed: COL1A1, COL3A1, fibronectin, TGFβ1, ITGAV (due to its significant upregulation in KRJ-I cells exposed to HEK conditioned media, as shown in our RT PCR Profiler data), ITGAX (due to its significant upregulation [2.1-fold, $p < 0.0001$] in KRJ-I cells exposed to HEK conditioned media, as shown in our RNA sequencing data). We used the following Assays-on-Demand primers: COL1A1 (Hs00164004), COL3A1 (Hs00943809), FN1 (Hs01549976), TGFβ1 (Hs00998133), ITGAV (Hs00233808), ITGAX (Hs00174217) and GAPDH (Hs02786624). Normalised gene expression was evaluated in both the primary tumour and mesenteric metastasis of all patients, using normal SI mucosa as control and GAPDH as a housekeeping gene. Statistical comparisons were performed using parametric or non-parametric tests, as appropriate, and GraphPad Prism® version 8 was used for the statistical analysis.

ii. **Immunohistochemistry (protein localisation)**. The following proteins were assessed: collagen I and III, fibronectin, TGFβ1, ITGAV, ITGAX and proliferation index Ki67. The immunohistochemistry for most of these proteins was performed by Mr Andrew Hall (Sheila Sherlock Liver Centre, Royal Free Hospital) except for Ki67 which was performed by the NHS laboratory of the Academic Department of Cellular Pathology as part of the routine diagnostic evaluation of resected tumours. Tissue samples of 3 patients per group (non-fibrotic, minimally fibrotic, mildly and severely fibrotic) were used for evaluation by immunohistochemistry. Sections from normal SI mucosa, primary and mesenteric tumours were submitted for immunohistochemical examination. **Antibody optimisation** for each of the evaluated proteins was based on suggested guidelines in the antibody data sheet provided by the vendor. The optimisation was carried

out on positive and negative control material by using variable antigen retrieval times, primary anybody dilutions and detection kit incubation times. This was an iterative process that resulted in an individual optimised protocol for each of the 6 antibodies (Collagen I, Collagen III, TGFβ1, Fibronectin, Integrin alpha X, Integrin alpha v). Tissue sections were cut on a rotary microtome at 4µm thickness and placed on Leica X-tra® adhesive glass slides (**sectioning**). Slides were incubated overnight (16-20 hrs) at 37ºC (**incubation**), were deparaffinised in xylene and rehydrated in graded alcohols (**hydration**). Thereafter, **antigen retrieval** was performed as per summary in **Table 4.6**. Slides were either placed into 1 litre of Sodium Citrate buffer (pH 6.0) or Tris-EDTA buffer (pH 9.0) and micro-waved or pressure cooked for a length of time according to antibody optimisation (**Table 4.6**) or trypsinised. Trypsinisation was carried out with 0.5% Trypsin and 0.5% Chymotrypsin in a pH 7.4 TBS with 1% calcium chloride at 37ºC. Next, **staining** was performed: On a staining tray, a hydrophobic pen was used to draw round the slides and the section was covered in TBS Tween wash buffer and left for 5 minutes. Slides were washed with TBS for 5 minutes at room temperature between each of the subsequent steps. Appropriate H_2O_2 and protein blocks were applied for 5 minutes each. Slides were incubated for 1 hour in optimised concentration of primary antibody, then the detection kit was applied (25 minutes post primary block, followed by NovoLink[TM] polymer for 25 minutes). The slides were then developed by incubation with diaminobenzidine (DAB) horseradish peroxidase (HRP) substrate for 3-5 minutes. Finally, the slides were counterstained in haematoxylin and mounted (**counterstaining**).

Primary antibody	Host	Company	Product code	Pre-treatment	Dilution
Collagen I	Rabbit pAb	AbCam	ab34710	Trypsinisation for 30 mins	1:200
Collagen III	Rabbit pAb	AbCam	ab7778	Citrate buffer and microwave for 20 mins	1:300
Fibronectin	Rabbit pAb	Abcam	ab2413	Citrate buffer and microwave for 10 mins	1:200
CD11c (Integrin alpha-X/beta-2)	Rabbit pAb	Abcam	ab52632	Tris-EDTA and microwave for 10 mins	1:500
Integrin alpha v	Rabbit pAb	Abcam	ab179475	Citrate buffer and microwave for 20 mins	1:250
TGFβ1	Rabbit pAb	Abcam	ab92486	Citrate buffer and microwave for 20 mins	1:75

Table 4.6. Summary of primary antibodies, pre-treatments and dilutions used for immunohistochemistry.

iii. **Western blot analysis (protein quantitation)**. Western blotting was performed using tissue samples of randomly selected patients from each of the mesenteric fibrosis groups (non-fibrotic [n=3], minimally fibrotic [n=3], mildly fibrotic [n=6] and severely fibrotic [n=3]). Normal mucosa, primary tumour and mesenteric metastatic tissue (5mg/sample) was lysed in protein lysis buffer (300 µl/sample) and protein concentrations were measured with a microBCA assay (ThermoFisher Scientific). Samples were pooled using a Western blot design which is shown in **Figure 4.33**. During sample pooling equal amounts of protein (8µg) were loaded for each sample and thus a total of 24µg of protein was loaded in each well. Total proteins were separated on 4-12% GenScript SurePAGE™ gels and transferred to PVDF membranes. The membranes were incubated with blocking buffer (5% BSA) for 1h and incubated with primary antibodies overnight at 4ºC. Primary antibodies used were as follows: ITGAV (1:2,000; AbCam), p44/42 MAPK (Erk 1/2) (1:1,000; Cell Signaling), phospho-p44/42 MAPK (Erk 1/2) (1:1,000; Cell Signaling), S6 ribosomal protein (1:1,000; Cell Signaling), phospho-S6 ribosomal protein (1:1,000; Cell Signaling), GAPDH (1:200; Santa Cruz). Blots were incubated with peroxidase-coupled secondary antibodies (1:10,000 anti-rabbit IgG, HRP-linked antibody; Cell Signaling for all of the above primary antibodies except for GAPDH, or 1:10,000 goat anti-mouse IgG-HRP secondary antibody; Santa Cruz for GAPDH) for 1 h, and protein expression was detected with SuperSignal West Pico Chemiluminescent Substrate (ThermoFisher Scientific).

Band intensity was measured using Image J and GAPDH served as a loading control.
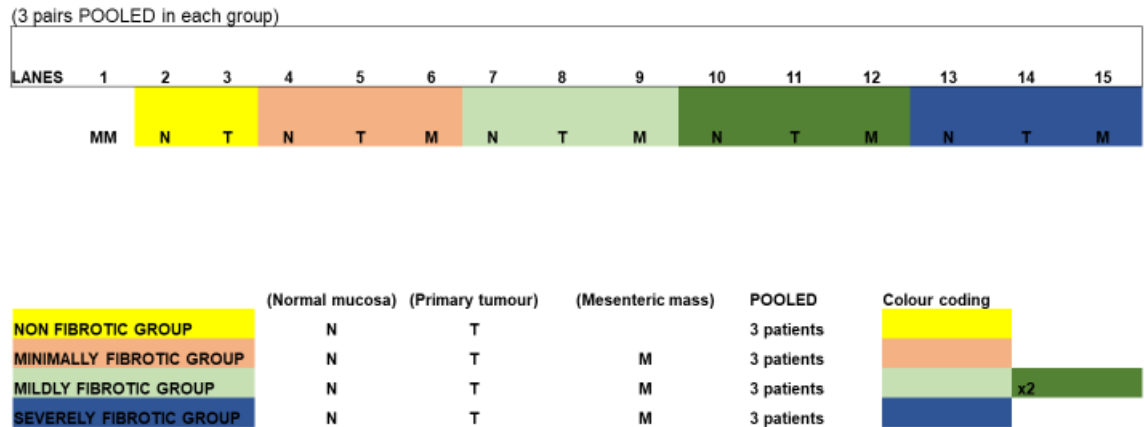
Figure 4.33. Design of Western blot analysis. Sample pooling was performed (3 samples pooled in each well), in order to allow evaluation of all the different mesenteric fibrosis groups in the same blot (Non-fibrotic [n=3], minimally fibrotic [n=3], mildly fibrotic [n=6] and severely fibrotic patients [n=3]). MM: Molecular Marker.

4.3.2.2. Results

4.3.2.2.1. qPCR results

In **non-fibrotic tumours**, there were no significant differences in gene expression between the primary tumour and normal SI mucosa for any of the evaluated genes (TGFβ1, COL1A1, COL3A1, fibronectin, ITGAV and ITGAX), as shown in **Figure 4.34**.
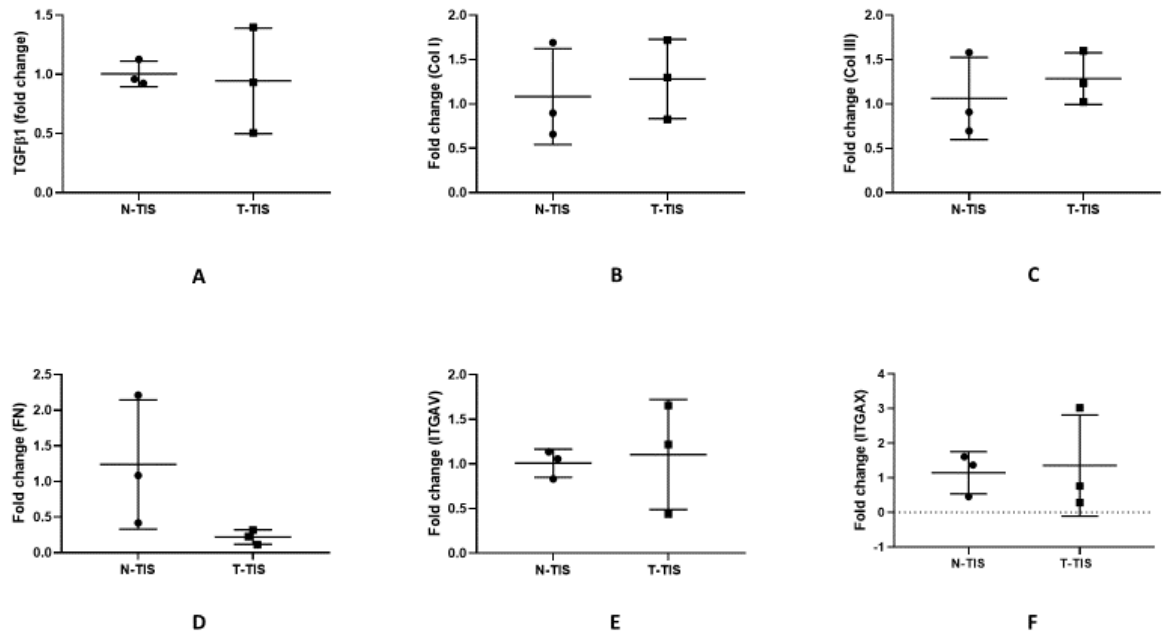
Figure 4.34. Normalised gene expression of several genes involved in the integrin signalling pathway (A-F) in non-fibrotic midgut NETs. No significant differences were seen between the primary tumour and control (normal SI mucosa). N-TIS: normal small intestinal mucosa, T-TIS: primary tumour tissue.

In contrast, in **fibrotic midgut NETs**, there was a significantly higher expression of all the evaluated genes in the mesenteric mass compared to control (normal SI mucosa) and primary tumour tissue. In addition, gene expression in the primary tumour was higher compared to control (normal SI mucosa) for most genes (TGFβ1, COL1A1, COL3A1, ITGAV, ITGAX). These results are shown in **Figures 4.35-4.40** collectively for the entire group of fibrotic midgut NETs (panel A), as well as separately for each of the different groups of mesenteric fibrosis severity, i.e. minimally fibrotic (panel B), mildly (panel C) and severely fibrotic (panel D).
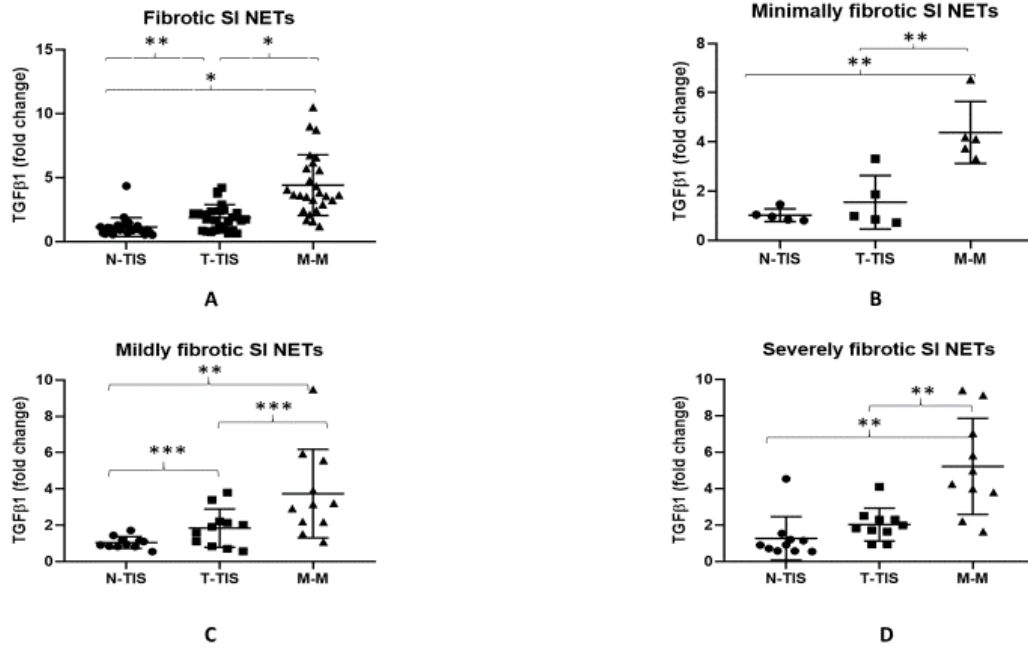
Figure 4.35. Changes in gene expression of TGFβ1 in fibrotic midgut NETs. **(A)** In the entire group of fibrotic midgut NETs (n=26) a significant stepwise increase was noted in TGFβ1 expression in the primary tumour and mesenteric mass, suggesting that this profibrotic gene is highly expressed in the fibrotic mesenteric metastasis. **(B-D)** Patterns of TGFβ1 gene expression are shown separately for each of the different groups of mesenteric fibrosis severity, i.e. minimally fibrotic (n=5), mildly fibrotic (n=11) and severely fibrotic (n=10). Levels of statistical significance are indicated by asterisks: *p<0.001, **p<0.01, ***p<0.05. N-TIS: normal small intestinal mucosa, T-TIS: primary tumour tissue, M-M: mesenteric mass.
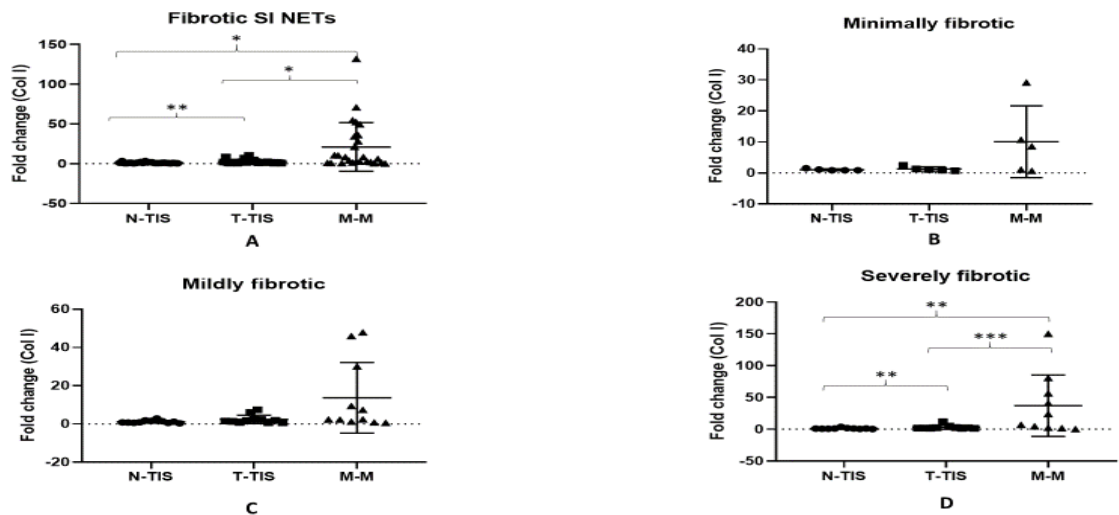
Figure 4.36. Changes in gene expression of collagen I (COL1A1) in fibrotic midgut NETs. (A) In the entire group of fibrotic midgut NETs (n=26) a significant stepwise increase was noted in collagen I expression in the primary tumour and mesenteric mass, suggesting that this profibrotic gene is highly expressed in the fibrotic mesenteric metastasis. **(B-D)** Patterns of collagen I gene expression are shown separately for each of the different groups of mesenteric fibrosis severity, i.e. minimally fibrotic (n=5), mildly fibrotic (n=11) and severely fibrotic (n=10). Levels of statistical significance are indicated by asterisks: $*p<0.001$, $**p<0.01$, $***p<0.05$. N-TIS: normal small intestinal mucosa, T-TIS: primary tumour tissue, M-M: mesenteric mass.

Figure 4.37. Changes in gene expression of collagen III (COL3A1) in fibrotic midgut NETs. (A) In the entire group of fibrotic midgut NETs (n=26) a significant stepwise increase was noted in collagen III expression in the primary tumour and mesenteric mass, suggesting that this profibrotic gene is highly

expressed in the fibrotic mesenteric metastasis. **(B-D)** Patterns of collagen III gene expression are shown separately for each of the different groups of mesenteric fibrosis severity, i.e. minimally fibrotic (n=5), mildly fibrotic (n=11) and severely fibrotic (n=10). Levels of statistical significance are indicated by asterisks: *p<0.001, **p<0.01, ***p<0.05. N-TIS: normal small intestinal mucosa, T-TIS: primary tumour tissue, M-M: mesenteric mass.
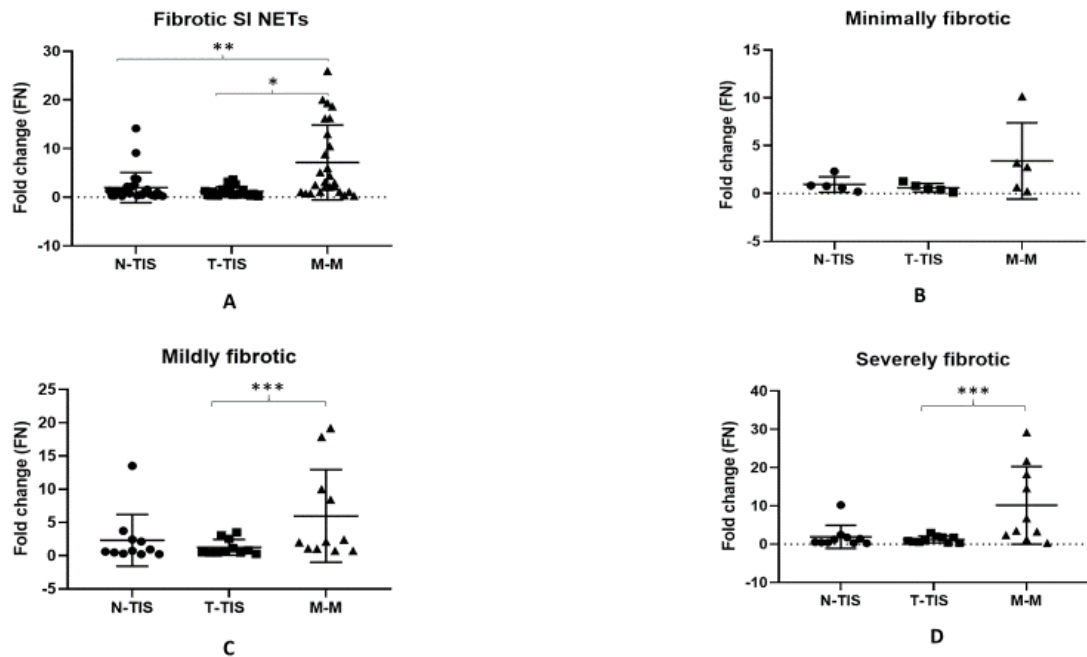
Figure 4.38. Changes in gene expression of fibronectin in fibrotic midgut NETs. (A) A significantly higher gene expression of fibronectin was observed in the mesenteric mass compared to the primary tumour and normal mucosa. **(B-D)** Patterns of fibronectin gene expression are shown separately for each of the different groups of mesenteric fibrosis severity, i.e. minimally fibrotic (n=5), mildly fibrotic (n=11) and severely fibrotic (n=10). Levels of statistical significance are indicated by asterisks: *p<0.001, **p<0.01, ***p<0.05. N-TIS: normal small intestinal mucosa, T-TIS: primary tumour tissue, M-M: mesenteric mass.
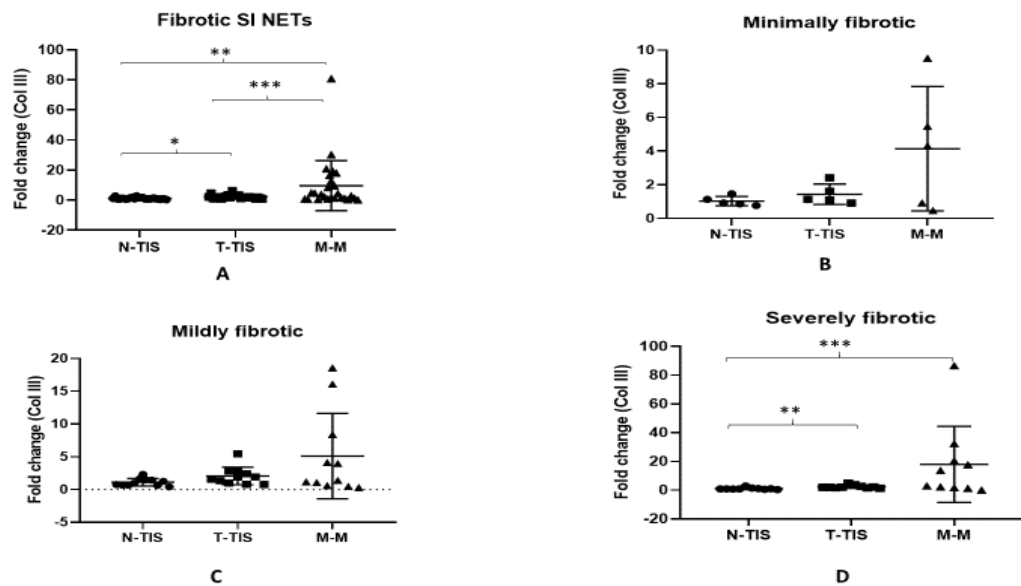
Figure 4.39. Changes in gene expression of ITGAV in fibrotic midgut NETs. (A) In the entire group of fibrotic midgut NETs (n=26) a significant stepwise increase was noted in ITGAV expression in the primary tumour and mesenteric mass, suggesting that this profibrotic gene is highly expressed in the fibrotic mesenteric metastasis. **(B-D)** Patterns of ITGAV gene expression are shown separately for each of the different groups of mesenteric fibrosis severity, i.e. minimally fibrotic (n=5), mildly fibrotic (n=11) and severely fibrotic (n=10). Levels of statistical significance are indicated by asterisks: *p<0.001, **p<0.01, ***p<0.05. N-TIS: normal small intestinal mucosa, T-TIS: primary tumour tissue, M-M: mesenteric mass.

Figure 4.40. Changes in gene expression of ITGAX in fibrotic midgut NETs. (A) In the entire group of fibrotic midgut NETs (n=26) a significant stepwise increase was noted in ITGAX expression in the primary tumour and mesenteric mass, suggesting that this profibrotic gene is highly expressed in the

fibrotic mesenteric metastasis. **(B-D)** Patterns of ITGAX gene expression are shown separately for each of the different groups of mesenteric fibrosis severity, i.e. minimally fibrotic (n=5), mildly fibrotic (n=11) and severely fibrotic (n=10). Levels of statistical significance are indicated by asterisks: *p<0.001, **p<0.01, ***p<0.05. N-TIS: normal small intestinal mucosa, T-TIS: primary tumour tissue, M-M: mesenteric mass.

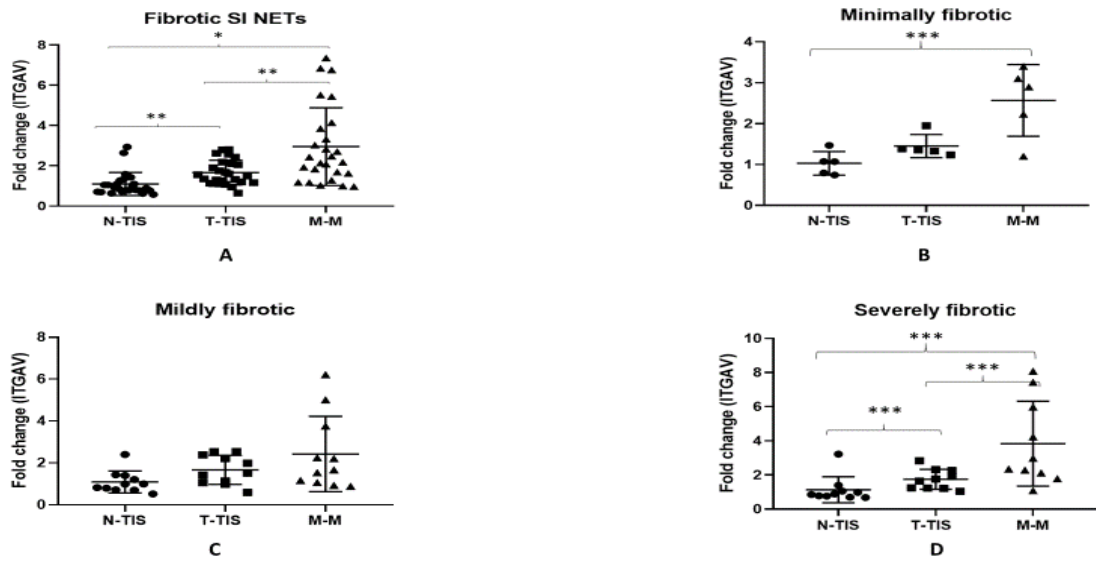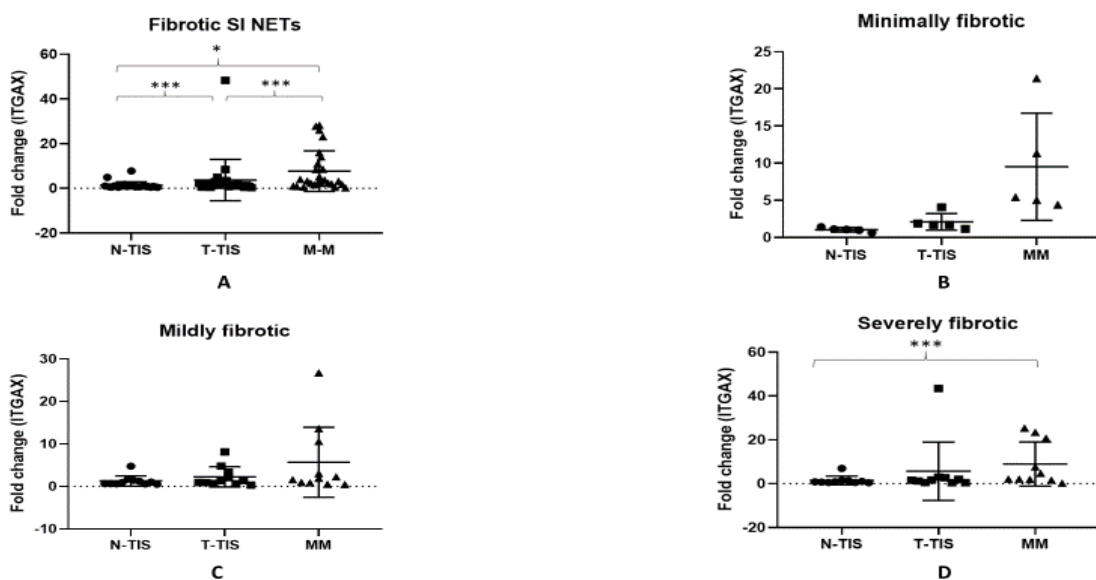Finally, we assessed **normalised gene expression in the primary tumour and mesenteric mass across different groups of mesenteric fibrosis severity**. As shown in **Figures 4.41-4.46**, generally a significantly higher expression of the evaluated genes was seen in the mesenteric mass of midgut neuroendocrine tumours, which was consistently elevated particularly in patients with severe fibrosis. This further validates the role of the evaluated genes of the integrin signalling pathway in the neoplastic fibrotic microenvironment of midgut NETs.
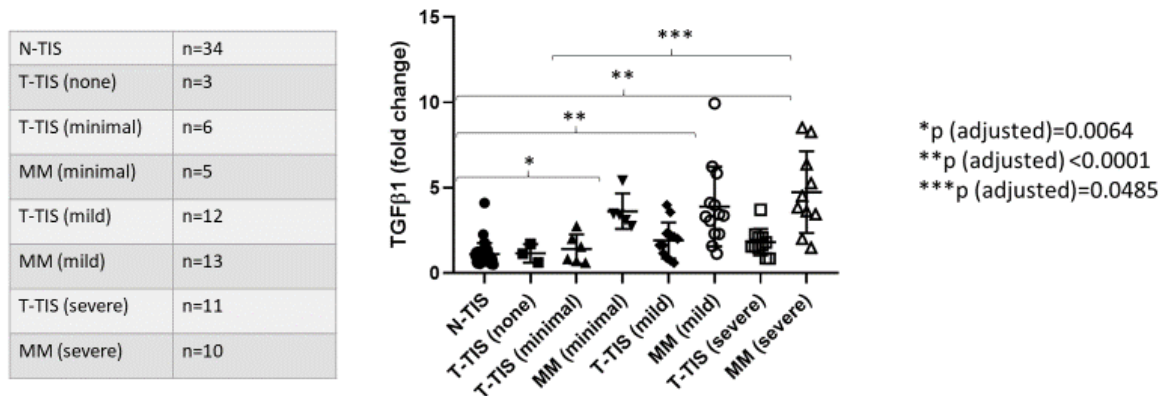
Figure 4.41. Normalised gene expression of TGFβ1 in the primary tumour and mesenteric mass of midgut NETs across different groups of mesenteric fibrosis severity (unpaired samples). TGFβ1 gene expression was significantly higher in the mesenteric mass of minimally, mildly and severely fibrotic patients compared to normal SI mucosa. In addition, TGFβ1 gene expression was significantly higher in the mesenteric mass of patients with severe fibrosis compared to the primary tumour of non-fibrotic patients. A Dunn's correction for multiple comparisons was performed and adjusted p-values are shown. N-TIS: normal SI mucosa, T-TIS: primary tumour tissue, MM: mesenteric mass.

N-TIS	n=34
T-TIS (none)	n=3
T-TIS (minimal)	n=6
MM (minimal)	n=5
T-TIS (mild)	n=12
MM (mild)	n=13
T-TIS (severe)	n=11
MM (severe)	n=10

*p (adjusted)=0.0006
**p (adjusted)=0.0011
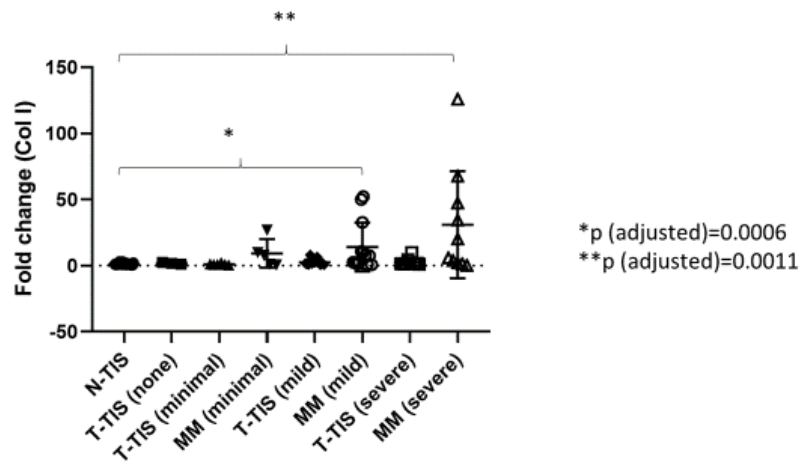
Figure 4.42. Normalised gene expression of collagen I (COL1A1) in the primary tumour and mesenteric mass of midgut NETs across different groups of mesenteric fibrosis severity (unpaired samples). COL1A1 gene expression was significantly higher in the mesenteric mass of mildly and severely fibrotic patients compared to normal SI mucosa. A Dunn's correction for multiple comparisons was performed and adjusted p-values are shown. N-TIS: normal SI mucosa, T-TIS: primary tumour tissue, MM: mesenteric mass.

N-TIS	n=34
T-TIS (none)	n=3
T-TIS (minimal)	n=6
MM (minimal)	n=5
T-TIS (mild)	n=12
MM (mild)	n=13
T-TIS (severe)	n=11
MM (severe)	n=10

*p (adjusted)=0.0044
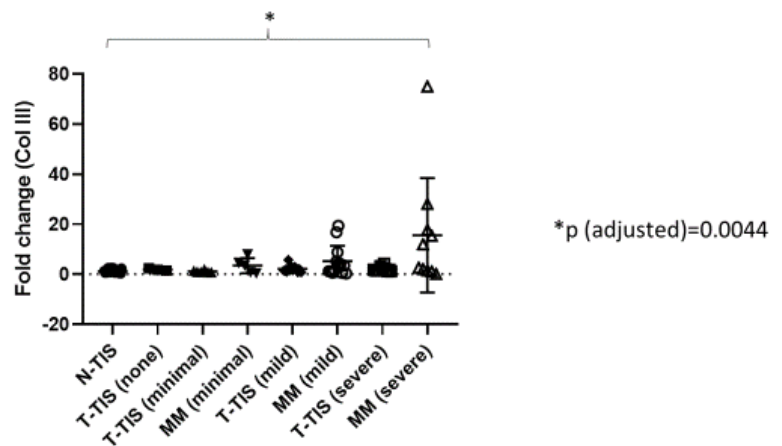
Figure 4.43. Normalised gene expression of collagen III (COL3A1) in the primary tumour and mesenteric mass of midgut NETs across different groups of mesenteric fibrosis severity (unpaired samples). COL3A1 gene expression was significantly higher in the mesenteric mass of severely fibrotic patients compared to normal SI mucosa. A Dunn's correction for multiple comparisons was performed and adjusted p-values are shown. N-TIS: normal SI mucosa, T-TIS: primary tumour tissue, MM: mesenteric mass.

N-TIS	n=34
T-TIS (none)	n=3
T-TIS (minimal)	n=6
MM (minimal)	n=5
T-TIS (mild)	n=12
MM (mild)	n=13
T-TIS (severe)	n=11
MM (severe)	n=10
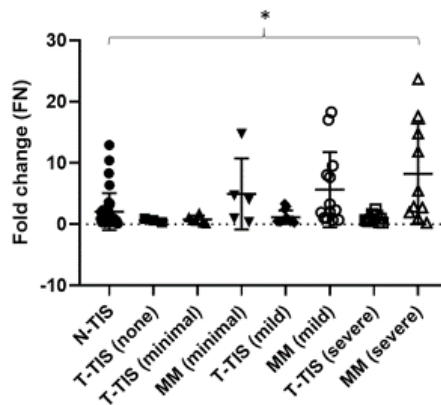
*p (adjusted)=0.0362

Figure 4.44. Normalised gene expression of fibronectin in the primary tumour and mesenteric mass of midgut NETs across different groups of mesenteric fibrosis severity (unpaired samples). Fibronectin gene expression was significantly higher in the mesenteric mass of severely fibrotic patients compared to normal SI mucosa. A Dunn's correction for multiple comparisons was performed and adjusted p-values are shown. N-TIS: normal SI mucosa, T-TIS: primary tumour tissue, MM: mesenteric mass.

N-TIS	n=34
T-TIS (none)	n=3
T-TIS (minimal)	n=6
MM (minimal)	n=5
T-TIS (mild)	n=12
MM (mild)	n=13
T-TIS (severe)	n=11
MM (severe)	n=10
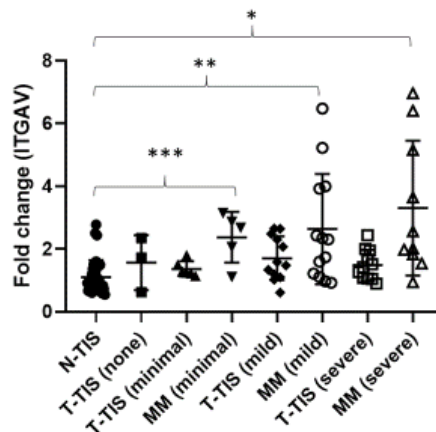
*p (adjusted)=0.0003
**p (adjusted)=0.0024
***p (adjusted)=0.0256

Figure 4.45. Normalised gene expression of ITGAV in the primary tumour and mesenteric mass of midgut NETs across different groups of mesenteric fibrosis severity (unpaired samples). ITGAV gene expression was significantly higher in the mesenteric mass of minimally, mildly and severely fibrotic patients compared to normal SI mucosa. A Dunn's correction for multiple comparisons was performed and adjusted p-values are shown. N-TIS: normal SI mucosa, T-TIS: primary tumour tissue, MM: mesenteric mass.

| N-TIS | n=34 |
T-TIS (none)	n=3
T-TIS (minimal)	n=6
MM (minimal)	n=5
T-TIS (mild)	n=12
MM (mild)	n=13
T-TIS (severe)	n=11
MM (severe)	n=10

*p (adj)=0.0049
**p (adj)=0.0097
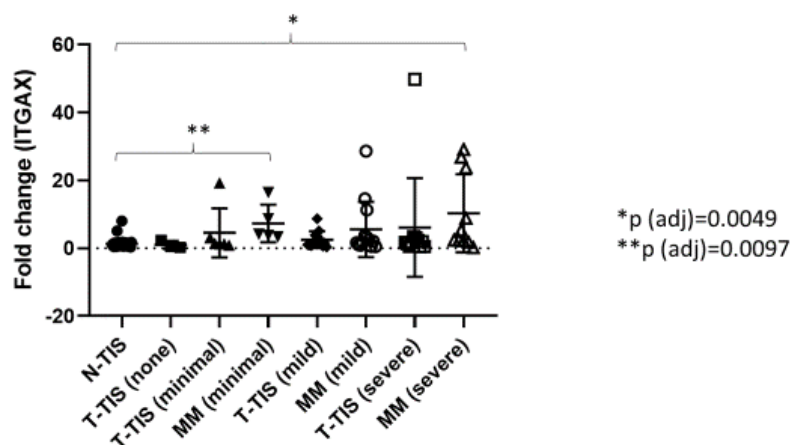
Figure 4.46. Normalised gene expression of ITGAX in the primary tumour and mesenteric mass of midgut NETs across different groups of mesenteric fibrosis severity (unpaired samples). ITGAX gene expression was significantly higher in the mesenteric mass of minimally and severely fibrotic patients compared to normal SI mucosa. A Dunn's correction for multiple comparisons was performed and adjusted p-values are shown. N-TIS: normal SI mucosa, T-TIS: primary tumour tissue, MM: mesenteric mass.

4.3.2.2.2. Immunohistochemistry

The localisation of these proteins (i.e. in the tumour cells, stromal cells or the extra-cellular matrix) was further investigated by immunohistochemistry in the tissue of 12 patients (3 patients per fibrosis severity group).

TGFβ1 was present in the cytoplasm of both tumour cells and stromal cells and was weakly expressed in the extracellular matrix. An example is shown in **Figure 4.47**, which illustrates the localisation of TGFβ1 within the primary tumour of a mildly fibrotic midgut NET.
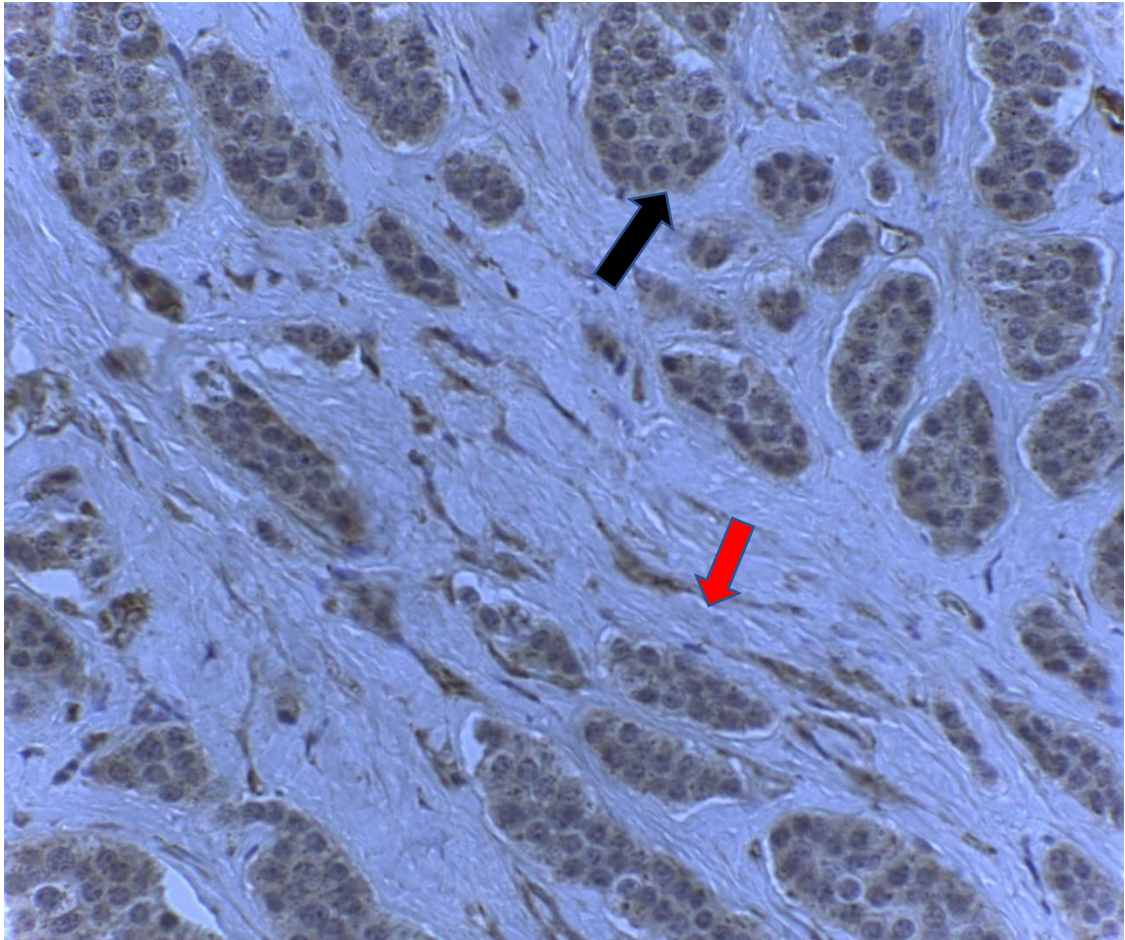
Figure 4.47. TGFβ1 expression in the primary tumour of a mildly fibrotic midgut NET. TGFβ1 was expressed in the cytoplasm of both cancer (black arrow) and stromal cells (red arrow) but was weakly expressed in the extracellular matrix (40x magnification).

Collagen I and III and fibronectin were highly expressed in the extracellular matrix, while the tumour cells did not stain for any of these proteins. Some examples are shown in **Figures 4.48-4.51**.
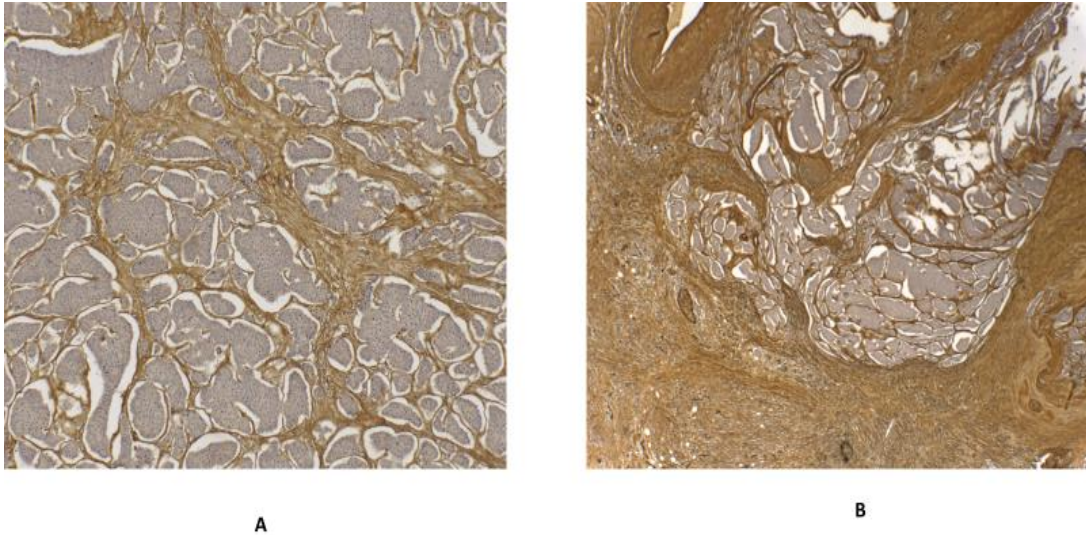
Figure 4.48. Collagen I expression in the primary tumour (A) and mesenteric mass (B) of a patient with advanced mesenteric fibrosis. The collagen I was present in the extracellular matrix, while the tumour cells did not stain. The mesenteric mass contained more stroma compared to the primary tumour, as expected. (Magnification 10x in primary tumour, 4x in mesenteric mass).
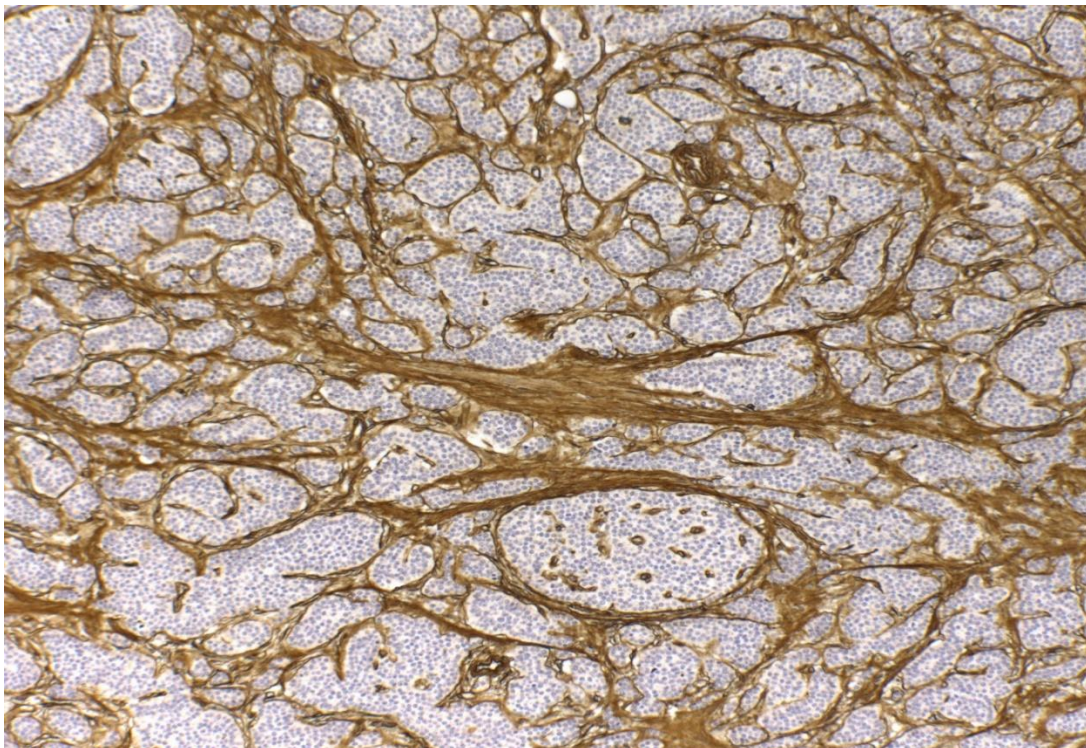
Figure 4.49. Collagen I expression in the primary tumour of a non-fibrotic patient. This patient had no mesenteric metastasis and therefore no fibrosis in the mesentery. However, it is clearly seen that collagen I was expressed in the stroma of the primary tumour. The tumour cells did not stain for collagen I. (magnification 10x)
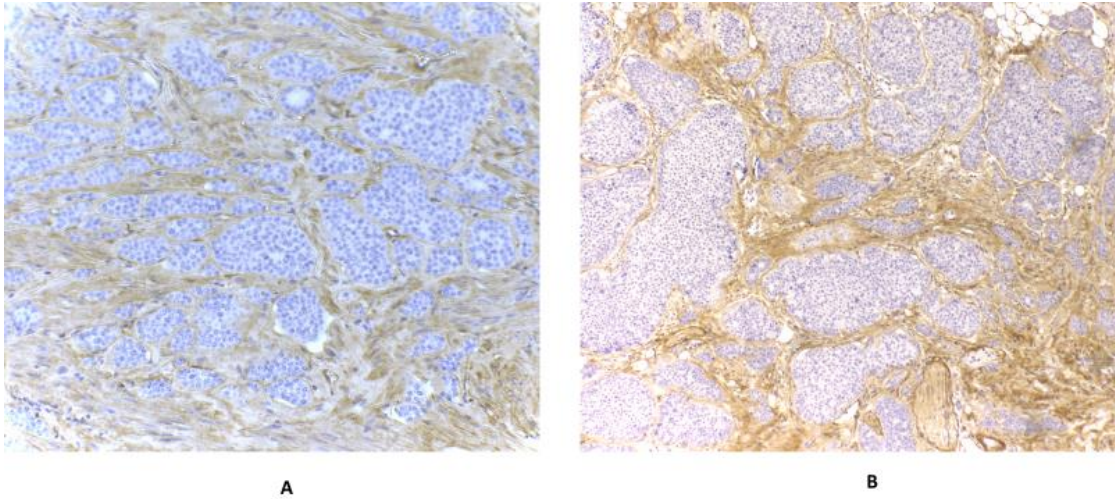
Figure 4.50. Collagen III expression in the primary tumour (A) and mesenteric mass (B) of a patient with mild fibrosis. Collagen III was present in the extracellular matrix, while the tumour cells did not stain for collagen III. (Magnification 10x in both the primary and mesenteric mass).
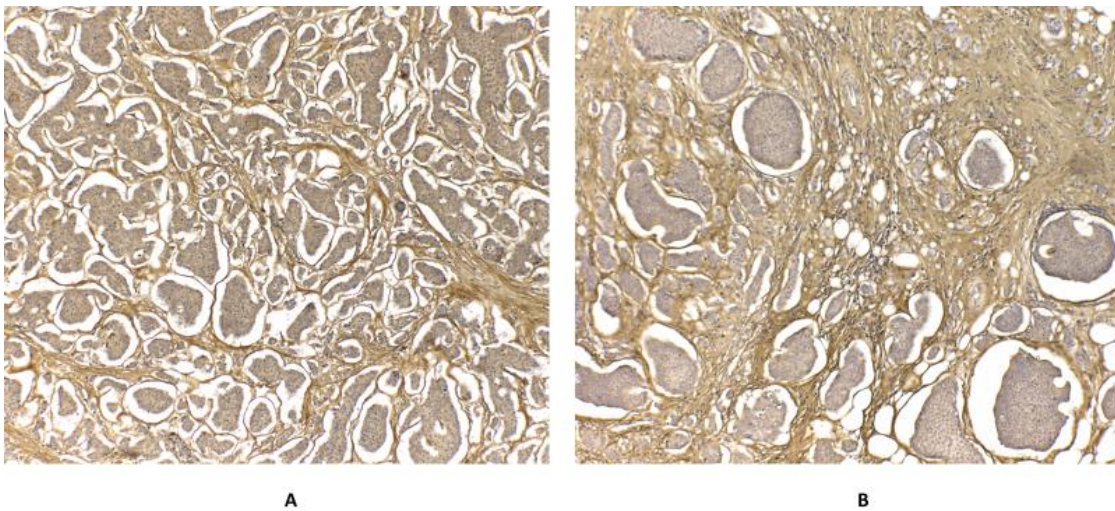
Figure 4.51. Fibronectin expression in the primary tumour (A) and mesenteric mass (B) of a patient with severe fibrosis. Fibronectin was expressed in the extracellular matrix, while the tumour cells did not stain for fibronectin. (magnification 10x in both the primary tumour and mesenteric mass).

Integrin α subunit v (ITGAV) was expressed in both tumour and stromal cells, and generally ITGAV expression was stronger in stromal cells compared to tumour cells, as shown in **Figure 4.52**. In some cases, ITGAV expression was weak in the cancer cells, as shown in **Figure 4.53**.
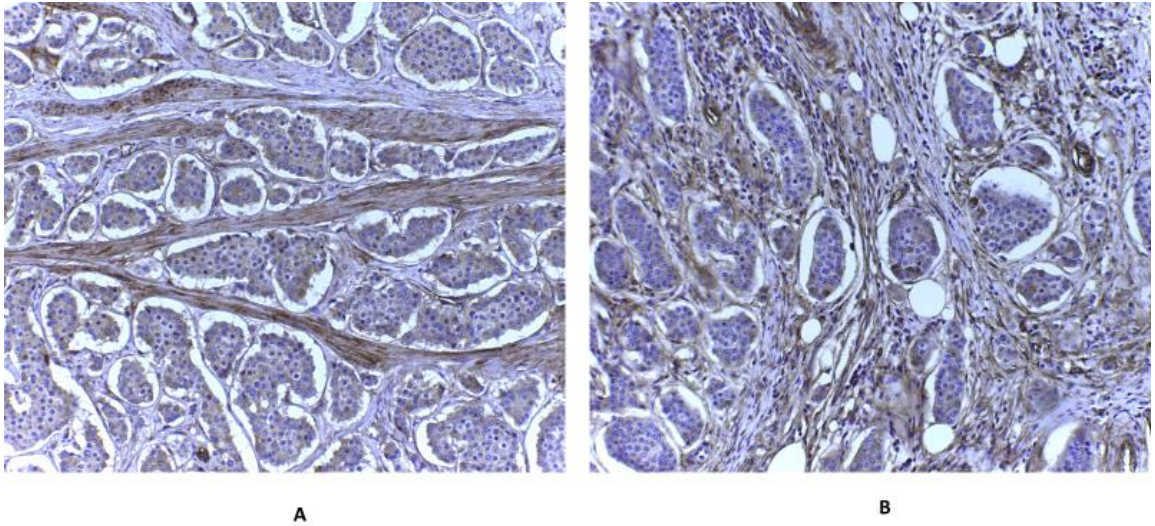
Figure 4.52. ITGAV expression in the primary tumour (A) and mesenteric mass (B) of a patient with severe mesenteric fibrosis. ITGAV was expressed in both the tumour and stromal cells. (Magnification 20x in both the primary tumour and mesenteric mass).
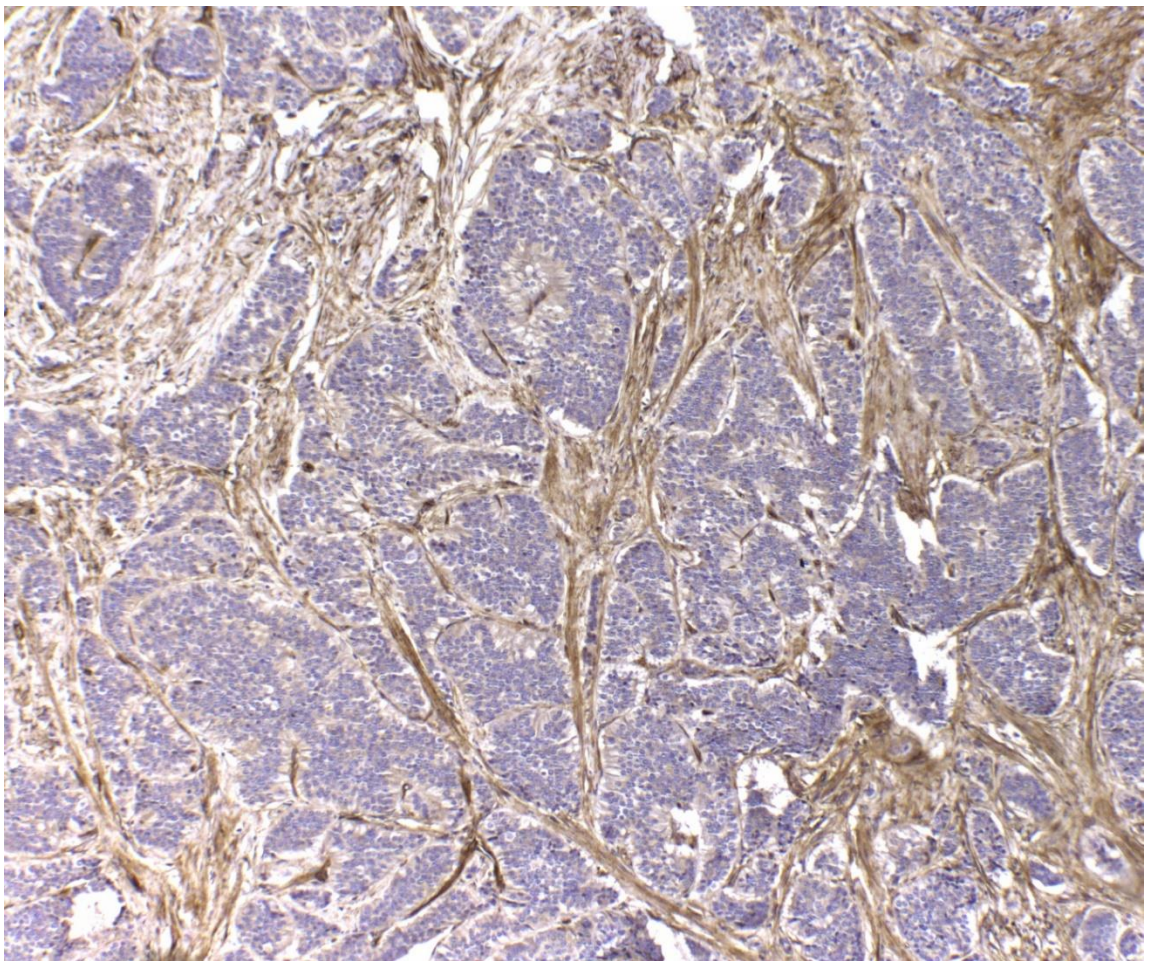
Figure 4.53. ITGAV expression in the primary tumour of a non-fibrotic patient. ITGAV was expressed in the stroma, while the tumour cells showed weak expression (magnification 10x).

Integrin α subunit X was expressed in inflammatory cell aggregates, although there were only few inflammatory cells within the midgut neuroendocrine tumours, as shown in **Figure 4.54**.
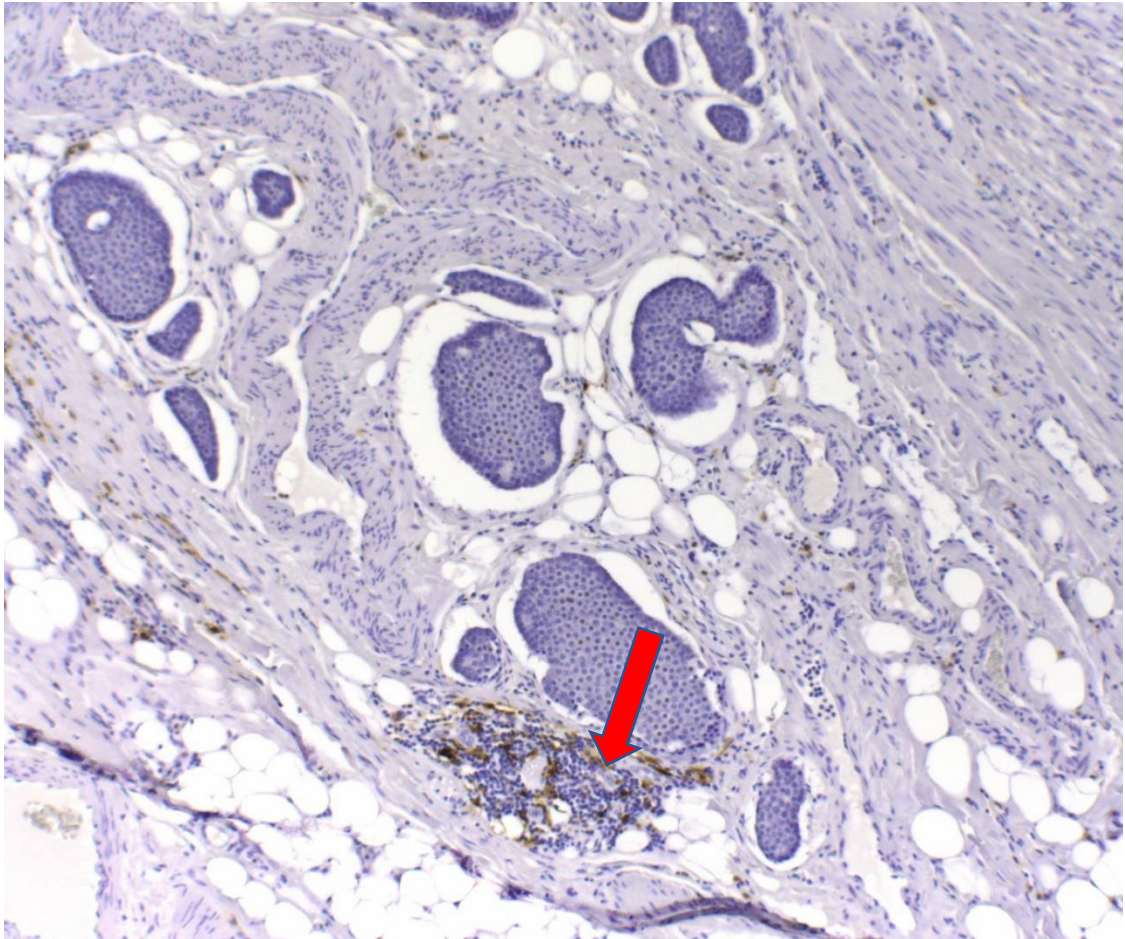
Figure 4.54. ITGAX expression in the mesenteric mass of a patient with severe mesenteric fibrosis. ITGAX was expressed within inflammatory cell aggregates (red arrow), but both the tumour and stromal cells did not stain for ITGAX. (magnification 10x).

The Ki67 proliferation index was also evaluated in the primary tumour and mesenteric mass of these 12 cases (3 patients per mesenteric fibrosis severity group). As shown in **Figure 4.55**, there were no significant differences between Ki67 proliferation indices in the primary tumour and mesenteric mass in any of the patient groups. Generally, the Ki67 index in the mesenteric mass was similar to the Ki67 index in the primary tumour, except for one patient in the advanced fibrosis group, in whom the Ki67 index was 5% in the mesenteric mass and 1% in the primary tumour.
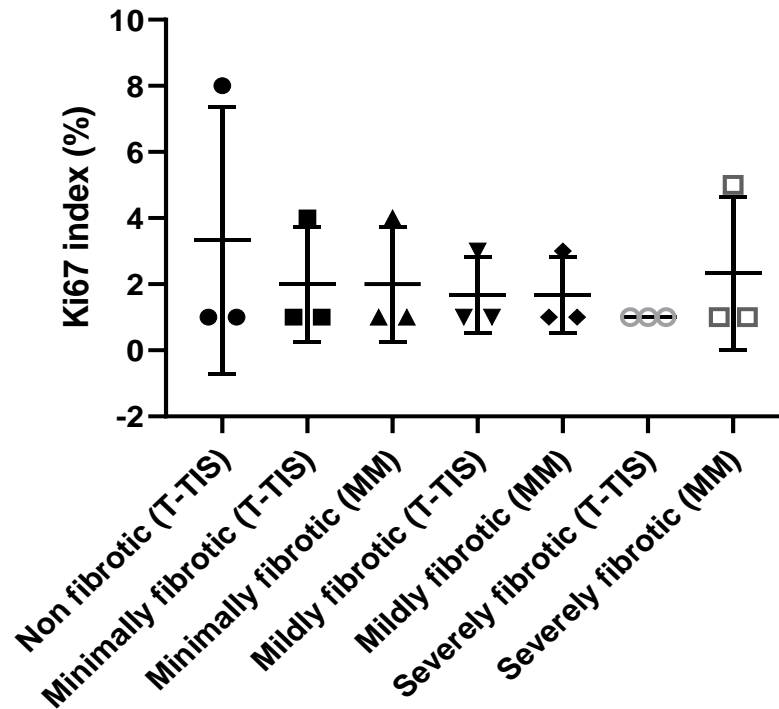
Figure 4.55. Ki67 proliferation index in the primary tumour and mesenteric mass across different patient groups of mesenteric fibrosis severity. There were no statistically significant differences among different types of tissue and across different patient groups (Kruskal Wallis test, p=0.9586).

4.3.2.2.3. Western blot

Two Western blots were performed, which evaluated the protein expression of ITGAV and the activation of its downstream signalling pathways, mTOR (S6 and phospho-S6) and MAPK (Erk 1/2 and phospho-Erk 1/2), as shown in **Figures 4.56-4.57**.
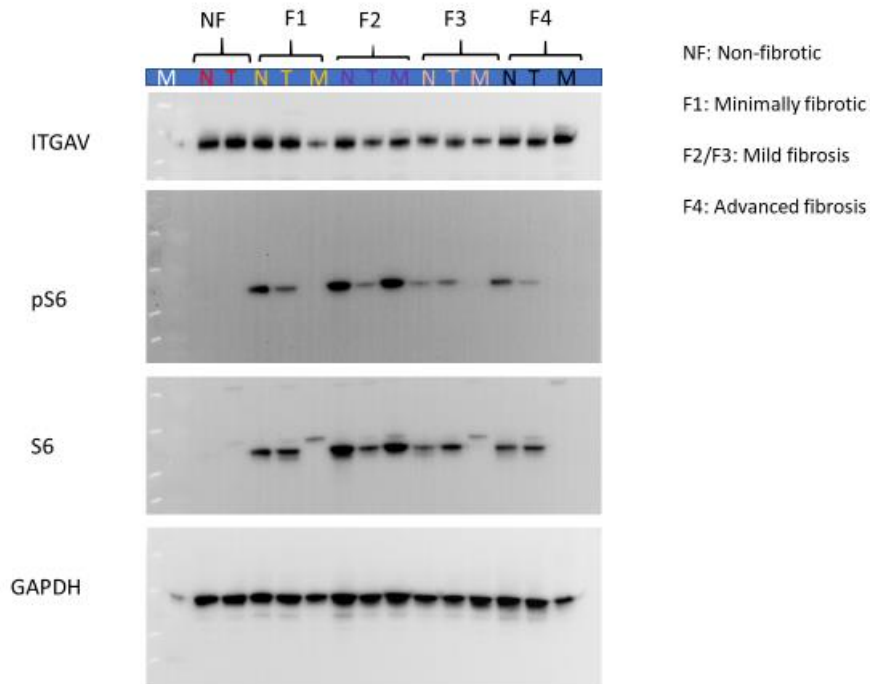
Figure 4.56. Western blot of pooled samples demonstrating the protein expression of ITGAV and downstream mTOR signalling (S6, phospho-S6) in fibrotic and non-fibrotic patients with SI NETs. GAPDH served as loading control. N: normal mucosa, T: Primary tumour, M: Mesenteric mass
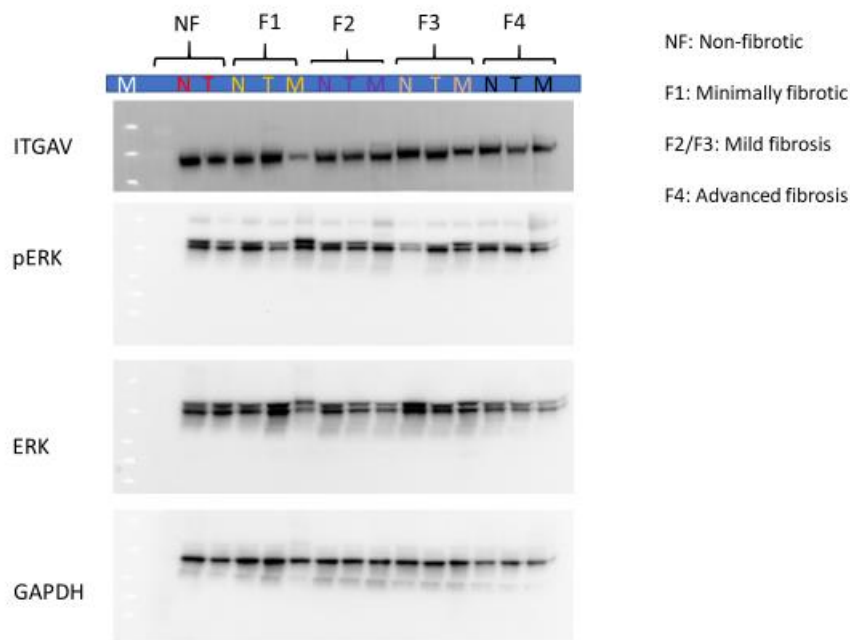
Figure 4.57. Western blot of pooled samples demonstrating the protein expression of ITGAV and downstream MAPK signalling (Erk 1/2, phospho-Erk 1/2) in fibrotic and non-fibrotic patients with SI NETs. GAPDH served as loading control. N: normal mucosa, T: Primary tumour, M: Mesenteric mass

4.3.2.2.3.1. ITGAV protein expression

ITGAV protein expression was highest in the mesenteric metastasis of patients with advanced fibrosis as shown in **Figures 4.56 and 4.58**. However, ITGAV protein expression was not significantly different between normal tissue, tumour tissue and metastasis, when all samples were pooled together in these 3 tissue categories. As shown in **Figure 4.58**, this is due to heterogeneity in protein expression among patients. For example, ITGAV expression was lower in the metastasis of minimally fibrotic patients (F1) compared to control (normal mucosa), while in patients with advanced fibrosis (F4) the expression was higher than that in normal mucosa.
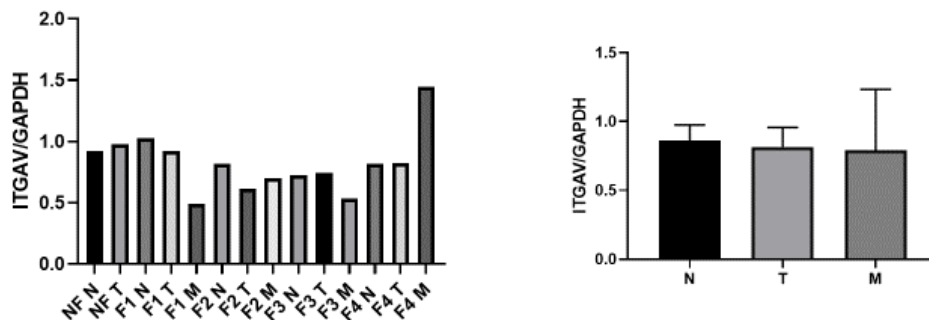
Figure 4.58. Densitometry analysis of Western blot shown in Figure 4.56. ITGAV protein expression was highest in the mesenteric metastasis of patients with advanced fibrosis (F4). NF: Non-fibrotic, F1: Minimally fibrotic, F2/F3: Mildly fibrotic, F4: Severely fibrotic.

4.3.2.2.3.2. mTOR signalling pathway

The presence and activation (phosphorylation) of protein S6 (a downstream mediator of the mTOR pathway) was evaluated, as illustrated in **Figures 4.56** and **4.59**. As shown in **Figure 4.59**, significant heterogeneity was noted in the activation of the S6 protein within the mesenteric metastasis of SI NETs. For example, in some cases (F1, F3 and F4 groups) there was lack of protein expression, while in other cases (F2) there was an increased p-S6:S6 ratio suggesting pathway activation.
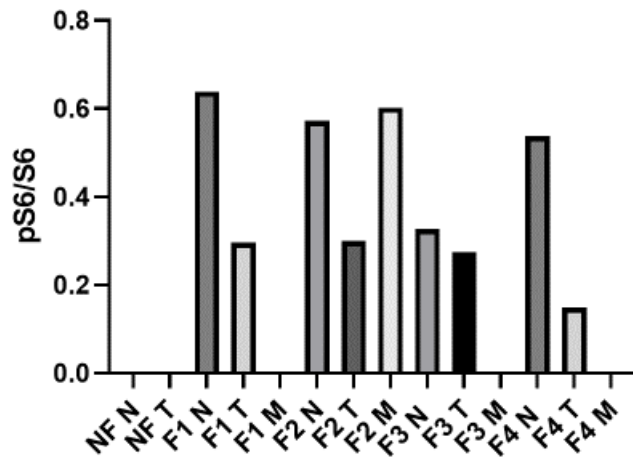
Figure 4.59. Densitometry analysis of Western blot shown in Figure 4.56. There was substantial heterogeneity in S6 protein expression and activation within the fibrotic mesenteric mass of patients with SI NETs. In some cases (F2) there was an elevated pS6:S6 ratio, suggesting activation of the mTOR pathway, while in other cases (F1, F3 and F4) there was lack of protein expression. NF: Non-fibrotic, F1: Minimally fibrotic, F2/F3: Mildly fibrotic, F4: Severely fibrotic.

4.3.2.2.3.3. MAPK signalling pathway

The presence and activation (phosphorylation) of Erk1 and Erk2 (downstream mediators of the MAPK signalling pathway) were assessed, as illustrated in **Figures 4.57** and **4.60**. As shown in **Figure 4.60**, the p-Erk1/2: Erk1/2 ratio was consistently higher in the mesenteric mass of patients with SI NETs compared to normal mucosa and when samples were grouped together in 3 tissue categories (normal, primary tumour and metastasis), the p-Erk1/2:Erk1/2 ratio was significantly higher ($p < 0.05$) in the metastasis compared to control (normal mucosa).
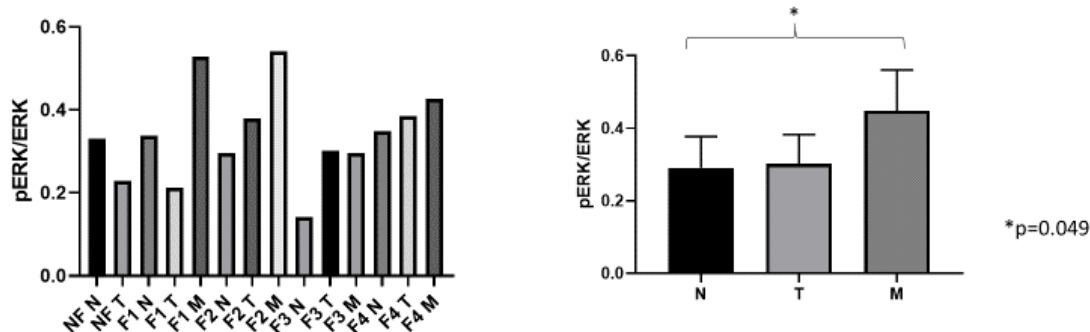
Figure 4.60. Densitometry analysis of Western blot shown in Figure 4.57. The p-Erk1/2: Erk1/2 ratio was significantly higher in the mesenteric metastasis of SI NETs compared to normal mucosa, suggesting activation of the oncogenic MAPK pathway in the metastasis. NF: Non-fibrotic, F1: Minimally fibrotic, F2/F3: Mildly fibrotic, F4: Severely fibrotic.

4.4. Discussion

The present study is the first report of a prospective correlation of surgical, radiological and histopathological findings of mesenteric fibrosis associated with midgut NETs. In general, these different evaluation methods of mesenteric fibrosis correlated well with each other, but in certain cases some discrepancies were noted. In this section we will discuss in more detail the triangulation of different methodological approaches for the evaluation of mesenteric fibrosis. It is quite surprising that we could identify only one old, small, retrospective study published by Pantongrag-Brown *et al* nearly 25 years ago, that evaluated the severity of mesenteric fibrosis by both radiological and histological criteria in midgut NETs with a mesenteric mass. Interestingly, in this study 21 cases with an associated mesenteric mass were evaluated by both methods (computed tomography and histology) and fibrotic tissue was detected histologically in all those cases[8]. This is in keeping with our finding that the presence of a mesenteric mass was invariably associated with the development of fibrosis, although sometimes this was not detected on imaging studies and was only

seen histologically as a 'fibrous capsule' (**Figure 4.8**). This is a quite unusual pattern which has not been reported previously and is distinct to the typical 'stellate' or 'spoke-wheel' appearance, which is described in the literature as a pathognomonic sign of a midgut carcinoid with associated mesenteric desmoplasia. Although typically the diagnosis of mesenteric desmoplasia is based on **radiological** criteria and is defined as a mesenteric mass with surrounding soft tissue strands, our data demonstrate clearly that cross-sectional imaging often underestimates the presence of fibrosis. As illustrated in **Figure 4.7**, despite the absence of mesenteric fibrosis on cross-sectional imaging in 15 of our cases, there was often histological evidence of fibrosis which could be quantified by histopathological measurements (CPA or width of fibrous bands). This is also demonstrated in **Table 4.3**, which shows that in 12 out of 15 cases with no radiological evidence of a desmoplastic reaction, there was histological evidence of fibrosis (graded using the histological fibrosis grade of the mesenteric mass). These patients had a histological fibrosis grade of 1 (n=6), 2 (n=3) or 3 (n=3), indicating that in some cases there was histologically dense fibrous tissue around the mesenteric tumour, which was not detected on cross-sectional imaging. Furthermore, it is interesting that in 6 out of 15 cases without mesenteric fibrosis at radiological assessment, there was evidence of mesenteric desmoplasia intra-operatively (macroscopically), which was usually graded by the operating surgeon as mild (n=5), or less often as moderate (n=1). This suggests that cross-sectional imaging may not only underestimate microscopic mesenteric fibrosis (that can be detected histologically), but also more pronounced fibrosis that can be detected macroscopically at the time of surgery. Perhaps, it is for this reason that in a previous study on the role of CTGF in mesenteric fibrogenesis published by Kidd *et al*, the authors decided to use surgical criteria for the determination of mesenteric fibrosis with additional histological confirmation, rather than the usual/standard radiological criteria, which appear to be less accurate[22]. We found however that the radiological and surgical grading of mesenteric fibrosis tended to correlate at a statistically significant level (Fisher's exact test, *p*=0.014), suggesting that the number and thickness of soft tissue strands detected radiologically were predictive of the amount of desmoplasia encountered intra-operatively. This indicates that there was a statistically significant correlation between macroscopic evaluations (radiological and surgical) of mesenteric fibrosis. In addition, the radiological assessment of mesenteric fibrosis correlated at a statistically significant level with the CPA (*p*=0.02), while its

association with the width of fibrous bands did not quite reach the level of statistical significance ($p=0.08$). This may suggest that the CPA is a better predictor of the radiological severity of mesenteric desmoplasia. A retrospective study by Pantongrag-Brown *et al* demonstrated that in a group of 21 midgut NETs associated with a mesenteric mass, a correlation was noted between the histological fibrosis grade (determined by the width of fibrous bands) and the radiological severity of mesenteric desmoplasia, which marginally missed the threshold of statistical significance (Fisher's exact test, $p=0.06$)[8]. Although several studies have shown that the **presence** of soft tissue strands around a mesenteric mass correlates with the presence of fibrosis on histology[8,118], this is the first study to show that the **absence** of mesenteric desmoplasia on imaging studies does not rule out the presence of mesenteric fibrosis, which was often detected during surgery or histologically.

It is interesting to note that the **surgical** assessment of mesenteric fibrosis correlated at a statistically significant level with both the radiological assessment (Fisher's exact test, $p=0.014$), as well as the histological parameters CPA ($p=0.02$) and width of fibrous bands ($p=0.01$). Although this indicates that the intra-operative assessment of mesenteric desmoplasia may be more accurate than the radiological assessment, it is important to note that the macroscopic surgical appearances were not always very precise either. For example, as shown in **Table 4.2**, in 3 out of 12 cases without macroscopic evidence of mesenteric fibrosis at surgery, there was mild fibrosis on imaging (<10 thin strands). In addition, as demonstrated in **Table 4.4**, in 9 out of 12 cases without obvious macroscopic fibrosis at surgery, there was histological evidence of fibrosis. These patients had a histological fibrosis grade of 1 (n=3), 2 (n=3) or 3 (n=3), indicating the histological presence of dense fibrosis around the mesenteric tumour in some cases.

These observations suggest that macroscopic assessments of mesenteric fibrosis are often inaccurate and that **histological** measurements should be the gold standard for the determination of mesenteric fibrosis. The CPA was able to predict the presence of clinical (radiologically and/or surgically detected) desmoplasia at a statistically significant level (p=0.007) with an AUC of 0.804. The width of fibrous bands was also predictive of clinically detectable fibrosis (p=0.027) with an AUC of 0.751. Obviously, although these histological measurements appear to be accurate measures for the presence of mesenteric fibrosis, the most significant limitation is that a surgical

179

resection specimen is required for histological assessment. Therefore, the development of circulating biomarkers for the pre-operative detection of image-negative mesenteric desmoplasia may have important clinical utility and will be discussed in more detail in **Chapter 5**. As with other histological measurements, another limiting factor is that the histological parameters are subject to sampling error and that they do not capture residual or unresectable fibrosis that is not included in the resection specimen.

Given the fact that each methodological approach of mesenteric fibrosis assessment has inherent limitations, we decided to use a multidimensional assessment of mesenteric desmoplasia, which incorporated radiological, surgical and histological measurements. Although this methodology has not been validated in other patient cohorts, it is more likely to accurately reflect the severity of mesenteric fibrosis. Using this multidimensional evaluation, we grouped patients in different categories of mesenteric fibrosis severity, i.e. non-fibrotic, minimally fibrotic, mildly and severely fibrotic, as described earlier.

Initially, we performed a preliminary study which included the first 26 patients recruited in our study and investigated a set of profibrotic genes that have been previously implicated in the pathogenesis of mesenteric fibrosis. In this initial study we observed a significant upregulation of CTGF expression in the mesenteric mass of fibrotic SI NETs compared to control (normal SI mucosa) and the primary tumour (matched samples). The role of CTGF in fibrosis development was first shown in a previous study by Kidd *et al*, in which 5 patients with midgut NETs (2 of those had intra-operative and histological evidence of fibrosis) and 5 patients with type 1 gastric NETs (considered as 'non-fibrotic' controls) were enrolled. The authors demonstrated a significantly higher expression of CTGF and TGFβ1 in primary SI NET tissue compared to normal mucosa and type 1 gastric NET tissue. These differences were also shown at protein level (by immunostaining for CTGF and TGFβ1 and use of an automated tissue microarray reader to determine protein expression) in a different group of 36 SI NET cases (of which 15 were associated with fibrosis) and 7 cases with type 1 gastric NETs. The authors also showed that serum CTGF levels were higher in patients with SI NETs (n=16), compared to patients with type 1 gastric NETs (n=7), other GI carcinoids (n=6) and normal controls (n=10). Finally, the intestinal stellate cell was isolated from one patient with a fibrotic SI NET. Functional studies with

TGFβ1 stimulation of the intestinal stellate cells led to significant upregulation of CTGF expression compared to unstimulated cells, demonstrating that CTGF acts as a downstream mediator of TGFβ signalling pathways in the tumour microenvironment of a midgut NET[22]. Although this study is quite interesting, perhaps its most significant limitations are the small number of SI NET patients evaluated in the gene expression (n=5) and functional (n=1) studies, the heterogeneous patient cohorts used in the different analyses (midgut NETs, type 1 gastric NETs, other GI carcinoids), and most importantly the fact that the mesenteric mass (which is the main area of fibrosis development) was not evaluated in any of the assessments (instead, only the primary tumour was assessed). The role of CTGF in the cross-talk of SI NET and stromal cells was also shown in another study by Svejda *et al*[21], which has been described in **Chapter 1**.

In addition, we found that in fibrotic SI NETs, TGFβ1 and TGFβ3 were significantly over-expressed in the mesenteric mass, compared to control (normal SI mucosa) and the primary SI tumour (matched samples). The involvement of TGFβ1 in the development of fibrosis associated with midgut NETs was shown in the studies of Kidd *et al* and Svejda *et al*, which have been described in **Chapter 1**[21,22]. In an older study from Uppsala, Chaudhry *et al* investigated the expression of TGFβ1, 2 and 3, as well as the latent TGFβ-binding protein (LTBP) and TGFβ receptor II (TGFβRII) in a mixed patient cohort with midgut (n=20), foregut (n=1) and pancreatic (n=7) NETs. The authors observed that most tumour tissues expressed all TGFβ isoforms, while LTBP was only weakly expressed (by immunohistochemistry). On the other hand, stromal cells expressed mainly TGFβ2 and LTBP, whereas TGFβ1 and TGFβ3 were only weakly expressed. TGFβRII was expressed mainly in the stromal cells. The authors suggested that the TGFβ signalling pathway may be involved in the interaction of tumour and stromal cells, thus contributing to the desmoplasia observed in carcinoid tumours[82]. However, this study was limited by the lack of functional experiments (to demonstrate a cause-effect relationship), the significant heterogeneity of the patient cohort and the evaluation of mainly primary tumours (liver metastases were also included in 3 cases, but the mesenteric mass which is the main area of fibrosis development was not included).

Moreover, we observed a significant upregulation of PDGF-β-R in the mesenteric mass of fibrotic midgut NETs, compared to control (SI mucosa) and primary tumour

tissue (matched samples). The involvement of PDGF pathways in the development of NET-associated fibrosis was shown in two old studies from Uppsala published in the 1990s. In the first study, Chaudhry *et al* examined 20 cases of midgut NETs and 5 pancreatic NETs. They demonstrated by immunohistochemistry and in situ hybridisation that PDGF and PDGF α receptor were expressed by both tumour and stromal cells, while PDGF β receptors were expressed only in the stroma. They therefore hypothesised that PDGF may be involved in the growth of carcinoid tumours in an autocrine fashion and in the stimulation of stromal cells by paracrine and possibly autocrine mechanisms[90]. In the second study, Funa *et al* examined a heterogeneous cohort of patients that included midgut NETs (n=26), pancreatic NETs (n=8), phaeochromocytoma (n=1), parathyroid carcinoma (n=1) and non-neuroendocrine carcinomas (n=22). The authors investigated the presence of PDGF β receptor by immunohistochemistry and demonstrated that while PDGF β receptors were expressed in the majority of carcinoid tumours, they were expressed rarely (10%) in the non-neuroendocrine carcinomas. In addition, stromal cells adjacent to tumour cells demonstrated a higher expression of PDGF β receptors compared to stromal cells located distant to the tumour cell clusters, suggesting that the tumour cells may induce the expression of PDGF β receptors on adjacent stromal cells. Furthermore, stromal cells in the mesenteric lymph nodes showed a higher expression of PDGF β receptors compared to stromal cells in liver metastases and the primary tumour[91]. The latter finding is in keeping with our gene expression analysis in fibrotic midgut NETs.

In addition, in this study we found that FGF2 (also known as bFGF) was expressed at similar levels in the primary tumour, mesenteric mass and normal mucosa, but its receptor FGFR1 was expressed at higher levels in the primary tumour compared to control (normal SI mucosa) and at even higher levels in the mesenteric mass. The role of FGF pathways in NET-related fibrogenesis has been explored in only a few studies. FGF2 was shown to be overexpressed by KRJ-I and HEK293 cells as a result of their cross-talk in the study by Svejda *et al*, which has been described in **Chapter 1**[21]. Chaudhry *et al* examined 23 midgut NETs and 7 pancreatic NETs and showed that FGF2 was expressed by both tumour and stromal cells, while its receptor was expressed only by stromal cells[205]. Bordi *et al* examined 27 patients with type 1 or 2 gastric carcinoids and 17 patients with type 3 gastric carcinoids and showed by immunohistochemistry that FGF2 was expressed in the majority of these tumours.

mRNA analysis (Northern blot) was also performed in 2 of these cases and demonstrated FGF2 gene expression in the tumour tissue (one case was a type 1 gastric NET and the other case was a type 3 gastric NET). The authors also observed diffuse stromal fibrosis associated with some of these tumours and suggested that FGF2 may be involved in fibrogenesis. FGF2 is also thought to be involved in the development of desmoplasia associated with other cancers, such as scirrhous gastric carcinoma[93].

We also investigated several genes (COL1A1, COL3A1, TNF) which have been implicated in the pathogenesis of fibrosis in other conditions but have not been evaluated in the field of NETs. COL1A1 was significantly upregulated in the mesenteric mass of fibrotic NETs compared to control (normal SI mucosa) and the primary tumour. COL3A1 was also over-expressed in the mesenteric mass compared to control (SI mucosa). COL1A1 and COL3A1 are known stromal markers. COL1A1 is one of the genes involved in the synthesis of type I collagen, which represents approximately 85% of collagen synthesized by fibroblasts of the skin and internal organs[206]. TGFβ is the major cytokine acting extracellularly which stimulates the transcription of the proalpha1 and proalpha2 (Type I) collagen genes during tissue fibrosis[206]. Therefore, it is not surprising that the TGFβ1 upregulation observed in the mesenteric mass was accompanied by an upregulation of COL1A1, as this is a downstream mediator in the development of tissue fibrosis. In addition, COL3 is another type of collagen that also forms part of the extracellular matrix[207] and its gene (COL3A1) was upregulated in the mesenteric mass, where the desmoplastic reaction is known to develop. We also investigated TNF expression in this study but did not find a significant difference in gene expression between the mesenteric mass and the normal SI mucosa or the primary tumour. TNF is a proinflammatory cytokine involved in the pathogenesis of many inflammatory diseases, such as rheumatoid arthritis and Crohn's disease[208]. It is known to have both profibrotic and antifibrotic properties[208]. Its profibrotic effects are mediated through inflammation, tissue destruction and repair, while it is also known to have antifibrotic effects by directly inhibiting extracellular matrix protein synthesis in fibroblasts *in vitro*[208]. Therefore, it may be that we did not observe significant changes in TNF expression, as fibrosis in the mesenteric mass is not primarily driven by inflammation, unlike other diseases, such as Crohn's disease or non-alcoholic steatohepatitis (NASH), where longstanding inflammation is the main driver of fibrosis development.

Finally, in this preliminary study we investigated EGFR gene expression in the tissue of patients with midgut NETs and found no significant change between the mesenteric mass and normal mucosa in fibrotic SI NETs. However, EGFR expression was significantly lower in the primary tumour tissue, and the reason for this is at present unclear. The role of Transforming Growth Factor α (TGFα) and its receptor EGFR in relation to desmoplasia development has been investigated in a previous study from Uppsala. This study included a heterogeneous group of gastroenteropancreatic NETs, and TGFα was found to be expressed in approximately 90% of cases, but EGFR expression was significantly higher in the tumour and stromal component of midgut compared to pancreatic neuroendocrine neoplasms. The authors suggested that this difference may account for the more pronounced fibrosis observed in midgut carcinoids. They also hypothesized that TGFα produced by tumour cells could bind to EGFR expressed by stromal and tumour cells and contribute to the associated desmoplastic reaction and neovascularisation perhaps by a paracrine mechanism and to tumour cell growth by an autocrine mechanism[98]. These are assumptions and the role of TGFα/EGFR would need to be further explored in other studies that include functional experiments to demonstrate their involvement in the development of fibrosis in midgut NETs.

This preliminary study is one of the largest studies on mesenteric fibrogenesis associated with midgut NETs. It essentially confirmed the involvement of many of the known profibrotic genes in mesenteric fibrogenesis, such as TGFβ1 and CTGF, but showed that other factors (such as FGF2) that were previously implicated in carcinoid-related fibrosis may not be so important, since no significant changes in gene expression were seen in the fibrotic mesenteric mass. We also explored the role of some profibrotic genes that have not been previously assessed, such as TNF. In addition, perhaps more importantly, this was a useful way to assess our study methodology and it was encouraging to see clear differences in gene expression of known profibrotic genes within the mesenteric mass compared to the normal SI mucosa and the primary tumour. We were then able perform a larger study which included 34 cases with midgut neuroendocrine tumours using the same methodology and investigated a new pathway (the integrin signalling pathway), that we identified in our *in vitro* functional cell line experiments.

We investigated several components of the integrin signalling pathway in SI NETs using a variety of techniques, namely qPCR (gene expression), immunohistochemistry (protein localisation) and Western blot (protein quantitation). At gene expression level, there was a significant upregulation of the evaluated genes (TGFβ1, COL1A1, COL3A1, fibronectin, ITGAV and ITGAX) in the mesenteric mass compared to control (normal SI mucosa) in fibrotic patients. In addition, the expression of most of the evaluated genes (TGFβ1, COL1A1, COL3A1, ITGAV, ITGAX) was significantly higher in the primary tumour of fibrotic patients compared to control, while in non-fibrotic patients there was no significant difference in gene expression of any of the evaluated genes between the primary tumour and SI mucosa. This suggests a significant activation of the integrin pathway at mRNA level. The protein localisation of these components of the integrin pathway was assessed by immunohistochemistry. We also evaluated integrin ITGAV and the activation of downstream signalling pathways mTOR (protein S6) and MAPK (proteins Erk1/2) by Western blot analysis in a subgroup of patients (n=15) with representation of all the different mesenteric fibrosis severity groups. The protein expression of ITGAV was highest within the mesenteric metastasis of patients with advanced fibrosis, but some heterogeneity was noted in the protein expression of this integrin subunit within the mesenteric mass of other patient groups. In addition, there was a significantly ($p<0.05$) higher p-Erk1/2: Erk1/2 ratio within the mesenteric metastasis of fibrotic patients (compared to normal mucosa), suggesting activation of the MAPK pathway. Given the heterogeneous expression of ITGAV in the mesenteric mass of fibrotic subjects, the activation of the MAPK pathway in the metastasis may be mediated by additional, non-ITGAV related pathways. However, this finding supports the hypothesis that the fibrotic tumour microenvironment exerts a pro-proliferative effect in cancer cells and plays a role in cancer progression, likely through multiple pathways as suggested by our in vitro cell line experiments (**Chapter 3**). Furthermore, there was some heterogeneity in the phosphorylation of protein S6 within the mesenteric metastasis of fibrotic patients, but it is interesting that this protein was absent in the primary tumour tissue of non-fibrotic patients. Protein S6 is a downstream mediator of the mTOR pathway that stimulates protein synthesis, cell growth and cell proliferation[209]. Collectively, these results suggest activation of the integrin pathway at least in some patients with mesenteric fibrosis. The heterogeneity observed in the expression of some of the investigated proteins most likely reflects the small sample size (n=3 patients per fibrosis group)

and possibly biological variation in the tissue. Therefore, evaluation of the involvement of these proteins in an independent and larger patient cohort would be required.

The integrin signalling pathway is known to play a role in carcinogenesis and affect the metastatic potential of many cancers and the role of integrin αv has been investigated in the context of various malignancies, such as laryngeal and hypopharyngeal squamous cell carcinomas[210], metastatic melanoma[211,212], colorectal[213], lung[214,215], breast[216,217] and prostate cancer[209]. In laryngeal squamous cell carcinomas increased ITGAV protein expression has been shown to be associated with poor differentiation and lymph node metastases, indicating its role in the tumour microenvironment for invasive and metastatic growth[210,218]. In addition, in metastatic melanoma ITGAV protein expression was strongly associated with the duration of disease-free survival[211], while in colorectal cancer increased ITGAV gene and protein expression were associated with a higher prevalence of perineural invasion[213,219]. Furthermore, in lung adenocarcinoma increased ITGAV expression was associated with a higher frequency of lymph node metastases[214] and in the human lung cancer cell line A549 integrin αv was found to exert a proliferative effect through the downstream activation of Erk1/2[215]. Further evidence for the involvement of ITGAV in cancer cell migration and metastasis was demonstrated in athymic rats, in which high αv integrin expression in several cancer cell lines of different origins led to a higher frequency of brain metastases. In this animal model, αv integrin appeared to mainly regulate cancer cell adhesion, invasion and metastasis, rather than cell proliferation and tumour growth, since the mean brain tumour volume after direct intracerebral inoculation of cancer cells overexpressing ITGAV (using a pTag-integrin expression vector) versus cancer cells with normal ITGAV expression (using an empty vector) was not significantly different [220]. This is interesting and mirrors our observations in which an increased ITGAV gene expression was noted in the mesenteric metastatic lymph node of fibrotic SI NETs, compared to the primary tumour and normal mucosa, but the proliferation index Ki67 was not significantly different between the primary tumour and the metastasis. Thus, ITGAV may be involved more in the metastatic potential of cancer cells, rather than cell proliferation. In addition, ITGAV is involved in angiogenesis, which may also facilitate tumour growth independently to the direct effects of the integrin signalling pathway on cancer

cell proliferation[221]. Interestingly, integrin αvβ3 has been investigated in a heterogeneous group of neuroendocrine tumours due to its known role in angiogenesis and the potential for therapeutic targeting, but large variations were noted in gene expression (>100-fold)[222]. The use of ^{64}Cu-NODAGA-c(RGDyK), a novel PET tracer targeting integrin αvβ3, has also been evaluated in nude mice with human neuroendocrine tumour xenografts (H727 cell line derived from a human bronchial carcinoid)[223]. A significant correlation was noted between tumour tracer uptake and integrin αvβ3 expression, indicating the potential of this novel PET tracer to detect angiogenesis in this animal model of neuroendocrine neoplasia[223]. Furthermore, ITGAV is known to play an important role in fibrosis development in many chronic fibrotic conditions and some malignancies, mainly through regulation of TGFβ activity in the extracellular matrix, and a variety of inhibitors have been evaluated in animal models[224]. Several small molecule inhibitors (such as cilengitide) and function-blocking monoclonal antibodies have been developed and have shown promising results as antifibrotic agents in this context[224]. This may be an interesting avenue to explore in cell line models evaluating the interaction of SI NET cell lines (or primary SI NET cells) and fibroblasts. A recent study assessed the effect of a novel integrin αvβ3-targeted dendrimer that was modified to deliver the mTOR inhibitor, rapamycin, in an *in vitro* co-culture model of prostate cancer cells and fibroblasts[209]. This study demonstrated that this agent could effectively reduce fibroblast-mediated prostate tumour progression and metastasis, indicating the potential use of such drugs in the context of carcinogenesis induced by the fibrotic microenvironment[209].

We also investigated another integrin, ITGAX, also known as CD11c. This integrin subunit was significantly (2.1-fold, $p<0.0001$) upregulated in KRJ-I cells exposed to HEK293 conditioned media, as shown in our RNA sequencing data. Although this integrin was highly upregulated in the mesenteric metastasis of fibrotic SI NETs compared to normal mucosa and the primary tumour, the immunohistochemistry demonstrated that this integrin subunit was expressed in inflammatory cell aggregates within the tumour. This may suggest an involvement of inflammatory cells in the fibrotic process within the tumour microenvironment. ITGAX is mainly expressed in dendritic cells, and at lower levels in granulocytes, monocytes, natural killer cells and activated T- and B- lymphocytes[225,226]. Thus, this integrin plays a role in antigen presentation and immune stimulation, but is also known to interact with the certain

components of the coagulation system, such as fibrinogen and kininogen[226]. ITGAX has been investigated in the context of various malignancies, such as chronic lymphocytic leukaemia[226] and prostate cancer[227], where it is considered to be a poor prognostic marker, while in other malignancies, such as gastric cancer, it is associated with a more favourable prognosis[228]. In addition, ITGAX is known to play a role in cancer angiogenesis by activating the PI3K/Akt downstream signalling pathway, which in turn stimulates VEGF-A overexpression in blood vessel endothelial cells[229]. Interestingly, this integrin seems to also play a role in fibrogenesis. For example, bone-marrow derived CD11c+ dendritic cells contribute to the development of cardiac inflammation and fibrosis in the context of haemodynamic overload in mice, through the presentation of cardiac self-antigens to T-cells[230]. In addition, CD11c+ resident macrophages surround dead hepatocytes and are able to trigger hepatic fibrosis development in a murine model of non-alcoholic steatohepatitis[231]. Therefore, the role of the immune cells within the tumour microenvironment in fibrogenesis of SI NETs requires further exploration.

In conclusion, in this study we used a multidimensional assessment of mesenteric fibrosis to accurately classify patients in terms of their desmoplasia severity. In an initial pilot study, we evaluated the expression of several known profibrotic genes and showed a significant upregulation of most of these genes within the fibrotic mesenteric mass. Subsequently, we assessed a novel pathway, the integrin signalling pathway, in the tissue of patients with SI NETs and demonstrated significant differences between fibrotic and non-fibrotic subjects. Therefore, this pathway appears to play a role in carcinogenesis and may promote the invasion, metastasis and survival of cancer cells (together with other pathways) within the fibrotic microenvironment but may also contribute to fibrosis development through its known interaction with the TGFβ pathway. Since ITGAV inhibitors are available, functional co-culture studies evaluating their role as antifibrotic agents should be undertaken. This will provide further evidence for the involvement of this pathway in the crosstalk of SI NET cells with fibroblasts and may lead to the development of novel drug treatments. The role of the immune system in the fibrotic neoplastic microenvironment also needs to be investigated further. Clearly, the mesenteric fibrotic microenvironment is a nidus of complex interactions that promote both carcinogenesis and fibrogenesis. These mechanisms need to be evaluated in a systematic way, in order to better understand

the underlying pathophysiology and develop effective antifibrotic and antineoplastic drugs.

Chapter 5

Development of a circulating biomarker for the prediction of mesenteric fibrosis in midgut neuroendocrine tumours

5. Development of a circulating biomarker for the prediction of mesenteric fibrosis in midgut neuroendocrine tumours

5.1. Introduction

As discussed in Chapters 1 and 2, the presence of mesenteric fibrosis in midgut NETs is associated with significant morbidity and may affect patient prognosis. The mortality observed in fibrotic tumours may be related to direct complications of the fibrotic mesenteric mass, such as the development of bowel obstruction or perforation secondary to advanced mesenteric ischaemia, but it is also possible that the liaison of cancer cells with resident fibroblasts can promote tumour cell survival, proliferation and migration leading to disease progression. This is supported by a retrospective study conducted in Munich, Germany, which demonstrated that fibrotic SI NETs were associated with a significantly higher prevalence of distant metastases, lymphatic vessel invasion, perineural infiltration and a shorter progression-free survival compared to non-fibrotic tumours[118]. In addition, our basic science data on the crosstalk of SI NET cell lines KRJ-I and P-STS with stromal cells (HEK293) suggest that many pro-proliferative pathways are activated in cancer cells as a result of the paracrine effect (Chapter 3). Therefore, the early detection of mesenteric fibrosis in SI NETs is important for patient management and prognostication.

However, as discussed in Chapter 4, the assessment of mesenteric desmoplasia remains a problematic area and several discrepancies were noted between different methods of assessment (radiological, surgical and histological). In particular, the radiological detection of fibrosis, which is the standard method of diagnosis of mesenteric desmoplasia in clinical practice, was inaccurate in many cases, especially when small amounts of fibrosis were present, which could be measured histologically using the width of fibrous bands or the Collagen Proportionate Area (CPA), as detailed in Chapter 4 (**Figure 5.1**). Thus, the development of non-invasive biomarkers with high accuracy for the early detection of desmoplasia would be of critical importance. Currently, there is a lack of clinically useful biomarkers for fibrosis in midgut NETs. Although several non-invasive biomarkers (plasma activin A, serum CTGF, urinary 5-HIAA, plasma neuropeptide and substance P, plasma neurokinin A) have been investigated in the context of carcinoid heart disease[9], only a few studies have assessed

the utility of non-invasive biomarkers in mesenteric fibrosis. This reflects the notion that mesenteric desmoplasia is a 'local' process confined to the mesentery, while carcinoid heart disease is a 'systemic' process[10]. The presence of mesenteric fibrosis has shown significant correlation with urinary 5-HIAA levels in some studies[11,71], suggesting that circulating serotonin may play a role in its development. In addition, serum CTGF levels were significantly higher in fibrotic SI NETs compared to controls and non-fibrotic gastrointestinal NETs (type 1 gastric carcinoids)[22]. However, these biomarkers have not gained acceptance in the detection of mesenteric fibrosis and require further validation.

*p=0.01
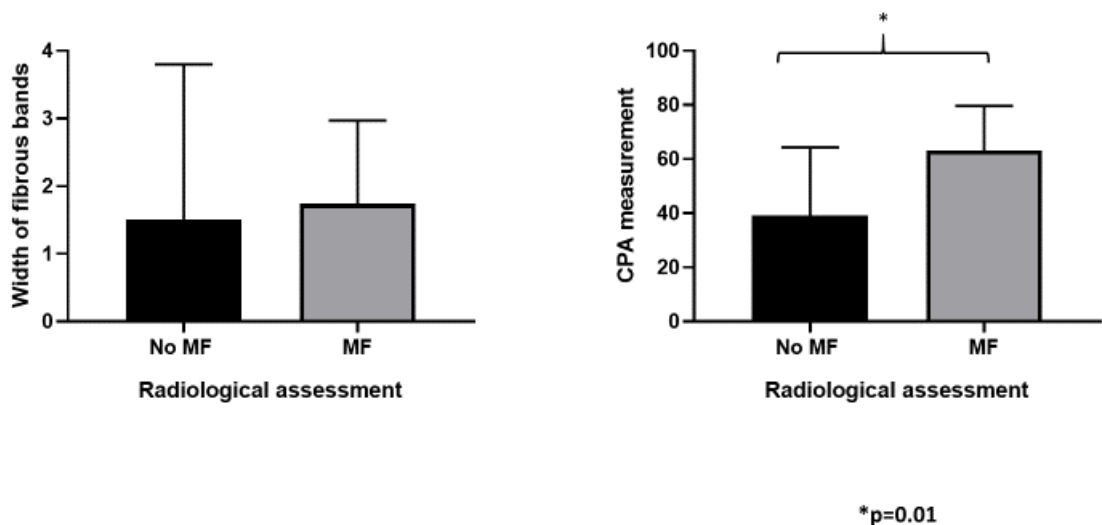
Figure 5.1. Correlation of radiological detection of mesenteric fibrosis with histological findings (width of fibrous bands around the mesenteric mass and collagen proportionate area [CPA]) in 34 patients with midgut NETs. Microscopic evidence of fibrosis was identified histologically in cases where the radiology (CT imaging) did not show clear evidence of desmoplasia. While the width of fibrous bands did not differ significantly (median 0.75mm vs. 1.47mm in non-fibrotic and fibrotic tumours, respectively, p=0.1349, Mann-Whitney test), the CPA was significantly different (median 33.4% vs. 65.40%, in non-fibrotic and fibrotic tumours, respectively, p=0.01, Mann-Whitney test). Data are from 34 patients classified as non-fibrotic (n=15) and fibrotic (n=19) by radiological detection.

The NETest is a PCR-based tool that measures a panel of 51 circulating transcripts (mRNA), which are specific to neuroendocrine neoplasia. This blood-based multianalyte was derived through complex mathematical algorithms and has shown,

albeit in limited publications, an excellent sensitivity and specificity for the diagnosis of neuroendocrine tumours, the prediction of disease progression and response to therapy[232]. This molecular signature is often described as the 'fingerprint' of a neuroendocrine tumour due to its excellent performance metrics and its ability to capture the hallmarks of neuroendocrine neoplasia[232,233]. We hypothesised that a subset of genes within this 51-gene panel with defined roles in fibrosis development may be predictive of mesenteric desmoplasia. We therefore analysed blood samples of patients taken pre-operatively (prior to surgical resection of the primary SI NET and desmoplastic mesenteric mass) and assessed the predictive accuracy of this blood-based biomarker for the detection of mesenteric fibrosis. This study was performed in collaboration with the Wren laboratories, Branford, USA (Dr Mark Kidd and Prof Irvin Modlin), that developed the NETest. A Mutual Transfer Agreement was signed between the UCL-RFH Biobank and the Wren Laboratories LLC in September 2017 to facilitate this study.

5.2. Methods

A total of 20 patients were included in the biomarker assessment study (a subset of 19 patients from the mesenteric desmoplasia evaluation study described in **Chapter 4**, and an additional patient who had extensive mesenteric fibrosis and unresectable disease, who was not included in the desmoplasia assessment study, since no histology was available). The demographic and clinical characteristics of this patient cohort are provided in **Table 5.1**. No patients had carcinoid heart disease or other fibrotic conditions.

	Patients with midgut NETs who underwent surgery (n=20) n (%)
Age (mean±SD)	63±10
Sex	
Male	13 (65%)
Female	7 (35%)
Grade	
1	13 (65%)
2	7 (35%)
Extent of disease	
Localised	2 (10%)
Locoregional	5 (25%)
Metastatic	13 (65%)
Mesenteric mass	18 (90%)
Liver metastases	10 (50%)
Distant extrahepatic metastases	5 (25%)
Macroscopic mesenteric fibrosis	17 (85%)
Medical therapy	
Octreotide LAR	6 (30%)
Lanreotide Autogel	7 (35%)
Surgical therapy	
Small bowel resection	1 (5%)
Gastro-jejunal bypass	1 (5%)
Right hemicolectomy (R0)	10 (50%)
Right hemicolectomy (R1)	8 (40%)

Table 5.1. Demographic and clinical characteristics of patients with midgut NETs included in the study.

The presence of mesenteric fibrosis was assessed using a multidimensional approach, incorporating radiological, surgical and histological parameters, as described in Chapter 4. Two analyses were performed (**Figure 5.2**). In the first analysis, the fibrosis assessment was based on *macroscopic* criteria (radiology, surgical assessment) and confirmed histologically (where tissue was available for assessment). This grouping method resulted in 3 patients classified as 'non-fibrotic' and 17 as 'fibrotic'. In the second analysis, patients were grouped based on the presence or absence of *microscopic* fibrosis. This grouping strategy resulted in 2 patients classified as 'non-fibrotic' and 18 as 'fibrotic'. This methodology was used to assess the predictive ability of the biomarker for the detection of 'established' (clinically evident or macroscopic), as well as 'early' (preclinical or microscopic) fibrosis.

n=20 patients with midgut NETs

Radiological and/or surgical detection of mesenteric fibrosis

n=17 patients
(Macroscopic evidence of fibrosis)

Histological assessment of mesenteric fibrosis

(possible in n=16 cases; 1 case with extensive unresectable fibrosis)

n=17 patients

(Fibrosis confirmed histologically in 16 cases with available tissue)

n=1 patient

(No clear macroscopic evidence of fibrosis, but microscopic fibrosis present)

n=3 patients
(No macroscopic evidence of fibrosis)

Histological assessment of mesenteric fibrosis

n=2 patients

(No macro- or microscopic fibrosis)

Figure 5.2. Schematic overview of mesenteric fibrosis assessment and allocation of patients with midgut NETs into fibrotic and non-fibrotic groups. In the first analysis (blue dashed line) patients with macroscopic (radiological and/or surgical) evidence of fibrosis were included in the fibrosis group and their fibrosis was confirmed histologically (where tissue was available), while the non-fibrotic group consisted of patients without macroscopic fibrosis. In the second analysis, patients with macroscopic and microscopic evidence of fibrosis were included in the fibrotic group (red dashed line).

A total of 31 blood samples were collected pre-operatively (within 24h of surgery) in 5ml EDTA tubes and stored in -80ºC within 2 hours of collection (samples immediately stored on ice/4ºC after sampling). These samples were shipped on dry ice to the Wren laboratories, USA for analysis (NETest measurements).

A two-step manual technique protocol (RNA isolation with cDNA synthesis and qPCR) was used, as previously described[234]. In brief, transcripts (mRNA) were isolated from 1ml EDTA-collected blood samples using the mini blood kit (Qiagen). The RNA quantity was 50µl (RNA quality >1.8 $A_{260:280}$ ratio, RIN>5.0). cDNA was produced from 50µl RNA using a High Capacity Reverse transcriptase kit (Life Technologies: cDNA production 2000-2500 ng/µl) and stored in -80ºC. qPCR was performed (384-well plate, HT-7900) with the cDNA (200 ng/µl) and 16µl of reagents/well (Universal Master mix II with UNG, Life Technologies, triplicate wells) (50ºC 2 min, 95ºC 10 min, then 95ºC 15s, 60ºC 60s for 40 cycles). PCR values of NET

marker genes were normalised to the housekeeping gene (ALG9) and gene expression was quantified against a population control (calibration sample), as previously described[235,236].

For this study, which was conducted in collaboration with Wren Laboratories, Branford, CT USA, we assessed a subset of 5 circulating transcripts (from the entire 51-gene molecular signature) with known roles in fibrosis, namely: CTGF, CD59, APLP2 (amyloid precursor-like protein 2), FZD7 (frizzled homolog 7) and BNIP3L (BCL2 Interacting Protein 3 Like). Statistical analysis was performed with Mann-Whitney test, ROC curve analysis and binary logistic regression, as appropriate, using Graphpad Prism version 8 and SPSS version 25 statistical packages.

5.3. Results

In this small cohort of patients there was one patient who did not appear to have obvious mesenteric desmoplasia at macroscopic assessments of fibrosis (radiological and surgical), although some minimal fibrosis was detected histologically (**Figure 5.3**). In this case, a thin fibrous capsule was seen around a small (~14mm) mesenteric lymph node. Although the natural history of mesenteric mass formation is not well documented in the literature, this small fibrotic lymph node would conceivably have developed into a larger fibrotic mesenteric mass, if it had been left *in situ*. Therefore, the ability of a biomarker to detect both macroscopic and microscopic fibrosis may be of clinical utility in anticipating the development of fibrosis, when this is not evident using clinical macroscopic assessments. On the other hand, a biomarker that can detect 'established' desmoplasia may also be useful, particularly if this is not seen at radiology (and can be noted only intra-operatively). Thus, we performed two analyses looking at the predictive ability of the 5 circulating transcripts from the NETest (CTGF, CD59, APLP2, FZD7 and BNIP3L) to define a profibrotic phenotype by *macroscopic* (i.e. established, clinically evident fibrosis) and *microscopic* (i.e. including cases with so called 'pre-clinical' or minimal fibrosis) criteria.
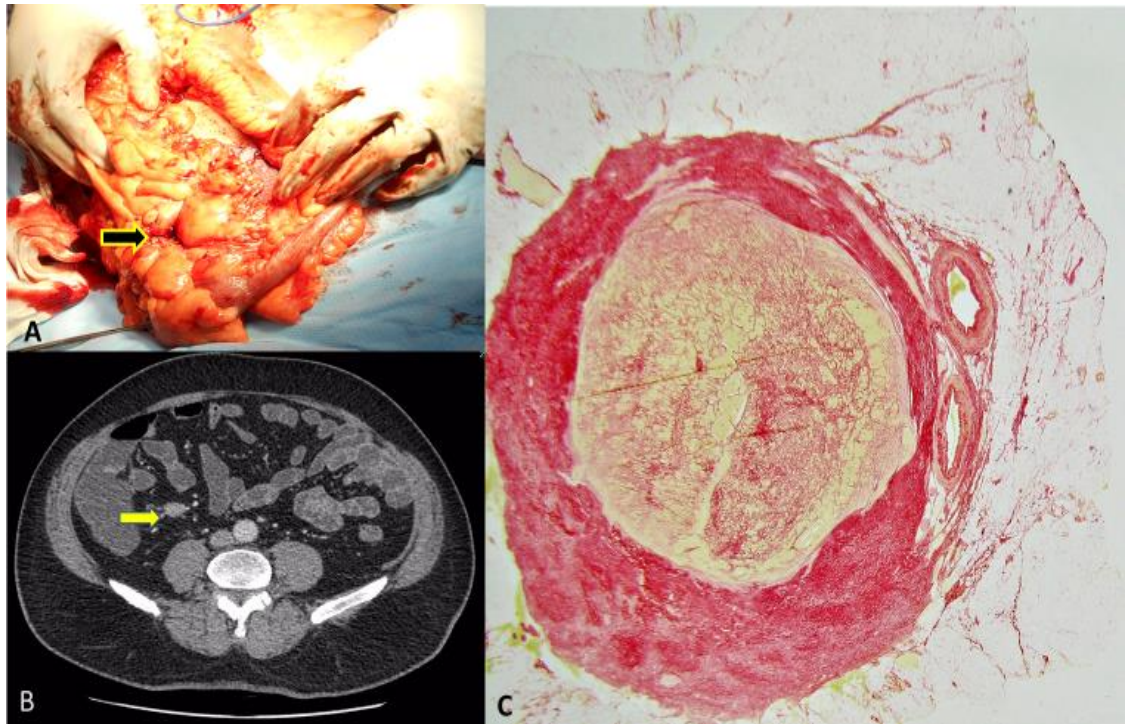
Figure 5.3. Review of surgical (A), radiological (B) and histological (C) assessments in a patient with a midgut NET. (A) The midgut primary tumour and mesenteric lymph node were removed laparoscopically. A small, soft palpable lymph node was seen intraoperatively with no obvious surrounding fibrosis. **(B)** Similarly, the CT scan showed a small lymph node with some subtle spiculation, but no evident desmoplasia with the typical 'stellate pattern'. **(C)** The histological slide of the lymph node with Sirius red staining showed a fibrotic capsule around the small (~14mm) metastatic lymph node. This minimal amount of fibrous tissue, as expected, was not obvious at macroscopic assessments.

5.3.1. Analysis using a macroscopic assessment of mesenteric fibrosis to define a fibrotic phenotype

Circulating transcript levels of APLP2, BNIP3L, CD59 and CTGF were significantly higher in non-fibrotic compared to fibrotic tumours. FZD7 levels did not differ significantly between the two groups (**Figure 5.4**).
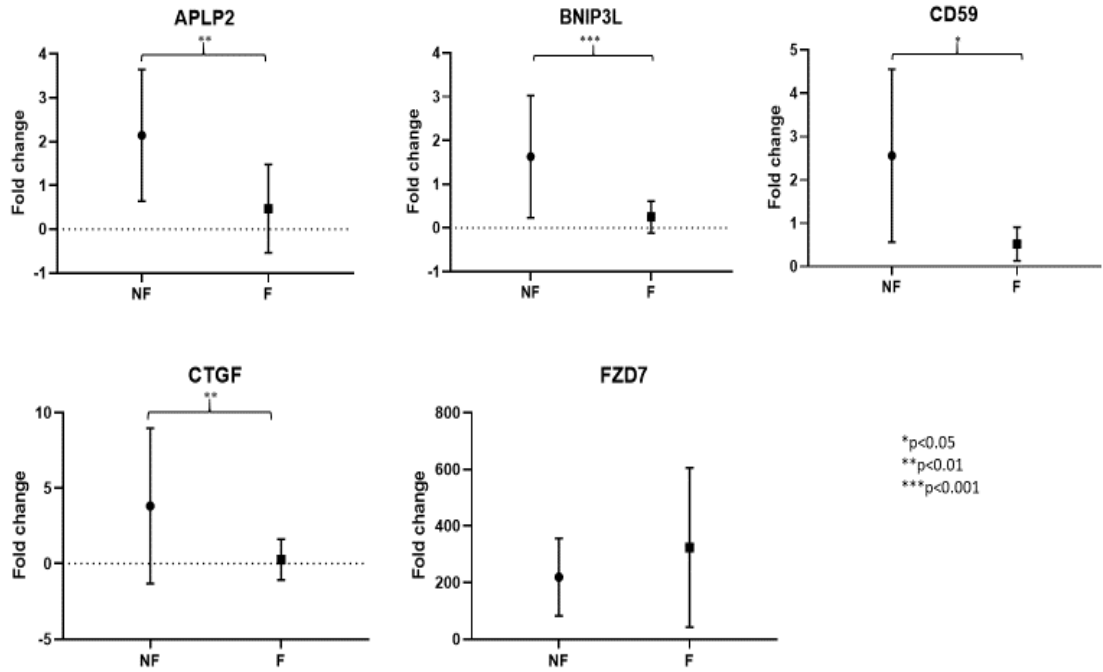
Figure 5.4. Normalised circulating gene expression in fibrotic (F) and non-fibrotic (NF) patients using macroscopic criteria to define a fibrotic phenotype. APLP2, BNIP3L, CD59 and CTGF transcript levels were significantly higher in the blood of non-fibrotic patients.

ROC curve analysis demonstrated that three of the selected circulating transcripts from the NETest (APLP2, BNIP3L and CD59) could independently predict a fibrotic phenotype at a statistically significant level (p<0.05). The metrics of each individual transcript for the detection of clinically-evident mesenteric fibrosis were the following: APLP2 (AUC 0.830, 95% CI 0.584, 1.000, p=0.13), BNIP3L (AUC 0.940, 95% CI 0.855, 1.000, p=0.001), CD59 (AUC 0.820, 95% CI 0.548, 1.000, p=0.016), CTGF (AUC 0.733, 95% CI 0.466, 1.000, p=0.08) and FZD7 (AUC 0.427, 95% CI 0.166, 0.688, p=0.582) (**Figure 5.5**).

ROC Curve

Diagonal segments are produced by ties.
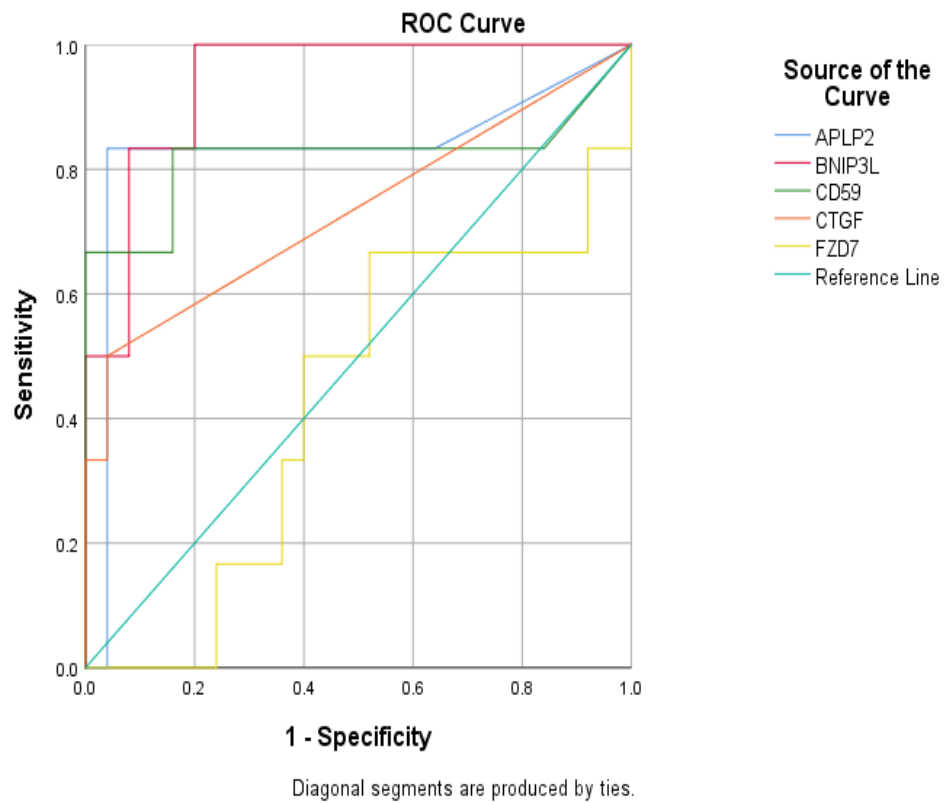
Figure 5.5. Receiver Operating Characteristic (ROC) Curve analysis demonstrating the ability of 5 circulating transcripts from the NETest (APLP2, BNIP3L, CD59, CTGF and FZD7) to define a fibrotic phenotype by macroscopic criteria. Three of these circulating transcripts (APLP2, BNIP3L and CD59) could independently predict a fibrotic phenotype at a statistically significant level ($p<0.05$).

In addition, the mathematical combination of these 5 circulating transcripts achieved an AUC 0.867 (95% CI 0.625, 1.000, p=0.006) (**Figure 5.6**) and could differentiate between fibrotic and non-fibrotic patients with an accuracy of 93.5% (**Table 5.2**).
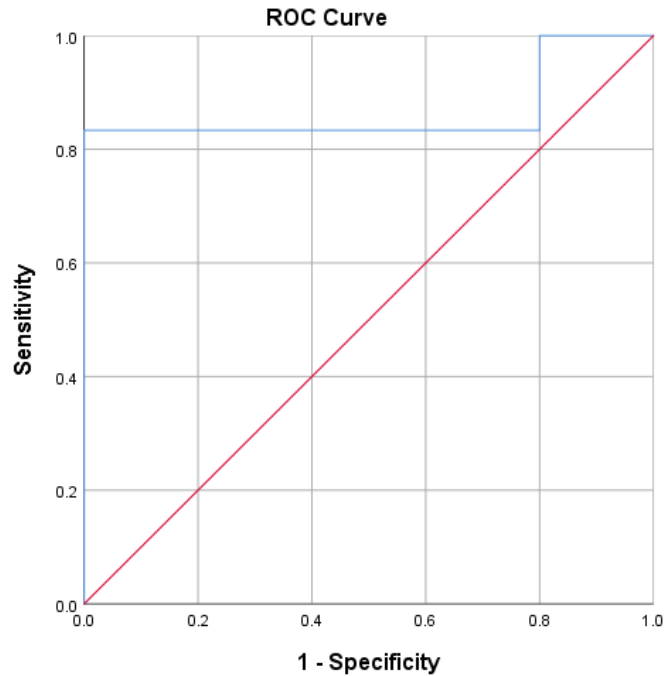
Figure 5.6. Receiver Operating Characteristic (ROC) Curve analysis demonstrating the ability of the combination of 5 circulating transcripts from the NETest (APLP2, BNIP3L, CD59, CTGF and FZD7) to define a fibrotic phenotype by macroscopic criteria. The mathematical combination of these transcripts achieved an AUC 0.867 (95% CI 0.625, 1.000, p=0.006).

| Observed | | Predicted | | |
| | | Fibrosis | | |
		F	NF	Percentage Correct
Fibrosis	F	25	0	100.0
	NF	2	4	66.7
Overall Percentage				93.5

Table 5.2. A predictive model utilising 5 circulating transcripts from the NETest (APLP2, BNIP3L, CD59, CTGF and FZD7) was able to predict the presence of macroscopic (evident by radiology and/or surgical assessment) mesenteric fibrosis with an accuracy of 93.5%. F: Fibrotic group, NF: Non-fibrotic group

5.3.2. Analysis using a microscopic assessment of mesenteric fibrosis to define a fibrotic phenotype

In this analysis, we included patients with macroscopic and microscopic (minimal) mesenteric fibrosis in the fibrotic group and assessed the ability of the 5 circulating transcripts from the NETest (APLP2, BNIP3L, CD59, CTGF and FZD7) to define a fibrotic phenotype. Circulating mRNA levels of APLP2, BNIP3L, CD59 and CTGF were higher in non-fibrotic compared to fibrotic tumours, while FZD7 mRNA levels did not differ significantly (**Figure 5.7**).
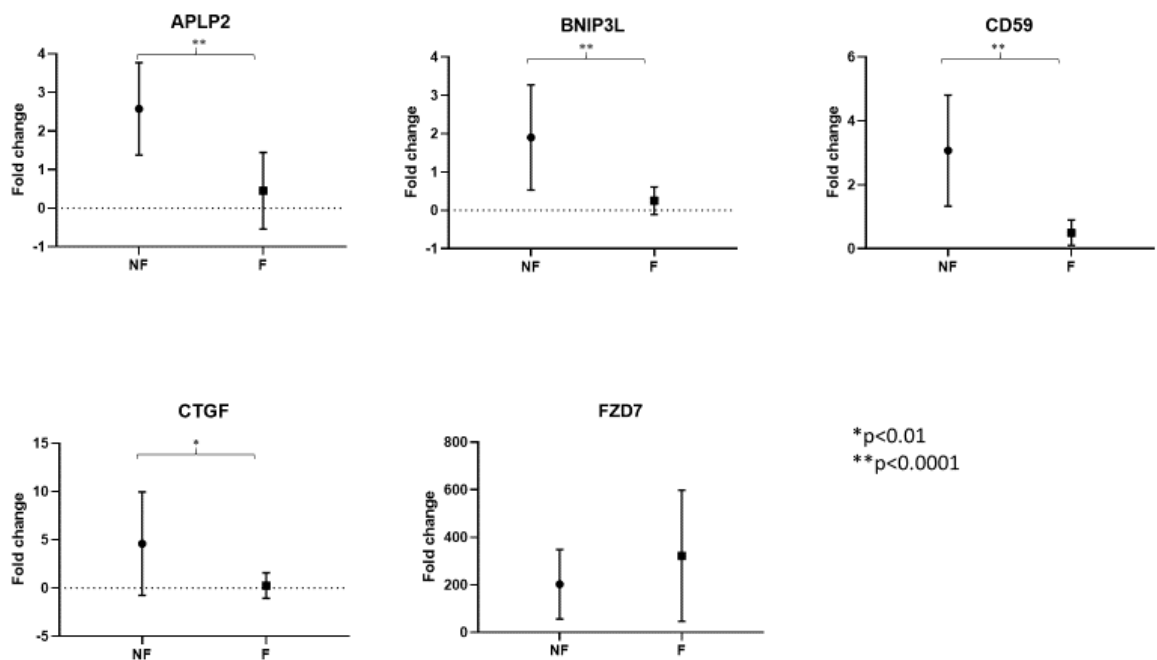
Figure 5.7. Normalised circulating gene expression in fibrotic (F) and non-fibrotic (NF) patients using microscopic (histological) criteria to define a fibrotic phenotype. APLP2, BNIP3L, CD59 and CTGF transcript levels were significantly higher in the blood of non-fibrotic patients.

ROC curve analysis demonstrated that four circulating transcripts (APLP2, BNIP3L, CD59 and CTGF) could independently predict the presence of mesenteric fibrosis at a statistically significant level ($p < 0.05$). More specifically, the metrics for each individual transcript were the following: APLP2 (AUC 0.962, 95% CI 0.888, 1.000, p=0.001), BNIP3L (AUC 0.969, 95% CI 0.912, 1.000, p=0.001), CD59 (AUC 0.969,

95% CI 0.904, 1.000, p=0.001), CTGF (AUC 0.785, 95% CI 0.510, 1.000, p=0.047) and FZD7 (AUC 0.377, 95% CI 0.095, 0.659, p=0.390) (**Figure 5.8**).
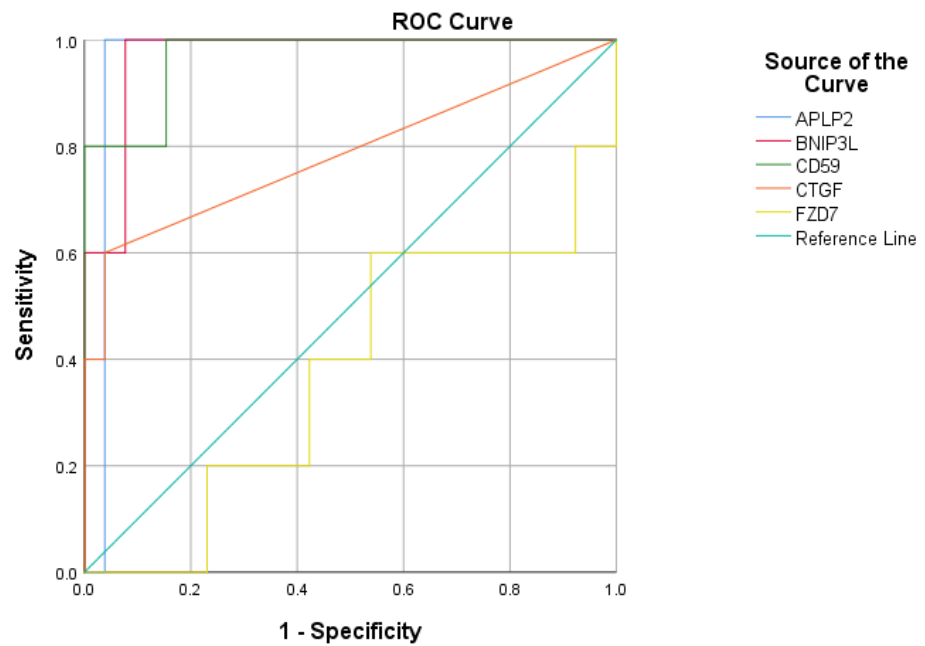
Diagonal segments are produced by ties.

Figure 5.8. Receiver Operating Characteristic (ROC) Curve analysis demonstrating the ability of 5 circulating transcripts from the NETest (APLP2, BNIP3L, CD59, CTGF and FZD7) to define a fibrotic phenotype by microscopic criteria. Four circulating transcripts (APLP2, BNIP3L, CD59 and CTGF) could independently predict a fibrotic phenotype at a statistically significant level (p<0.05).

The mathematical combination of the 5 circulating transcripts achieved an AUC of 1.000 (95% CI 1.000, 1.000, p<0.001) (**Figure 5.9**) and a predictive model based on the combination of these transcripts exhibited an accuracy of 100% for predicting the presence of mesenteric fibrosis (**Table 5.3**). This demonstrated the ability of these 5 circulating transcripts to determine the presence of desmoplasia, not only when it was clinically (macroscopically) evident, but also at a very early stage, when it was detected only histologically.
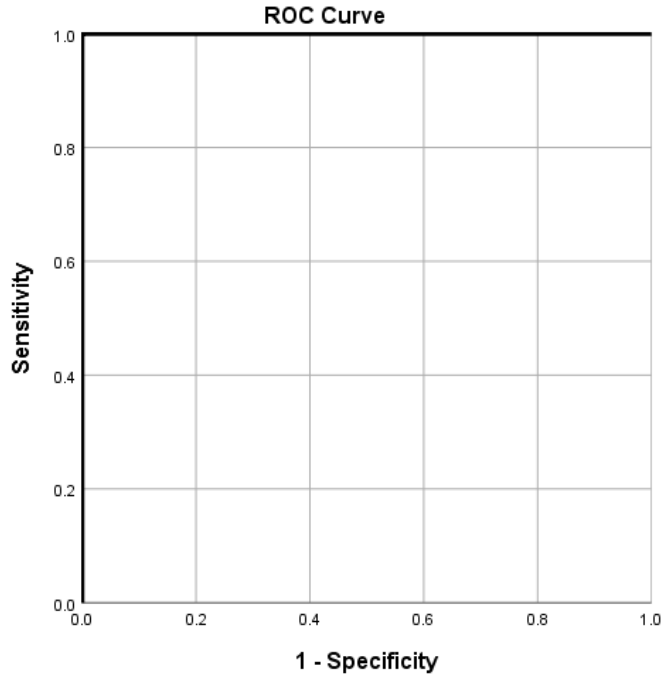
Figure 5.9. Receiver Operating Characteristic (ROC) Curve analysis demonstrating the ability of the combination of 5 circulating transcripts from the NETest (APLP2, BNIP3L, CD59, CTGF and FZD7) to define a fibrotic phenotype by microscopic criteria. The mathematical combination of these transcripts achieved an AUC of 1.000 (95% CI 1.000, 1.000, p<0.001).

		Predicted		
		Fibrosis		
Observed		F	NF	Percentage Correct
Fibrosis	F	26	0	100.0
	NF	0	5	100.0
Overall Percentage				100.0

Table 5.3. A predictive model utilising 5 circulating transcripts from the NETest (APLP2, BNIP3L, CD59, CTGF and FZD7) was able to predict the presence of microscopic mesenteric fibrosis with an accuracy of 100%. F: Fibrotic group, NF: Non-fibrotic group.

5.4. Discussion

The assessment of mesenteric fibrosis is a problematic area and an accurate classification is important for clinical and research purposes. We have shown that a radiological diagnosis, which represents the standard method of assessment in clinical practice, is not a sensitive tool, as it has significant limitations, particularly in cases of minimal fibrosis. A predictive biomarker with a high sensitivity and specificity for mesenteric fibrosis may therefore be of clinical utility. Although serum CTGF has been shown to be elevated in midgut NETs compared to normal controls and non-fibrotic gastrointestinal NETs[22], these results have not been validated in other studies and therefore this biomarker has not gained acceptance. In the present study we evaluated a subset of 5 genes from the NETest that are related to fibrosis and assessed their performance metrics in the detection of macroscopic and minimal (microscopic) fibrosis.

The NETest is a PCR-based 51 transcript signature that has an excellent (>90%) sensitivity and specificity for the diagnosis of gastroenteropancreatic NETs, and is known to outperform conventional secretory biomarkers, such as chromogranin A[233-235,237,238]. In addition, this molecular signature correlates with disease status[239,240] and captures the hallmarks of neuroendocrine neoplasia (proliferome, growth factor signalome, metabolome, secretome [general and progressive], epigenome, apoptome, plurome and SSTRome)[241]. The NETest has also been shown to predict response to somatostatin analogue therapy[236], peptide receptor radionuclide therapy (PRRT)[242,243], operative resection and ablation strategies[244].

Given the ability of this multianalyte to act as a "liquid biopsy" that can yield biologically relevant, real-time information about the tumour and capture the multidimensionality of neuroendocrine neoplasia, we hypothesised that a subset of 5 genes from the NETest (APLP2, BNIP3L, CTGF, CD59 and FZD7) that are involved in fibrosis may be a clinically useful and accurate biomarker of mesenteric fibrosis. In this small cohort of 20 patients, who did not have carcinoid heart disease or other fibrotic disorders, these 5 circulating transcripts could accurately predict the presence of macroscopic and microscopic fibrosis (100%). These genes (with the exception of CTGF) have not been investigated in the context carcinoid-driven fibrosis, although they have been linked to fibrosis in other conditions. **FZD (Frizzled)** are seven-

transmembrane receptors that bind Wnt proteins and mediate the canonical and non-canonical Wnt signalling pathways. Wnt signalling plays important roles in tissue development and repair, as well as carcinogenesis, but more recently it has also been implicated in fibrogenesis[245,246]. FZD7 in particular has been shown to mediate TGFβ-induced pulmonary fibrosis via the non-canonical Wnt signalling pathway and lead to the expression of collagen I, fibronectin, CTGF and α-SMA in lung fibroblasts[247]. FZD7 has also been assessed in SI NETs as part of a molecular signature that was able to differentiate primary SI neuroendocrine tumours from normal EC (enterochromaffin) cell preparations[248]. Although FZD7 could not independently predict the presence of mesenteric fibrosis, its use within the 5 circulating transcript predictive model led to an accurate classification of fibrosis. In addition, **CTGF** is a known mediator of fibrosis, which acts downstream of TGFβ, and has been investigated in carcinoid-related desmoplasia and other fibrotic conditions[9,22,249]. It is somewhat surprising however that circulating CTGF mRNA levels were significantly higher in non-fibrotic compared to fibrotic tumours. This may reflect some discordance between tissue and blood CTGF mRNA levels, since in our preliminary tissue analyses (**Chapter 4**) CTGF gene expression was higher in the mesenteric mass of fibrotic tumours compared to primary tumours and normal mucosa. **BNIP3L** is also implicated in cardiac fibrosis, where it is known to promote TGFβ expression in cardiac fibroblasts[250]. It is noteworthy that circulating BNIP3L mRNA levels were higher in non-fibrotic compared to fibrotic tumours, which seems paradoxical, but (similar to CTGF) these may not necessarily accurately reflect BNIP3L gene expression at tissue level. Conceivably the levels of circulating transcripts in the blood might be affected not only by the levels of gene expression in the tissue, but also the size of the primary tumour and fibrotic mesenteric mass, as well as treatments (e.g. somatostatin analogues), and although this is currently not known, such factors may account for some of the possible differences between tissue and blood transcript levels. Moreover, **CD59** is a regulator of complement activation and inhibits the formation of the membrane attack complex (MAC). The complement system is involved not just in innate immunity and adaptive responses, but also in tissue repair and fibrosis[251,252]. Thus, CD59 may be viewed as a regulator of fibrosis and the increased circulating transcript levels observed in non-fibrotic compared to fibrotic tumours may be pathophysiologically relevant. Finally, **APLP2** is widely expressed in human cells and has been implicated in cancer progression. A recent study in Drosophila demonstrated

that APLP2 expression promotes cell migration by inducing matrix metalloproteinase MMP1 expression, which in turn leads to basement membrane degradation[253]. Therefore, this protein may play a role in extracellular matrix remodelling and its precise role in carcinoid-related fibrosis needs to be further investigated.

In conclusion, this study has investigated the role of a novel circulating biomarker (derived from the NETest) in the detection of mesenteric fibrosis. This biomarker exhibited excellent metrics with an accuracy of 100% for macroscopic and microscopic mesenteric fibrosis, which suggests that it may provide additional information and perhaps guide patient management in cases of image-negative mesenteric desmoplasia. Of course, these findings would need to be externally validated in additional and larger patient cohorts. In addition, it would be useful to assess expression of these genes in the tissue (both primary tumour and mesenteric metastasis) at both mRNA and protein level to gain a better understanding of their role in fibrosis development. Furthermore, the role of this molecular signature in other fibrotic complications of neuroendocrine tumours (such as carcinoid heart disease) would need to be explored, as well as its specificity for carcinoid-related fibrosis in patients with other fibrotic conditions (such as scleroderma). These studies will define the role of this promising novel biomarker and delineate its clinical utility in a variety of clinical applications.

Chapter 6

Concluding remarks

6. Concluding remarks

NETs often are associated with diverse fibrotic complications, which can lead to devastating clinical sequelae and cause considerable morbidity and mortality. However, our knowledge of the biologic basis of this relationship is relatively limited. Because to our knowledge there are no established medical therapies for the prevention or regression of fibrosis in patients with NETs, there is an unmet need for meaningful investigations into the pathophysiology of this association. In this thesis we have investigated several clinical aspects of mesenteric fibrosis as well as its pathophysiology in small intestinal neuroendocrine neoplasms and have evaluated a biomarker for fibrosis detection. The area of mesenteric fibrogenesis has not been adequately explored in the literature.

Our clinical retrospective studies highlighted the clinical importance of this condition and demonstrated that patients with mesenteric fibrosis have a worse prognosis compared to non-fibrotic patients. Interestingly, the shorter overall survival in these patients was mainly due to disease progression rather than local intra-abdominal complications, such as bowel obstruction. This led us to hypothesise that the development of fibrosis may have an impact on the natural history of the disease, which is a new concept in neuroendocrine neoplasia. At the same time, a few other retrospective studies from different centres were published and these also showed that desmoplastic tumours were associated with a shorter progression-free survival. This further supported our original hypothesis. Although our clinical studies were limited by their retrospective design and the fact that they were based at a tertiary referral centre, they provided important information about clinical outcomes in desmoplastic neuroendocrine neoplasms and were published as original articles in *Neuroendocrinology*.

We then investigated the pathophysiology of mesenteric fibrosis *in vitro* and in human tissue. The *in vitro* studies were performed in collaboration with the University of Graz in Austria. Although this collaboration was fruitful and useful for allowing the utilisation of appropriate small intestinal neuroendocrine tumour cell lines for our project, there were significant limitations in terms of our ability to independently manage the cell line experiments and further validate the results *in vitro* by altering various experimental conditions. However, these cell line experiments revealed that

multiple genes, cytokines and pathways could potentially be implicated in the cross-talk of cancer and stromal cells within the tumour microenvironment. Many of these pathways are involved not only in fibrosis development but also cancer progression, thus highlighting a possible bidirectional effect in the interplay of cancer cells and fibroblasts within the mesenteric microenvironment. This work was presented as an oral lecture at the Digestive Disease Week (San Diego, 2019) and received positive feedback due to novel concepts that it introduced in the field. However, it is clearly limited by the fact that it was based on one independent experiment and the results were not validated *in vitro* with the use of other co-culture models (for example, the use of another stromal cell line or primary fibroblasts).

We then validated one of the pathways in human tissue of patients that we recruited prospectively during the period of the study. The prospective nature of the project was critically important, because it allowed us to investigate the accuracy of radiological measurements of mesenteric fibrosis and correlate these with intra-operative appearances and histological measurements. This triangulation of methods to assess mesenteric desmoplasia demonstrated that radiological evaluations of fibrosis (which are the standard technique to diagnose mesenteric fibrosis in clinical practice) are often inadequate. Using this methodology, we were able to classify our patients more accurately with a multidimensional assessment of fibrosis. This may be an approach that other researchers in the field could potentially use to further investigate this area. In our *in vivo* study we evaluated the integrin signalling pathway (which was activated in KRJ-I cancer cells in the functional *in vitro* experiments) in fibrotic and non-fibrotic subjects. We showed that several components of this pathway were transcriptionally upregulated in the mesenteric mass of fibrotic patients, but we observed some heterogeneity in protein expression among fibrotic subjects. This work demonstrated a new pathway that could be involved in the pathophysiology of mesenteric fibrogenesis which has additional roles in carcinogenesis and angiogenesis, thus showing how the fibrotic microenvironment may potentially promote cancer growth. This study has been accepted as an oral lecture at the Digestive Disease Week (Chicago, 2020). The main limitations of this study are the relatively small numbers of patients, particularly non-fibrotic subjects. Due to the lack of symptoms and abdominal complications in patients without mesenteric fibrosis, these patients do not usually undergo surgical resection, and so enrolling such cases in the study becomes

very challenging. Multicentre studies may allow the inclusion of more cases for tissue analyses.

Finally, in collaboration with the Wren Laboratories (USA) we investigated a new biomarker for fibrosis detection in small intestinal NETs - the 'NETest Fibrosome'. The NETest is a panel of 51 circulating transcripts that have demonstrated a sensitivity and specificity of about 95% for the diagnosis of neuroendocrine neoplasia in several previous studies. Here, we evaluated a subset of 5 circulating transcripts from the NETest in terms of their ability to predict a fibrotic phenotype in a small cohort of 20 patients, of who only 2 had no evidence of fibrosis histologically. The NETest Fibrosome showed very promising results in this setting and this work has now been published as an original article in *Endocrine*. However, clearly this study is limited by small patient numbers and a disproportionately low number of non-fibrotic cases. Therefore, it is difficult to draw safe conclusions from this study and the results will need to be validated in additional, larger and ideally multicentre patient cohorts.

In summary, this project was based on international collaborations with both the University of Graz (Austria) and the Wren laboratories (USA). We have attempted to address several clinical aspects of mesenteric fibrosis and also look at the pathophysiology of this process. Future clinical studies could aim to investigate why only some patients with mesenteric fibrosis tend to develop severe abdominal complications while others remain asymptomatic. Our data have shown that the amount of fibrous tissue is not a determining factor, as patients with mild, moderate and severe desmoplasia did not have significant differences in terms of survival and abdominal symptoms. Other clinical factors, such as the size of the mesenteric mass and its location in relation to other vital structures (e.g. mesenteric vessels, bowel loops) may be more important and require investigation as predictors of fibrotic complications. The use of computer-based technologies to analyse imaging studies (radionomics) and predict surgical complications may be an interesting avenue to explore and other centres are currently evaluating this approach.

More basic science studies evaluating the cross-talk of cancer cells with fibroblasts in the mesenteric microenvironment are needed. The use of appropriate cancer cell lines is particularly important and only a few small intestinal neuroendocrine tumour cell lines are available, which are not very well characterised and not widely available and

this is a challenging issue. It may be more appropriate to use primary fibroblasts and primary cancer cells isolated from patients with small bowel NETs in co-culture models. To this date only simple co-culture systems have been used to investigate the interplay of cancer and stomal cells in NETs (e.g. Transwell system). The role of more complex co-culture systems (such as 3D systems) requires consideration. In addition, the role of other cell types, such as endothelial, epithelial and inflammatory cells in this process requires further investigation, as these cells may play an important role in fibrosis development and may be appropriate therapeutic targets. Furthermore, it is important to validate the role of any identified pathways by selecting appropriate drug targets and assessing the role of therapeutic agents in cell line models. Unfortunately, there are currently no suitable animal models or organoids for small intestinal NETs to evaluate drug treatments.

In addition, further studies are needed using human tissue to better understand the pathophysiology of mesenteric fibrosis. As mentioned earlier, it is important to develop a clear definition of mesenteric fibrosis in order to be able to accurately classify patients in appropriate categories. Collaborative programs are essential to increase patient numbers for such studies, particularly the number of non-fibrotic cases, which are difficult to recruit. Tissue microdissection would be useful to separate cancer cells from fibrotic stroma and study gene and protein expression separately in these tissue types. This may provide further insight into the underlying mechanisms of mesenteric fibrogenesis and oncogenesis. The investigation of epigenetic changes in NETs as a driver of fibrogenesis is another promising area for future research. Common epigenetic alterations (DNA methylation, posttranscriptional modifications of histones, and noncoding RNAs) are known to contribute toward the pathogenesis of fibrosis in many chronic fibrotic disorders, such as systemic scleroderma and cardiac, kidney, and pulmonary fibrosis. This may be an exciting avenue for future research in NET-related fibrosis. The role of oxidative stress in the development of fibrosis in patients with NETs is another interesting research area that requires further exploration.

Furthermore, the evaluation and development of non-invasive biomarkers of fibrosis could have important clinical implications. Such biomarkers potentially could predict the development of fibrosis at an early preclinical stage or help to stratify patients into different categories of risk of fibrotic complications, perhaps alongside other clinical

information. This would be important not only for prognostication purposes, but also for targeting patients at highest risk of poor outcomes with experimental antifibrotic therapies. Our study has also highlighted the various limitations of radiological assessments and clearly cases of image-negative fibrosis are common. Therefore, a non-invasive, circulating biomarker of fibrosis may have important clinical utility for the identification of microscopic fibrosis. Collaborative efforts are needed to increase patient numbers for such studies, especially the number of non-fibrotic subjects. The evaluation of proteins as circulating biomarkers also requires consideration, as proteins are more stable than circulating transcripts and may have better applicability and clinical utility.

In conclusion, our study has advanced our existing knowledge regarding the clinical implications and pathophysiology of mesenteric fibrosis. This process appears to be complex and remains poorly understood. More research is needed using appropriate cell line models, which may also serve as a platform for the evaluation of antifibrotic drug therapies. Collaborative studies are also required to better understand the pathophysiology of this process using human tissue and to develop non-invasive biomarkers in order to detect and monitor fibrosis development in these patients. Finally, there is a lot to be learnt from other disciplines where research in fibrosis has progressed more rapidly (such as rheumatology or hepatology) and therefore collaboration with researchers in the field of fibrosis in such disciplines would be beneficial to further advance our knowledge in this field.

References:

1. Dasari A, Shen C, Halperin D, et al. Trends in the Incidence, Prevalence, and Survival Outcomes in Patients With Neuroendocrine Tumors in the United States. JAMA Oncol 2017 Oct 1;3(10):1335-1342 doi: 101001/jamaoncol20170589.
2. Modlin IM, Shapiro MD, Kidd M. Carcinoid tumors and fibrosis: an association with no explanation. Am J Gastroenterol 2004 Dec;99(12):2466-78 doi: 101111/j1572-0241200440507x.
3. Gustafsson BI, Hauso O, Drozdov I, Kidd M, Modlin IM. Carcinoid heart disease. Int J Cardiol 2008 Oct 13;129(3):318-24 doi: 101016/jijcard200802019 Epub 2008 Jun 20.
4. Makridis C, Ekbom A, Bring J, et al. Survival and daily physical activity in patients treated for advanced midgut carcinoid tumors. Surgery 1997 Dec;122(6):1075-82.
5. Pellikka PA, Tajik AJ, Khandheria BK, et al. Carcinoid heart disease. Clinical and echocardiographic spectrum in 74 patients. Circulation 1993 Apr;87(4):1188-96.
6. Druce MR, Bharwani N, Akker SA, Drake WM, Rockall A, Grossman AB. Intra-abdominal fibrosis in a recent cohort of patients with neuroendocrine ('carcinoid') tumours of the small bowel. QJM 2010 Mar;103(3):177-85 doi: 101093/qjmed/hcp191 Epub 2010 Feb 1.
7. Daskalakis K, Karakatsanis A, Stalberg P, Norlen O, Hellman P. Clinical signs of fibrosis in small intestinal neuroendocrine tumours. Br J Surg 2017 Jan;104(1):69-75 doi: 101002/bjs10333 Epub 2016 Nov 10.
8. Pantongrag-Brown L, Buetow PC, Carr NJ, Lichtenstein JE, Buck JL. Calcification and fibrosis in mesenteric carcinoid tumor: CT findings and pathologic correlation. AJR Am J Roentgenol 1995 Feb;164(2):387-91 doi: 102214/ajr16427839976.
9. Laskaratos FM, Rombouts K, Caplin M, Toumpanakis C, Thirlwell C, Mandair D. Neuroendocrine tumors and fibrosis: An unsolved mystery? Cancer 2017 Dec 15;123(24):4770-4790 doi: 101002/cncr31079 Epub 2017 Nov 7.
10. Laskaratos FM, Diamantopoulos L, Walker M, et al. Prognostic Factors for Survival among Patients with Small Bowel Neuroendocrine Tumours Associated with Mesenteric Desmoplasia. Neuroendocrinology 2018;106(4):366-380 doi: 101159/000486097 Epub 2018 Jan 10.
11. Laskaratos FM, Walker M, Wilkins D, et al. Evaluation of Clinical Prognostic Factors and Further Delineation of the Effect of Mesenteric Fibrosis on Survival in Advanced Midgut Neuroendocrine Tumours. Neuroendocrinology 2018;107(3):292-304 doi: 101159/000493317 Epub 2018 Aug 28.
12. Blazevic A, Zandee WT, Franssen GJH, et al. Mesenteric fibrosis and palliative surgery in small intestinal neuroendocrine tumours. Endocr Relat Cancer 2018 Mar;25(3):245-254 doi: 101530/ERC-17-0282 Epub 2017 Dec 18.
13. Hellman P, Lundstrom T, Ohrvall U, et al. Effect of surgery on the outcome of midgut carcinoid disease with lymph node and liver metastases. World J Surg 2002 Aug;26(8):991-7 doi: 101007/s00268-002-6630-z Epub 2002 May 21.
14. Taylor JK. Retroperitoneal fibrosis, regional enteritis, and carcinoid tumors. JAMA 1971 Sep 27;217(13):1864.
15. Ratnavel RC, Burrows NP, Pye RJ. Scleroderma and the carcinoid syndrome. Clin Exp Dermatol 1994 Jan;19(1):83-5.
16. Moss SF, Lehner PJ, Gilbey SG, et al. Pleural involvement in the carcinoid syndrome. Q J Med 1993 Jan;86(1):49-53.

17. Blazevic A, Hofland J, Hofland LJ, Feelders RA, de Herder WW. Small intestinal neuroendocrine tumours and fibrosis: an entangled conundrum. Endocr Relat Cancer 2018 Mar;25(3):R115-R130 doi: 101530/ERC-17-0380 Epub 2017 Dec 12.

18. Schuppan D, Somasundaram R, Dieterich W, Ehnis T, Bauer M. The extracellular matrix in cellular proliferation and differentiation. Ann N Y Acad Sci 1994 Sep 15;733:87-102.

19. Cirri P, Chiarugi P. Cancer-associated-fibroblasts and tumour cells: a diabolic liaison driving cancer progression. Cancer Metastasis Rev 2012 Jun;31(1-2):195-208 doi: 101007/s10555-011-9340-x.

20. Carloni V, Luong TV, Rombouts K. Hepatic stellate cells and extracellular matrix in hepatocellular carcinoma: more complicated than ever. Liver Int 2014 Jul;34(6):834-43 doi: 101111/liv12465 Epub 2014 Feb 12.

21. Svejda B, Kidd M, Giovinazzo F, et al. The 5-HT(2B) receptor plays a key regulatory role in both neuroendocrine tumor cell proliferation and the modulation of the fibroblast component of the neoplastic microenvironment. Cancer 2010 Jun 15;116(12):2902-12 doi: 101002/cncr25049.

22. Kidd M, Modlin I, Shapiro M, et al. CTGF, intestinal stellate cells and carcinoid fibrogenesis. World J Gastroenterol 2007 Oct 21;13(39):5208-16.

23. Spatz M. Pathogenetic Studies of Experimentally Induced Heart Lesions and Their Relation to the Carcinoid Syndrome. Lab Invest 1964 Mar;13:288-300.

24. Jackson LN, Chen LA, Larson SD, et al. Development and characterization of a novel in vivo model of carcinoid syndrome. Clin Cancer Res 2009 Apr 15;15(8):2747-55 doi: 101158/1078-0432CCR-08-2346 Epub 2009 Mar 31.

25. McKinney B, Crawford MA. Fibrosis in guineapig heart produced by plantain diet. Lancet 1965 Oct 30;2(7418):880-2.

26. Gustafsson BI, Tommeras K, Nordrum I, et al. Long-term serotonin administration induces heart valve disease in rats. Circulation 2005 Mar 29;111(12):1517-22 doi: 101161/01CIR00001593564206448 Epub 2005 Mar 21.

27. Musunuru S, Carpenter JE, Sippel RS, Kunnimalaiyaan M, Chen H. A mouse model of carcinoid syndrome and heart disease. J Surg Res 2005 Jun 1;126(1):102-5 doi: 101016/jjss200501003.

28. Mekontso-Dessap A, Brouri F, Pascal O, et al. Deficiency of the 5-hydroxytryptamine transporter gene leads to cardiac fibrosis and valvulopathy in mice. Circulation 2006 Jan 3;113(1):81-9 doi: 101161/CIRCULATIONAHA105554667 Epub 2005 Dec 27.

29. Elangbam CS, Job LE, Zadrozny LM, et al. 5-hydroxytryptamine (5HT)-induced valvulopathy: compositional valvular alterations are associated with 5HT2B receptor and 5HT transporter transcript changes in Sprague-Dawley rats. Exp Toxicol Pathol 2008 Aug;60(4-5):253-62 doi: 101016/jetp200803005 Epub 2008 Jun 3.

30. Lancellotti P, Nchimi A, Hego A, et al. High-dose oral intake of serotonin induces valvular heart disease in rabbits: Int J Cardiol. 2015 Oct 15;197:72-5. doi: 10.1016/j.ijcard.2015.06.035. Epub 2015 Jun 19.

31. Janssen W, Schymura Y, Novoyatleva T, et al. 5-HT2B receptor antagonists inhibit fibrosis and protect from RV heart failure. Biomed Res Int 2015;2015:438403 doi: 101155/2015/438403 Epub 2015 Feb 1.

32. Hauso O, Gustafsson BI, Loennechen JP, Stunes AK, Nordrum I, Waldum HL. Long-term serotonin effects in the rat are prevented by terguride. Regul Pept 2007 Oct 4;143(1-3):39-46 doi: 101016/jregpep200702009 Epub 2007 Mar 1.

33. Tornebrandt K, Eskilsson J, Nobin A. Heart involvement in metastatic carcinoid disease. Clin Cardiol 1986 Jan;9(1):13-9.

34. Jacobsen MB, Nitter-Hauge S, Bryde PE, Hanssen LE. Cardiac manifestations in mid-gut carcinoid disease. Eur Heart J 1995 Feb;16(2):263-8.

35. Lundin L, Norheim I, Landelius J, Oberg K, Theodorsson-Norheim E. Carcinoid heart disease: relationship of circulating vasoactive substances to ultrasound-detectable cardiac abnormalities. Circulation 1988 Feb;77(2):264-9.

36. Denney WD, Kemp WE, Jr., Anthony LB, Oates JA, Byrd BF, 3rd. Echocardiographic and biochemical evaluation of the development and progression of carcinoid heart disease. J Am Coll Cardiol 1998 Oct;32(4):1017-22.

37. Robiolio PA, Rigolin VH, Wilson JS, et al. Carcinoid heart disease. Correlation of high serotonin levels with valvular abnormalities detected by cardiac catheterization and echocardiography. Circulation 1995 Aug 15;92(4):790-5.

38. Zuetenhorst JM, Bonfrer JM, Korse CM, Bakker R, van Tinteren H, Taal BG. Carcinoid heart disease: the role of urinary 5-hydroxyindoleacetic acid excretion and plasma levels of atrial natriuretic peptide, transforming growth factor-beta and fibroblast growth factor. Cancer 2003 Apr 1;97(7):1609-15 doi: 101002/cncr11226.

39. Bhattacharyya S, Jagroop A, Gujral DM, et al. Circulating plasma and platelet 5-hydroxytryptamine in carcinoid heart disease: a pilot study. J Heart Valve Dis 2013 May;22(3):400-7.

40. Dobson R, Burgess MI, Banks M, et al. The association of a panel of biomarkers with the presence and severity of carcinoid heart disease: a cross-sectional study. PLoS One 2013 Sep 12;8(9):e73679 doi: 101371/journalpone0073679 eCollection 2013.

41. Westberg G, Wangberg B, Ahlman H, Bergh CH, Beckman-Suurkula M, Caidahl K. Prediction of prognosis by echocardiography in patients with midgut carcinoid syndrome. Br J Surg 2001 Jun;88(6):865-72 doi: 101046/j0007-1323200101798x.

42. Ross EM, Roberts WC. The carcinoid syndrome: comparison of 21 necropsy subjects with carcinoid heart disease to 15 necropsy subjects without carcinoid heart disease. Am J Med 1985 Sep;79(3):339-54.

43. Himelman RB, Schiller NB. Clinical and echocardiographic comparison of patients with the carcinoid syndrome with and without carcinoid heart disease. Am J Cardiol 1989 Feb 1;63(5):347-52.

44. Moller JE, Connolly HM, Rubin J, Seward JB, Modesto K, Pellikka PA. Factors associated with progression of carcinoid heart disease. N Engl J Med 2003 Mar 13;348(11):1005-15 doi: 101056/NEJMoa021451.

45. From the Centers for Disease Control and Prevention. Cardiac valvulopathy associated with exposure to fenfluramine or dexfenfluramine: US Department of Health and Human Services interim public health recommendations, November 1997. JAMA 1997 Dec 3;278(21):1729-31.

46. Connolly HM, Crary JL, McGoon MD, et al. Valvular heart disease associated with fenfluramine-phentermine. N Engl J Med 1997 Aug 28;337(9):581-8 doi: 101056/NEJM199708283370901.

47. Hendrikx M, Van Dorpe J, Flameng W, Daenen W. Aortic and mitral valve disease induced by ergotamine therapy for migraine: a case report and review of the literature. J Heart Valve Dis 1996 Mar;5(2):235-7.

48. Antonini A, Poewe W. Fibrotic heart-valve reactions to dopamine-agonist treatment in Parkinson's disease. Lancet Neurol 2007 Sep;6(9):826-9 doi: 101016/S1474-4422(07)70218-1.

49. Waller EA, Kaplan J. Pergolide-associated valvular heart disease. Compr Ther 2006 Summer;32(2):94-101.

50. Zanettini R, Antonini A, Gatto G, Gentile R, Tesei S, Pezzoli G. Valvular heart disease and the use of dopamine agonists for Parkinson's disease. N Engl J Med 2007 Jan 4;356(1):39-46 doi: 101056/NEJMoa054830.

51. Horvath J, Fross RD, Kleiner-Fisman G, et al. Severe multivalvular heart disease: a new complication of the ergot derivative dopamine agonists. Mov Disord 2004 Jun;19(6):656-62 doi: 101002/mds20201.

52. Schade R, Andersohn F, Suissa S, Haverkamp W, Garbe E. Dopamine agonists and the risk of cardiac-valve regurgitation. N Engl J Med 2007 Jan 4;356(1):29-38 doi: 101056/NEJMoa062222.

53. Roth BL. Drugs and valvular heart disease. N Engl J Med 2007 Jan 4;356(1):6-9 doi: 101056/NEJMp068265.

54. Mason JW, Billingham ME, Friedman JP. Methysergide-induced heart disease: a case of multivalvular and myocardial fibrosis. Circulation 1977 Nov;56(5):889-90.

55. Reimund E. Methysergide and retroperitoneal fibrosis: Lancet. 1987 Feb 21;1(8530):443.

56. Graham JR, Suby HI, LeCompte PR, Sadowsky NL. Fibrotic disorders associated with methysergide therapy for headache. N Engl J Med 1966 Feb 17;274(7):359-68 doi: 101056/NEJM196602172740701.

57. Rothman RB, Baumann MH, Savage JE, et al. Evidence for possible involvement of 5-HT(2B) receptors in the cardiac valvulopathy associated with fenfluramine and other serotonergic medications. Circulation 2000 Dec 5;102(23):2836-41.

58. Smith SA, Waggoner AD, de las Fuentes L, Davila-Roman VG. Role of serotoninergic pathways in drug-induced valvular heart disease and diagnostic features by echocardiography. J Am Soc Echocardiogr 2009 Aug;22(8):883-9 doi: 101016/jecho200905002 Epub 2009 Jun 23.

59. Hutcheson JD, Setola V, Roth BL, Merryman WD. Serotonin receptors and heart valve disease--it was meant 2B. Pharmacol Ther 2011 Nov;132(2):146-57 doi: 101016/jpharmthera201103008 Epub 2011 Apr 2.

60. Setola V, Hufeisen SJ, Grande-Allen KJ, et al. 3,4-methylenedioxymethamphetamine (MDMA, "Ecstasy") induces fenfluramine-like proliferative actions on human cardiac valvular interstitial cells in vitro. Mol Pharmacol 2003 Jun;63(6):1223-9 doi: 101124/mol6361223.

61. Nebigil CG, Launay JM, Hickel P, Tournois C, Maroteaux L. 5-hydroxytryptamine 2B receptor regulates cell-cycle progression: cross-talk with tyrosine kinase pathways. Proc Natl Acad Sci U S A 2000 Mar 14;97(6):2591-6 doi: 101073/pnas050282397.

62. Kidd M, Modlin IM. Small intestinal neuroendocrine cell pathobiology: 'carcinoid' tumors. Curr Opin Oncol 2011 Jan;23(1):45-52 doi: 101097/CCO0b013e328340d006.

63. Seuwen K, Magnaldo I, Pouyssegur J. Serotonin stimulates DNA synthesis in fibroblasts acting through 5-HT1B receptors coupled to a Gi-protein. Nature 1988 Sep 15;335(6187):254-6 doi: 101038/335254a0.

64. Launay JM, Birraux G, Bondoux D, et al. Ras involvement in signal transduction by the serotonin 5-HT2B receptor. J Biol Chem 1996 Feb 9;271(6):3141-7.

65. Gooz M, Gooz P, Luttrell LM, Raymond JR. 5-HT2A receptor induces ERK phosphorylation and proliferation through ADAM-17 tumor necrosis factor-alpha-converting enzyme (TACE) activation and heparin-bound epidermal growth factor-like growth factor (HB-EGF) shedding in mesangial cells. J Biol Chem 2006 Jul 28;281(30):21004-12 doi: 101074/jbcM512096200 Epub 2006 May 31.

66. Banes A, Florian JA, Watts SW. Mechanisms of 5-hydroxytryptamine(2A) receptor activation of the mitogen-activated protein kinase pathway in vascular smooth muscle. J Pharmacol Exp Ther 1999 Dec;291(3):1179-87.

67. Lee SL, Wang WW, Lanzillo JJ, Fanburg BL. Serotonin produces both hyperplasia and hypertrophy of bovine pulmonary artery smooth muscle cells in culture. Am J Physiol 1994 Jan;266(1 Pt 1):L46-52 doi: 101152/ajplung19942661L46.

68. Dolivo DM, Larson SA, Dominko T. Tryptophan metabolites kynurenine and serotonin regulate fibroblast activation and fibrosis. Cell Mol Life Sci 2018 Oct;75(20):3663-3681 doi: 101007/s00018-018-2880-2 Epub 2018 Jul 20.

69. Xu J, Jian B, Chu R, et al. Serotonin mechanisms in heart valve disease II: the 5-HT2 receptor and its signaling pathway in aortic valve interstitial cells. Am J Pathol 2002 Dec;161(6):2209-18 doi: 101016/S0002-9440(10)64497-5.

70. Jian B, Xu J, Connolly J, et al. Serotonin mechanisms in heart valve disease I: serotonin-induced up-regulation of transforming growth factor-beta1 via G-protein signal transduction in aortic valve interstitial cells. Am J Pathol 2002 Dec;161(6):2111-21.

71. Rodriguez Laval V, Pavel M, Steffen IG, et al. Mesenteric Fibrosis in Midgut Neuroendocrine Tumors: Functionality and Radiological Features. Neuroendocrinology 2018;106(2):139-147 doi: 101159/000474941 Epub 2017 Apr 7.

72. Woodard PK, Feldman JM, Paine SS, Baker ME. Midgut carcinoid tumors: CT findings and biochemical profiles. J Comput Assist Tomogr 1995 May-Jun;19(3):400-5.

73. McCall CM, Shi C, Klein AP, et al. Serotonin expression in pancreatic neuroendocrine tumors correlates with a trabecular histologic pattern and large duct involvement. Hum Pathol 2012 Aug;43(8):1169-76 doi: 101016/jhumpath201109014 Epub 2012 Jan 4.

74. Johnson A, Wright JP, Zhao Z, et al. Cadherin 17 is frequently expressed by 'sclerosing variant' pancreatic neuroendocrine tumour. Histopathology 2015 Jan;66(2):225-33 doi: 101111/his12535 Epub 2014 Oct 28.

75. Shi C, Siegelman SS, Kawamoto S, et al. Pancreatic duct stenosis secondary to small endocrine neoplasms: a manifestation of serotonin production? Radiology 2010 Oct;257(1):107-14 doi: 101148/radiol10100046 Epub 2010 Aug 16.

76. Kawamoto S, Shi C, Hruban RH, et al. Small serotonin-producing neuroendocrine tumor of the pancreas associated with pancreatic duct obstruction. AJR Am J Roentgenol 2011 Sep;197(3):W482-8 doi: 102214/AJR105428.

77. La Rosa S, Franzi F, Albarello L, et al. Serotonin-producing enterochromaffin cell tumors of the pancreas: clinicopathologic study of 15 cases and comparison with intestinal enterochromaffin cell tumors. Pancreas 2011 Aug;40(6):883-95 doi: 101097/MPA0b013e31822041a9.

78. Ignotz RA, Massague J. Transforming growth factor-beta stimulates the expression of fibronectin and collagen and their incorporation into the extracellular matrix. J Biol Chem 1986 Mar 25;261(9):4337-45.

79. Wang B, Omar A, Angelovska T, et al. Regulation of collagen synthesis by inhibitory Smad7 in cardiac myofibroblasts. Am J Physiol Heart Circ Physiol 2007 Aug;293(2):H1282-90 doi: 101152/ajpheart009102006 Epub 2007 May 18.

80. Kidd M, Modlin IM, Pfragner R, et al. Small bowel carcinoid (enterochromaffin cell) neoplasia exhibits transforming growth factor-beta1-mediated regulatory abnormalities including up-regulation of C-Myc and MTA1. Cancer 2007 Jun 15;109(12):2420-31 doi: 101002/cncr22725.

81. Leu FP, Nandi M, Niu C. The effect of transforming growth factor beta on human neuroendocrine tumor BON cell proliferation and differentiation is mediated through somatostatin signaling. Mol Cancer Res 2008 Jun;6(6):1029-42 doi: 101158/1541-7786MCR-07-2073.

82. Chaudhry A, Oberg K, Gobl A, Heldin CH, Funa K. Expression of transforming growth factors beta 1, beta 2, beta 3 in neuroendocrine tumors of the digestive system. Anticancer Res 1994 Sep-Oct;14(5B):2085-91.

83. Waltenberger J, Lundin L, Oberg K, et al. Involvement of transforming growth factor-beta in the formation of fibrotic lesions in carcinoid heart disease. Am J Pathol 1993 Jan;142(1):71-8.

84. Bergestuen DS, Edvardsen T, Aakhus S, et al. Activin A in carcinoid heart disease: a possible role in diagnosis and pathogenesis. Neuroendocrinology 2010;92(3):168-77 doi: 101159/000318014 Epub 2010 Aug 18.

85. Zhang PJ, Furth EE, Cai X, Goldblum JR, Pasha TL, Min KW. The role of beta-catenin, TGF beta 3, NGF2, FGF2, IGFR2, and BMP4 in the pathogenesis of mesenteric sclerosis and angiopathy in midgut carcinoids. Hum Pathol 2004 Jun;35(6):670-4.

86. Bergestuen DS, Gravning J, Haugaa KH, et al. Plasma CCN2/connective tissue growth factor is associated with right ventricular dysfunction in patients with neuroendocrine tumors. BMC Cancer 2010 Jan 6;10:6 doi: 101186/1471-2407-10-6.

87. Iwayama T, Olson LE. Involvement of PDGF in fibrosis and scleroderma: recent insights from animal models and potential therapeutic opportunities. Curr Rheumatol Rep 2013 Feb;15(2):304 doi: 101007/s11926-012-0304-0.

88. Ostendorf T, Boor P, van Roeyen CR, Floege J. Platelet-derived growth factors (PDGFs) in glomerular and tubulointerstitial fibrosis. Kidney Int Suppl (2011) 2014 Nov;4(1):65-69 doi: 101038/kisup201412.

89. Borkham-Kamphorst E, Weiskirchen R. The PDGF system and its antagonists in liver fibrosis. Cytokine Growth Factor Rev 2016 Apr;28:53-61 doi: 101016/jcytogfr201510002 Epub 2015 Oct 30.

90. Chaudhry A, Papanicolaou V, Oberg K, Heldin CH, Funa K. Expression of platelet-derived growth factor and its receptors in neuroendocrine tumors of the digestive system. Cancer Res 1992 Feb 15;52(4):1006-12.

91. Funa K, Papanicolaou V, Juhlin C, et al. Expression of platelet-derived growth factor beta-receptors on stromal tissue cells in human carcinoid tumors. Cancer Res 1990 Feb 1;50(3):748-53.

92. Beenken A, Mohammadi M. The FGF family: biology, pathophysiology and therapy. Nat Rev Drug Discov 2009 Mar;8(3):235-53 doi: 101038/nrd2792.

93. Bordi C, Falchetti A, Buffa R, et al. Production of basic fibroblast growth factor by gastric carcinoid tumors and their putative cells of origin. Hum Pathol 1994 Feb;25(2):175-80.

94. La Rosa S, Chiaravalli AM, Capella C, Uccella S, Sessa F. Immunohistochemical localization of acidic fibroblast growth factor in normal human enterochromaffin cells and related gastrointestinal tumours. Virchows Arch 1997 Feb;430(2):117-24.

95. Cai YC, Barnard G, Hiestand L, Woda B, Colby J, Banner B. Florid angiogenesis in mucosa surrounding an ileal carcinoid tumor expressing transforming growth factor-alpha. Am J Surg Pathol 1997 Nov;21(11):1373-7.

96. Nilsson O, Wangberg B, Kolby L, Schultz GS, Ahlman H. Expression of transforming growth factor alpha and its receptor in human neuroendocrine tumours. Int J Cancer 1995 Mar 3;60(5):645-51.

97. Kidd M, Schimmack S, Lawrence B, Alaimo D, Modlin IM. EGFR/TGFalpha and TGFbeta/CTGF Signaling in Neuroendocrine Neoplasia: Theoretical Therapeutic Targets. Neuroendocrinology 2013;97(1):35-44 doi: 101159/000334891 Epub 2012 Jun 15.

98. Oberg K. Expression of growth factors and their receptors in neuroendocrine gut and pancreatic tumors, and prognostic factors for survival. Ann N Y Acad Sci 1994 Sep 15;733:46-55.

99. Wulbrand U, Wied M, Zofel P, Goke B, Arnold R, Fehmann H. Growth factor receptor expression in human gastroenteropancreatic neuroendocrine tumours. Eur J Clin Invest 1998 Dec;28(12):1038-49.

100. Nilsson O, Wangberg B, Theodorsson E, Skottner A, Ahlman H. Presence of IGF-I in human midgut carcinoid tumours--an autocrine regulator of carcinoid tumour growth? Int J Cancer 1992 May 8;51(2):195-203.

101. Nilsson O, Wangberg B, Wigander A, Ahlman H. Immunocytochemical evidence for the presence of IGF-I and IGF-I receptors in human endocrine tumours. Acta Physiol Scand 1992 Feb;144(2):211-2 doi: 101111/j1748-17161992tb09288x.

102. Nilsson O, Wangberg B, McRae A, Dahlstrom A, Ahlman H. Growth factors and carcinoid tumours. Acta Oncol 1993;32(2):115-24.

103. Froesch ER, Schmid C, Schwander J, Zapf J. Actions of insulin-like growth factors. Annu Rev Physiol 1985;47:443-67 doi: 101146/annurevph47030185002303.

104. Sartelet H, Decaussin M, Devouassoux G, et al. Expression of vascular endothelial growth factor (VEGF) and its receptors (VEGF-R1 [Flt-1] and VEGF-R2 [KDR/Flk-1]) in tumorlets and in neuroendocrine cell hyperplasia of the lung. Hum Pathol 2004 Oct;35(10):1210-7.

105. He P, Gu X, Wu Q, Lin Y, Gu Y, He J. Pulmonary carcinoid tumorlet without underlying lung disease: analysis of its relationship to fibrosis. J Thorac Dis 2012 Dec;4(6):655-8 doi: 103978/jissn2072-143920120611.

106. Amoury RA. Heart disease and the malignant carcinoid syndrome. A case report and review of pathophysiologic and pathogenetic mechanisms. Am J Surg 1970 May;119(5):585-94.

107. Strickman NE, Rossi PA, Massumkhani GA, Hall RJ. Carcinoid heart disease: a clinical pathologic, and therapeutic update. Curr Probl Cardiol 1982 Feb;6(11):1-42.

108. Oates JA, Melmon K, Sjoerdsma A, Gillespie L, Mason DT. Release of a Kinin Peptide in the Carcinoid Syndrome. Lancet 1964 Mar 7;1(7332):514-7.

109. Nilsson J, von Euler AM, Dalsgaard CJ. Stimulation of connective tissue cell growth by substance P and substance K. Nature 1985 May 2-8;315(6014):61-3.

110. Katayama I, Nishioka K. Substance P augments fibrogenic cytokine-induced fibroblast proliferation: possible involvement of neuropeptide in tissue fibrosis. J Dermatol Sci 1997 Sep;15(3):201-6.

111. Koperek O, Bergner O, Pichlhofer B, et al. Expression of hypoxia-associated proteins in sporadic medullary thyroid cancer is associated with desmoplastic stroma reaction and lymph node metastasis and may indicate somatic mutations in the VHL gene. J Pathol 2011 Sep;225(1):63-72 doi: 101002/path2926 Epub 2011 Jun 1.

112. Koperek O, Scheuba C, Puri C, et al. Molecular characterization of the desmoplastic tumor stroma in medullary thyroid carcinoma. Int J Oncol 2007 Jul;31(1):59-67.

113. Oba H, Nishida K, Takeuchi S, et al. Diffuse idiopathic pulmonary neuroendocrine cell hyperplasia with a central and peripheral carcinoid and multiple tumorlets: a case report emphasizing the role of neuropeptide hormones and human gonadotropin-alpha. Endocr Pathol 2013 Dec;24(4):220-8 doi: 101007/s12022-013-9265-8.

114. Druce M, Rockall A, Grossman AB. Fibrosis and carcinoid syndrome: from causation to future therapy. Nat Rev Endocrinol 2009 May;5(5):276-83 doi: 101038/nrendo200951.

115. Jacob N, Targan SR, Shih DQ. Cytokine and anti-cytokine therapies in prevention or treatment of fibrosis in IBD. United European Gastroenterol J 2016 Aug;4(4):531-40 doi: 101177/2050640616649356 Epub 2016 May 10.

116. Aoki T, Narumiya S. Prostaglandins and chronic inflammation. Trends Pharmacol Sci 2012 Jun;33(6):304-11 doi: 101016/jtips201202004 Epub 2012 Mar 28.

117. Niederle MB, Hackl M, Kaserer K, Niederle B. Gastroenteropancreatic neuroendocrine tumours: the current incidence and staging based on the WHO and European Neuroendocrine Tumour Society classification: an analysis based on

prospectively collected parameters. Endocr Relat Cancer 2010 Oct 5;17(4):909-18 doi: 101677/ERC-10-0152 Print 2010 Dec.

118. Bosch F, Bruewer K, D'Anastasi M, et al. Neuroendocrine tumors of the small intestine causing a desmoplastic reaction of the mesentery are a more aggressive cohort. Surgery 2018 Nov;164(5):1093-1099 doi: 101016/jsurg201806026 Epub 2018 Jul 31.

119. Landry CS, Lin HY, Phan A, et al. Resection of at-risk mesenteric lymph nodes is associated with improved survival in patients with small bowel neuroendocrine tumors. World J Surg 2013 Jul;37(7):1695-700 doi: 101007/s00268-013-1918-8.

120. Daskalakis K, Karakatsanis A, Hessman O, et al. Association of a Prophylactic Surgical Approach to Stage IV Small Intestinal Neuroendocrine Tumors With Survival. JAMA Oncol 2018 Feb 1;4(2):183-189 doi: 101001/jamaoncol20173326.

121. Niederle B, Pape UF, Costa F, et al. ENETS Consensus Guidelines Update for Neuroendocrine Neoplasms of the Jejunum and Ileum. Neuroendocrinology 2016;103(2):125-38 doi: 101159/000443170 Epub 2016 Jan 12.

122. Drozdov I, Kidd M, Gustafsson BI, et al. Autoregulatory effects of serotonin on proliferation and signaling pathways in lung and small intestine neuroendocrine tumor cell lines. Cancer 2009 Nov 1;115(21):4934-45 doi: 101002/cncr24533.

123. van der Horst-Schrivers AN, Post WJ, Kema IP, et al. Persistent low urinary excretion of 5-HIAA is a marker for favourable survival during follow-up in patients with disseminated midgut carcinoid tumours. Eur J Cancer 2007 Dec;43(18):2651-7 doi: 101016/jejca200707025 Epub 2007 Sep 6.

124. Laskaratos F-M, Rombouts K, Caplin M, Toumpanakis C, Thirlwell C, Mandair D. Neuroendocrine tumors and fibrosis: An unsolved mystery? Cancer.123(24):4770-90.

125. Kidd M, Eick GN, Modlin IM, Pfragner R, Champaneria MC, Murren J. Further delineation of the continuous human neoplastic enterochromaffin cell line, KRJ-I, and the inhibitory effects of lanreotide and rapamycin. J Mol Endocrinol 2007 Feb;38(1-2):181-92 doi: 101677/jme102037.

126. Beauchamp RD, Coffey RJ, Jr., Lyons RM, Perkett EA, Townsend CM, Jr., Moses HL. Human carcinoid cell production of paracrine growth factors that can stimulate fibroblast and endothelial cell growth. Cancer Res 1991 Oct 1;51(19):5253-60.

127. Pfragner R, Behmel A, Hoger H, et al. Establishment and characterization of three novel cell lines - P-STS, L-STS, H-STS - derived from a human metastatic midgut carcinoid. Anticancer Res 2009 Jun;29(6):1951-61.

128. Pfragner R, Wirnsberger G, Niederle B, et al. Establishment of a continuous cell line from a human carcinoid of the small intestine (KRJ-I). Int J Oncol 1996 Mar;8(3):513-20.

129. Stepanenko AA, Dmitrenko VV. HEK293 in cell biology and cancer research: phenotype, karyotype, tumorigenicity, and stress-induced genome-phenotype evolution. Gene 2015 Sep 15;569(2):182-90 doi: 101016/jgene201505065 Epub 2015 May 27.

130. Hantel C, Ozimek A, Lira R, et al. TNF alpha signaling is associated with therapeutic responsiveness to vascular disrupting agents in endocrine tumors. Mol Cell Endocrinol 2016 Mar 5;423:87-95 doi: 101016/jmce201512009 Epub 2016 Jan 6.

131. Ishizuka J, Beauchamp RD, Sato K, Townsend CM, Jr., Thompson JC. Novel action of transforming growth factor beta 1 in functioning human pancreatic carcinoid cells. J Cell Physiol 1993 Jul;156(1):112-8 doi: 101002/jcp1041560116.

132. Jack GD, Garst JF, Cabrera MC, et al. Long term metabolic arrest and recovery of HEK293 spheroids involves NF-kappaB signaling and sustained JNK activation. J Cell Physiol 2006 Feb;206(2):526-36 doi: 101002/jcp20499.

133. Kumar Pachathundikandi S, Brandt S, Madassery J, Backert S. Induction of TLR-2 and TLR-5 expression by Helicobacter pylori switches cagPAI-dependent signalling leading to the secretion of IL-8 and TNF-alpha. PLoS One 2011 May 9;6(5):e19614 doi: 101371/journalpone0019614.

134. Mendez-Samperio P, Trejo A, Perez A. Mycobacterium bovis bacillus Calmette-Guerin induces CCL5 secretion via the Toll-like receptor 2-NF-kappaB and -Jun N-terminal kinase signaling pathways. Clin Vaccine Immunol 2008 Feb;15(2):277-83 doi: 101128/CVI00368-07 Epub 2007 Nov 7.

135. Zhou X, Fragala MS, McElhaney JE, Kuchel GA. Conceptual and methodological issues relevant to cytokine and inflammatory marker measurements in clinical research. Curr Opin Clin Nutr Metab Care 2010 Sep;13(5):541-7 doi: 101097/MCO0b013e32833cf3bc.

136. Hofving T, Arvidsson Y, Almobarak B, et al. The neuroendocrine phenotype, genomic profile and therapeutic sensitivity of GEPNET cell lines. Endocr Relat Cancer 2018 Mar;25(3):367-380 doi: 101530/ERC-17-0445.

137. Grozinsky-Glasberg S, Shimon I, Rubinfeld H. The role of cell lines in the study of neuroendocrine tumors. Neuroendocrinology 2012;96(3):173-87 doi: 101159/000338793 Epub 2012 Jun 7.

138. Yoshimura T. The chemokine MCP-1 (CCL2) in the host interaction with cancer: a foe or ally? Cell Mol Immunol 2018 Apr;15(4):335-345 doi: 101038/cmi2017135 Epub 2018 Jan 29.

139. Morris GF. An alternative to lung inflammation and fibrosis. Am J Pathol 2010 Jun;176(6):2595-8 doi: 102353/ajpath2010100272 Epub 2010 Apr 22.

140. Yang L, Cui H, Wang Z, et al. Loss of negative feedback control of nuclear factor-kappaB2 activity in lymphocytes leads to fatal lung inflammation. Am J Pathol 2010 Jun;176(6):2646-57 doi: 102353/ajpath2010090751 Epub 2010 Apr 2.

141. Gal P, Varinska L, Faber L, et al. How Signaling Molecules Regulate Tumor Microenvironment: Parallels to Wound Repair. Molecules 2017 Oct 26;22(11) pii: molecules22111818 doi: 103390/molecules22111818.

142. Cingarlini S, Bonomi M, Corbo V, Scarpa A, Tortora G. Profiling mTOR pathway in neuroendocrine tumors. Target Oncol 2012 Sep;7(3):183-8 doi: 101007/s11523-012-0226-9 Epub 2012 Aug 14.

143. Liu F, Yang X, Geng M, Huang M. Targeting ERK, an Achilles' Heel of the MAPK pathway, in cancer therapy. Acta Pharm Sin B 2018 Jul;8(4):552-562 doi: 101016/japsb201801008 Epub 2018 Feb 16.

144. Svejda B, Kidd M, Kazberouk A, Lawrence B, Pfragner R, Modlin IM. Limitations in small intestinal neuroendocrine tumor therapy by mTor kinase inhibition reflect growth factor-mediated PI3K feedback loop activation via ERK1/2 and AKT. Cancer 2011 Sep 15;117(18):4141-54 doi: 101002/cncr26011 Epub 2011 Mar 8.

145. Qian ZR, Ter-Minassian M, Chan JA, et al. Prognostic significance of MTOR pathway component expression in neuroendocrine tumors. J Clin Oncol 2013 Sep 20;31(27):3418-25 doi: 101200/JCO2012466946 Epub 2013 Aug 26.

146. Pavel ME, Hainsworth JD, Baudin E, et al. Everolimus plus octreotide long-acting repeatable for the treatment of advanced neuroendocrine tumours associated with carcinoid syndrome (RADIANT-2): a randomised, placebo-controlled, phase 3 study. Lancet 2011 Dec 10;378(9808):2005-2012 doi: 101016/S0140-6736(11)61742-X Epub 2011 Nov 25.

147. Yao JC, Fazio N, Singh S, et al. Everolimus for the treatment of advanced, non-functional neuroendocrine tumours of the lung or gastrointestinal tract (RADIANT-4): a randomised, placebo-controlled, phase 3 study. Lancet 2016 Mar 5;387(10022):968-977 doi: 101016/S0140-6736(15)00817-X Epub 2015 Dec 17.

148. Wu PK, Park JI. MEK1/2 Inhibitors: Molecular Activity and Resistance Mechanisms. Semin Oncol 2015 Dec;42(6):849-62 doi: 101053/jseminoncol201509023 Epub 2015 Sep 24.

149. Flum M, Kleemann M, Schneider H, et al. miR-217-5p induces apoptosis by directly targeting PRKCI, BAG3, ITGAV and MAPK1 in colorectal cancer cells. J Cell Commun Signal 2018 Jun;12(2):451-466 doi: 101007/s12079-017-0410-x Epub 2017 Sep 14.

150. Feldkoren B, Hutchinson R, Rapoport Y, Mahajan A, Margulis V. Integrin signaling potentiates transforming growth factor-beta 1 (TGF-beta1) dependent down-regulation of E-Cadherin expression - Important implications for epithelial to mesenchymal transition (EMT) in renal cell carcinoma. Exp Cell Res 2017 Jun 15;355(2):57-66 doi: 101016/jyexcr201703051 Epub 2017 Mar 29.

151. Zhang C, Wu M, Zhang L, Shang LR, Fang JH, Zhuang SM. Fibrotic microenvironment promotes the metastatic seeding of tumor cells via activating the fibronectin 1/secreted phosphoprotein 1-integrin signaling. Oncotarget 2016 Jul 19;7(29):45702-45714 doi: 1018632/oncotarget10157.

152. Jean C, Gravelle P, Fournie JJ, Laurent G. Influence of stress on extracellular matrix and integrin biology. Oncogene 2011 Jun 16;30(24):2697-706 doi: 101038/onc201127 Epub 2011 Feb 21.

153. Faull RJ, Ginsberg MH. Inside-out signaling through integrins. J Am Soc Nephrol 1996 Aug;7(8):1091-7.

154. Xiao G, Rabson AB, Young W, Qing G, Qu Z. Alternative pathways of NF-kappaB activation: a double-edged sword in health and disease. Cytokine Growth Factor Rev 2006 Aug;17(4):281-93 doi: 101016/jcytogfr200604005 Epub 2006 Jun 21.

155. Chen H, Liu H, Qing G. Targeting oncogenic Myc as a strategy for cancer treatment. Signal Transduct Target Ther 2018 Feb 23;3:5 doi: 101038/s41392-018-0008-7 eCollection 2018.

156. Giubellino A, Burke TR, Jr., Bottaro DP. Grb2 signaling in cell motility and cancer. Expert Opin Ther Targets 2008 Aug;12(8):1021-33 doi: 101517/147282221281021

157. Derakhshan A, Chen Z, Van Waes C. Therapeutic Small Molecules Target Inhibitor of Apoptosis Proteins in Cancers with Deregulation of Extrinsic and Intrinsic Cell Death Pathways. Clin Cancer Res 2017 Mar 15;23(6):1379-1387 doi: 101158/1078-0432CCR-16-2172 Epub 2016 Dec 30.

158. Strasser A, Newton K. FADD/MORT1, a signal transducer that can promote cell death or cell growth. Int J Biochem Cell Biol 1999 May;31(5):533-7.

159. Lopez-Otin C, Palavalli LH, Samuels Y. Protective roles of matrix metalloproteinases: from mouse models to human cancer. Cell Cycle 2009 Nov 15;8(22):3657-62 doi: 104161/cc8229956 Epub 2009 Dec 1.

160. Dejonckheere E, Vandenbroucke RE, Libert C. Matrix metalloproteinase8 has a central role in inflammatory disorders and cancer progression. Cytokine Growth Factor Rev 2011 Apr;22(2):73-81 doi: 101016/jcytogfr201102002 Epub 2011 Mar 8.

161. Lichtman MK, Otero-Vinas M, Falanga V. Transforming growth factor beta (TGF-beta) isoforms in wound healing and fibrosis. Wound Repair Regen 2016 Mar;24(2):215-22 doi: 101111/wrr12398 Epub 2016 Mar 2.

162. Sgonc R, Wick G. Pro- and anti-fibrotic effects of TGF-beta in scleroderma. Rheumatology (Oxford) 2008 Oct;47 Suppl 5:v5-7 doi: 101093/rheumatology/ken275.

163. Markovics JA, Araya J, Cambier S, et al. Interleukin-1beta induces increased transcriptional activation of the transforming growth factor-beta-activating integrin subunit beta8 through altering chromatin architecture. J Biol Chem 2011 Oct 21;286(42):36864-74 doi: 101074/jbcM111276790 Epub 2011 Aug 30.

164. Margadant C, Sonnenberg A. Integrin-TGF-beta crosstalk in fibrosis, cancer and wound healing. EMBO Rep. Feb;11(2):97-105.

165. Danen EH, Yamada KM. Fibronectin, integrins, and growth control. J Cell Physiol 2001 Oct;189(1):1-13 doi: 101002/jcp1137.

166. Ritzenthaler JD, Han S, Roman J. Stimulation of lung carcinoma cell growth by fibronectin-integrin signalling. Mol Biosyst. 2008 Dec;4(12):1160-9.

167. Sun SC, Cesarman E. NF-kappaB as a target for oncogenic viruses. Curr Top Microbiol Immunol 2011;349:197-244 doi: 101007/82_2010_108.

168. Pillai S, Moran ST. Tec kinase pathways in lymphocyte development and transformation. Biochim Biophys Acta 2002 Jun 21;1602(2):162-7.

169. Ma Y, Shurin GV, Peiyuan Z, Shurin MR. Dendritic cells in the cancer microenvironment. J Cancer 2013;4(1):36-44 doi: 107150/jca5046 Epub 2012 Dec 15.

170. Hammer GE, Ma A. Molecular control of steady-state dendritic cell maturation and immune homeostasis. Annu Rev Immunol 2013;31:743-91 doi: 101146/annurev-immunol-020711-074929 Epub 2013 Jan 17.

171. Dalod M, Chelbi R, Malissen B, Lawrence T. Dendritic cell maturation: functional specialization through signaling specificity and transcriptional programming. EMBO J 2014 May 16;33(10):1104-16 doi: 101002/embj201488027 Epub 2014 Apr 15.

172. Tessarz AS, Cerwenka A. The TREM-1/DAP12 pathway. Immunol Lett. 2008 Mar 15;116(2):111-6.

173. Pan MG, Xiong Y, Chen F. NFAT gene family in inflammation and cancer. Curr Mol Med. May;13(4):543-54.

174. Garg R, Benedetti LG, Abera MB, Wang H, Abba M, Kazanietz MG. Protein kinase C and cancer: what we know and what we do not. Oncogene 2014 Nov 6;33(45):5225-37 doi: 101038/onc2013524 Epub 2013 Dec 16.

175. Follo MY, Manzoli L, Poli A, McCubrey JA, Cocco L. PLC and PI3K/Akt/mTOR signalling in disease and cancer. Adv Biol Regul. Jan;57:10-6.

176. Kim JG, Islam R, Cho JY, et al. Regulation of RhoA GTPase and various transcription factors in the RhoA pathway. J Cell Physiol 2018 Sep;233(9):6381-6392 doi: 101002/jcp26487 Epub 2018 Mar 25.

177. Qadir MI, Parveen A, Ali M. Cdc42: Role in Cancer Management. Chem Biol Drug Des 2015 Oct;86(4):432-9 doi: 101111/cbdd12556 Epub 2015 Apr 7.

178. Jellusova J, Rickert RC. The PI3K pathway in B cell metabolism. Crit Rev Biochem Mol Biol. Sep;51(5):359-78.

179. Ting AT, Bertrand MJM. More to Life than NF-kappaB in TNFR1 Signaling. Trends Immunol 2016 Aug;37(8):535-545 doi: 101016/jit201606002 Epub 2016 Jul 13.

180. Singh JK, Simoes BM, Howell SJ, Farnie G, Clarke RB. Recent advances reveal IL-8 signaling as a potential key to targeting breast cancer stem cells. Breast Cancer Res 2013;15(4):210 doi: 101186/bcr3436.

181. Shabab T, Khanabdali R, Moghadamtousi SZ, Kadir HA, Mohan G. Neuroinflammation pathways: a general review. Int J Neurosci. Jul;127(7):624-33.

182. Tham YK, Bernardo BC, Ooi JY, Weeks KL, McMullen JR. Pathophysiology of cardiac hypertrophy and heart failure: signaling pathways and novel therapeutic targets. Arch Toxicol 2015 Sep;89(9):1401-38 doi: 101007/s00204-015-1477-x Epub 2015 Feb 24.

183. Proud CG. eIF2 and the control of cell physiology. Semin Cell Dev Biol 2005 Feb;16(1):3-12 doi: 101016/jsemcdb200411004 Epub 2004 Dec 10.

184. Walewska A, Szewczyk A, Koprowski P. Gas Signaling Molecules and Mitochondrial Potassium Channels. Int J Mol Sci 2018 Oct 18;19(10) pii: ijms19103227 doi: 103390/ijms19103227.

185. Huttemann M, Lee I, Samavati L, Yu H, Doan JW. Regulation of mitochondrial oxidative phosphorylation through cell signaling. Biochim Biophys Acta 2007 Dec;1773(12):1701-20.

186. Carrasquillo JA, Chen CC. Molecular imaging of neuroendocrine tumors. Semin Oncol 2010 Dec;37(6):662-79 doi: 101053/jseminoncol201010015.

187. Gorin A, Gabitova L, Astsaturov I. Regulation of cholesterol biosynthesis and cancer signaling. Curr Opin Pharmacol 2012 Dec;12(6):710-6 doi: 101016/jcoph201206011 Epub 2012 Jul 21.

188. Amelio I, Cutruzzola F, Antonov A, Agostini M, Melino G. Serine and glycine metabolism in cancer. Trends Biochem Sci 2014 Apr;39(4):191-8 doi: 101016/jtibs201402004 Epub 2014 Mar 20.

189. Kung T, Murphy KA, White LA. The aryl hydrocarbon receptor (AhR) pathway as a regulatory pathway for cell adhesion and matrix metabolism. Biochem Pharmacol 2009 Feb 15;77(4):536-46 doi: 101016/jbcp200809031 Epub 2008 Oct 1.

190. Antonioli L, Colucci R, Pellegrini C, et al. The AMPK enzyme-complex: from the regulation of cellular energy homeostasis to a possible new molecular target in the management of chronic inflammatory disorders. Expert Opin Ther Targets 2016;20(2):179-91 doi: 101517/1472822220161086752 Epub 2015 Sep 28.

191. Kaspar JW, Niture SK, Jaiswal AK. Nrf2:INrf2 (Keap1) signaling in oxidative stress. Free Radic Biol Med 2009 Nov 1;47(9):1304-9 doi: 101016/jfreeradbiomed200907035 Epub 2009 Aug 7.

192. Pena-Silva RA, Miller JD, Chu Y, Heistad DD. Serotonin produces monoamine oxidase-dependent oxidative stress in human heart valves. Am J Physiol Heart Circ Physiol 2009 Oct;297(4):H1354-60 doi: 101152/ajpheart005702009 Epub 2009 Aug 7.

193. Andrews RK, Arthur JF, Gardiner EE. Targeting GPVI as a novel antithrombotic strategy. J Blood Med 2014 May 21;5:59-68 doi: 102147/JBMS39220 eCollection 2014.

194. Pu M, Chen J, Tao Z, et al. Regulatory network of miRNA on its target: coordination between transcriptional and post-transcriptional regulation of gene expression. Cell Mol Life Sci 2019 Feb;76(3):441-451 doi: 101007/s00018-018-2940-7 Epub 2018 Oct 29.

195. Malczewska A, Kidd M, Matar S, Kos-Kudla B, Modlin IM. A Comprehensive Assessment of the Role of miRNAs as Biomarkers in Gastroenteropancreatic Neuroendocrine Tumors. Neuroendocrinology 2018;107(1):73-90 doi: 101159/000487326 Epub 2018 Mar 22.

196. Mansour MA. Ubiquitination: Friend and foe in cancer. Int J Biochem Cell Biol 2018 Aug;101:80-93 doi: 101016/jbiocel201806001 Epub 2018 Jun 1.

197. Olzscha H. Posttranslational modifications and proteinopathies: how guardians of the proteome are defeated. Biol Chem 2019 Jun 26;400(7):895-915 doi: 101515/hsz-2018-0458.

198. Yoshimura T. The production of monocyte chemoattractant protein-1 (MCP-1)/CCL2 in tumor microenvironments. Cytokine 2017 Oct;98:71-78 doi: 101016/jcyto201702001 Epub 2017 Feb 8.

199. Karin N. Chemokines and cancer: new immune checkpoints for cancer therapy. Curr Opin Immunol 2018 Apr;51:140-145 doi: 101016/jcoi201803004 Epub 2018 Mar 24.

200. Frangogiannis NG, Entman ML. Chemokines in myocardial ischemia. Trends Cardiovasc Med 2005 Jul;15(5):163-9 doi: 101016/jtcm200506005.

201. Brownell J, Polyak SJ. Molecular pathways: hepatitis C virus, CXCL10, and the inflammatory road to liver cancer. Clin Cancer Res 2013 Mar 15;19(6):1347-52 doi: 101158/1078-0432CCR-12-0928 Epub 2013 Jan 15.

202. Siddique ZL, Drozdov I, Floch J, et al. KRJ-I and BON cell lines: defining an appropriate enterochromaffin cell neuroendocrine tumor model. Neuroendocrinology 2009;89(4):458-70 doi: 101159/000209330 Epub 2009 Mar 18.

203. Tsochatzis E, Bruno S, Isgro G, et al. Collagen proportionate area is superior to other histological methods for sub-classifying cirrhosis and determining prognosis. J Hepatol 2014 May;60(5):948-54 doi: 101016/jjhep201312023 Epub 2014 Jan 8.

204. Tsipouras MG, Giannakeas N, Tzallas AT, et al. A methodology for automated CPA extraction using liver biopsy image analysis and machine learning techniques. Comput Methods Programs Biomed 2017 Mar;140:61-68 doi: 101016/jcmpb201611012 Epub 2016 Nov 29.

205. Chaudhry A, Funa K, Oberg K. Expression of growth factor peptides and their receptors in neuroendocrine tumors of the digestive system. Acta Oncol 1993;32(2):107-14 doi: 103109/02841869309083898.

206. Cutroneo KR. How is Type I procollagen synthesis regulated at the gene level during tissue fibrosis. J Cell Biochem 2003 Sep 1;90(1):1-5 doi: 101002/jcb10599.

207. Cutroneo KR, White SL, Chiu JF, Ehrlich HP. Tissue fibrosis and carcinogenesis: divergent or successive pathways dictate multiple molecular therapeutic targets for oligo decoy therapies. J Cell Biochem 2006 Apr 15;97(6):1161-74 doi: 101002/jcb20750.

208. Distler JH, Schett G, Gay S, Distler O. The controversial role of tumor necrosis factor alpha in fibrotic diseases. Arthritis Rheum 2008 Aug;58(8):2228-35 doi: 101002/art23645.

209. Hill EE, Kim JK, Jung Y, et al. Integrin alpha V beta 3 targeted dendrimer-rapamycin conjugate reduces fibroblast-mediated prostate tumor progression and metastasis. J Cell Biochem 2018 Nov;119(10):8074-8083 doi: 101002/jcb26727 Epub 2018 Jun 22.

210. Lu JG, Sun YN, Wang C, Jin DJ, Liu M. Role of the alpha v-integrin subunit in cell proliferation, apoptosis and tumor metastasis of laryngeal and hypopharyngeal squamous cell carcinomas: a clinical and in vitro investigation. Eur Arch Otorhinolaryngol 2009 Jan;266(1):89-96 doi: 101007/s00405-008-0675-z Epub 2008 Apr 22.

211. Nikkola J, Vihinen P, Vlaykova T, Hahka-Kemppinen M, Heino J, Pyrhonen S. Integrin chains beta1 and alphav as prognostic factors in human metastatic melanoma. Melanoma Res 2004 Feb;14(1):29-37.

212. Mitjans F, Meyer T, Fittschen C, et al. In vivo therapy of malignant melanoma by means of antagonists of alphav integrins. Int J Cancer 2000 Sep 1;87(5):716-23.

213. Viana Lde S, Affonso RJ, Jr., Silva SR, et al. Relationship between the expression of the extracellular matrix genes SPARC, SPP1, FN1, ITGA5 and ITGAV and clinicopathological parameters of tumor progression and colorectal cancer dissemination. Oncology 2013;84(2):81-91 doi: 101159/000343436 Epub 2012 Oct 31.

214. Clarke MR, Landreneau RJ, Finkelstein SD, Wu TT, Ohori P, Yousem SA. Extracellular matrix expression in metastasizing and nonmetastasizing adenocarcinomas of the lung. Hum Pathol 1997 Jan;28(1):54-9.

215. Fu S, Fan L, Pan X, Sun Y, Zhao H. Integrin alphav promotes proliferation by activating ERK 1/2 in the human lung cancer cell line A549. Mol Med Rep 2015 Feb;11(2):1266-71 doi: 103892/mmr20142860 Epub 2014 Nov 4.

216. Meyer T, Marshall JF, Hart IR. Expression of alphav integrins and vitronectin receptor identity in breast cancer cells. Br J Cancer 1998 Feb;77(4):530-6 doi: 101038/bjc199886.

217. Townsend PA, Villanova I, Uhlmann E, et al. An antisense oligonucleotide targeting the alphaV integrin gene inhibits adhesion and induces apoptosis in breast cancer cells. Eur J Cancer 2000 Feb;36(3):397-409.

218. Lu JG, Li Y, Li L, Kan X. Overexpression of osteopontin and integrin alphav in laryngeal and hypopharyngeal carcinomas associated with differentiation and metastasis. J Cancer Res Clin Oncol 2011 Nov;137(11):1613-8 doi: 101007/s00432-011-1024-y Epub 2011 Aug 19.

219. Denadai MV, Viana LS, Affonso RJ, Jr., et al. Expression of integrin genes and proteins in progression and dissemination of colorectal adenocarcinoma. BMC Clin Pathol 2013 May 24;13:16 doi: 101186/1472-6890-13-16 eCollection 2013.

220. Wu YJ, Pagel MA, Muldoon LL, Fu R, Neuwelt EA. High alphav Integrin Level of Cancer Cells Is Associated with Development of Brain Metastasis in Athymic Rats. Anticancer Res 2017 Aug;37(8):4029-4040 doi: 1021873/anticanres11788.

221. Brooks PC, Montgomery AM, Rosenfeld M, et al. Integrin alpha v beta 3 antagonists promote tumor regression by inducing apoptosis of angiogenic blood vessels. Cell 1994 Dec 30;79(7):1157-64.

222. Oxboel J, Binderup T, Knigge U, Kjaer A. Quantitative gene-expression of the tumor angiogenesis markers vascular endothelial growth factor, integrin alphaV and integrin beta3 in human neuroendocrine tumors. Oncol Rep 2009 Mar;21(3):769-75.

223. Oxboel J, Schjoeth-Eskesen C, El-Ali HH, Madsen J, Kjaer A. (64)Cu-NODAGA-c(RGDyK) Is a Promising New Angiogenesis PET Tracer: Correlation between Tumor Uptake and Integrin alpha(V)beta(3) Expression in Human Neuroendocrine Tumor Xenografts. Int J Mol Imaging 2012;2012:379807 doi: 101155/2012/379807 Epub 2012 Oct 2.

224. Conroy KP, Kitto LJ, Henderson NC. alphav integrins: key regulators of tissue fibrosis. Cell Tissue Res 2016 Sep;365(3):511-9 doi: 101007/s00441-016-2407-9 Epub 2016 May 2.

225. Marotta G, Raspadori D, Sestigiani C, Scalia G, Bigazzi C, Lauria F. Expression of the CD11c antigen in B-cell chronic lymphoproliferative disorders. Leuk Lymphoma 2000 Mar;37(1-2):145-9 doi: 103109/10428190009057637.

226. Umit EG, Baysal M, Durmus Y, Demir AM. CD11c expression in chronic lymphocytic leukemia revisited, related with complications and survival. Int J Lab Hematol 2017 Oct;39(5):552-556 doi: 101111/ijlh12695 Epub 2017 Jun 12.

227. Williams KA, Lee M, Hu Y, et al. A systems genetics approach identifies CXCL14, ITGAX, and LPCAT2 as novel aggressive prostate cancer susceptibility genes. PLoS Genet 2014 Nov 20;10(11):e1004809 doi: 101371/journalpgen1004809 eCollection 2014 Nov.

228. Wang Y, Xu B, Hu WW, et al. High expression of CD11c indicates favorable prognosis in patients with gastric cancer. World J Gastroenterol 2015 Aug 21;21(31):9403-12 doi: 103748/wjgv21i319403.

229. Wang J, Yang L, Liang F, Chen Y, Yang G. Integrin alpha x stimulates cancer angiogenesis through PI3K/Akt signaling-mediated VEGFR2/VEGF-A overexpression in blood vessel endothelial cells. J Cell Biochem 2019 Feb;120(2):1807-1818 doi: 101002/jcb27480 Epub 2018 Sep 14.

230. Wang H, Kwak D, Fassett J, et al. Role of bone marrow-derived CD11c(+) dendritic cells in systolic overload-induced left ventricular inflammation, fibrosis and hypertrophy. Basic Res Cardiol 2017 May;112(3):25 doi: 101007/s00395-017-0615-4 Epub 2017 Mar 27.

231. Itoh M, Suganami T, Kato H, et al. CD11c+ resident macrophages drive hepatocyte death-triggered liver fibrosis in a murine model of nonalcoholic steatohepatitis. JCI

Insight 2017 Nov 16;2(22) pii: 92902 doi: 101172/jciinsight92902 eCollection 2017 Nov 16.

232. Modlin IM, Bodei L, Kidd M. Neuroendocrine tumor biomarkers: From monoanalytes to transcripts and algorithms. Best Pract Res Clin Endocrinol Metab 2016 Jan;30(1):59-77 doi: 101016/jbeem201601002 Epub 2016 Jan 18.

233. Modlin IM, Drozdov I, Kidd M. Gut neuroendocrine tumor blood qPCR fingerprint assay: characteristics and reproducibility. Clin Chem Lab Med 2014 Mar;52(3):419-29 doi: 101515/cclm-2013-0496.

234. Modlin IM, Drozdov I, Alaimo D, et al. A multianalyte PCR blood test outperforms single analyte ELISAs (chromogranin A, pancreastatin, neurokinin A) for neuroendocrine tumor detection. Endocr Relat Cancer 2014 Aug;21(4):615-28 doi: 101530/ERC-14-0190.

235. Modlin IM, Drozdov I, Kidd M. The identification of gut neuroendocrine tumor disease by multiple synchronous transcript analysis in blood. PLoS One 2013 May 15;8(5):e63364 doi: 101371/journalpone0063364 Print 2013.

236. Cwikla JB, Bodei L, Kolasinska-Cwikla A, Sankowski A, Modlin IM, Kidd M. Circulating Transcript Analysis (NETest) in GEP-NETs Treated With Somatostatin Analogs Defines Therapy. J Clin Endocrinol Metab 2015 Nov;100(11):E1437-45 doi: 101210/jc2015-2792 Epub 2015 Sep 8.

237. Modlin IM, Aslanian H, Bodei L, Drozdov I, Kidd M. A PCR blood test outperforms chromogranin A in carcinoid detection and is unaffected by proton pump inhibitors. Endocr Connect 2014 Dec;3(4):215-23 doi: 101530/EC-14-0100 Epub 2014 Oct 14.

238. Modlin IM, Kidd M, Bodei L, Drozdov I, Aslanian H. The clinical utility of a novel blood-based multi-transcriptome assay for the diagnosis of neuroendocrine tumors of the gastrointestinal tract. Am J Gastroenterol 2015 Aug;110(8):1223-32 doi: 101038/ajg2015160 Epub 2015 Jun 2.

239. Pavel M, Jann H, Prasad V, Drozdov I, Modlin IM, Kidd M. NET Blood Transcript Analysis Defines the Crossing of the Clinical Rubicon: When Stable Disease Becomes Progressive. Neuroendocrinology 2017;104(2):170-182 doi: 101159/000446025 Epub 2016 Apr 15.

240. Bodei L, Kidd M, Modlin IM, et al. Gene transcript analysis blood values correlate with (6)(8)Ga-DOTA-somatostatin analog (SSA) PET/CT imaging in neuroendocrine tumors and can define disease status. Eur J Nucl Med Mol Imaging 2015 Aug;42(9):1341-52 doi: 101007/s00259-015-3075-9 Epub 2015 May 7.

241. Kidd M, Drozdov I, Modlin I. Blood and tissue neuroendocrine tumor gene cluster analysis correlate, define hallmarks and predict disease status. Endocr Relat Cancer 2015 Aug;22(4):561-75 doi: 101530/ERC-15-0092 Epub 2015 Jun 2.

242. Bodei L, Kidd M, Modlin IM, et al. Measurement of circulating transcripts and gene cluster analysis predicts and defines therapeutic efficacy of peptide receptor radionuclide therapy (PRRT) in neuroendocrine tumors. Eur J Nucl Med Mol Imaging 2016 May;43(5):839-51 doi: 101007/s00259-015-3250-z Epub 2015 Nov 23.

243. Bodei L, Kidd MS, Singh A, et al. PRRT genomic signature in blood for prediction of (177)Lu-octreotate efficacy. Eur J Nucl Med Mol Imaging 2018 Jul;45(7):1155-1169 doi: 101007/s00259-018-3967-6 Epub 2018 Feb 26.

244. Modlin IM, Frilling A, Salem RR, et al. Blood measurement of neuroendocrine gene transcripts defines the effectiveness of operative resection and ablation strategies. Surgery 2016 Jan;159(1):336-47 doi: 101016/jsurg201506056 Epub 2015 Oct 9.

245. Edeling M, Ragi G, Huang S, Pavenstadt H, Susztak K. Developmental signalling pathways in renal fibrosis: the roles of Notch, Wnt and Hedgehog. Nat Rev Nephrol 2016 Jul;12(7):426-39 doi: 101038/nrneph201654 Epub 2016 May 3.

246. Perugorria MJ, Olaizola P, Labiano I, et al. Wnt-beta-catenin signalling in liver development, health and disease. Nat Rev Gastroenterol Hepatol 2018 Nov 19 pii: 101038/s41575-018-0075-9 doi: 101038/s41575-018-0075-9.

247. Guan S, Zhou J. Frizzled-7 mediates TGF-beta-induced pulmonary fibrosis by transmitting non-canonical Wnt signaling. Exp Cell Res 2017 Oct 1;359(1):226-234 doi: 101016/jyexcr201707025 Epub 2017 Jul 20.

248. Drozdov I, Kidd M, Nadler B, et al. Predicting neuroendocrine tumor (carcinoid) neoplasia using gene expression profiling and supervised machine learning. Cancer 2009 Apr 15;115(8):1638-50 doi: 101002/cncr24180.

249. Kidd M, Modlin IM, Eick GN, Camp RL, Mane SM. Role of CCN2/CTGF in the proliferation of Mastomys enterochromaffin-like cells and gastric carcinoid development. Am J Physiol Gastrointest Liver Physiol 2007 Jan;292(1):G191-200 doi: 101152/ajpgi001312006 Epub 2006 Aug 31.

250. Liu W, Wang X, Mei Z, et al. BNIP3L promotes cardiac fibrosis in cardiac fibroblasts through [Ca(2+)]i-TGF-beta-Smad2/3 pathway. Sci Rep 2017 May 15;7(1):1906 doi: 101038/s41598-017-01936-5.

251. Danobeitia JS, Djamali A, Fernandez LA. The role of complement in the pathogenesis of renal ischemia-reperfusion injury and fibrosis. Fibrogenesis Tissue Repair 2014 Nov 1;7:16 doi: 101186/1755-1536-7-16 eCollection 2014.

252. Nafar M, Kalantari S, Samavat S, Rezaei-Tavirani M, Rutishuser D, Zubarev RA. The novel diagnostic biomarkers for focal segmental glomerulosclerosis. Int J Nephrol 2014;2014:574261 doi: 101155/2014/574261 Epub 2014 Mar 26.

253. Wang X, Guo X, Ma Y, Wu C, Li W, Xue L. APLP2 Modulates JNK-Dependent Cell Migration in Drosophila. Biomed Res Int 2018 Jul 29;2018:7469714 doi: 101155/2018/7469714 eCollection 2018.

List of publications during PhD research fellowship

*Laskaratos FM, Mandair D, Hall A, Alexander S, von Stempel C, Bretherton J, Luong T, Watkins J, Ogunbiyi O, Rombouts K, Caplin M, Toumpanakis C. Clinicopathological correlations of mesenteric fibrosis and evaluation of a novel biomarker for fibrosis detection in small bowel neuroendocrine neoplasms. Endocrine. 2019 Oct 9. doi: 10.1007/s12020-019-02107-4. PMID: 31598848

Laskaratos FM, Armeni E, Shah H, Megapanou M, Papantoniou D, Hayes AR, Navalkissoor S, Gnanasegaran G, von Stempel C, Phillips E, Furnace M, Kamieniarz L, Kousteni M, Luong TV, Watkins J, Mandair D, Caplin M, Toumpanakis C. Predictors of antiproliferative effect of lanreotide autogel in advanced gastroenteropancreatic neuroendocrine neoplasms. Endocrine. 2020 Jan;67(1):233-242. doi: 10.1007/s12020-019-02086-6. PMID: 31556004

Koffas A, Laskaratos FM, Epstein O. Training in video capsule endoscopy: Current status and unmet needs. World J Gastrointest Endosc. 2019 Jun 16;11(6):395-402. doi: 10.4253/wjge. v11.i6.395. PMID: 31236192

Koffas A, Laskaratos FM, Epstein O. Non-small bowel lesion detection at small bowel capsule endoscopy: A comprehensive literature review. World J Clin Cases. 2018 Dec 6;6(15):901-907. doi: 10.12998/wjcc. v6.i15.901. PMID: 30568944

Laskaratos FM, El-Mileik H. Gastric diverticulum of the antrum: An unusual endoscopic finding. Clin Case Rep. 2018 Nov 5;6(12):2515-2516. doi: 10.1002/ccr3.1910. eCollection 2018 Dec.PMID: 30564363

Laskaratos FM, Caplin M. Treatment challenges in and outside a network setting: Gastrointestinal neuroendocrine tumours. Eur J Surg Oncol. 2019 Jan;45(1):52-59. doi: 10.1016/j.ejso.2018.03.012. PMID: 29685756

*Laskaratos FM, Walker M, Wilkins D, Tuck A, Ramakrishnan S, Phillips E, Gertner J, Megapanou M, Papantoniou D, Shah R, Banks J, Vlachou E, Garcia-Hernandez J, Woodbridge L, Papadopoulou A, Grant L, Theocharidou E, Watkins J, Luong TV, Mandair D, Caplin M, Toumpanakis C. Evaluation of clinical prognostic factors and further delineation of the effect of mesenteric fibrosis on survival in advanced midgut neuroendocrine tumours. Neuroendocrinology. 2018;107(3):292-304. doi: 10.1159/000493317. PMID: 30153671

*Laskaratos FM, Diamantopoulos L, Walker M, Walton H, Khalifa M, El-Khouly F, Koffas A, Demetriou G, Caplin M, Toumpanakis C, Mandair D. Prognostic factors for survival among patients with small bowel neuroendocrine tumours associated with mesenteric desmoplasia. Neuroendocrinology. 2018;106(4):366-380. doi: 10.1159/000486097. PMID: 29320779

*<u>Laskaratos FM</u>, Rombouts K, Caplin M, Toumpanakis C, Thirlwell C, Mandair D. Neuroendocrine tumors and fibrosis: An unsolved mystery? Cancer. 2017 Dec 15;123(24):4770-4790. doi: 10.1002/cncr.31079. Epub 2017 Nov 7. PMID: 29112233

<u>Laskaratos FM</u>, Walker M, Naik K, Maragkoudakis E, Oikonomopoulos N, Grant L, Meyer T, Caplin M, Toumpanakis C. Predictive factors of antiproliferative activity of octreotide LAR as first-line therapy for advanced neuroendocrine tumours. Br J Cancer. 2016 Nov 22;115(11):1321-1327. doi: 10.1038/bjc.2016.349. Epub 2016 Nov 3. PMID: 27811856

(* directly arising from the PhD thesis)

List of conference abstracts during PhD research fellowship

2019:

*Laskaratos F, Levi A, Schwach G, Pfragner R, Xia D, Toumpanakis C, Mandair D,Rombouts K, Caplin M. Delineation of the pathogenesis of mesenteric fibrosis in midgut neuroendocrine tumours using an in vitro model of the neoplastic fibrotic microenvironment. Oral lecture at DDW, San Diego, USA, May 2019

*Laskaratos F, Hall A, Alexander S, von Stempel C, Bretherton J, Luong TV, Watkins J, Ogunbiyi O, Toumpanakis C, Mandair D, Caplin M. Is computed tomography an accurate diagnostic modality for the detection of mesenteric fibrosis in midgut neuroendocrine tumours? Poster presentation at DDW, San Diego, USA, May 2019

*Laskaratos F, Mandair D, Shah R, Luong TV, Watkins J, Ogunbiyi O, Caplin M, Toumpanakis C. Circulating transcripts of profibrotic genes in the NETest can identify mesenteric fibrosis in midgut neuroendocrine tumours. Poster presentation at 16th Annual ENETS conference, Barcelona, Spain, March 2019

*Laskaratos F, Shah R, Ogunbiyi O, Mandair D, Caplin M, Toumpanakis C. Circulating transcript analysis (NETest) assessment in the follow-up of resected midgut neuroendocrine tumours. Poster presentation at 16th Annual ENETS conference, Barcelona, Spain, March 2019.

Laskaratos F, Cox N, Woo WL, Khalifa M, Ewang M, Navalkissoor S, Quigley A, Mandair D, Caplin M, Toumpanakis C. Assessment of changes in mesenteric fibrosis after Peptide Receptor Radionuclide Therapy (PRRT) in midgut neuroendocrine tumours. Poster presentation at 16th Annual ENETS conference, Barcelona, Spain, March 2019.

2018:

Laskaratos FM, Megapanou M , Papantoniou D , Hayes A, von Stempel C, Phillips E, Furnace M, Kousteni M, Shah H, Mandair D, Caplin M, Toumpanakis C. Predictors of antiproliferative effects of Lanreotide Autogel as first-line therapy for gastroenteropancreatic neuroendocrine tumours. Oral lecture at Digestive Disease Week (DDW) conference, Washington DC, USA, June 2018

Laskaratos F, Shah R, Banks J, Smith J, Jacobs B, Galanopoulos M, Walton H, Khalifa M, Mandair D, Caplin M, Toumpanakis C. Antiproliferative effect of above-

label doses of somatostatin analogues for the management of gastroenteropancreatic neuroendocrine tumours. Poster presentation at DDW conference, Washington DC, USA, June 2018

Galanopoulos M, McFadyen R, Evans N, Naik R, Drami I, Varcada M, Ogunbiyi O, Luong TV, Watkins J, Clark I, Laskaratos F, Mandair D, Caplin M, Toumpanakis C. Challenging the current criteria for right hemicolectomy in appendiceal neuroendocrine neoplasms. Poster presentation at DDW conference, Washington DC, USA, June 2018

Laskaratos FM, Megapanou M , Papantoniou D , Hayes A, von Stempel C, Phillips E, Furnace M, Kousteni M, Shah H, Mandair D, Caplin M, Toumpanakis C. Predictors of Antiproliferative Effect of Lanreotide Autogel (LA) as First-Line Therapy for Advanced Neuroendocrine Tumors (NETs). Poster presentation at the 15th Annual ENETS Conference, Barcelona, Spain, March 2018

Laskaratos FM, Shah R, Banks J, Smith J, Jacobs B, Galanopoulos M, Walton H, Khalifa M, Mandair D, Caplin M, Toumpanakis C Antiproliferative Effect of Above-Label Doses of Somatostatin Analogues (SSA) for the Management of Neuroendocrine Tumors (NETs). Poster presentation at the 15th Annual ENETS Conference, Barcelona, Spain, March 2018

Galanopoulos M, McFadyen R, Evans N, Naik R, Drami I, Varcada M, Ogunbiyi O, Luong TV, Watkins J, Clark I, Laskaratos F, Mandair D, Caplin M, Toumpanakis C. Reassessment of Risk Factors Associated with Locoregional Lymph Nodal Metastases in Well-Differentiated Appendiceal Neuroendocrine Neoplasms. Poster presentation at the 15th Annual ENETS Conference, Barcelona, Spain, March 2018

2017:

Laskaratos FM, Shah R, Banks J, Jacobs B, Smith J, Galanopoulos M, Mandair D, Caplin M, Toumpanakis C. Shortened interval of octreotide LAR administration for the treatment of advanced neuroendocrine tumours (NETs). Poster at UKINETS 2017, London, UK

Laskaratos FM, Banks J, Shah R, Smith J, Jacobs B, Galanopoulos M, Caplin M, Mandair D, Toumpanakis C. Above-label doses of lanreotide Autogel for the treatment of advanced neuroendocrine tumours (NETs). Poster at UKINETS 2017, London, UK

Galanopoulos M, McFadyen R, Evans N, Naik R, Drami I, Varcada M, Ogunbiyi O, Luong T, Watkins J, Clark I, Laskaratos FM, Mandair D, Caplin M, Toumpanakis C. Prophylactic right hemicolectomy in Appendiceal Neuroendocrine Neoplasms: challenging the current indications. Poster at UKINETS 2017, London, UK

Telese A, Murino A, Phillips E, Laskaratos FM, Luong T, Koukias N, Mandair D, Toumpanakis C, Caplin M, Despott E. Double-balloon enteroscopy (DBE) is useful and effective for the diagnosis, assessment and management of small

bowel neuroendocrine tumours (SBNETs): a case series from a national tertiary referral centre. Poster at UKINETS 2017, London, UK

Murino A, Bailey J, Telese A, Laskaratos FM, Koukias N, Vlachou E, Luong T, Mandair D, Caplin M, Toumpanakis C, Despott E. Endoscopic submucosal dissection (ESD) of gastric and rectal neuroendocrine tumours (NETs). Poster at UKINETS 2017, London, UK

*Laskaratos F, Diamantopoulos L, Walker M, Khalifa M, Walton H, Koffas A, Demetriou G, Toumpanakis C, Caplin M, Mandair D. Predictors of survival in patients with small bowel neuroendocrine tumours associated with mesenteric desmoplasia. Poster of distinction at the DDW 2017 conference in Chicago, USA. Also accepted as poster at the 14th ENETS 2017 conference in Barcelona, Spain.

Koffas A, Demetriou G, Gvozdanovic A, Brooks PR, Horan CJ, Laskaratos FM, Garcia Hernandez J, Mullan M, Grant L, Papadopoulou AM, Mandair D, Caplin ME, Toumpanakis C. Predictive factors of survival in patients with pancreatic neuroendocrine tumors. Poster at the DDW 2017 conference in Chicago, USA. Also accepted as poster at the 14th ENETS 2017 conference in Barcelona, Spain.

Mandair D, Demetriou G, Diamantopoulos L, Devakumar H, Popat R, Laskaratos F, Caplin M, Toumpanakis C. Predictors of outcome in patients treated with Peptide Radio-labelled Receptor target therapy (PRRT). Poster presentation at the American Society of Clinical Oncology (ASCO) conference, Chicago, USA, June 2017. Also presented as poster at the 14th ENETS 2017 conference in Barcelona, Spain.

Mandair D, Diamantopoulos L, Demetriou G, Laskaratos F, Toumpanakis C, Caplin M. Typical bronchial NETs as a misleading biology. Poster presentation at the American Society of Clinical Oncology (ASCO) conference, Chicago, USA, June 2017. Also presented as poster at the 14th ENETS 2017 conference in Barcelona, Spain.

Demetriou G, Crawford A, Guarino S , Ogunbiyi O , Varcada M , Koffas A , Laskaratos FM , Hernandez Garcia J , Mandair D , Caplin M , Toumpanakis C. Clinical Outcomes in Small Neuroendocrine Tumours Treated with Intestinal Surgery in Tertiary Centre. Poster at the 14th ENETS 2017 conference in Barcelona, Spain.

(* directly arising from the PhD thesis)

Prizes/awards during PhD research fellowship

06/2019: *AGA (American Gastroenterological Association) Certificate of Recognition* for DDW oral lecture 'Delineation of the pathogenesis of mesenteric fibrosis in midgut neuroendocrine tumours using an in vitro model of the neoplastic fibrotic microenvironment', San Diego, USA

03/2019: *European Neuroendocrine Tumour Society (ENETS) Travel Grant*. This travel grant (awarded by ENETS to a maximum of 10 candidates annually) covered the costs of participation at the Annual ENETS conference in Barcelona, Spain.

01/2019: *IPSEN research grant* (£96,500) awarded following several research meetings with IPSEN and a competitive application, to investigate the pathophysiology of mesenteric fibrosis in midgut neuroendocrine tumours and the effect of telotristat etiprate on fibrogenesis

03/2018: *Second prize for best poster in Clinical Category at 15th Annual ENETS Conference* (abstract: "Antiproliferative Effect of Above-Label Doses of Somatostatin Analogues for the Management of Neuroendocrine Tumours")

12/2017: *UK and Ireland Neuroendocrine Tumour Society (UKINETS) Travel Grant*

03/2017: *European Neuroendocrine Tumour Society (ENETS) Travel Grant*